# Characterizing a novel interaction between ecdysone receptor and the AP-1 transcription factor in the regulation of gene expression during *Drosophila* dorsal closure

**by**

**Byoung Joo Yoo**

B.Sc., Simon Fraser University, 2011

Thesis submitted in Partial Fulfillment of the
Requirements for the Degree of
Master of Science

in the
Department of Molecular Biology and Biochemistry
Faculty of Science

© Byoung Joo Yoo 2020
SIMON FRASER UNIVERSITY
Spring 2020

Copyright in this work rests with the author. Please ensure that any reproduction or re-use is done in accordance with the relevant national copyright legislation.

# Approval

| | |
|---|---|
| **Name:** | **Byoung Joo Yoo** |
| **Degree:** | **Master of Science** |
| **Title:** | **Characterizing a novel interaction between ecdysone receptor and the AP-1 transcription factor in the regulation of gene expression during *Drosophila* dorsal closure** |
| **Examining Committee:** | **Chair: Edgar C. Young**<br>Associate Professor |
| | **Nicholas Harden**<br>Senior Supervisor<br>Professor |
| | **Esther M. Verheyen**<br>Supervisor<br>Professor |
| | **Charles Krieger**<br>Supervisor<br>Professor<br>Department of Biomedical Physiology and Kinesiology |
| | **Nancy Hawkins**<br>Internal Examiner<br>Associate Professor and Chair |
| **Date Defended/Approved:** | April 15, 2020 |

## Abstract

Dorsal closure (DC) of the *Drosophila* embryo is a well-characterized model system for studying morphogenetic events in wound healing and other developmental fusions such as palate fusion and neural tube closure. Prior to DC, a hole occupied with an extraembryonic tissue called amnioserosa (AS) is naturally left at the dorsal side of the embryo. DC begins when the epithelial sheets migrate over a hole and fuse to form a continuous epidermis. A commonly used secretable signal is a member of the transforming growth factor β (TGFβ) family, such as Dpp in Drosophila. During DC, the leading edge cells secrete Dpp into the AS cells to produce the steroid hormone, ecdysone (20E), which then drives AS morphogenesis by triggering gene expression. Here, we provide evidence that ecdysone-mediated gene expression is achieved through a novel interaction between the ecdysone receptor (EcR) and a subunit of the JNK-activated AP-1 transcription factor, Jun. While steroid hormone receptor interactions with AP-1 have been described in vertebrates, to our knowledge they have not been described in invertebrates and our work suggests that these interactions are ancient, predating the split between the vertebrate and invertebrate lineages.



**Keywords**: *Drosophila*; Dorsal Closure; Epithelial morphogenesis; AP-1; EcR ; 20E Hydroxyecdysone

*To my husband and family*

## Acknowledgements

Foremost, I wish to express my sincere gratitude to my senior supervisor, Dr. Nicholas Harden, for all the support and guidance over the years. His passion for research was always very inspiring and motivating. I deeply value the opportunities he gave me to develop my scientific skills during my graduate studies.

I would also like to extend my appreciation to my committee members, Dr. Esther Verheyen and Dr. Charles Krieger for their insightful and constructive feedback. I am grateful towards my examining committee, Dr.Nancy Hawkins (the internal examiner) and Dr. Edgar Young (Chair) for taking the time to evaluate my thesis.

I am deeply indebted to Dr. Simon Wang for his valuable supports. He has been a great mentor for over the years since I was an undergraduate student. He has provided me invaluable lessons regarding molecular biology and research. Words cannot express my gratitude for his encouragements and the countless hours he has spent to help me get through my project. Without his constructive advice and insightful suggestions, I could not have completed my thesis. Thank you for always being so patient and generous.

Thanks should also go to the past and present lab members. Fist of all, two of my best friends Hae-yoon Kim and Nicole Yoo. I have been blessed by your friendship and support which always uplifted me inside and outside the lab. I had pleasure working with hard working undergraduate students. I appreciate Claire Shih, Brian Lam and Sydney Schwartz for all their help. It was also great having Lionel Pereira, Shaianne Stein and Tiffany Schulz whose cheerfulness brightened the lab. I am also grateful to have met MBB friends who went through this journey together.

I wish to acknowledge the support and great love of my family and friends. Especially to my husband who have always believed in me. Thank you for letting me pursue my graduate studies. Even if we are geographically far away, I was always encouraged by your unconditional love.

# Table of Contents

## List of Tables

## List of Figures

# List of Acronyms

| | |
|---|---|
| 20E | 20-Hydroxyecdysone-*ecdysone steroid hormone* |
| AEL | After egg laying |
| A-P | Anterior-posterior |
| AS | Amnioserosa |
| DC | Dorsal closure |
| Dib | Disembodied – *Halloween gene required for ecdysone biosynthesis* |
| DME | Dorsal-most epidermal |
| D-V | Dorsal-ventral |
| Dpp | Decapentaplegic – *member of the transforming growth factor β (TGF-β) family* |
| EcR | Ecdysone receptor – *heterodimerizes with Usp to bind to EcREs* |
| EcRE | Ecdysone response element -*sequence bound by the EcR/Usp transcription factor complex* |
| FISH | Fluorescent *in situ* hybridization |
| Fos | Fos – *heterodimerizes with Jun to form the JNK-activated AP-1 transcription factor* |
| GBR | Germband retraction |
| JNK | Jun N-terminal kinase |
| Jun | Jun – *heterodimerizes with Jun to form the JNK-activated AP-1 transcription factor* |
| Kay | Kayak – *homologous of Fos* |
| LE | Leading edge |
| PLA | Proximity ligation assay |
| Spo | Spook – *Halloween gene required for ecdysone biosynthesis* |
| TGF-β | Transforming growth factor β |
| Usp | Ultraspiracle – *heterodimerizes with EcR to bind to EcREs* |
| Zip | Zipper – *encodes for non-muscle myosin II* |

# Chapter 1. Introduction

## 1.1. Dorsal closure

Dorsal closure (DC) during late *Drosophila* embryonic development is a well-characterized paradigm of epithelial migration and fusion. Many of the proteins that are known to regulate DC have also been implicated in a diverse range of epithelial migration and fusion events in other animals, including but not limited to epiboly, neural tube closure, palate fusion, and eyelid closure in vertebrates, and ventral enclosure in *Caenorhabditis elegans* (Simske and Hardin, 2001). Due to the striking parallels between DC and these other developmental processes, knowledge gained from the study of DC can be used to better understand epithelial morphogenesis in general (Harden, 2002; Jacinto et al., 2002). Most importantly, DC is of considerable medical interest as it is a genetic model for scarless wound healing (Martin and Parkhurst, 2004). DC may also provide critical insights concerning birth defects that result from failed epithelial fusions such as cleft palate, spina bifida and anencephaly.

DC corresponds to stages 13-15 during embryonic development (Atlas of *Drosophila* Development), which occurs approximately 9-13 hours after egg laying (AEL) at 25°C (Harden, 2002). Following germband retraction (GBR) (stages 11-12), a large hole is naturally left in the dorsal side of the epidermis and is occupied by an extraembryonic, unilayered epithelium called the amnioserosa (AS) (Figure 1.1.1 A) (Harden, 2002; Kiehart et al., 2017). At the onset of DC, the lateral epidermal flanks that abut both sides of the hole migrate dorsally towards each other up and over the AS (Figure 1.1.1 B,C). The epidermal flanks eventually meet and fuse at the dorsal midline, consequently internalizing the AS and sealing the hole to shut to form a continuous epidermis (Figure 1.1.1 D). Sealing of the hole progressively occurs from both canthi at the anterior and posterior ends of the hole in a zipper-like fashion (Jacinto and Martin 2001; Jacinto et al. 2002).

Though dozens of genes required for animal epithelial migration and fusion have already been identified, how they fit within the complex network of signaling pathways that control these processes is poorly understood. *Drosophila* is a powerful genetic model for studying epithelial morphogenesis, such as DC, for many reasons: they are easy and inexpensive to culture in the lab, they have a short developmental life cycle, they produce

large numbers of externally laid embryos, and there are numerous advanced genetic and developmental biological techniques available to Drosophilists (Jennings, 2011). Furthermore, identifying genes required for DC is relatively easy. If DC fails to complete, the embryo will die since there is no epidermis where the hole is to secrete a cuticle which is necessary for insect life. This makes identifying genes required for the process simple as mutations in these genes can result in a visible dorsal hole in the embryonic cuticle (Harden, 2002).

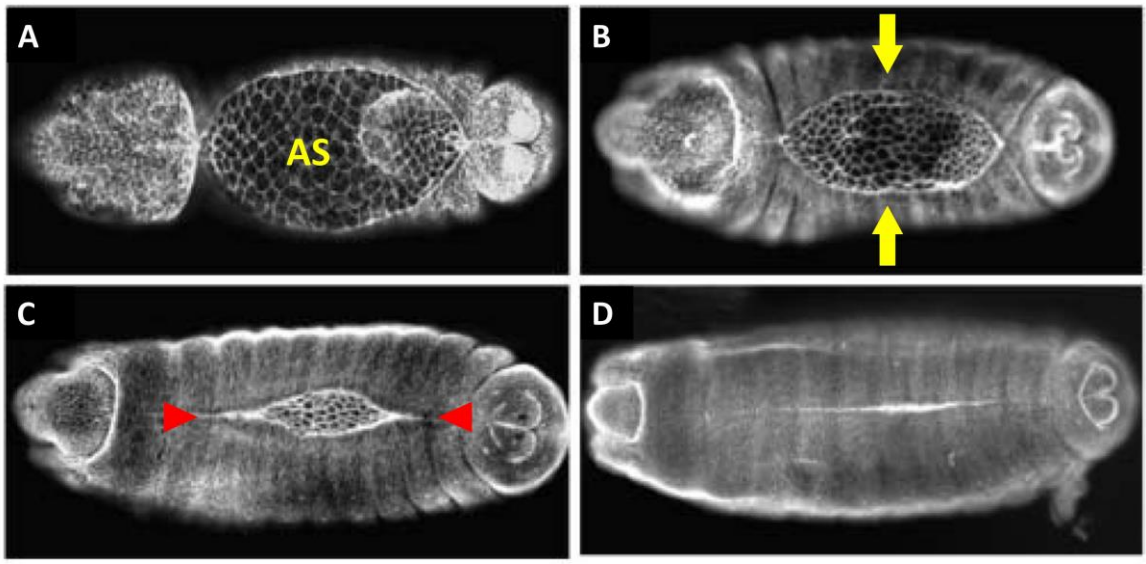


**Figure 1.1.1 DC of the *Drosophila* embryo.**

Confocal z-stacked images showing dorsal views of progressively older embryos throughout DC. The fixed embryos were stained with anti-phospho-tyrosine, which marks cell membranes. The anterior end is on the left. (A) Prior to the onset of DC, a hole is present in the dorsal epidermis of the embryo, which is occupied by an extraembryonic tissue called the AS. (B) As DC proceeds, the epidermal flanks that surround both sides of the hole start to migrate dorsally towards each other. Yellow arrows indicate the direction of the migration. (C) The opposing epidermal flanks begin to meet at the dorsal midline, and fuse at the canthi (indicated by red arrows) of the hole in a zipper-like fashion. (D) Upon DC completion, the hole is completely sealed to form a smooth, continuous epidermis. These images were modified from Harden, 2002. AS = amnioserosa.

## 1.2. Actomyosin contractility

Cell shape change, motility, and force generation are driven by actomyosin, as non-muscle myosin-II (referred to as myosin hereafter) motor proteins are able to crosslink and slide actin filaments past each other, leading to contraction (Harden, 2002; Young et al., 1993). Myosin exists as a hexamer composed of two heavy chains and two pairs of regulatory and essential light chains (Liu et al., 2008). Each heavy chain consists of three main regions: an N-terminal head region, a neck region, and a C-terminal tail region (Harrington and Rodgers, 1984; Kiehart and Feghali, 1986; Ricketson et al., 2010). The head region, also known as the motor domain, binds to actin filaments where it catalyzes the hydrolysis of ATP to initiate actomyosin constriction (Vasquez et al., 2016). The neck region is bound by the two light chains, which play structural and regulatory roles (Heissler and Sellers, 2014). The tail regions of the two heavy chains within a hexamer twist together to form a supercoil, which in turn interacts with the tails of heavy chains from other myosin subunits to form bipolar filaments (Kiehart and Feghali, 1986; Liu et al., 2008; Ricketson et al., 2010; Vasquez et al., 2016).

Closure of the dorsal hole is due to coordinated contraction between the dorsal epidermis and the AS. For DC to proceed properly, actomyosin networks must assemble in the form of a cable at the leading edge (LE) of the dorsal-most epidermal (DME) cells (*i.e.* the first row of epidermal cells that directly abut the dorsal hole) (Harden, 2002). Actomyosin networks are also formed across a medial array at the apical surface in AS cells (Blanchard et al., 2010; Solon et al., 2009; Wells et al., 2014).

### 1.2.1. DME cells

As DC proceeds, the shape of the DME cells change from polygonal to elongated along the dorsal-ventral (D-V) axis, which is due to the polarized accumulation of actomyosin at the LE membrane (Kiehart et al., 2017). This actomyosin network, which connects from cell-to-cell via adherens junctions, forms a continuous cable along the entire length of the LE of both epidermal flanks, and thus surrounds the dorsal hole. Contraction of the cable causes the DME cells to constrict in the anterior-posterior (A-P) direction, consequently resulting in D-V stretching towards the dorsal midline in a process that has been likened to the action of a purse string (Young et al. 1993; Mizuno, Tsutsui, and Nishida 2002). The purse string model is supported in studies where DME cells

lacking components of the actomyosin cable are observed to be unable to elongate, leading to a dorsal open phenotype (Harden et al., 1996). In addition, laser ablation of the actomyosin cable resulted in recoiling of the dorsal epidermis, indicating that the tissue is under tension and, most importantly, is not being passively drawn forward (Kiehart et al., 2000; Lacy and Hutson, 2016; Rodriguez-Diaz et al., 2008; Wells et al., 2014).

In addition to the actomyosin cable, the DME cells also extend towards the dorsal hole dynamic, actin-rich filopodial and lamellipodial protrusions, similar to those found in migratory cells (Jacinto et al., 2000; Mueller, 1999). Upon DC completion, the two epidermal flanks fuse seamlessly at the dorsal midline. Fusion is achieved by progressive zipping at both canthi of the “eye-shaped” dorsal hole (Toyama et al., 2008). Some studies indicate that this zipping process also contributes a DC driving force. For example, during the late stages of DC, embryos with impaired zipping show a significant reduction in closure rates (Jankovics and Brunner, 2006). The filopodia and lamellipodia appear to interact with both the AS and, at each canthus, DME cells from the opposing epidermal flank (Harden, 2002; Jacinto et al., 2000). Contact between the epidermal filopodia and lamellipodia may play roles in strengthening adhesion between opposing DME cells when they meet, in addition to responding to guidance cues that orient the protrusions towards opposing segments of the same identity to ensure perfect segmental matching (Hayes and Solon, 2017; Pasakarnis et al., 2016).

### 1.2.2. AS cells

The AS also plays a prominent mechanical role in DC, generating forces that contribute to the proper dorsal-ward movement of the epidermis. As DC proceeds, the AS cells contain cortical and medio-apical arrays of actomyosin that contract in wave-like pulses to constrict the apical surface of the cells leading to ingression (Solon et al., 2009). These pulsed contractions dampen sequentially from the outermost row of AS cells to the most dorsal ones, with the AS cells at the periphery sliding underneath the advancing epidermis. It has been proposed that the pulsations promote the progression of DC in coordination with the actomyosin cable at the LE of the DME cells, in what has been described as a ratchet-like motion. Direct irradiation of the AS, in which individual cells or clusters of cells are ablated, cause AS cells surrounding the ablated area to expand (Kiehart et al., 2000). This suggests that the AS cells are under tension. Laser ablation of the AS also caused retraction of the epidermis in the ventral direction, indicating that the

AS is not just being passively compressed by the advancing epidermal flanks. In addition to cell ingression, reduction in AS surface area is also attributed to apoptosis (Muliyil and Narasimha, 2014; Sokolow et al., 2012; Toyama et al., 2008). In support of this, studies have shown that reducing or enhancing apoptosis can greatly slow or speed up the rate of DC, respectively (Diaz et al. 2010; Muliyil, Krishnakumar, and Narasimha 2011; Toyama et al. 2008).

### 1.2.3. Zipper, the *Drosophila* myosin heavy chain

As mentioned in the previous sections, actomyosin contractility in both the DME cells and the AS is essential for DC to proceed properly. In *Drosophila*, the myosin heavy chain is encoded by a single locus, *zipper* (*zip*) (Vasquez et al., 2016). Likewise, *spaghetti squash* (*sqh*) and *myosin light chain cytoplasmic* (*mlc-c*) are the only *Drosophila* genes to encode for the myosin regulatory and essential light chains, respectively (Edwards et al., 1995; Karess et al., 1991). Prior work has shown that *zip* mutant embryos display dorsal open phenotypes (Young et al., 1993), which is described in more detail below. Potential DC defects cannot be evaluated for *sqh* null alleles, as the mutant embryos can survive to larval stages (Karess et al., 1991). This may be attributed to maternal loading. The role of *mlc-c* during DC has yet to be genetically evaluated (Jordan and Karess, 1997; Karess et al., 1991; Young et al., 1993). Thus, only *zip* will be focused on in this study.

Owing to its importance in the process, *zip* was one of the first DC genes to be studied in detail (Harden 2002; Hayes and Solon 2017; Nusslein-Vulhard 1984). Its name was derived from a severe defect in fusion between opposing epidermal flanks that was observed in DC-staged mutants (Young et al., 1993). During late embryonic development, the expression of the *zip* gene is dynamically regulated (Harden, 2002). *zip* expression is highly elevated in the AS at the onset of GBR (Figure 1.2.1 D). During mid to late GBR, expression in the DME cells begins to be upregulated (Figure 1.2.1 E). As DC proceeds, however, the expression levels abate in the AS but persist in the DME cells (Figure 1.2.1 F). In *zip* mutant embryos, cell shape change in both the DME cells and AS is aberrant, and DC fails to go to completion (Young et al., 1993). This is attributed to a disruption in the organization of the actomyosin cytoskeleton, which is needed to form the supracellular purse string in the DME cells and the cortical and medio-apical arrays in the AS cells (Franke et al., 2005). Tissue-specific expression of *zip* in either the LE epidermis or the AS in *zip* mutant embryos can rescue the dorsal open phenotype (Franke et al., 2005),

thus indicating that regulation of *zip* expression in both the DME cells and AS is critical for DC.

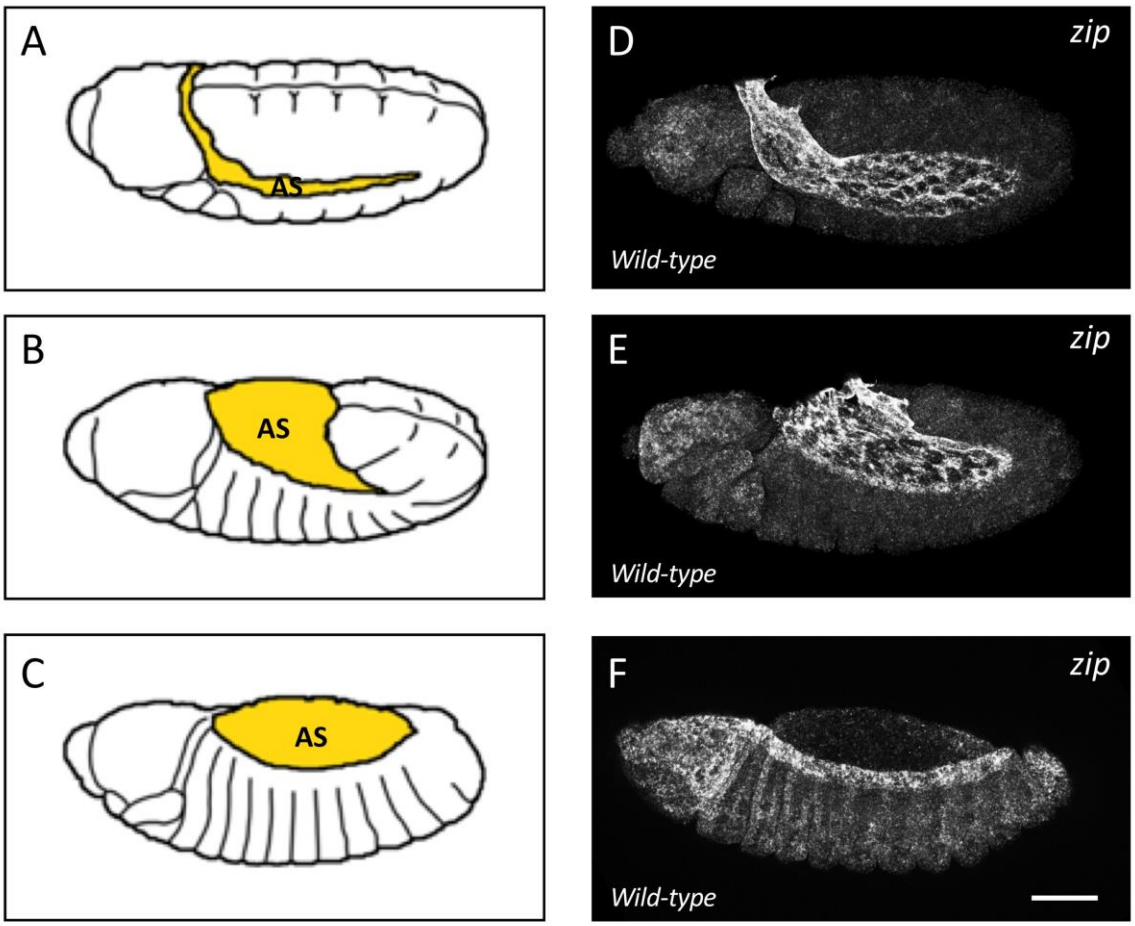


**Figure 1.2.1 *zip* expression during GBR and DC.**

(A-C) Illustrations showing lateral views of embryos at the onset of GBR (stage 11) (A), during GBR (stage 12) (B), and during DC (stage 13) (C). The anterior ends are on the left. The AS is highlighted in yellow. (D-F) Corresponding confocal images showing similarly-staged, wild-type embryos. *zip* transcripts are detected with FISH. *zip* is highly expressed in the AS at the onset of GBR (D). As GBR proceeds, the expression of *zip* begins to be elevated in the DME cells (E). Once DC begins, *zip* expression subsides in the AS but is maintained in the DME cells. Upregulated expression in the head can also be observed (D-F). AS = amnioserosa. Scale bar: 50μm. Illustrations were modified from the Atlas of *Drosophila* Development.

## 1.3. Signaling pathways that regulate DC

A recurring finding in studies of epithelial fusions during development and wound healing is that cells occupying the hole contribute to closure by contracting in response to signaling from the surrounding tissue margin via TGF-β superfamily ligands (Werner et al., 2007). This mechanism is conserved in DC where, in response to a JNK cascade, the DME cells secrete the *Drosophila* TGF-β ligand, Dpp, into the AS, thereby activating signaling pathways that stimulate its morphogenesis (Fernández et al., 2007; Wada et al., 2007; Zahedi et al., 2008). In a search for pathways downstream of Dpp in the AS, the lab has considered signaling by the steroid hormone, ecdysone. The AS is a major source of ecdysone during embryogenesis, and mutants of the Halloween group of genes, which encode enzymes in the ecdysone biosynthetic pathway, display DC defects (Chavez et al., 2000; Giesen et al., 2003; Kozlova and Thummel, 2003; Niwa et al., 2010; Ono et al., 2006). Interestingly, Dpp is required for the expression of at least one of these enzymes (Chen, 2014). In the following sections, the main signaling pathways involved in regulating DC will be discussed in greater detail.

### 1.3.1. c-Jun N-terminal kinase cascade

A key feature of DC is the formation of an actomyosin cable at the LE of DME cells (Harden, 2002). A similar structure is observed in wound healing (Grose and Martin, 1999; Martin and Parkhurst, 2004). Formation of the actomyosin cable in both processes is dependent on the c-Jun N-terminal kinase (JNK) pathway, which is a member of the family of mitogen-activated protein kinase (MAPK) cascades (Bosch et al., 2005).

MAPK cascades are central signaling pathways that regulate a wide range of stimulated cellular processes such as proliferation, differentiation, apoptosis and stress response (Ip and Davis, 1998). Thus, disruption of these cascades can lead to various disorders including cancer, diabetes, autoimmune diseases, and developmental abnormalities (Biteau et al., 2011; Fu et al., 2009; Hotamisligil, 2006; Kuan et al., 1999; Riesgo-Escovar et al., 1996). Each cascade consists of three core kinases (*i.e.* MAPK kinase kinase (MAPKKK), MAPK kinase (MAPKK), and MAPK), though additional upstream and downstream kinases can be involved (Cargnello and Roux, 2011; Harden, 2002). Signaling through the cascade is propagated by sequential phosphorylation and activation of the kinases. MAPKKKs are serine/threonine kinases that are often activated

by small GTPases or through phosphorylation by a MAPK kinase kinase kinase (MAPKKKK) in response to extracellular stimuli. Activated MAPKKKs, in turn, phosphorylate and activate MAPKKs, which are dual-specificity kinases that act as tyrosine and serine/threonine kinases that phosphorylate MAPKs at conserved Thr-X-Tyr activation loops. Finally, activated MAPKs phosphorylate serine and threonine residues of downstream targets, which can vary from transcription factors, cytoskeletal proteins, kinases and other enzymes. In mammals, there are five families of the MAPK cascades, which are divided based on the MAPK: extracellular signal-regulated kinase 1 and 2 (ERK1/2), JNK, p38, ERK3/4 and ERK5 (Cargnello and Roux 2011; Qi and Elion 2005).

The JNK signaling cascade is conserved between vertebrates and invertebrates (Glise et al., 1995; Martin-blanco, 1997; Riesgo-Escovar and Hafen, 1997a). In *Drosophila*, JNK regulates numerous developmental events including, but not limited to, follicle cell morphogenesis, imaginal disc morphogenesis, and thorax closure during metamorphosis (Agnès et al., 1999; Dobens et al., 2001; Igaki, 2009; Johnson and Nakamura, 2007; Martín-Blanco et al., 2000; Zeitlinger and Bohmann, 1999). Involvement of the JNK cascade during DC was first revealed when cloning the *hemipterous* (*hep*) locus. *hep* encodes a MAPKK that is most similar to the mammalian JNKK, MKK7 (Bourbon 1995; Harden 2002; Stronach and Perrimon 2001). A subsequent study revealed that *basket* (*bsk*), a homologue to human JNK, is the only JNK present in *Drosophila* (Riesgo-Escovar et al., 1996; Sluss et al., 1996). Mutations in *hep* and *bsk* both disrupt the DC process, resulting in embryos with dorsal holes (Bourbon 1995; Riesgo-escovar et al. 1996; Riesgo-escovar and Hafen 1997b; Sluss et al. 1996; Hou 1997; Zeitlinger et al. 1997). Their DC phenotypes are similar to each other including disrupted D-V elongation of the DME cells and loss of the actomyosin cable along the LE.

In *Drosophila*, several JNKKKs have been identified that can activate the Hep-Bsk cassette: dTAK1, DASK1, dMLK and dMekk1 (Igaki 2009). The JNKKKs are activated by different upstream, intracellular proteins, which can include GTPases, the Ste20-related kinase, Misshapen (Msn), and the tumor necrosis factor receptor-associated factors (TRAFs), DTRAF1 and DTRAF2. Among these different JNKKKs, the *Drosophila* mixed lineage kinase (dMLK), encoded by *slipper* (*slpr)* locus, is the only kinase that has been shown to directly phosphorylate Hep and activate the JNK pathway during DC (Sathyanarayana et al. 2003; Stronach and Perrimon 2002). Based on various genetic and biochemical experiments, evidence suggests that dMLK can be activated by the Rac1

GTPase and Msn in both *Drosophila* and mammals (Gallo and Johnson 2002; Leung and Lassam 2001; Stronach and Perrimon 2002). However, upstream regulation of the JNK pathway during DC remains poorly understood.

The *Drosophila* JNK pathway acts as a classic MAPK cascade that culminates in the activation of Jun (Riesgo-Escovar and Hafen, 1997a). When activated, Jun forms the AP1 transcription upon dimerization with Fos, which is encoded by *kayak* (*kay*) (Mihaly et al. 2001; Riesgo-escovar and Hafen 1997a; Zeitlinger et al. 1997). *jun* and *kay* mutations both result in similar DC phenotypes to those observed with loss of *hep* and *bsk*, indicating that activation of the AP-1 transcription factor via the JNK pathway is a major signaling route for DC to proceed properly. This is supported through expression of constitutively active Jun, which can rescue DC defects in embryos lacking upstream JNK kinase components (Martin-blanco, 1997; Riesgo-Escovar and Hafen, 1997b; Riesgo-Escovar et al., 1996; Sluss and Davis, 1997; Sluss et al., 1996; Stronach and Perrimon, 2002). In a genetic screen identifying mutations that affect DC, a multidomain protein, Connector of kinase to AP-1 (Cka), was also found to be part of the JNK pathway (Chen et al., 2002). CKA can form a complex with Hep, Bsk, Jun and Fos during embryonic development, and is believed to act as a scaffolding protein that brings the upstream and downstream pathway components together (Figure 1.3.1).

JNK cascade activation during DC occurs in the DME cells to drive gene expression (Figure 1.3.1) (Glise et al., 1995; Hou et al., 1997; Riesgo-Escovar and Hafen, 1997a; Riesgo-Escovar et al., 1996; Sluss et al., 1996; Stronach and Perrimon, 2002; Zeitlinger et al., 1997). Extensive studies have focused on two target genes: *puckered* (*puc*) and *decapentaplegic* (*dpp*). *puc* encodes a dual specificity MAPK phosphatase, which dephosphorylates Bsk and serves as a negative feedback loop for the JNK pathway (Glise et al., 1995; Martín-Blanco et al., 1998). *dpp* encodes a key morphogen of the transforming growth factor-β (TGF-β) pathway (Jackson and Hoffmann, 1994), which will be discussed further in the next section. It has previously been shown that mutations in JNK cascade components result in loss of *puc* and *dpp* expression in the DME cells (Riesgo-Escovar and Hafen, 1997a).

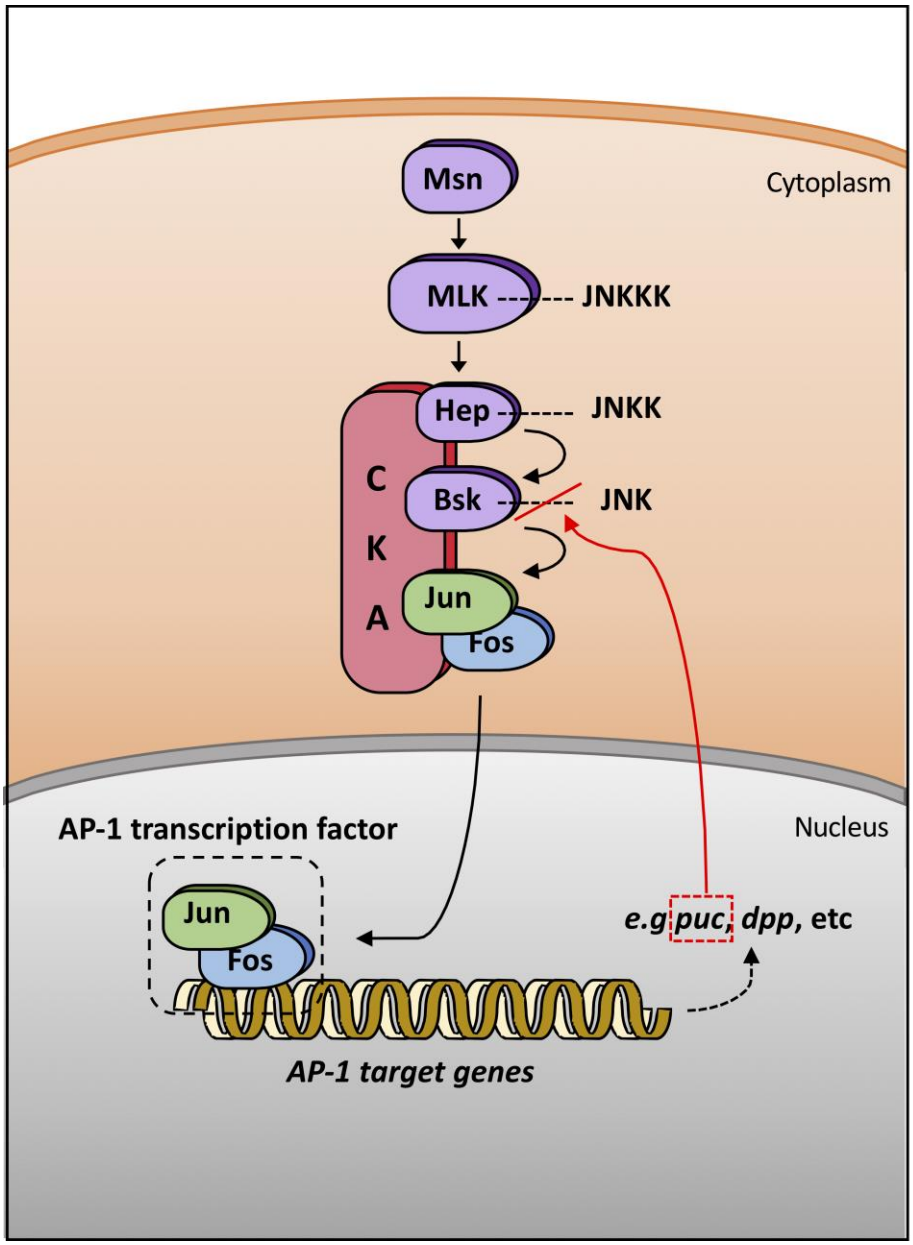


**Figure 1.3.1 A schematic of the JNK signaling cascade in DME cells during DC.**

In DME cells during DC, the Ste20-related kinase, Msn, transduces an unknown upstream signal to activate the core JNK signaling cascade module, which involves the stepwise phosphorylation of dMLK (JNKKK), Hep (JNKK) and Bsk (JNK). Bsk then phosphorylates and activates the AP-1 transcription factor, consisting of a heterodimeric complex between Jun and Kay/Fos, to drive target gene expression (*e.g. puc* and *dpp*). Puc is a MAPK phosphatase that dephosphorylates Bsk, and serves as a negative feedback loop for the JNK pathway. Dpp is a key ligand of the TGF-β pathway. Stepwise phosphorylation and activation are aided by Cka, which is a scaffolding protein that can form a complex with Hep, Bsk, Jun and Fos.

### 1.3.2. The Rho small GTPase as an upstream activator of JNK-Dpp pathway

Among candidate upstream activators of the JNK pathway, the Rho family small GTPases have been investigated for involvement in DC. The small GTPases cycle between two states, a GDP-bound “off” state and a GTP-bound “on” state, thus acting as a molecular switch to regulate diverse cellular processes by transducing extracellular and intracellular signals to downstream effectors. The Rho GTPases which consists of Rac, Cdc42 and Rho subgroups have been shown to be involved in the regulation of the actin cytoskeleton and upstream activators of the JNK and other MAPK cascades. For example, an embryo with dominant negative Rac1 ($Rac^{N17}$) showed loss of the cytoskeleton at the leading edge of the DME which suppressed the elongation of LE cells and resulted in a DC defect (Harden, 2002; Harden et al., 1999). The DC defect induced by dominant negative Rac1 was comparable to the defect caused by the loss of JNK components. Loss of the LE cytoskeleton in Rac1 mutant embryo was rescued by constitutively active Jun (Hou 1997). Constitutively active Rac1 causes ectopic expression of *dpp* and *puc* which also suggests that Rac1 is part of the upregulation of the JNK-Dpp pathway (Glise et al., 1995). However, the rescue of DC defects by Jun was only partial, thus it suggests the presence of another pathway in which Rac1 is involved. Cdc42 has a similar effect on the JNK-Dpp pathway and DC like seen in Rac1. Rac1 and Cdc42 seem to have a role in upregulating the JNK pathway in DC, but the rescue experiments suggest other players in the JNK pathway regulation.

Rho1 on the otherhand, has been shown to regulate myosin accumulation at the LE and the interaction of Rho1 with myosin seems to be associated with the Rho-associated kinases (ROKs). ROKs are downstream effectors of Rho1 in mammalian cells and phosphorylate the regulatory light chain of myosin which activates the myosin ATPase, ultimately promoting the assembly and function of the actomyosin cytoskeleton (Bishop and Hall, 2000; Bresnick, 1999). Rho1-ROK-MyosinII activity in cooperation with Ras has been shown to be involved in up-regulation of the JNK signaling (Khoo et al., 2013). Previous study done in our lab (unpublished) demonstrated elevated *zip* transcript levels during DC through overexpression of Rho1. RhoGEF2 likely to have a role in activating Rho1 since overexpression of RhoGEF2 led to slight increase in *zip* transcript levels during DC (Figure 1.3.2) (Kim, 2017).

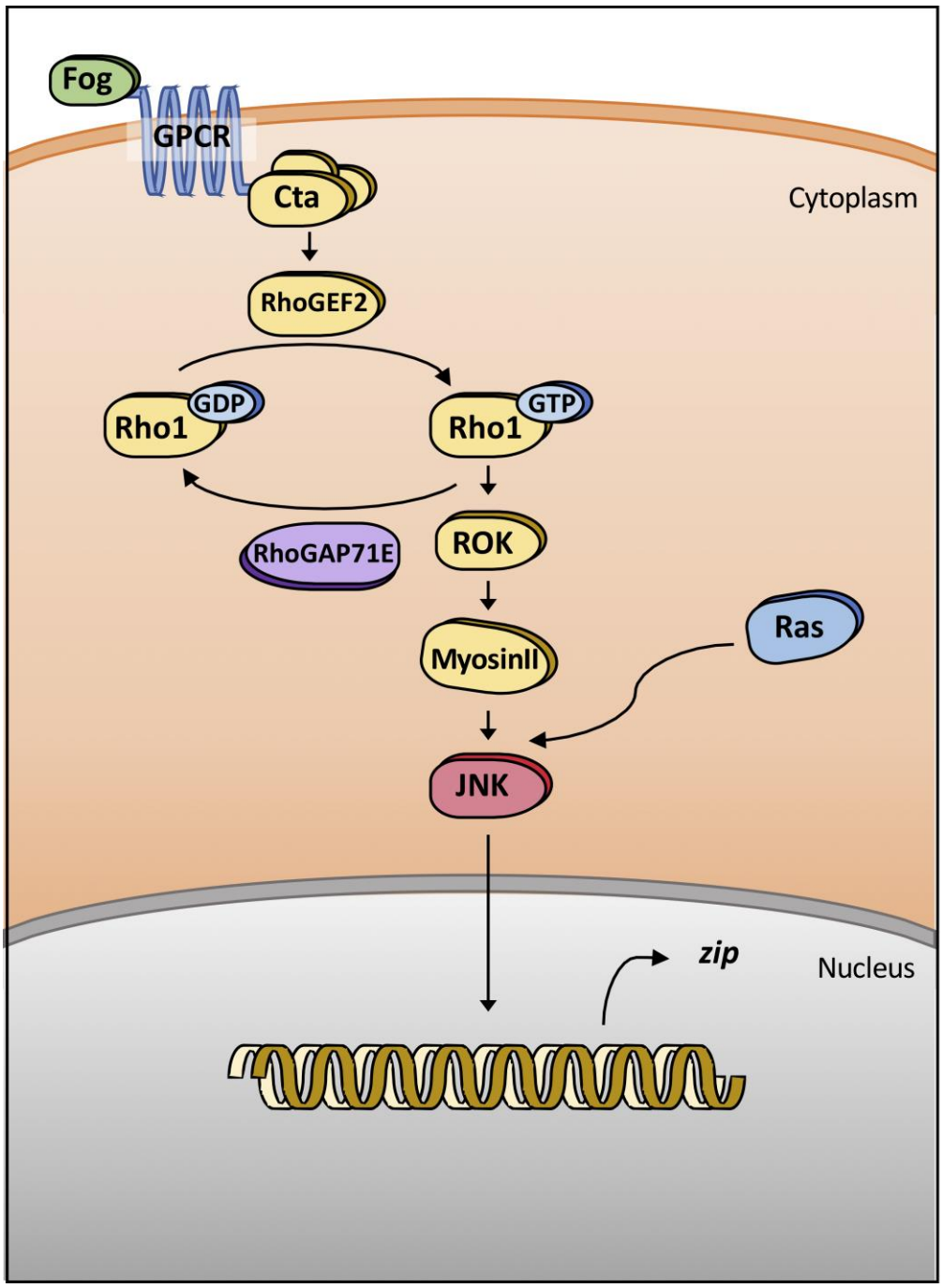


**Figure 1.3.2 A simplified schematic represenation of possible RhoGAP71E involvement during DC by deactivating Rho1**

Fog regulation of *zip* through the GPCR-mediated Rho1-ROK-Myosin II pathway has previously been demonstrated by several tests. In this study, RhoGAP71E is hypothesized to be acting as a GAP to turn off Rho1.

### 1.3.3. Transforming growth factor-β pathway

*Drosophila* Dpp is a member of the TGF-β superfamily that plays fundamental roles in controlling tissue specification, growth and patterning (Inoue et al., 1998; Letsou et al., 1995; Sekelsky et al., 1995). Homologous to vertebrate bone morphogenetic proteins (BMPs), Dpp serves as a morphogen that diffuses in a spatial concentration gradient to activate the TGF-β pathway in surrounding tissues (Raftery and Sutherland, 1999). Signaling begins when the Dpp ligand is recognized by the receiving cell through a heterodimeric receptor complex consisting of the type I receptor, Thickveins (Tkv), and the type II receptor, Punt (Put) (Figure 1.3.3) (Affolter et al., 2001). When Tkv is bound by Dpp, Put, a constitutively active kinase, is recruited and activates Tkv through phosphorylation at a type I receptor-specific, juxtamembrane GS domain. Activated Tkv then phosphorylates the Smad, Mothers against Dpp (Mad), which in turn translocates into the nucleus with the Co-Smad, Medea (Med). Once in the nucleus, the Mad-Med complex binds to *cis*-acting elements in target genes, and either activates or represses their expression. The Dpp pathway can also control gene expression indirectly by downregulating the expression of *brk,* which encodes a transcription factor that binds to *cis*-acting elements in Dpp target genes acting as a gene repressor (Campbell and Tomlinson, 1999). Daughters against dpp (Dad), another product from the Dpp pathway, blocks Tkv and Mad interaction by associating with Tkv, thus antagonizing the Dpp pathway. (Inoue et al., 1998; Minami et al., 1999). These positive and negative feedback loops are important in maintaining the Dpp pathway.

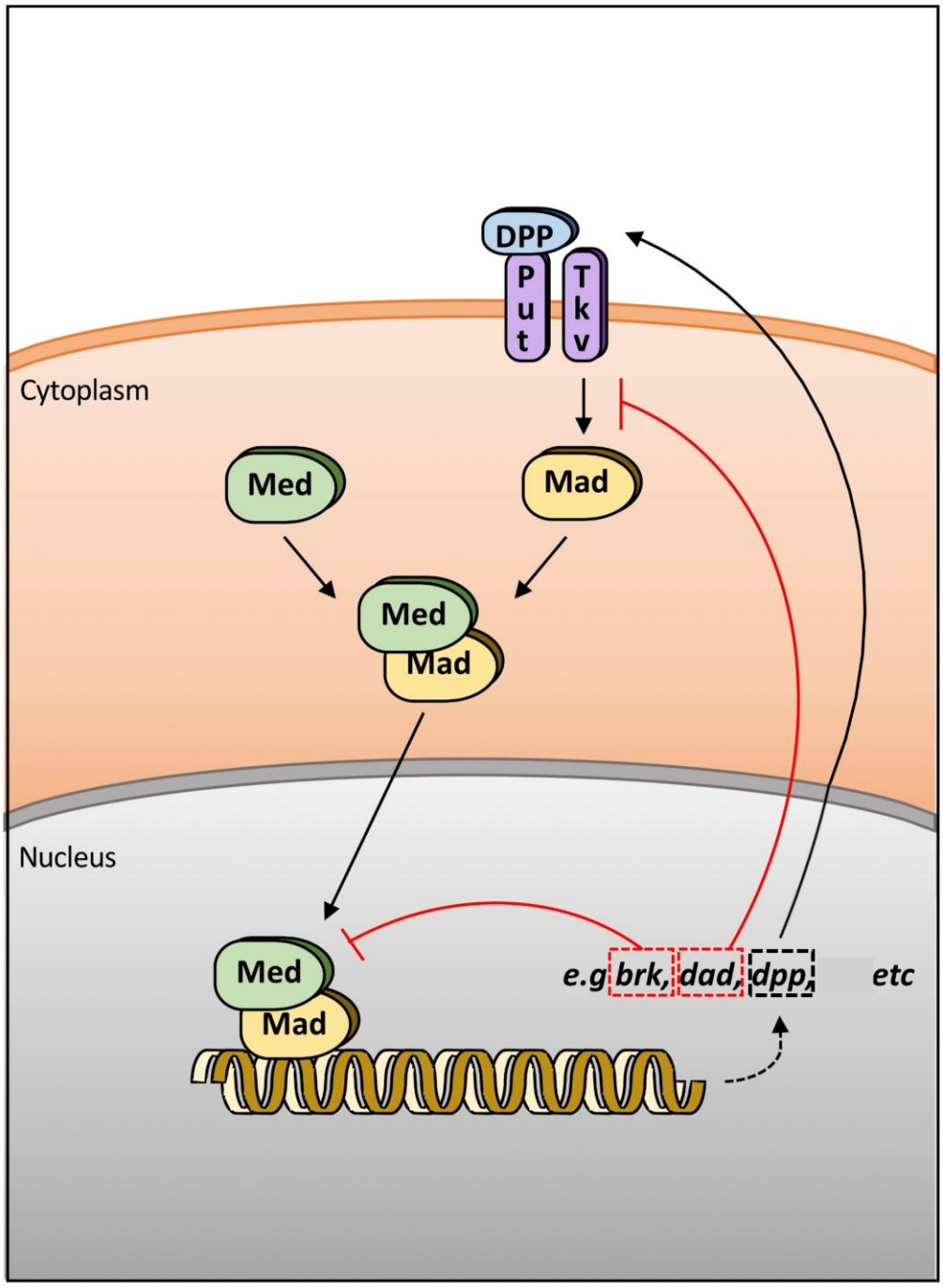


**Figure 1.3.3 A schematic of Dpp signaling in AS cells during DC.**

During DC, DME cells secrete Dpp to neighboring AS (and other DME) cells. Dpp binds to Put of the receiving cell, which in turn recruits and activates Tkv. Upon phosphorylation by activated Tkv, Mad translocates into the nucleus with Med, and the transcription factor binds to *cis*-acting elements in target genes to drive their expression. Brk and Dad expression creates negative feedback loops, whereas expression of more Dpp provides a positive feedback loop.

During DC, the epidermal expression of Dpp is in two stripes. One in the DME cells and the other in few rows of ventral lateral cells (Jackson and Hoffmann, 1994). Only expression of Dpp in the DME cells is dependent on the JNK pathway (Bourbon 1995; Hou 1997; Riesgo-escovar and Hafen 1997b; Sluss and Davis 1997; Stronach and Perrimon 2002). Previous genetic studies have shown that mutations in Dpp pathway components such as *tkv, put* and *mad* all result in DC defects similar to those observed with mutations in components of the JNK cascade. Over-expression of Dpp or expression of constitutively active Tkv can rescue the DC defects caused by impaired JNK signaling (Brummel et al., 1994; Letsou et al., 1995; Riesgo-Escovar and Hafen, 1997a; Ruberte et al., 1995). These results strongly indicate that the Dpp pathway is downstream of the JNK signaling cascade during DC.

Knowing that *zip* is an important factor in the DC process and that it is highly expressed in the DME as well, there is a high possibility that the Dpp pathway is upstream regulator of *zip* during DC. It also has been shown that the *zip gene* levels in the AS were reduced during germband retraction and the LE expression of the *zip* during DC is lost in *tkv* mutant embryos (Arquier et al., 2001; Zahedi et al., 2008). A previous study also showed Dpp secreted from the DME cells were responsible for *zip* expression both in the DME and the AS. (Figure 1.3.4) It was demonstrated by observing Dpp activity pattern (by staining for pMad) which corresponded to *zip* expression pattern. (Zahedi et al., 2008). However these studies suggest *zip* expression was not dependent only on Dpp but required additional input because ectopically activated Dpp pathway in the embryo through constitutive active Tkv receptor or by expressing Dpp transgene (Dorfman and Shilo, 2001; Hoodless et al., 1996) using *prd-GAL4* was not enough to ectopically elevate *zip* transcripts. Dpp therefore, is necessary for regulating *zip* expression in both DME and AS but not sufficient and additional inputs are required.

Although there are some evidences that the JNK-Dpp pathways are cooperating in DC by regulating DC genes such as *zip*, the exact mechanism how the JNK-Dpp in the LE plays a key role in coordinating cellular behaviors in the DME and the AS is still elusive. Interesting fact is, the JNK pathway is turned off in the AS prior to DC but *zip* expression is still upregulated in this tissue (Figure 1.2.1) (Reed, Wilk, and Lipshitz 2001). Based on the knowledge that Dpp ligand activates a signaling pathway in the AS through its receptors Tkv and Punt and is responsible for the AS morphogenesis (Fernández et al., 2007; Wada et al., 2007; Zahedi et al., 2008), downstream of Dpp in the AS might be

regulating expression of DC genes including *zip*. Signaling by the steroid hormone 20-hydroxyecdysone (hereafter referred to as 20E) is becoming a good candidate for another key pathway in regulating DC cooperating with the JNK and the Dpp pathways. Evidence also shows that 20E biosynthetic pathway is activated by Dpp because reduced *spook (spo)* transcripts, which encode one of the enzymes required for this pathway, were confirmed in the AS of *tkv* mutant embryo. Reduced *zip* transcript levels in *tkv* mutant embryos were also rescued by incubating with exogenous 20E (Chen, 2014) which suggests 20E is a likely input that upregulates *zip* expression during DC in addition to Dpp pathway (Figure 1.3.4).

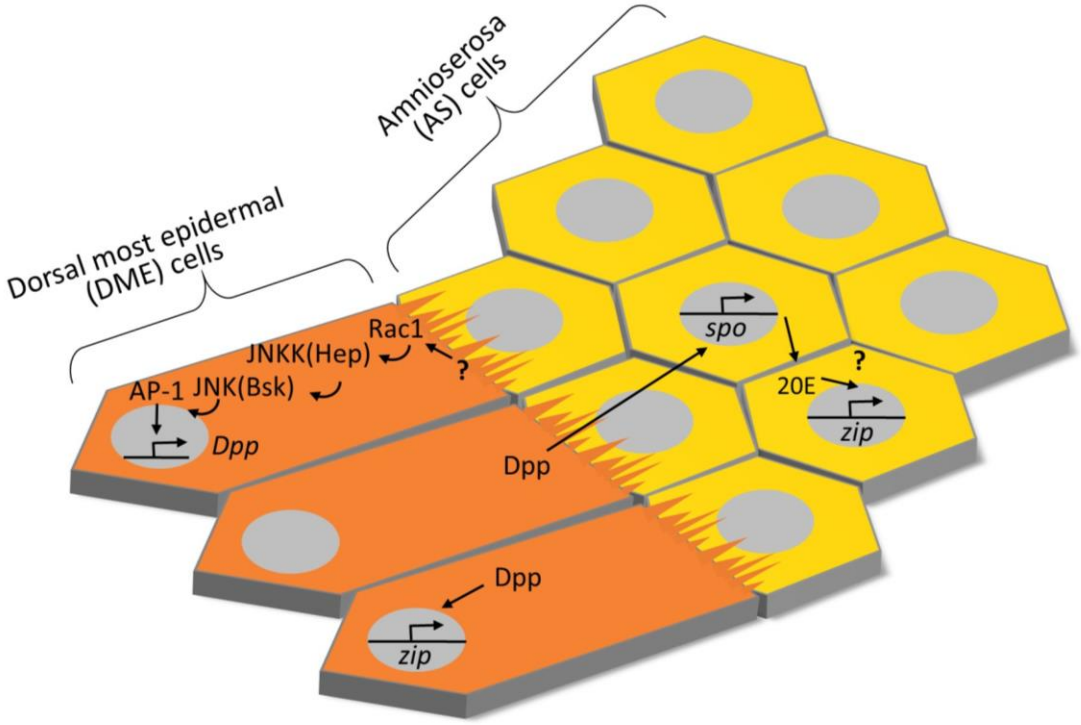


**Figure 1.3.4 A schematic of DME and AS cells showing the JNK-Dpp pathways are cooperating in regulation of DC genes such as *zip.***

*zip* expression in the DME cells is dependent on JNK pathway, but not in the AS since JNK pathway is turned off in this tissue. Dpp signaling is required but not sufficient for *zip* expression in both the DME and AS cells, which suggests additional input is required. Previous study has demonstrated that Dpp secreted to the AS activates 20E biosynthetic pathway. Therefore, 20E is a likely input that upregulates *zip* expression during DC in addition to Dpp pathway.

### 1.3.4. Ecdysone signaling

Steroid hormones are secreted chemical messengers that transmit signals to other cells, and regulate a variety of tissues and biological functions (Brennan et al., 1998; Chavez et al., 2000; Niwa and Niwa, 2014). Within target cells, the steroids can activate signaling pathways and mediate gene expression by binding to cytosolic or nuclear protein receptors. In humans, there are four major types of steroids: progestins, androgens, estrogens and corticoids (Holst et al., 2013). They are derived from free cholesterols in the cytoplasm that are transported to the mitochondria. Steroid hormones can also be the cause of cancer, steroid insensitivity, abnormal fertility and endocrine alterations (Miller, 2017; Zubeldia-Brenner et al., 2016). The principal steroid in insects is 20-hydroxyecdysone (henceforth referred to as 20E or ecdysone), which coordinates many processes during *Drosophila* development such as metamorphosis, molting and diapause (Bender et al., 1997; Brennan et al., 1998; Chavez et al., 2000; Niwa and Niwa, 2014). 20E also plays roles in aging by regulating multiple events during the transition from larval to pupal stages including cell proliferation, movement of the morphogenetic furrow in eye discs, eversion of imaginal discs, apoptosis of larval cells, and deposition of pupal cuticle. Of interest to the lab, a number of studies have indicated that 20E is involved in DC. 20E is produced from dietary cholesterol by a biosynthetic pathway of cytochrome $P_{450}$ enzymes encoded by members of the Halloween genes, which include: *neverland* (*nvd*), *spook* (*spo*), *spookier* (*spok*)*, phantom* (*phm*)*, disembodied* (*dib*), *shadow* (*sad*) and *shade* (*shd*) (Niwa and Niwa, 2014). During embryogenesis, 20E levels rise between 6-10 hours AEL, with a peak at 8 hours (*i.e.* just prior to the onset of DC), and the AS has been identified as a major source of 20E production (Kozlova and Thummel, 2003). In addition, mutants of the Halloween genes cause DC defects (Chávez et al. 2000; Giesen et al. 2003; Kozlova and Thummel 2003; Ono et al. 2006; Niwa et al. 2010).

Canonical ecdysone signaling involves activation of a heterodimeric transcription factor consisting of Ecdysone receptor (EcR) and Ultraspiracle (Usp) (Thummel, 1995). EcR is orthologous to the liver X (LXR) and farnesoid X (FXR) receptors in vertebrates, whereas Usp is a homolog of the vertebrate retinoid X receptor (RXR) (Thummel 1995; Riddiford et al. 2001). In the absence of ecdysone, EcR-Usp is localized in the nucleus and bound to DNA where it is thought to act as a transcriptional repressor (Dobens et al., 1991; Tsai et al., 1999). Upon binding of 20E, the EcR-Usp complex acts as a transcriptional factor which associates with ecdysone response elements (EcREs) within

the genome to promote the expression of downstream genes (Cherbas et al., 1991; Riddiford et al., 2001). EcR binding to 20E is relatively weak on its own, however, ligand binding is greatly enhanced by the co-presence of Usp (Koelle et al., 1991; Yao et al., 1992). Reciprocally, 20E binding stabilizes the EcR-Usp heterodimer, and increases affinity of the complex to EcREs. Three protein isoforms are encoded by the *ecr* locus: EcR-A, EcR-B1 and EcR-B2 (Cherbas et al., 2003; Riddiford et al., 2001). Isoform expression is tissue specific, and is temporally regulated based on cell fates at different developmental stages (Talbot et al., 1993; Thummel, 1995). Differences between the isoforms occur at the N-terminus, which contains an activation function 1 (AF1) domain (Cherbas et al., 2003; Riddiford et al., 2001). Though the domain appears to be dispensable for development, it was revealed that only EcR-A can regulate wing disc margin development, whereas only EcR-B2 is involved in the development of the larval epidermis and the border cells of the egg chamber. Despite these differences, each isoform contains identical DNA binding domains that can associate with EcREs. Similar to the embryonic defects associated with loss of 20E production, reduced EcR or Usp function results in embryonic defects in head involution, tracheal morphogenesis and DC (Chavoshi et al., 2010).

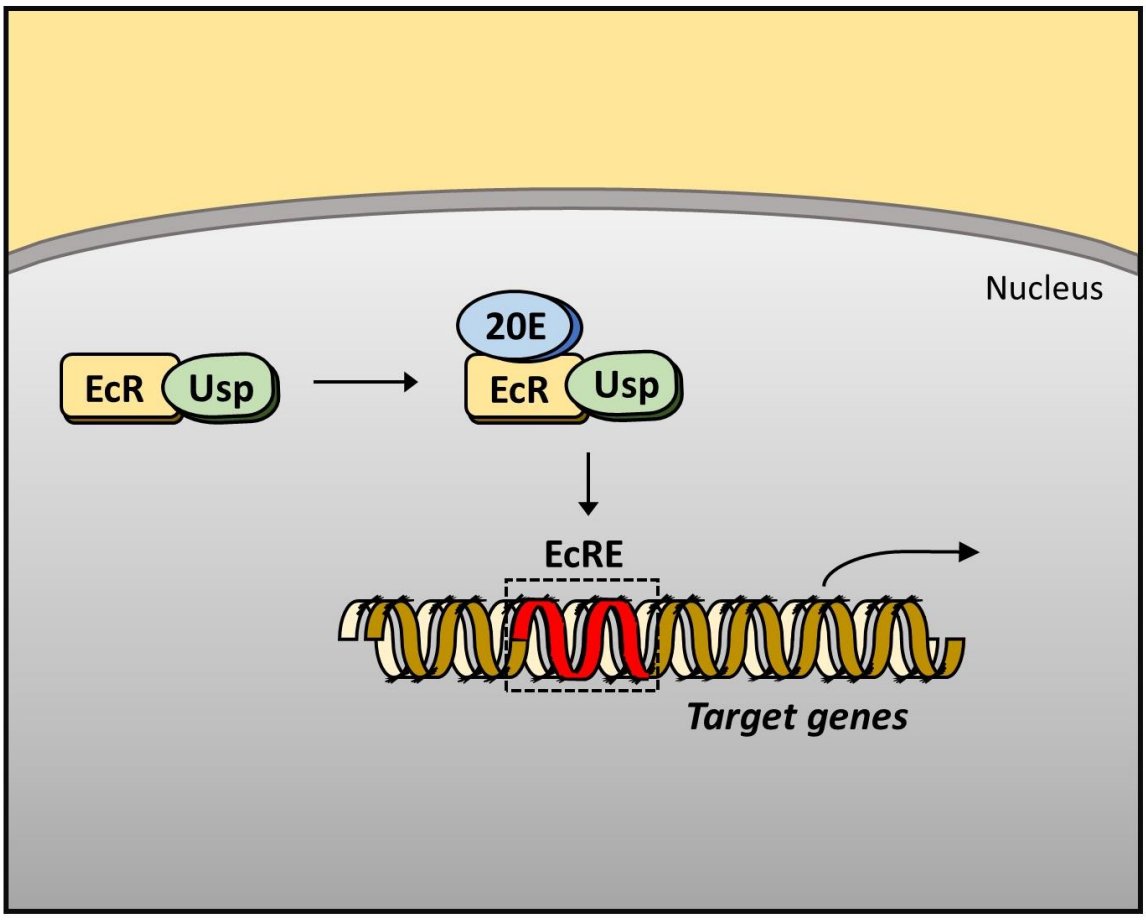


**Figure 1.3.5 A schematic of canonical ecdysone signaling.**

Upon binding of 20E, EcR and Usp heterodimers become activated binds to EcREs regulatory regions in the genome to drive target gene expression.

## 1.4. Objectives

As before mentioned, canonical ecdysone signaling involves the formation of a heterodimeric transcription factor complex consisting of EcR and Usp (Thummel, 1995). In the presence of ecdysone, EcR-Usp complex is stabilized and binds to EcREs within the genome to promote the expression of downstream genes (Cherbas et al., 1991; Riddiford et al., 2001). Ecdysone signaling is required for late embryonic development, as DC defects are observed in mutants for the Halloween genes, *spo* and *dib*, which encode for enzymes in the biosynthetic pathway that produces 20E (Chavez et al., 2000; Giesen et al., 2003; Kozlova and Thummel, 2003). Previous work in the lab has shown that *zip* transcript levels are reduced in the AS of both *spo* and *dib* mutant embryos (Figure 1.4.1), thus indicating that actomyosin contractility is disrupted (Chen, 2014). To confirm these results, dominant negative forms of EcR, which compete with endogenous EcR for Usp binding, were expressed during DC (Chen, 2014). As formation of the functional transcription factor complex is blocked even in the presence of ecdysone, *zip* expression was expected to be inhibited, similar to what is observed in *spo* and *dib* mutants. However, *zip* transcript levels remained unaffected (Figure 1.4.2), indicating that ecdysone does not regulate the expression of *zip* through the canonical signaling pathway.

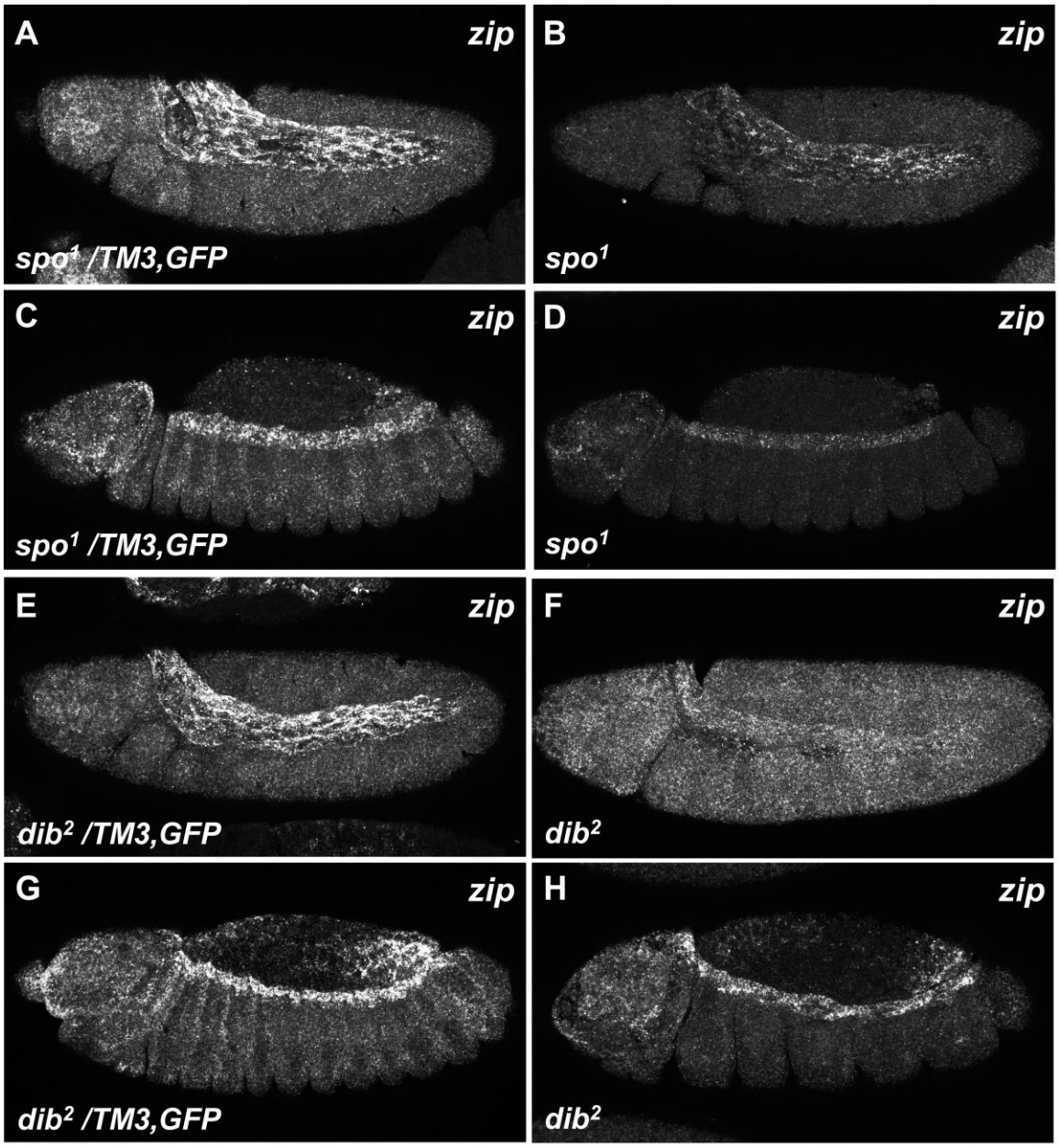


**Figure 1.4.1 Ecdysone signaling negatively regulates *zip* expression.**

FISH against *zip* on early GBR- and mid DC-staged embryos. (A,C) Embryos heterozygous mutant for *spo*$^{1}$, which served as a wild-type control, displayed typical *zip* transcript distributions during early GBR (A) and mid DC (C). (B,D) Homozygous mutant embryos showed a considerable loss of *zip* transcripts in the AS during early GBR (B), but only a slight reduction in the DME cells during DC (D). (E-H) Similar results were observed between *dib*$^{2}$ and *spo*$^{1}$ mutant embryos.

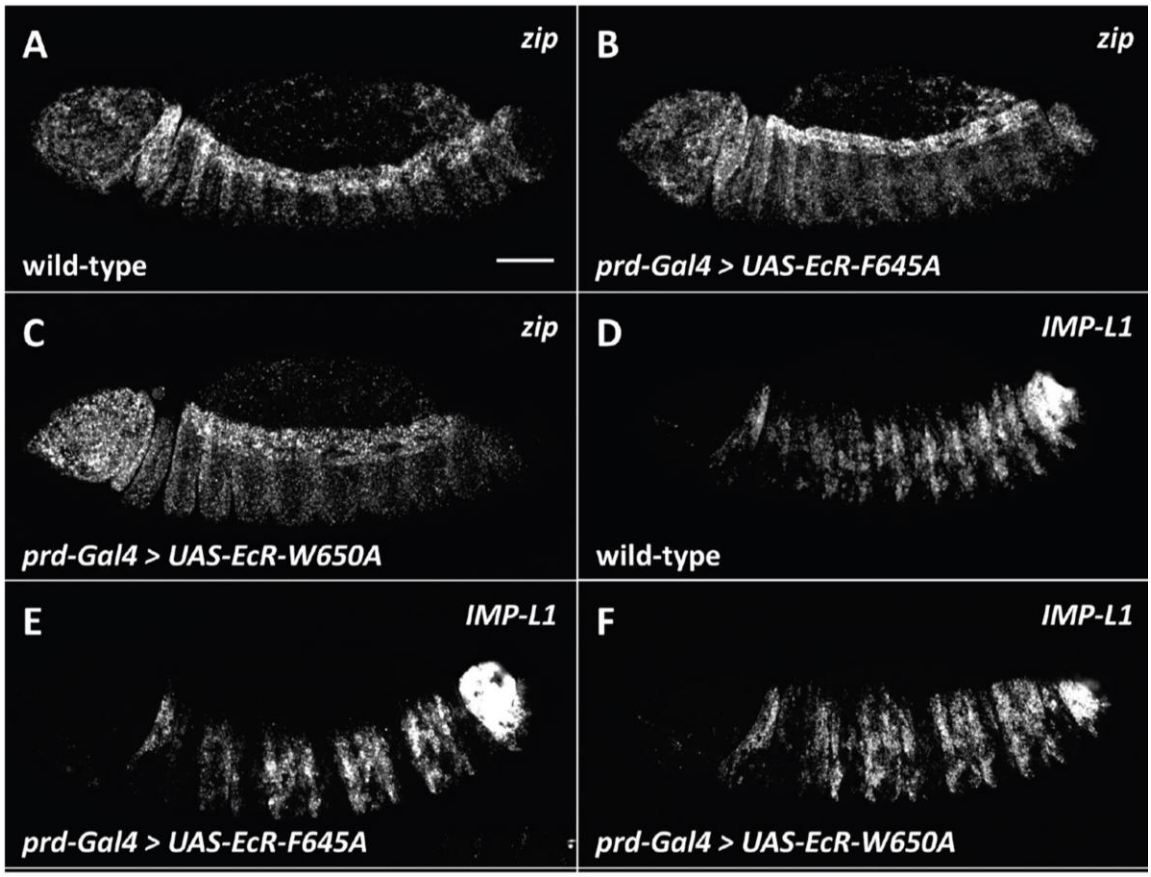


**Figure 1.4.2 Expression of EcR$^{DN}$ has no effects on *zip* transcript levels.**

FISH against *zip* and *IMP-L1* on DC-staged embryos. (A) Wild-type embryo displaying typical *zip* distribution. (B,C) Expression of dominant negative EcR (carrying either the F645A or W650A substitution) with the segmental *prd-Gal4* driver showed no effect on *zip* transcript levels. (D) Wild-type embryo displaying typical *IMP-L1* distribution. The *IMP-L1* locus is known to contain EcREs. (E,F) Expression of dominant negative EcR showed a loss of *IMP-L1* transcripts in prd[+] stripes. These images were modified from Chen, 2014.

An interesting alternative is that ecdysone-activated EcR can instead interact with the AP-1 transcription factor. In mammalian studies, there is evidence that the estrogen receptor, ERβ, a steroid nuclear receptor similar to EcR, can regulate gene expression in cooperation with AP-1 (Kushner et al., 2000; Teurich and Angel, 1995; Zhao et al., 2010). In MCF7 breast cancer cells, ChIP analysis revealed that the genomic region bound by ERβ also contained AP-1 binding sites that can bound by the AP-1 components, c-Jun and c-Fos. Remarkably, a study mapping EcR-binding regions in 20E-treated *Drosophila* Kc167 cells identified sites, including one within the *zip* locus, that contained consensus

AP-1 binding sequences but no EcREs (Gauhar et al., 2009). The purpose of this study is to provide further evidence that non-canonical ecdysone signaling, in the form of EcR and AP-1 cooperation, regulates the expression of DC-related genes, such as *zip*, during late embryonic development.

### 1.4.1. Part I: Provide genetic and molecular evidence for the EcR-Jun complex

The first part of this study will be to genetically and molecularly characterize the interaction of EcR and Jun (a component of the AP-1 transcription factor). Past work has shown that ecdysone and JNK signaling are required for the expression of *zip* during GBR and DC (Chen, 2014; Zahedi et al., 2008). However, interaction amongst the two pathways in this process has never been extensively studied. Interestingly, an interaction between JNK and hormone signaling has been reported in mouse eyelid closure (Sanchis et al., 2010). In this study, the glucocorticoid receptor (GR), which is a steroid hormone receptor, regulates closure through a mechanism involving GR binding to AP-1.

To determine whether EcR and Jun cooperate to regulate *zip* expression, epistatic analysis was performed. This was accomplished by assessing *zip* transcript levels in *jun* mutant embryos treated with exogenous 20E. If ecdysone-activated EcR and Jun function independently of each other, then exposure to exogenous 20E should still result in elevated *zip* transcript levels in embryos lacking Jun, similar to what has previously been observed with 20E-treated wild-type embryos (see Figure 3.1.3 A,B) (Chen, 2014).

Complex formation between EcR and Jun has previously been shown in our lab via proximity ligation assay (PLA) (Chen, 2014). PLA is a technique used to detect *in vivo* associations between endogenous proteins that are in close proximity (*i.e.* within 40nm) to each other (Söderberg et al., 2006). In wild-type embryos, PLA signal between EcR and Jun was observed in both the nuclei and cytoplasm of AS and DME cells during DC (Figure 1.4.3 A-A”). Strikingly, the PLA signal was reduced in *zip* deficient embryos (Figure 1.4.3 B-B”), suggesting that EcR and Jun form a complex at the *zip* locus to possibly drive its expression. Here, further work was carried out to molecularly characterize this EcR-Jun complex. In order to determine if EcR and Jun can directly bind to each other, pull-down assays involving bacterially expressed tagged constructs were performed. Chromatin

immunoprecipitations (ChIPs) were also be done to assess whether EcR and Jun can actually bind to the *zip* locus.

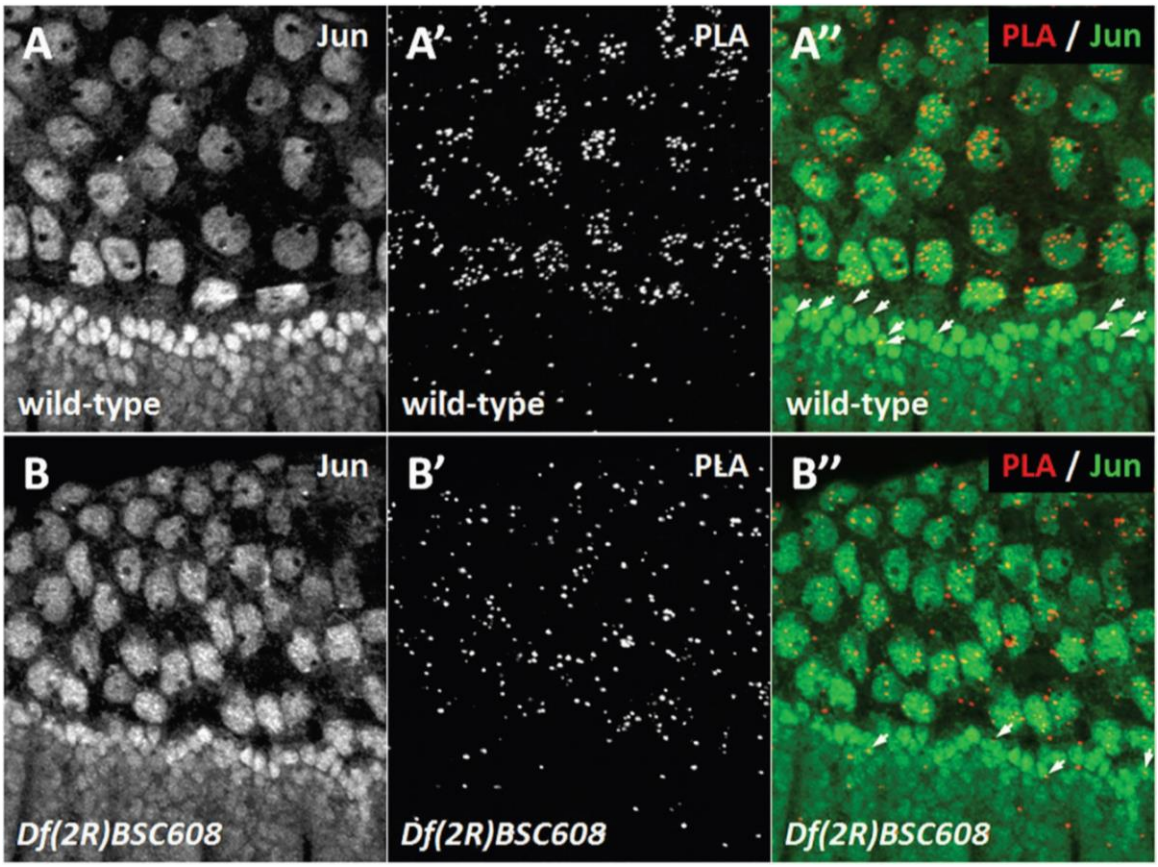


**Figure 1.4.3 EcR and Jun form a complex at the *zip* gene in AS and DME cell nuclei.**

PLA between EcR and Jun on DC-staged embryos. (A) Jun immunostain on a wild-type embryo. (A',A'') PLA signal, in the form of puncta, indicates complex formation between Jun and EcR (A'), which mostly localizes within AS cell nuclei (A''). Lower levels are also be observed in DME cell nuclei (A'', white arrows). (B) Jun immunostain on a *zip* deficient embryo. (B',B'') PLA puncta levels are significantly reduced in both AS and DME (white arrows) cell nuclei. Note that some PLA signal still remains even in the absence of the *zip* locus. These images were modified from Chen, 2014.

### 1.4.2. Part II: Identify other DC-related genes regulated by the EcR-Jun complex

The second part of this study will be to investigate whether the EcR-Jun complex can regulate the expression of other DC-related genes. As mentioned above, a study that mapped EcR-binding sites in *Drosophila* Kc167 cells identified a region within the *zip* locus that contained consensus AP-1 binding sites but no EcREs (Gauhar et al., 2009). Through a bioinformatics screen, our lab has identified at least 49 other similar regions throughout the genome, some of which are nearby known or presumed (based on cellular function) DC genes (Chen, 2014; Kim, 2017). PLA between EcR and Jun on *zip* deficient embryos, discussed above, strongly indicates that EcR-Jun complexes are binding to other genomic regions in addition to the *zip* locus (Chen, 2014). This is because the PLA signal was only reduced, not eliminated, in the AS and DME cell nuclei of *zip* deficient embryos (see Figure 1.4.3), which means other binding sites are still present.

Investigation of only the DC-related candidate genes was done to determine if their expressions are also controlled by the EcR-Jun complex during late embryogenesis, similar to *zip*. Fluorescent *in situ* hybridization (FISH) against each candidate was performed on wild-type embryos in order to observe their transcript distributions during GBR and DC. Expression patterns similar to *zip* were sought after, as this may indicate that the genes are regulated by a similar mechanism. The expression of promising candidates were then assessed in *spo*, *dib* and *jun* mutant embryos. For candidates whose expressions are determined to be dependent on both ecdysone and JNK signaling, epistatic analysis, as described in the previous section, was performed.

### 1.4.3. Part III: Determine if one of the candidates, RhoGAP71E, supresses Rho1 activity during DC

Lastly, one of the candidates analyzed in this project is RhoGAP71E. It has earlier been reported that RhoGAP71E is required for ventral furrow formation, where it apically localizes with myosin in ventral furrow cells (Mason et al., 2016). However, little is known about RhoGAP71E function regarding epithelial morphogenesis during DC (Greenberg and Hatini, 2011). Rho1 is required for myosin activity during DC and wound repair (Abreu-Blanco et al., 2014; Harden, 2002; Harden et al., 1999). Previous results in the lab have shown that over-expression of Rho1 during DC causes ectopic *zip* expression, which

leads to morphological defects due to excessive contraction (Kim, 2017). The role of the diffusible ligand Fog, a well-known activator of the Rho1 actomyosin contractility pathway during gastrulation (Barrett et al., 1997; Costa et al., 1994; Dawes-Hoang et al., 2005) was also assessed. It was demonstrated that overexpression of Fog caused elevated levels of *zip* in the DME cells during DC, which led to assessments of known downstream components of the Fog pathway such as GTPase Rho1 and RhoGEF2. Mutation of RhoGEF2 led to a decrease in *zip* levels suggesting RhoGEF2 has a role in activating Rho1 that is upstream of the JNK pathway during DC. (Kim, 2017)(Figure 1.3.2).

As mentioned before, Rho1 regulation during DC is not fully understood. Thus, it is worthwhile to investigate if RhoGAP71E can serve as a GAP to modulate Rho1 activation. To accomplish this, RhoGAP71E was over-expressed with Rho1 during DC. If RhoGAP71E does indeed function as a Rho1 GAP, then RhoGAP71E will be able to block Rho1 over-expression phenotypes.

# Chapter 2. Materials and Methods

## 2.1. Fly stocks and crosses

Flies were maintained under standard conditions at 25°C (Ranz et al., 2007). $w^{1118}$ served as a wild-type control unless otherwise stated. The following stocks were ordered from the Bloomington *Drosophila* Stock Center (Indiana University): $w^{1118}$ (3605); $spo^{1}$ (3276); $dib^{2}$ (2776); *Df(2R)BSC303* (23686); $jun^{76\text{-}19}$ (9880); $jun^{lA109}$ (3273); *c381-Gal4* (3734); *prd-Gal4* (1947); *UAS-kay*$^{DN}$ (7215); *UAS-ecr* (6469); *UAS-rho1* (28872, 58819); *TM3/TM6B* (2537); *Gla/CyO, twi-Gal4, UAS-GFP* (6662); and *Dr/TM3, twi-Gal4, UAS-GFP* (6663). *UAS-rhogap71e* ORF lines (F001171 and F001319) were obtained from FlyORF (University of Zurich) (Bischof et al., 2013).

For mutant analyses, homozygous mutant lethal lines were re-balanced over GFP-containing balancers so that homozygous mutant embryos (GFP-negative) could be distinguished from heterozygous mutant embryos (GFP-positive). Genotypes were identified by immunostaining the embryos for GFP and viewing them under confocal fluorescent microscopy. Heterozygous mutant embryos were often used as the "wild-type" control for experiments, as opposed to a separate wild-type control done in parallel, since they were treated in the same tube under identical conditions as their homozygous mutant siblings. For transgenic analyses, homozygous *Gal4*-bearing virgin females were crossed to homozygous *UAS*-transgenic males to ensure that all F1 progeny contained one copy of both. A separate wild-type control done in parallel was used for comparison. In cases where either the *Gal4* or *UAS*-transgenic stock was homozygous lethal, the stock was also re-balanced over a GFP-containing balancer. In subsequent crosses, GFP-negative embryos carried both the *Gal4* and *UAS*-transgene, whereas GFP-positive embryos, which served as an internal control, lacked either the *Gal4* or *UAS*-transgene and, therefore, had no transgenic expression.

Recombination:

Recombination between *UAS-rho1* (BDSC, 2882) and *UAS-rhogap71e* (FlyORF, F001171) was accomplished by using standard methods (Roote and Prokop, 2013) (see Appendix A for the genetic flow scheme). First, *UAS-rhogap71e* homozygous males were crossed to *UAS-rho1* homozygous virgin females (cross one), ensuring that all F1 progeny

carried one copy of each transgene. Resulting F1 virgin females were then collected and crossed to a *TM3/TM6B* balancer stock (cross two). Female meiotic recombination was expected to generate the following gametes: 1.) +, + (recombinant chromosome); 2.) *UAS-rho1,* + (parental chromosome); 3.) +, *UAS-rhogap71e* (parental chromosome); and 4.) *UAS-rho1, UAS-rhogap71e* (desired recombinant chromosome). From the F1 progeny of cross two, single males balanced with either *TM3* or *TM6B* were individually crossed back to *TM3/TM6B* (cross three). Only ten crosses were set up as it was assumed that the transgenes were not linked and that a 50% recombination frequency would be achieved. In addition, both transgenes are marked with the *mini-white* (*mw+*) gene, which confers eye colour. Thus, F1 males from cross two that had darker eye colours were purposefully chosen as they were more likely to carry two copies of *mw+*, and consequently both transgenes. For each male that was crossed to *TM3/TM6B* (*i.e.* cross three), brother-sister crosses from the F1 progeny (cross four) were done to generate a stable stock. To determine if a stock contained both transgenes, males were first crossed to *prd-Gal4* virgin females. Embryos were then collected (see section 2.5) and FISH (see section 2.8) against *rho1* and *rhogap71e* transcripts were performed in parallel. Stocks that carried both transgenes were identified when both stains showed elevation of FISH signal in prd[+] stripes when viewed under fluorescent microscopy.

## 2.2. cDNAs

All cDNA clones were ordered from the *Drosophila* Genomics Research Center (Indiana University): *cbt* (RE07124), *ecr* (RE06878), *jar* (FI18104), *jun* (LD25202), *jupiter* (GH10365), *kay* (LP01201), *mes2* (SD09884), *rho1* (LD03419), *rhogap71e* (LD04071), *step* (RE34385), *ush* (LD12631), *usp* (LD09973), *zasp52* (RH03424), and *zip* (LD21871). Each clone was received as DNA on a Whatman FTA disc in a microcentrifuge tube. The following steps were done using sterile technique. The disc was first washed by adding 50µL of **Tris-EDTA (TE)** to the tube, quickly pipetting up and down twice, then immediately discarding the buffer. 50µL of DH5α competent cells (Invitrogen, 18265-017) were next added to the disc and the tube was incubated on ice for 30 minutes. Following heat shock at 37°C for 2 minutes, the cells were transferred into a new microcentrifuge tube containing 1mL of **Super Optimal broth with Catabolite repression (SOC)** and incubated at 37°C with shaking for one hour. The entire transformation mix was then plated onto multiple **Lysogeny Broth (LB) agar** plates with the appropriate antibiotics (see Appendix B for

more information). Resulting single colonies were individually liquid cultured in 3mL of **LB** with the appropriate antibiotics at 37°C with shaking for 16-18 hours. Plasmid DNA was extracted with the QIAprep Spin Miniprep Kit (QIAGEN, 27106), and the concentration and purity of the preps were measured with a NanoDrop. The preps were further verified through test digestions and checking for the correct banding pattern via agarose gel analysis (see Appendix B for more information). Confirmed plasmid DNA were stored at -20°C until ready to be used.

**Tris-EDTA (TE):** 10mM Tris, 1mM EDTA, pH 8.0. Autoclave.

**Super Optimal Broth with Catabolite Repression (SOC):** 20g/L Tryptone, 5g/L Yeast Extract, 2.5mM KCl, 10mM $MgCl_2$, 10mM $MgSO_4$, 10mM NaCl, 20mM Glucose [*], pH 7.5. Autoclave. [*] Cool to 55°C before adding filter sterilized glucose. Store at 4°C.

**Lysogeny Broth (LB) Agar:** 10g/L Tryptone, 5g/L Yeast Extract, 10g/L NaCl, 15g/L Agar. Autoclave. Cool to 55°C before adding the desired antibiotic: 50mg/L Ampicillin, 85mg/L Chloramphenicol, or 25mg/L Kanamycin. Pour into 100x15mm petri dishes. Store at 4°C.

**Lysogeny Broth (LB):** 10g/L Tryptone, 5g/L Yeast Extract, 10g/L NaCl. Autoclave. Store at 4°C. Before use, add the desired antibiotic: 50mg/L Ampicillin, 85mg/L Chloramphenicol, or 25mg/L Kanamycin.

## 2.3. RNA probe synthesis

cDNA derived from our genes of interest (see section 2.2) were previously inserted within the multiple cloning sites of different vectors (Rubin et al., 2000; Stapleton et al., 2002), and by consequence are flanked on both sides by a combination of two out of three possible RNA polymerase promoters: SP6, T3, and T7. In order to make a Digoxigenin-labeled, antisense RNA probe, the vector was first linearized at the 5' end of the coding strand of the cDNA insert with a restriction enzyme that leaves a 5' or blunt overhang (see Appendix B for more information). The reaction composition (100µL total volume) was as follows: 1-5µg of plasmid DNA, 3µL of FastDigest restriction enzyme (Thermo Fisher Scientific), 10µL of 10X FastDigest Buffer. After incubating the digest at 37°C for one hour, the linearized vector was purified using the QIAquik PCR Purification Kit (QIAGEN, 28106). The purified, linearized vector was next used as a template for RNA synthesis, using the promoter at the 3' end of the coding strand of the cDNA insert (see Appendix B

for more information), with the reaction composition (40µL total volume) consisting of the following: 0.5-2.5µg of linearized template DNA, 4µL of RNA polymerase (Roche), 4µL of DIG labeling mix (Roche, 11277073910), 2µL of RNase inhibitor (Roche, 03335399001), 4µL of 10X supplied buffer. Synthesis was performed at 37°C for four hours, then the probe was purified with an illustra MicroSpin S-200 HR Column (GE Healthcare Life Sciences, 27-5120-01). Finally, the concentration and purity was measured with a NanoDrop, and the integrity was checked by agarose gel analysis. Confirmed probes were stored at -80°C until ready to be used.

## 2.4. Antibodies

The following primary antibodies were used for immunostains: 1:5 mouse anti-EcR (Developmental Studies Hybridoma Bank, DDA2.7); 1:25 rabbit anti-Jun (Santa Cruz Biotechnology, sc-25763); 1:250 mouse anti-phospho-tyrosine (Cell Signaling, 9411); and 1:100 rabbit anti-GFP (Sigma-Aldrich, G1544). In order to detect the primaries via confocal microscopy, the following fluorophore-conjugated secondary antibodies were used at a 1:200 dilution: Fluorescein-labeled horse anti-mouse (Vector Laboratories, FI-2100); Fluorescein-labeled goat anti-rabbit (Vector, FI-1000); Texas Red-labeled horse anti-mouse (Vector, TI-2000); and Cy3-labeled donkey anti-rabbit (Jackson ImmunoResearch, 711-165-152). All antibodies were diluted with 1% BSA.

For immunoblots, 1:150 mouse anti-EcR (DSHB, DDA2.7) and 1:1000 rabbit anti-Jun (SCBT, sc-25763) were used for primaries. Horseradish peroxidase-conjugated horse anti-mouse (Vector, PI-2000) and donkey anti-rabbit (JIR, 711-035-152) antibodies were used at a 1:2000 dilution for secondaries. All antibodies were diluted with 1% milk.

## 2.5. Embryo collection and fixation

Embryo collection and fixation were performed as previously described (Rothwell and Sullivan, 2007a; Rothwell and Sullivan, 2007b; Rothwell and Sullivan, 2007c), but with some modifications. Experiments and their controls were always collected at the same time and treated under identical conditions. Cages consisted of a 100mL tri-cornered plastic beaker with several pinholes poked in for air circulation, and a 60x15mm petri dish to enclose the opening of the beaker. The petri dish contained **grape juice agar** with a dollop of **yeast paste** on top to encourage egg laying. Approximately 300 flies were placed

in each cage and were allowed to lay eggs on the agar for approximately 16 hours at 25°C unless otherwise stated. The embryos, which ranged in age from 0-16 hours after egg laying (AEL), were brushed off the plate and into a collecting basket (described in Rothwell and Sullivan, 2007a) with the aid of a fine paint brush and 0.01% Triton X-100. To remove the outer egg shells, the embryos were dechorionated by soaking the basket in **50% bleach** for 3.5 minutes. The basket was then soaked in 0.01% Triton X-100 three times for three minutes each to wash off the bleach. To remove the vitelline membrane, the embryos were next transferred from the mesh of the collecting basket to a 20mL scintillation vial that contained a biphasic devitellinization mixture consisting of 5mL of **4% paraformaldehyde (PFA)** (bottom aqueous layer) and 5mL of heptane (top organic layer). After vigorously shaking the vial for 25 minutes, the bottom aqueous layer was removed and replaced with 5mL of methanol. Upon shaking the vial again for one minute, properly devitellinized embryos will sink from the interphase into the bottom methanol layer, thus allowing the top heptane layer, along with any non-devitellinized embryos at the interphase, to be removed. Multiple rinses with methanol were then performed to ensure that all residual heptane was removed. Finally, with wide-bore tips, the embryos were transferred into a microcentrifuge tube containing fresh methanol, and stored at -20°C until ready to be used.

**Grape Juice Agar:** 25g/L Sugar, 22.5g/L Agar, 1.5g/L Tegosept [*], 25% Welch's Grape Juice [*]. Autoclave. [*] Cool to 55°C before adding the mold inhibitor and juice. Pour into 60x15mm petri dishes. Store at 4°C.

**Yeast Paste:** 50% White Vinegar, 50% Water, Active Dry Yeast [*]. [*] Continuously add yeast while stirring until a peanut butter consistency is achieved. Store at 4°C.

**50% Bleach:** 50% Clorox Bleach, 50% 0.01% Triton X-100. Make fresh each time.

**4% Paraformaldehyde (PFA):** 4% PFA, 1mM NaOH, 1X PBS (pH 7.0) [*]. [*] Dissolve PFA in deionized water with NaOH at 65°C before adding buffer. Make fresh each time.

**10X Phosphate Buffered Saline (PBS):** 3mM $NaH_2PO_4 \cdot H_2O$, 7mM $Na_2PO_4$, 1.3M NaCl, pH 7.0. Autoclave.

## 2.6. 20-hydroxyecdysone treatment of embryos

20-hydroxyecdysone (20E) treatment of stage 11-15 embryos was performed as previously described (Kozlova and Thummel, 2003). Flies were placed into cages (see section 2.5) and were allowed to lay eggs for 6 hours at 25°C. The embryos, which ranged in age from 0-6 hours AEL, were then transferred into a collecting basket with a fine paint brush and deionized water. To dechorionate the embryos, the collecting basket was first soaked in **50% bleach** for three-and-a-half minutes, then in deionized water three times for three minutes each. The embryos were next transferred from the mesh of the collecting basket into a scintillation vial containing 6mL of heptane and 2mL of **Modified Basic Incubation Medium (MBIM)** with **$5x10^{-6}$M 20-Hydroxyecdysone (20E)**. After swirling the vial gently to permeabilize the embryos, the heptane layer was completely removed and an additional 2mL of MBIM with $5x10^{-6}$M 20E was added to the vial. The embryos were transferred back into the collection basket and soaked in MBIM with $5x10^{-6}$M 20E at 25°C for 4 hours, using a humidity chamber to prevent evaporation. Note that half of the dechorionated embryos were used for the negative control, which was done in parallel under similar treatment, where all steps involving 20E was replaced with an equal volume of 100% ethanol. Upon completion of the incubation, the embryos were washed three times with 0.01% Triton X-100 for three minutes each, then fixed (see section 2.5). The fixed embryos were subsequently stored at -20°C until ready to be used.

**50% Bleach:** 50% Clorox Bleach, 50% Deionized Water. Make fresh each time.

**Modified Basic Incubation Medium (MBIM):** 10.82mM $MgCl_2$, 14.6mM $MgSO_4$ [*], 3.5mM $NaH_2PO_4$ [*], 82.2mM Glutamic acid [*], 80.6mM Glycine [*], 5mM Malic acid [*], 0.33mM Sodium acetate, 12.2mM Glucose [*], 8.92mM $CaCl_2 \cdot 2H_2O$, pH 6.8. Adjust pH using a 1:1 mixture of 5% NaOH and 5% KOH. Filter sterilize. [*] Reagents must be tissue culture grade.

**$5x10^{-6}$M 20-Hydroxyecdysone (20E):** Dissolve 5mg of 20E (Sigma-Aldrich, H5142) in 1.075mL of 100% ethanol (2000X stock). Store at -20°C. Dilute 1:2000 in MBIM for use.

## 2.7. Larval salivary gland dissection

Dissection of salivary glands from crawling third instar larvae was performed as previously described (Kennison, 2008).

## 2.8. Fluorescent *in situ* hybridization

Fluorescent *in situ* hybridization (FISH) was performed as previously described (Lécuyer et al., 2008), but with modifications. Experiments and their controls were always done at the same time under identical conditions. Unless stated otherwise, all incubations and washes were done at room temperature, and with agitation. All buffers and reagents were sterile and RNase-free.

Fixed embryos (see sections 2.5 and 2.6) were rehydrated by rinsing once with methanol, once with 1:1 methanol:PBTween, and twice with **Phosphate Buffered saline with Tween (PBTween)**. The embryos were then post-fixed with **4% PFA** for 20 minutes, followed by three PBTween washes for two minutes each. After incubating with **3µg/mL Proteinase K** for two minutes, the embryos were left to sit on ice for one hour to increase tissue permeability. Protease activity was stopped by washing the embryos twice with **2mg/mL glycine** for two minutes each, then twice with PBTween for two minutes each. The embryos were post-fixed a second time for 20 minutes in 4% PFA, followed by five PBTween washes for two minutes each. The embryos were next rinsed once in 1:1 PBTween:hybridization solution, and once in **hybridization solution** alone. In the meantime, a pre-hybridization solution, which served as the block, was prepared by boiling fresh hybridization solution for five minutes, then cooling it on ice for at least five minutes. After removing the hybridization solution rinse from the embryos, the prepared block solution was added to the embryos and incubated at 56°C for two hours. During the incubation, the Digoxigenin-labeled, RNA antisense probe was prepared as follows: 400ng of probe (see section 2.3) was added to 200µL of hybridization solution, heated at 80°C for three minutes, then cooled on ice for at least five minutes. After the blocking solution was removed, the embryos were incubated with the RNA probe solution at 56°C overnight without agitation.

The following day, the RNA probe solution was removed and the embryos were rinsed once in pre-warmed hybridization solution, and then washed in fresh pre-warmed

hybridization solution for 20 minutes at 56°C. The embryos were subsequently washed in pre-warmed 3:1, 1:1, and 1:3 mixtures of hybridization solution:PBTween for 15 minutes each at 56°C. The embryos were further washed in pre-warmed PBTween three times at 56°C for 15 minutes each, and one time at room temperature for an additional 15 minutes. After the washes, the embryos were blocked in **3% Bovine Serum Albumin (BSA)** for ten minutes, then incubated with a 1:200 dilution of POD-conjugated sheep anti-DIG antibody (Sigma Aldrich, 11207733910) in 3% BSA for 2 hours. Following three PBTween washes for ten minutes each and three **Phosphate Buffered Saline (PBS)** washes for five minutes each, the embryos were incubated with a 1:50 dilution of Cy3-labeled tyramide (Perkin Elmer Life Sciences, SAT705A) in the supplied amplification buffer at 4°C overnight. The embryos were kept in the dark for the remainder of the protocol to reduce photobleaching.

The following day, the tyramide solution was discarded and the embryos were blocked in 3% BSA twice for five minutes each. The embryos were next incubated with other desired primary antibodies (see section 2.4) that were diluted in 3% BSA for 2 hours, followed by three washes with 3% BSA for ten minutes each. Appropriate secondary antibodies (see section 2.4) diluted in 3% BSA were then added to the embryos and incubated for two hours. Following three final washes with PBS for 10 minutes each, the embryos were equilibrated in VECTASHIELD Mounting Medium (Vector Laboratories, H-1000) at 4°C overnight. The embryos were then mounted onto platform slides, and stored at -20°C until ready for imaging.

Images of stage 11-15 embryos were taken as merged z-stacks on a Nikon A1R laser scanning confocal microscope with NIS-Elements software. Experiments and their controls were always imaged in one sitting under identical acquisition settings. All images were subsequently processed with Adobe Photoshop.

**Phosphate Buffered Saline with Tween (PBTween):** 1X PBS (pH 7.0), 0.1% Tween 20.

**4% Paraformaldehyde (PFA):** 4% PFA, 1mM NaOH, 1X PBS (pH 7.0) [*], 0.1% Tween 20 [*]. [*] Dissolve PFA in RNase-free water with NaOH at 65°C before adding buffer and detergent. Make fresh each time.

**3µg/mL Proteinase K:** Dissolve 3mg of Proteinase K (Sigma-Aldrich, P6556) in 1mL of RNase-free water (1000X stock). Store at -20°C. Dilute 1:1000 in PBTween for use.

**2mg/mL Glycine:** Dissolve 1g of glycine in 50mL of PBTween (10X stock). Filter sterilize. Store at -20°C. Dilute 1:10 in PBTween for use.

**Hybridization Solution:** 50% Formamide, 4X SSC, 1X Denhardt's Reagent, 0.1% Tween 20, 5% Dextran sulfate (Sigma-Aldrich, D4911), 250µg/mL Salmon Sperm DNA, 50µg/mL Heparin. Filter sterilize. Store at -20°C.

**20X Saline-Sodium Citrate (SSC):** 3M NaCl, 0.3M Sodium citrate, pH 7.0. Autoclave.

**50X Denhardt's Reagent:** 1% BSA, 1% Ficoll 400, 1% Polyvinylpyrrolidone (Sigma-Aldrich, PVP10). Filter sterilize. Store at -20°C.

**3% Bovine Serum Albumin (BSA):** 3% BSA in PBTween. Filter sterilize. Store at 4°C.

**10X Phosphate Buffered Saline (PBS):** 3mM $NaH_2PO_4 \cdot H_2O$, 7mM $Na_2PO_4$, 1.3M NaCl, pH 7.0. Autoclave. Dilute 1:10 in RNase-free water for use.

## 2.9. Quantifications

### 2.9.1. FISH signal in the AS

Expression levels in the AS were quantified by counting the number of pixels that made up fluorescent signals derived from FISH. For each embryo, the z-stacked confocal image (see section 2.8) was first converted to grayscale with Adobe Photoshop. The AS was next hand-selected with the Lasso tool, and the surface area of the tissue was measured as pixel area. The selection was then copied and pasted into a new file, and opened under ImageJ. The selection was inverted and the threshold was adjusted to create a black and white image, where black represented the FISH signal and white represented the background. The FISH signal was then measured as the total number of black pixels. To standardize the measurement between embryos, the number of black pixels was divided by the pixel area of the AS (ratio). For each experiment, measurements were performed with a sample size of at least three embryos per genotype per embryonic stage. Data were expressed as absolute values, and presented as "mean of the ratios $\pm$ sem". Student's t-tests were performed for all statistical comparisons using GraphPad. Note that the parameters used for quantification were kept constant within data sets.

### 2.9.2. FISH intensity in the DME cells

Expression levels in the DME cells were quantified by measuring the intensities of fluorescent signals derived from FISH. For each embryo, the z-stacked confocal image (see section 2.8) was first converted to grayscale with Adobe Photoshop. A section of leading edge epidermis corresponding to one embryonic segment was next selected using the Rectangular Marquee tool with a fixed selection size. The fluorescence intensity of the FISH signal was then measured as mean gray value. For each experiment, measurements were performed with a minimum sample size of 35 leading edge segments from five embryos (*i.e.* seven segments per embryo) per genotype per embryonic stage. Data were expressed as absolute values, and presented as "mean $\pm$ sem". Student's t-tests were performed for all statistical comparisons using GraphPad. Note that the parameters used for quantification were kept constant within data sets.

### 2.9.3. FISH intensity for 20E-treated embryos

Expression levels in the AS and DME cells of 20E-treated embryos were quantified by measuring the intensities of fluorescent signals derived from FISH. For each embryo, the z-stacked confocal image (see section 2.8) was first converted to grayscale with Adobe Photoshop. Neighbouring regions of peripheral AS tissue and leading edge epidermis corresponding to one embryonic segment were next selected using the Rectangular Marquee tool with a fixed selection size. The fluorescence intensities of the FISH signal were then measured as mean gray value. To standardize the measurements between embryos, the intensities were divided by the intensity of a region of ventral epidermis that was not affected by 20E-treatment (ratios). Expression levels were also measured for ethanol-treated embryos, which served as a negative control. For each experiment, measurements were performed with a minimum sample size of 15 per genotype per embryonic stage per treatment. Data were expressed as absolute values, and presented as "mean of the ratios $\pm$ sem". Student's t-tests were performed for all statistical comparisons using GraphPad. Note that the parameters used for quantification were kept constant within data sets.

## 2.10. Immunohistochemistry

Immunostaining of embryos and third instar larval salivary glands were performed as previously described (Muller, 2008), but with some modifications. Experiments and their controls were always done at the same time under identical conditions. All steps were performed at room temperature and with rotation unless otherwise stated.

Fixed embryos (see section 2.5) and larval salivary glands (see section 2.7) were immunostained using the same protocol. Samples were first washed with **Phosphate Buffered saline with Triton (PBT)** three times for ten minutes each, then blocked with **1% BSA** for one hour. The samples were next incubated with primary antibodies (see section 2.4) diluted in 1% BSA overnight at 4°C. Following three washes with PBT for ten minutes each, the samples were then incubated with the appropriate secondary antibodies (see section 2.4) diluted in 1% BSA for two hours. As the fluorophore-labeled secondaries are light sensitive, the samples were kept in the dark for the remainder of the protocol. After incubation with the secondary antibodies, the samples were washed with PBT three times for ten minutes each, then equilibrated with VECTASHIELD Mounting Medium (Vector Laboratories, H-1000) overnight at 4°C. The samples were mounted onto platform slides and stored at -20°C until ready for imaging.

Images were taken as merged stacks, unless otherwise stated, on a Nikon A1R laser scanning confocal microscope with NIS-Elements software. Experiments and their controls were always imaged in one sitting under identical acquisition settings. All images were subsequently processed with Adobe Photoshop.

**Phosphate Buffered Saline with Triton (PBT):** 1X PBS (pH 7.0), 0.1% Triton X-100.

**1% Bovine Serum Albumin (BSA):** 1% BSA in PBT. Store at 4°C.

**10X Phosphate Buffered Saline (PBS):** 3mM $NaH_2PO_4 \cdot H_2O$, 7mM $Na_2PO_4$, 1.3M NaCl, pH 7.0. Autoclave.

## 2.11. Cuticle Preparation

Cuticle preparations were performed as previously described (Stern and Sucena, 2011), but with some modifications. Experiments and their controls were always collected

at the same time and treated under identical conditions. Approximately 100 flies were placed in each cage (see section 2.5) and were allowed to lay eggs for 24 hours at 25°C. The plate was then removed and aged for an additional 48 hours at 25°C. All the progeny, which ranged in age from 48 to 72 hours AEL, were transferred into a collecting basket with the aid of a fine paint brush and 0.01% Triton X-100. To dechorionate the embryos, the collecting basket was first soaked in **50% bleach** for three-and-a-half minutes, then in 0.01% Triton X-100 three times for three minutes each. With a fine paint brush, all the progeny were carefully mounted onto slides with **Hoyer's Medium**. Weights were added on top of the coverslips to flatten the samples, and the slides were incubated at 65°C for three days or until all the soft tissue was digested leaving behind only cleared cuticle. Embryonic phenotypes were quantified on a Nikon TMS inverted microscope with a minimum sample size of 500 progeny. Representative phenotypes were imaged under phase contrast, and the images were processed using Adobe Photoshop.

**50% Bleach:** 50% Clorox Bleach, 50% 0.01% Triton X-100. Make fresh each time.

**Hoyer's Medium:** 30g Gum arabic (Sigma-Aldrich, G9752), 200g Chloral hydrate (Sigma-Aldrich, C8383), 16mL Glycerol. Dissolve gum arabic, then chloral hydrate, in 50mL of water before adding glycerol. Once completely dissolved, centrifuge at 12,000 x g for three hours. Pour into glass amber drop dispensing bottles, taking care not to transfer black precipitates that were pelleted after centrifugation.

## 2.12. Subcloning

The following cDNA clones (see section 2.2) were used in subcloning experiments: *usp* (LD09973) and *kay* (LP01201). Coding regions from the clones were inserted in frame into pGEX-4T-1 (GE Healthcare, 28-9545-49) and pET-28a(+) (MilliporeSigma, 69864-3) to create N-terminal, GST- and His-tagged constructs, respectively. Tagged constructs for *ecr* (RE06878) and *jun* (LD25202) were previously created by Ms. Hae-yoon Kim using similar methods described below (Kim, 2017).

The coding region from each clone was PCR amplified using the Phusion High-Fidelity PCR Kit (New England Biolabs, M0531S). Reactions consisted of the following: 100-200ng of template plasmid, 0.5µM forward and reverse primer, 200µM dNTPs, 1U polymerase, 1X supplied buffer. Forward and reverse primers were made by Invitrogen

(see Appendix C for primer sequences and additional information). The thermocycler settings were as follows: 30 seconds initial denaturation at 98°C, [10 seconds denaturation at 98°C, 30 seconds annealing at 45-72°C, 30 seconds per kb extension at 72°C] x30 cycles, 10 minutes final extension at 72°C. After amplification, the PCR products were purified using the QIAquick PCR Purification Kit, then digested with the appropriate restriction enzymes (see Appendix C for more information). The digest composition (100µL total volume) was as follows: 1-5µg of PCR product, 3µL of each FastDigest restriction enzyme (Thermo Fisher Scientific), 10µL of 10X FastDigest Buffer. Upon incubating the reactions at 37°C for two hours, the digested PCR products were purified using the QIAquick PCR Purification Kit. The purified, digested PCR products were next ligated into linearized pGEX-4T-1 and pET-28a(+) vectors with T4 DNA Ligase (Invitrogen, 15224017), using a 6:1 insert:vector molar ratio, at 16°C for 24 hours. The ligation reaction was then transformed into DH5$\alpha$ competent cells, and the entire transformation mix was plated onto LB agar with the appropriate antibiotics and incubated at 37°C overnight (see section 2.2 for protocol). Resulting single colonies were tested via PCR colony screening, and putative positive colonies were liquid cultured in 3mL of LB with the appropriate antibiotics at 37°C with shaking for 16-18 hours. Plasmid DNA was extracted using the QIAprep Spin Miniprep Kit, and the concentration and purity of the preps were measured with a NanoDrop. The preps were verified through test digestions by using the appropriate restriction enzymes and checking for the correct banding pattern via agarose gel analysis. Positive clones were further confirmed through sequencing using GENEWIZ (see Appendix C for a list of the sequencing primers used). Confirmed constructs were stored at -20°C until ready to be used.

## 2.13. Pull-down assay

Protein expression and extraction:

To express the GST- and His-tagged proteins, each construct was transformed into BL21(DE3) competent cells (New England Biolabs, C2527) as per the manufacturer's instructions (refer to section 2.2 for a similar protocol). Single colonies that grew on the LB agar plates were then inoculated in 10mL of LB with the appropriate antibiotics. Upon incubating with shaking at 37°C for 16-18 hours, the cultures were subcultured into 200mL of pre-warmed LB with the appropriate antibiotics and grown with shaking at 37°C. When

the optical density (OD) at 600nm was between 0.5-1.0, 100µL of 1M IPTG was added to induce protein expression, and the cultures were incubated with shaking at 4°C for an additional three hours. The cultures were then centrifuged at 1,400 x g at 4°C for 20 minutes. Bacterial pellets were stored at -80°C until ready to be used. Note that the above steps were done using sterile technique.

Each bacterial pellet was next completely resuspended in 15mL of either **Cold Buffer** (for GST-tagged proteins) or **Lysis Buffer** (for His-tagged proteins). For lysis, the bacterial cells were sonicated on ice with a Virsonic 100 Ultrasonic Cell Disruptor (Virtis) using the following protocol: three ten second pulses with 20 second rests in between, followed by a final 15 second pulse, all at power setting four. 1.5mL of 10% Triton X-100 was then added, and the bacterial lysate was incubated with rotation at 4°C for one hour. After a 20 minute centrifugation at 15,600 x g at 4°C, the supernatant fraction containing soluble proteins was kept and stored at -80°C until ready to be used.

Test pull-downs were conducted in order to confirm the expression of the tagged proteins. Each step was done at 4°C, and with rotation for the incubations and washes. Glutathione Sepharose 4B (GE Healthcare, 17-0756-01) was used for GST-tagged proteins, whereas Ni-NTA Agarose (QIAGEN, 30210) was used for His-tagged proteins. For each construct, 1mL of the bacterial soluble protein fraction was added to 25µL of washed beads and incubated for two hours. Upon centrifuging at 800 x g for two minutes, the supernatant was discarded and the beads were washed three times with either **Buffer A** (for Glutathione beads) or Lysis Buffer (for Ni-NTA beads). Each wash involved a ten minute incubation, followed by centrifugation at 800 x g for two minutes, after which the supernatant was discarded. After the last wash, protein loading dye was added to the beads and each sample was boiled for ten minutes. The denatured samples were then run on a 10% discontinuous SDS-PAGE gel in **Running Buffer** at 100V until the dye front reached the bottom of the resolving gel. To visualize the amount of expression/purification from the bacterial soluble protein fraction for each construct, the gel was stained with **Coomassie Brilliant Blue** with agitation for 30 minutes, then de-stained twice with **Destain Solution** with agitation for 30 minutes each. The gel was finally soaked in a mixture of 20% ethanol, 10% glycerol overnight before drying on cellophane (Sigma-Aldrich, Z377597).

**Cold Buffer:** 50mM Tris (pH 7.5), 150mM NaCl, 10mM EDTA. Store at 4°C. Before use, add one protease inhibitor tablet (Sigma-Aldrich, 05892970001) to 10mL of buffer.

**Lysis Buffer:** 58mM $NaH_2PO_4 \cdot H_2O$, 300mM NaCl, 10mM Imidazole, pH 8.0. Store at 4°C. Before use, add one protease inhibitor tablet (Sigma-Aldrich, 05892791001) [*] to 10mL of buffer. [*] Ensure to use EDTA-free tablets.

**Buffer A:** 20mM Tris (pH 8.0), 1mM $MgCl_2$, 150mM NaCl, 0.1% NP-40, 10% Glycerol. Store at 4°C. Before use, add one protease inhibitor tablet (Sigma-Aldrich, 05892970001) to 10mL of buffer.

**Running Buffer:** 248mM Tris, 1.92M Glycine, 0.1% SDS.

**Coomassie Brilliant Blue:** 125mg/L Coomassie Brilliant Blue, 50% Methanol, 1% Acetic acid. Filter.

**Destain Solution:** 45% Methanol, 10% Acetic acid.

Pull-down assay:

All steps were performed at 4°C, and with rotation for the incubations and washes. Based on the analysis of the test pull-downs, equivalent amounts of bait protein (i.e. the GST-tagged protein from the bacterial soluble protein fraction) were added to 250µL of prey protein (i.e. the His-tagged protein from the bacterial soluble protein fraction). The final volume was topped up to 500µL with Buffer A, and the mix was incubated for 1.5 hours. In the meantime, 25µL of Glutathione Sepharose 4B beads were washed three times with **PBS**, then blocked with **1% BSA** for one hour. When the incubation of the bait and prey was done, the mix was added to the blocked beads and incubated for another 1.5 hours. One rinse and three washes with Buffer A were then performed. Each washing step involved a ten minute incubation, followed by centrifugation at 800 x g for two minutes, after which the supernatant was discarded. When necessary, the stringency of Buffer A was modified in order to reduce non-specific binding to the beads (see below). After the last wash, protein loading dye was added to the beads, and the samples were stored at -20°C until ready to be used.

**Buffer A:** See section 2.9 (under “Protein expression and extraction”). For pull-downs with His-EcR, non-modified Buffer A was used for the washes. For pull-downs with His-Jun, the amount of NP-40 in Buffer A was increased to 1%.

**Phosphate Buffered Saline (PBS):** 0.3mM $NaH_2PO_4 \cdot H_2O$, 0.7mM $Na_2PO_4$, 0.13M NaCl, pH 7.4.

**1% Bovine Serum Albumin (BSA):** 1% BSA in Buffer A.

Immunoblot analysis:

Upon boiling for ten minutes, the samples were loaded onto a 10% discontinuous SDS-PAGE gel. The samples were run at 100V in Running Buffer until the dye front migrated to the end of the resolving gel. The samples were then transferred onto a nitrocellulose membrane (Bio-Rad, 162-0115) at 15V with **Transfer Buffer** for one hour using a semi-dry transfer apparatus.

Unless stated otherwise, each step was done at room temperature and with agitation. The membrane was first washed three times with **Tris Buffered Saline (TBS)** for ten minutes each, then blocked with **5% milk** for one hour. The membrane was next incubated at 4°C overnight with the desired primary antibody (see section 2.4). The next day, the membrane was washed twice with **Tris Buffered Saline with Tween (TBST)** and blocked twice with **2.5% milk**, for ten minutes each step. The membrane was then incubated with the appropriate HRP-conjugated secondary antibody (see section 2.4) for two hours, followed by four TBST washes for 15 minutes each. BM Chemiluminescence Blotting Substrate (Roche, 11500694001) was used for imaging the membrane, and the signal was detected with an Amersham Imager 600 (GE Healthcare).

**Transfer Buffer:** 248mM Tris, 1.92M Glycine.

**Tris Buffered Saline (TBS):** 1.5M Tris, 0.5M NaCl, pH 7.5.

**Tris Buffered Saline with Tween (TBST):** TBS (pH 7.5), 0.1% Tween 20.

**5% Milk:** 5% Carnation Instant Skim Milk Powder in TBST.

**2.5% Milk:** 2.5% Carnation Instant Skim Milk Powder in TBST.

## 2.14. Chromatin immunoprecipitation from embryos

Chromatin immunoprecipitation (ChIP) from late-staged embryos was performed as previously described (Loubiere et al., 2017), but with modifications.

Embryo collection:

To amass enough embryos, at least ten cages were set up (see section 2.5). Stage 11-15 embryos were collected by allowing the flies to lay eggs on the grape juice agar plates for four hours at 25°C. The plates were then removed from the cages and left to incubate at 25°C for an additional nine hours. All the embryos on the plates, ranging in age from 9-13 hours AEL, were transferred into collecting baskets. The baskets were then soaked in 0.01% Triton X-100 three times for three minutes each to wash off the yeast paste. The embryos were next transferred into a pre-weighed microcentrifuge tube. Upon removing residual wash solution, the total embryonic weight was measured and the embryos were stored at -80°C until ready to be used.

DNA-protein crosslinking:

All steps were performed at 4°C, and with rotation for the incubations and washes, unless otherwise stated. 150mg of embryos was resuspended in 888µL of **Buffer A1**, then transferred into a tissue grinder. 112µL of **16% formaldehyde** (1.8% final concentration) was quickly added and the embryos were grinded by slowly moving the pestle up and down for five minutes at room temperature. The homogenate was next transferred into a new microcentrifuge tube and incubated for 15 minutes. To stop the crosslinking reaction, 300µL of 1.5M glycine (350mM final concentration) was added and the tube was incubated for an additional five minutes, then put on ice. The homogenate was subsequently centrifuged at 2000 x g for two minutes, and the supernatant was discarded. The pellet was then washed three times with Buffer A1, then once with **Lysis Buffer 1**. Each wash involved a 5 minute incubation, followed by centrifugation at 2000 x g for 2 minutes, after which the supernatant was discarded.

**Buffer A1:** 60mM KCl, 4mM $MgCl_2$, 15mM NaCl, 15mM HEPES (pH 7.5), 0.5% Triton X-100, 0.5mM DTT, 10mM Sodium butyrate. Before use, add one protease inhibitor tablet (Sigma-Aldrich, 05892791001) to 10mL of buffer.

**16% Formaldehyde:** 16% Paraformaldehyde, 8mM NaOH, 1X PBS (pH 7.0) [*]. [*] Dissolve PFA in deionized water with NaOH at 65°C before adding buffer. Make fresh each time.

**10X Phosphate Buffered Saline (PBS):** See section 2.5.

**Lysis Buffer 1:** 140mM NaCl, 15mM HEPES (pH 7.5), 1mM EDTA, 0.5mM EGTA, 1% Triton X-100, 0.5mM DTT, 0.1% Sodium deoxycholate, 10mM Sodium butyrate. Before use, add one protease inhibitor tablet (Sigma-Aldrich, 05892791001) to 10mL of buffer.

Chromatin fragmentation:

After the last wash, 750µL of **Lysis Buffer 2** was added to the pellet and the tube was incubated on ice for two hours. The sample was occasionally mixed by pipetting up and down every 20-30 minutes in order to prevent detergent precipitation. For chromatin fragmentation, a Virsonic 100 Ultrasonic Cell Disruptor (Virtis) was used with the following protocol: 20 second pulses with one minute rests on ice in between repeated 20 times, all at power setting 10. After sonication, the samples were stored at -80°C until ready for further use. For ChIP, the size of the DNA fragments should ideally be in the range of 100-500bp, which can be confirmed through agarose gel analysis.

**Lysis Buffer 2:** 0.5% N-lauroylsarcosine in Lysis Buffer 1.

Immunoprecipitation:

Each step was done at 4°C, and with rotation for the incubations. The sonicated extract was next centrifuged at 14,000 x g for five minutes. The resulting supernatant was then equally split into two new microcentrifuge tubes, with one tube designated for the experimental IP and the other tube designated for the negative control IP. To reduce non-specific binding, the aliquots were first pre-cleared. 15µL of washed Protein G magnetic beads (Invitrogen, 10003D) was added to both tubes and incubated for two hours. The pre-cleared samples were then transferred into new microcentrifuge tubes and, for the experimental IP, 5µg of either mouse anti-EcR (Developmental Studies Hybridoma Bank, DDA2.7) or rabbit anti-Jun (Santa Cruz Biotechnology, sc-25763) was added. For the negative control, an equal amount of species-specific normal IgG (SCBT, sc-2025; Cell Signaling Technology, 2729S) was instead added. Both IPs were incubated for 4 hours.

30µL of washed Protein G magnetic beads were subsequently added to each tube and incubated overnight.

DNA recovery:

The following day, the supernatant was discarded and **Lysis Buffer Wash** was added to the beads. Washing consisted of pipetting up and down briefly, incubating with rotation for five minutes at 4°C, and then removing the supernatant. Three more washes were done, followed by two washes with **TE**. After removing the last TE wash, a first elution was performed by adding 100µL of **Elution Buffer 1**. After briefly pipetting up and down, the beads were incubated with vigorous agitation for 15 minutes at 65°C. The supernatant was transferred into a new microcentrifuge tube, and a second elution was done by adding 150µL of **Elution Buffer 2** to the beads and using the same protocol as the first elution. The two elutions were then combined to make a final volume of 250µL. To de-crosslink DNA-protein interactions, the elutions were incubated with shaking overnight at 65°C. The next day, 3µL of 20mg/mL Proteinase K (Sigma-Aldrich, P2308) was added to the tube and incubated with shaking for an additional two hours at 56°C. One volume of phenol-chloroform was then added, and the beads were vortexed for 30 seconds followed by a 15 minute centrifugation at 16,300 x g. Consequently the samples will form two phases: a top aqueous phase containing the DNA, and a bottom organic phase containing proteins and hydrophobic lipids. The aqueous phase was transferred into a new microcentrifuge tube and the following was added: 1/10 volume of 3M Sodium acetate (pH 5.5), 75µg of glycogen, 2.5 volumes of 100% ethanol. After briefly vortexing, the samples were incubated overnight at -20°C. The next day, the samples were centrifuged at maximum speed for 30 minutes at 4°C. The supernatant was discarded and the pellet was washed with 500µL of ice-cold 75% ethanol, then centrifuged at maximum speed for 10 minutes at 4°C. The supernatant was subsequently removed, taking care not to disrupt the pellet which contains the DNA. Following air drying for 10 minutes, the pellet was resuspended in 15µL of nuclease free water and the concentration was measured with a NanoDrop.

**Lysis Buffer Wash:** 0.05% SDS in Lysis Buffer 1**.**

**Tris-EDTA (TE):** 10mM Tris (pH 8.0), 0.1mM EDTA.

**Elusion Buffer 1:** 50mM Tris (pH 8.0), 10mM EDTA, 1% SDS.

**Elusion Buffer 2:** 10mM Tris (pH 8.0), 0.1mM EDTA, 0.67% SDS.

PCR analysis:

Intronic regions of the *zip* locus were PCR amplified using PCR Taq MasterMix (Applied Biological Materials, G013). Reactions consisted of the following: 100 ng template, 0.5µM forward and reverse primer, 1X master mix. Forward and reverse primers were made by Invitrogen (see Appendix D for primer sequences and additional information). The thermocycler settings were as follows: three minutes initial denaturation at 94°C, [30 seconds denaturation at 94°C, 30 seconds annealing at 45-72°C, one minute per kb extension at 72°C] x27 cycles, five minutes final extension at 72°C. Following amplification, the PCR products were analyzed on a 2% agarose gel.

# Chapter 3. Results

## 3.1. EcR acts in a complex with Jun, a component of AP-1, to regulate *zip* expression during late embryogenesis

As mentioned in the introduction, ecdysone signaling may regulate DC in a novel manner that does not require its receptor, EcR, to bind to EcREs for promoting gene expression. Instead, EcR potentially interacts with AP-1 to bind to AP-1 consensus sites. A study mapping EcR binding regions in 20E-treated *Drosophila* Kc167 cells identified a subset of genomic regions that are bound by EcR but do not contain any EcREs (Gauhar et al., 2009). Interestingly, *zip*, a key DC gene that encodes for the myosin heavy chain, was revealed to have a 4-kb region bound by EcR, which contained five sequences matching the AP-1 consensus binding site but no consensus EcREs. The first part of this study involved genetically and molecularly characterizing the interaction between EcR and Jun, a component of the AP-1 transcription factor. Previous work has already shown that ecdysone and JNK signaling are required for the expression of *zip* during GBR and DC (Chen, 2014; Kim, 2017). However, with the exception of some PLA experiments that were previously done in the lab (see Figure 1.4.3) (Chen, 2014), interaction between components of the two pathways in this process has not been fully characterized.

### 3.1.1. EcR and Jun cooperate in the regulation of *zip* expression

Here, epistatic analysis as performed to provide genetic evidence that ecdysone-activated EcR and Jun interact with each other to regulate the expression of *zip* during late embryonic development. As mentioned in the introduction, *zip* expression is strongly upregulated in the AS at the onset of GBR (Figure 1.2.1 D). During mid to late GBR, elevated expression in the DME cells can begin to be observed (Figure 1.2.1 E). As DC proceeds, though, the expression levels diminish in the AS but persist in the DME cells (Figure 1.2.1 F). Prominent levels of *zip* expression are also readily observable in the head during these stages (Figure 1.2.1 D-F).

Ecdysone signaling is required late in embryonic development, as DC defects are observed in embryos lacking either Spo or Dib, enzymes in the biosynthetic pathway that produces 20E and in turn is required for EcR activation (Koelle et al., 1991; Kozlova and Thummel, 2003; Yao et al., 1992). Past work in the lab has shown that *zip* transcript levels

are considerably reduced in the AS of both *spo* and *dib* mutant embryos during GBR (Figure 1.4.1 A,B,E,F), thus indicating that ecdysone signaling is a key player in regulating *zip* expression and actomyosin contractility in the AS (Chen, 2014). During DC, however, *zip* transcripts are still relatively present in the DME cells, though the levels may be slightly reduced, suggesting that ecdysone signaling may only serve to "fine-tune" *zip* expression in the dorsal epidermis (Figure 1.4.1 C,D,G,H). In gain-of-function analysis, wild-type embryos treated with exogenous 20E show increased *zip* expression in the AS and DME cells, with ectopic expression extending into the ventral epidermis in segmental stripes, when compared to ethanol-treated embryos, which serve as a negative control (see Figure 3.1.3) (Chen, 2014). All of these results have been confirmed in this work.

Multiple studies have shown that JNK signaling is also required for *zip* expression during late embryogenesis (Franke et al., 2005; Young et al., 1993; Zahedi et al., 2008). For example, work done previously in the lab has shown that expression of a dominant negative *bsk* (JNK) transgene with the segmental *prd-Gal4* driver causes a loss of *zip* transcription in DME cells within prd[+] stripes during DC (Chen, 2014). To confirm this result with mutant analysis, FISH against *zip* transcripts was performed on embryos containing either the *jun* deficiency, *Df(2R)BSC303*, or one of the *jun* alleles, $jun^{76\text{-}19}$ and $jun^{lA109}$. *Df(2R)BSC303* contains a small chromosomal deletion that removes multiple genes including the entire *jun* locus, and is thus expected to produce no Jun protein (Parks et al., 2004). $jun^{76\text{-}19}$ and $jun^{lA109}$ are characterized amorphic alleles, which encode truncated proteins that lack both the DNA-binding and dimerization domains, in addition to N-terminal phosphorylation sites (Hou et al., 1997; Riesgo-Escovar and Hafen, 1997a). Both mutations result in a dorsal-open phenotype (Hou et al., 1997), whereas the deficiency has yet to be characterized during DC. When staining wild-type embryos with an antibody against Jun, Jun immunoreactivity was predominately observed within the nuclei of AS and DME cells during DC (Figure 3.1.1 A). Similar patterns were observed in heterozygous mutant embryos from all three *jun* loss-of-function lines (Figure 3.1.1 B,D,F). In contrast, Jun immunoreactivity was essentially absent in homozygous mutant embryos from each line (Figure 3.1.1 C,E,G), thus confirming the nature of the genetic alterations. In line with previous experiments, FISH results showed a considerable decrease in *zip* transcript levels in both the AS during GBR and the DME cells during DC in *Df(2R)BSC303*, $jun^{76\text{-}19}$ and $jun^{lA109}$ homozygous mutant embryos when compared to their heterozygous mutant siblings (Figure 3.1.2).

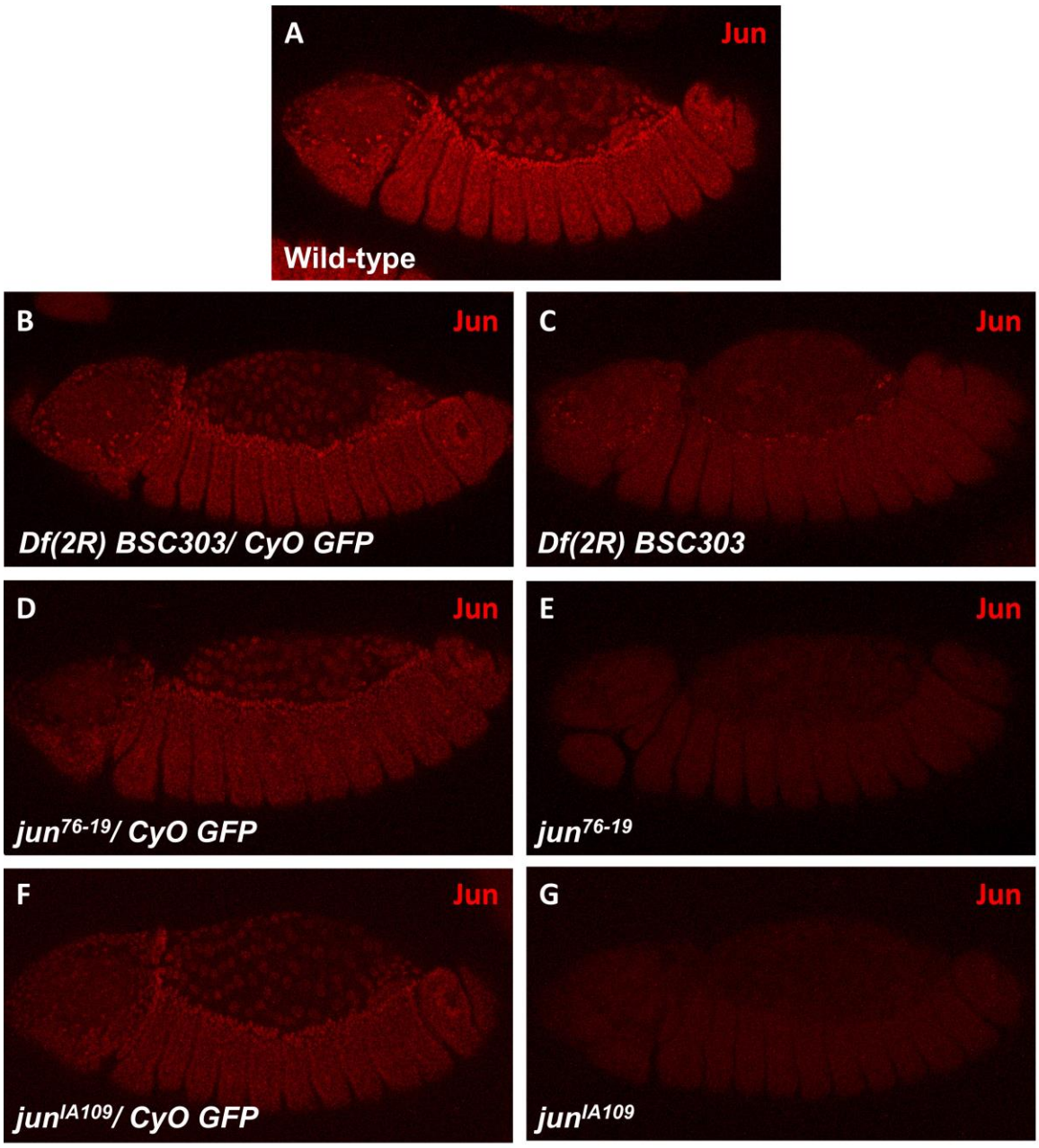


**Figure 3.1.1 Jun protein levels in *jun* loss-of-fuction lines.**

Jun immunostains on DC-staged embryos. (A) Wild-type embryo showing endogenous Jun protein levels and distribution. (B,D,F) Heterozygous mutant embryos carrying one copy of *Df(2R)BSC303*, $jun^{76\text{-}19}$ or $jun^{IA109}$ show comparable immunoreactivity patterns to wild-type, though the levels may be slightly reduced. (C,E,G) Homozygous mutants show little to no Jun immunoreactivity.

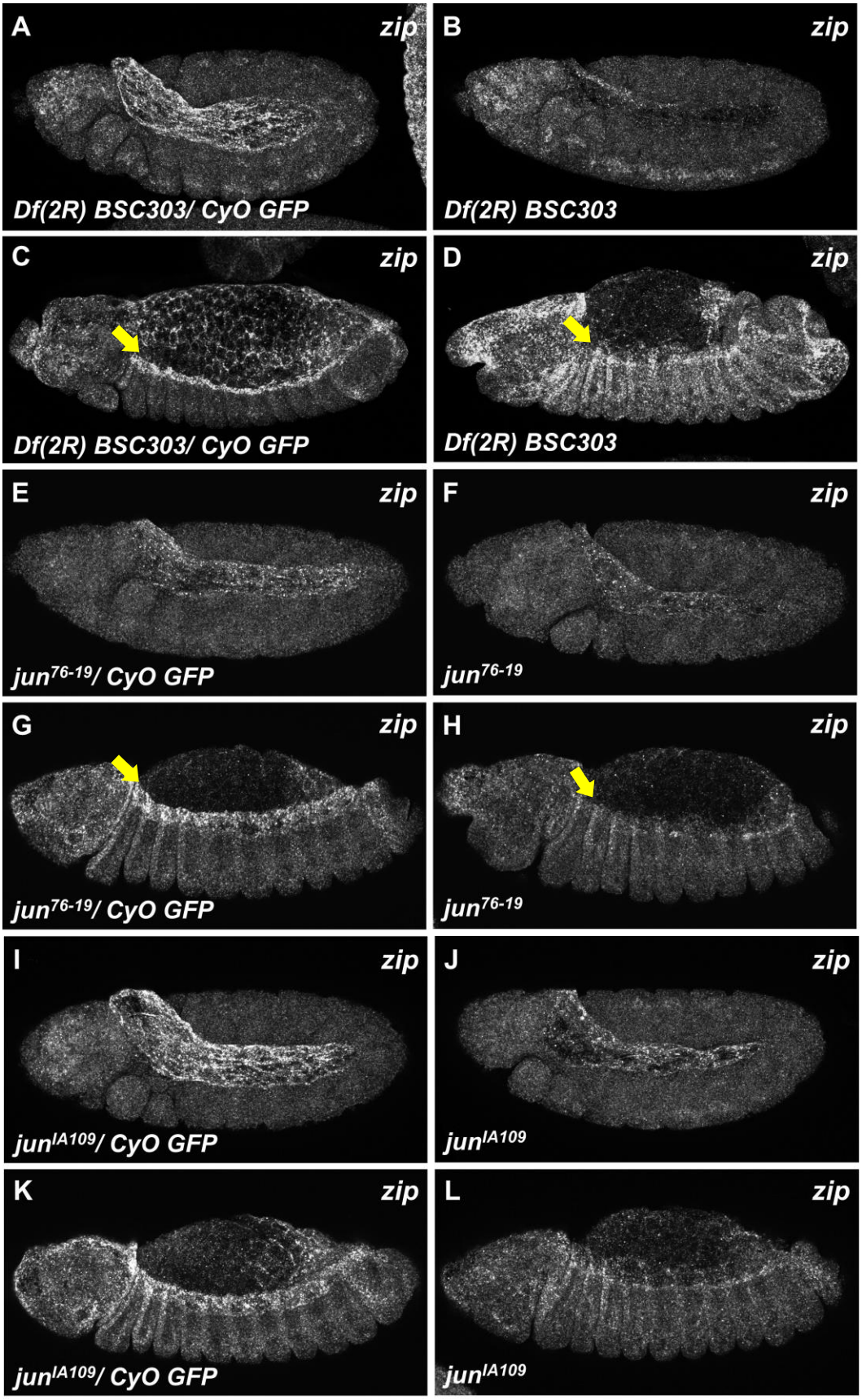
A
zip
Df(2R) BSC303/ CyO GFP
B
zip
Df(2R) BSC303
C
zip
Df(2R) BSC303/ CyO GFP
D
zip
Df(2R) BSC303
E
zip
jun76-19/ CyO GFP
F
zip
jun76-19
G
zip
jun76-19/ CyO GFP
H
zip
jun76-19
I
zip
junIA109/ CyO GFP
J
zip
junIA109
K
zip
junIA109/ CyO GFP
L
zip
junIA109

**Figure 3.1.2 *zip* transcript levels in *jun* loss-of-function lines.**

FISH against *zip* on early GBR- and DC-staged embryos. Yellow arrow indicates the boundary between the AS and DME. (A-D) Embryos heterozygous mutant for the *Df(2R)BSC303* deficiency, which served as a wild-type control, showed typical *zip* transcript distributions during GBR (A) and DC (C). Homozygous mutant embryos displayed a loss of *zip* transcripts specifically in the AS during GBR (B) and DME cells during DC (D). However, DC-staged mutants also unexpectantly showed an overall increase in *zip* throughout the epidermis (D). (E-H) $jun^{76\text{-}19}$ homozygous mutants had greatly diminished *zip* levels in the AS during GBR (F) and DME cells during DC (see yellow arrowhead) (H), when compared to their heterozygous mutant counterparts (E,G). (I-L) Similar results were observed between $jun^{IA109}$ and $jun^{76\text{-}19}$.

Work presented thus far has shown that both ecdysone-activated EcR and Jun are required for the expression of *zip* during late embryonic development. In order to provide evidence that EcR and Jun cooperate in the regulation of *zip* expression, epistatic analysis was performed. This was accomplished by assessing *zip* transcript levels in *jun* loss-of-function embryos exposed to exogenous 20E using FISH. If ecdysone-activated EcR and Jun function independently of each other, then exposure to exogenous 20E should still result in elevations of *zip* expression in the AS and DME cells of embryos lacking Jun, similar to what is observed with 20E-treated wild-type embryos (Figure 3.1.3 A,B) (Chen, 2014). However, 20E-treatment did not lead to any observable increases in *zip* transcript levels in DC-staged *Df(2R)BSC303* or $jun^{IA109}$ homozygous mutant embryos when compared to their heterozygous mutant siblings (Figure 3.1.3 C,D,G,H), which were used as a positive control that showed a similar up-regulation in signal as wild-type embryos treated with 20E. In fact, 20E-treated homozygous mutant embryos showed comparable levels of *zip* transcription as ethanol-treated homozygous mutant embryos (Figure 3.1.3 E,F,I,J), which served as a negative control, indicating that there was indeed no change in signal. Note that 20E and ethanol treatments were always done in parallel (see section 2.6), and that for each treatment, heterozygous and homozygous mutant embryos were in the same tube, and thus exposed to identical experimental conditions. $jun^{76\text{-}19}$ mutant embryos were not included in this analysis as $jun^{IA109}$ and $jun^{76\text{-}19}$ had similar effects on *zip* expression (see Figure 3.1.2). Taken together, the results described above strongly indicate that ecdysone-activated EcR cooperates with Jun to promote the expression of *zip* during late embryogenic development.

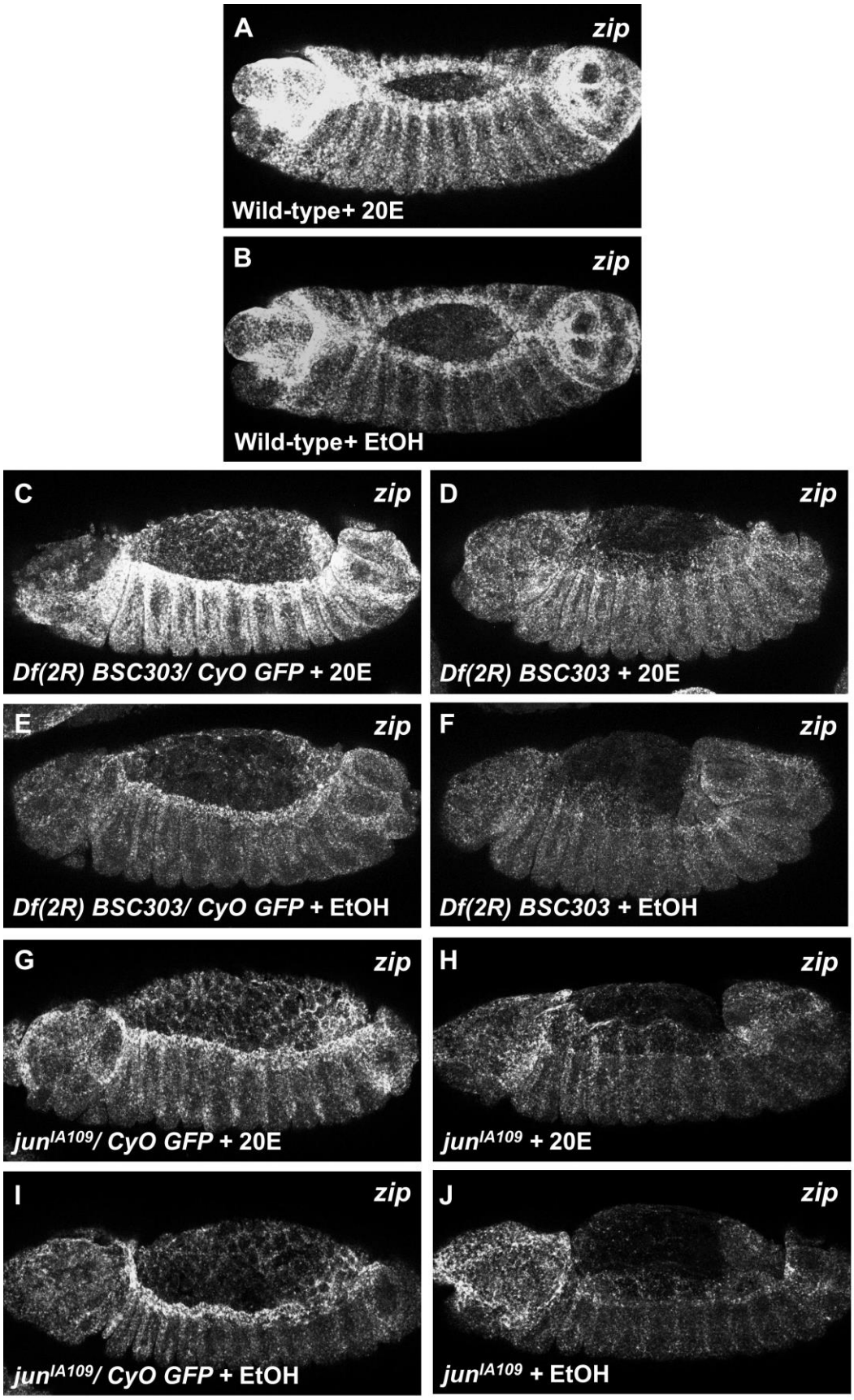
A
zip
Wild-type+ 20E
B
zip
Wild-type+ EtOH
C
zip
Df(2R) BSC303/ CyO GFP + 20E
D
zip
Df(2R) BSC303 + 20E
E
zip
Df(2R) BSC303/ CyO GFP + EtOH
F
zip
Df(2R) BSC303 + EtOH
G
zip
jun^lA109/ CyO GFP + 20E
H
zip
jun^lA109 + 20E
I
zip
jun^lA109/ CyO GFP + EtOH
J
zip
jun^lA109 + EtOH

**Figure 3.1.3 Epistatic analysis between ecdysone-activated EcR and Jun in the regulation the expression of *zip*.**

FISH against *zip* on DC-staged embryos. (A,B) Wild-type embryos treated with exogenous 20E showed elevated *zip* expression (A) in comparison to ethanol-treated embryos (B), which served as a negative control. (C-F) Heterozygous *Df(2R)BSC303* embryos treated with 20E displayed comparable elevations in *zip* transcript levels (C) to that of 20E-treated wild-type embryos. However, 20E-treated homozygous *Df(2R)BSC303* embryos showed no such elevations, as the *zip* transcript levels were similar to those observed in ethanol-treated homozygous embryos (F). (G-J) Similar results were observed between $jun^{IA109}$ and *Df(2R)BSC303*.

## 3.1.2. EcR and Jun can directly bind to each other *in vitro*

In the previous section, an interaction between ecdysone-activated EcR and Jun in the regulation of *zip* expression during late embryonic development was shown. However, this result does not reveal any information regarding the molecular nature of the interaction. To determine if EcR and Jun can directly bind to each other, *in vitro* pull-down assays were performed. Previous PLA experiments have indicated that EcR and Jun are in close proximity to each other (*i.e.* within 40nm) in both the nuclei and cytoplasm of AS and DME cells during DC (see Figure 1.4.3 A-A'') (Chen, 2014).

For both EcR and Jun, GST- and His-tagged fusion proteins were constructed and expressed in bacteria (see sections 2.12 and 2.13 for more detail). Note that the full-length proteins were N-terminally tagged, and were made by Ms. Hae-yoon Kim (Kim, 2017). GST-tagged EcR was first incubated with His-tagged Jun, and then pulled-down with Glutathione beads. Immunoblot analysis revealed a Jun immunoreactive band corresponding to His-Jun, which has an expected size of 34.9kDa (Figure 3.1.4 A). A negative control that was done in parallel involving GST alone and His-Jun resulted in no observable His-Jun band in the blot (Figure 3.1.4 A), thus indicating that the observed interaction between GST-EcR and His-Jun was specific between the two proteins and not the tags or beads. Binding was confirmed via reverse pull-downs between GST-Jun and His-EcR, which showed similar results (Figure 3.1.4 B). That is, immunoblot analysis of GST-Jun pull-downs revealed an EcR immunoreactive band corresponding to His-EcR, which has an expected size of 97.4kDa, whereas the negative control between GST alone and His-EcR resulted in no His-EcR band. Collectively, these results show that EcR and Jun can bind directly to each other, at least *in vitro*.

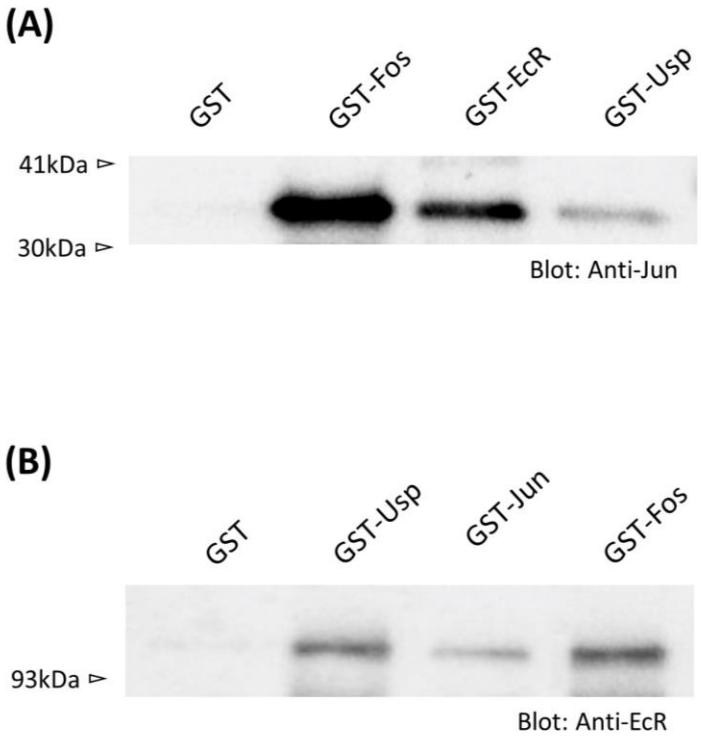


**Figure 3.1.4 Pull down assays between EcR and Jun.**

Immunoblot analysis of pull-down assays between EcR and Jun. (A) Jun immunoblots. GST-Fos (Kay) was able to pull-down His-Jun, resulting in an approximately 34.9kDa Jun-immunoreactive band in the blot. Kay/Fos is part of the AP-1 transcription factor complex with Jun. Thus, this pull-down served as a positive control. Both GST-EcR and GST-Usp were also able to pull-down His-Jun. No binding was observed in the negative control, which involved GST alone. (B) EcR immunoblots. GST-Usp was able to pull-down His-EcR, resulting in an approximately 97.4kDa EcR-immunoreactive band in the blot. This pull-down served as a positive control, as EcR and Usp are known binding partners during ecdysone signaling. Both GST-Jun and GST-Fos were also able to pull-down His-EcR, whereas no binding was observed with GST alone.

The binding of known interacting partners of EcR and Jun was also investigated by performing additional pull-down assays. As mentioned in the introduction, EcR forms a heterodimeric transcription factor complex with Usp during canonical ecdysone signaling (Koelle et al., 1991; Yao et al., 1992), whereas Jun binds to Kay/Fos to form AP-1 upon JNK activation (Mihaly et al. 2001; Riesgo-escovar and Hafen 1997a; Zeitlinger et al. 1997). Interestingly, GST-Kay (Fos) was able to bind to His-EcR with a similar affinity as GST-Usp, as immunoblot analysis revealed that the His-EcR band was roughly equal in band intensity in both GST pull-downs (Figure 3.1.4 B). The binding affinity, however, may

likely be affected by the presence of 20E, as 20E binding to EcR stabilizes the EcR-Usp heterodimer (Chavoshi et al., 2010; Koelle et al., 1991; Yao et al., 1992) Likewise, GST-Usp was observed to bind to His-Jun, though not as strongly as GST-Kay (Figure 3.1.4 A). Note that the starting amount of GST-tagged protein (*i.e.* the bait) was normalized for each pull-down experiment. These results indicate that EcR and Jun can directly bind to each other, and that Usp and Kay may also be components of this complex.

### 3.1.3. EcR and Jun can bind to the same region of the *zip* locus

EcR and Jun can bind directly to each other *in vitro*, but further work is needed, to determine that this interaction can serve as a novel transcription factor unit *in vivo*. To accomplish this, ChIP was performed to determine if EcR and Jun can bind to the *zip* locus. This is to further prior work, which has shown that PLA signal between EcR and Jun can be observed in both the nuclei and cytoplasm of AS and DME cells during DC (Figure 1.4.3 A-A") (Chen, 2014). In *zip* deficient embryos, the PLA signal is significantly reduced (Figure 1.4.3 B-B"), suggesting that EcR and Jun form a complex somewhere at the *zip* locus (Chen, 2014).

Stage 11-15 embryos (*i.e.* embryos between the start of GBR to the end of DC) were used for ChIP analysis. Following homogenization, protein-chromatin interactions were cross-linked and the DNA was sheared to an average size of 100 to 500 base pairs (bps). The extracts were next incubated with anti-EcR antibodies, then magnetic beads. Co-immunoprecipitated DNA was purified, and *zip*-specific primers were used for PCR amplification to assess whether parts of the *zip* locus form a complex with EcR (see Appendix D for more information regarding the primers). Upon agarose gel analysis, a band corresponding to a intron of the *zip* gene was observed (Figure 3.1.5 A). The area amplified was against the EcR-binding region discovered by Gauhar and colleagues, which contained AP-1 binding sites but no EcREs (Gauhar et al., 2009). No band was observed for a region corresponding to the 3' end of the *zip* genomic region, which was not expected to form a complex with EcR (Figure 3.1.5 B). Similar results were obtained when performing ChIP with anti-Jun antibodies (Figure 3.1.5 A,B). For each experiment, a negative control was done in parallel involving normal IgG. In all cases, no bands were observed (Figure 3.1.5 A,B), thus indicating that non-specific binding was not occurring. Taken together, the ChIP assays showed that EcR and Jun can bind to the same region of the *zip* locus where EcR binding region and AP-1 consensus sites co-exist during late

embryonic development. Note that the amount of product immunoprecipitated may be improved upon if 20E-treated wildtype embryos were used for the assay instead of non-treated wild-type embryos.

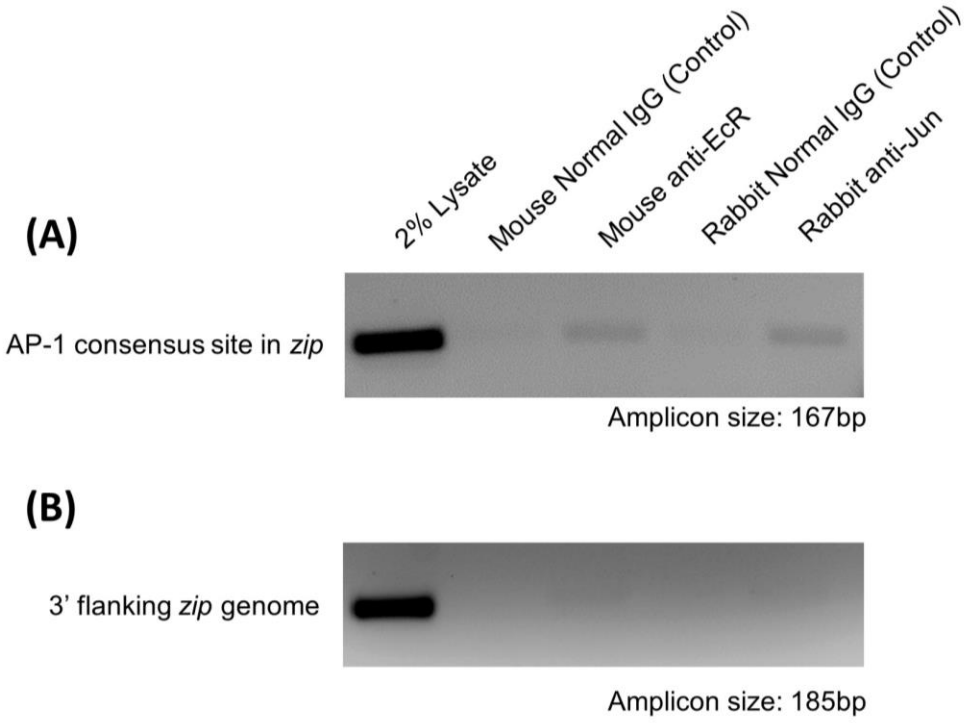


**Figure 3.1.5 ChIP analyses of EcR and Jun complex formation at the *zip* locus.**

Agarose gel analysis of PCR amplified *zip* fragments from EcR and Jun immunoprecipitates. (A) Amplification of a 167 bp fragment of a *zip* intron, corresponding to the EcR-binding region that contains AP-1 binding sites but no EcREs. The fragment was present in both EcR and Jun immunoprecipitates, but not the negative control immunoprecipitates involving just IgG. (B) Amplification of a 185 bp fragment corresponding to a region of the 3' *zip* genomic region. The fragment was not present in EcR or Jun immunoprecipitates.

Another way to potentially show that EcR and Jun are binding to the same genomic region is to immunostain polytene chromosomes. In a preliminary test, *Drosophila* salivary glands from third instar larvae were dissected and co-immunostained with EcR and Jun antibodies. Within intact salivary gland nuclei, a subset of the EcR-labeled and Jun-labeled chromatin bands appeared to overlap, which may be an indication of their co-localization at these chromosomal regions (Figure 3.1.6). Future work will involve co-immunostaining

chromosome squashes so that the chromosomal positions of overlapping signal can be determined. For example, co-localization at cytogenetic position 60E12 (FlyBase) can be determined in order to see if EcR and Jun bind at the region containing the *zip* locus. For increased sensitivity, this experiment could be repeated with PLA which would show regions specifically bound by EcR-Jun complexes.

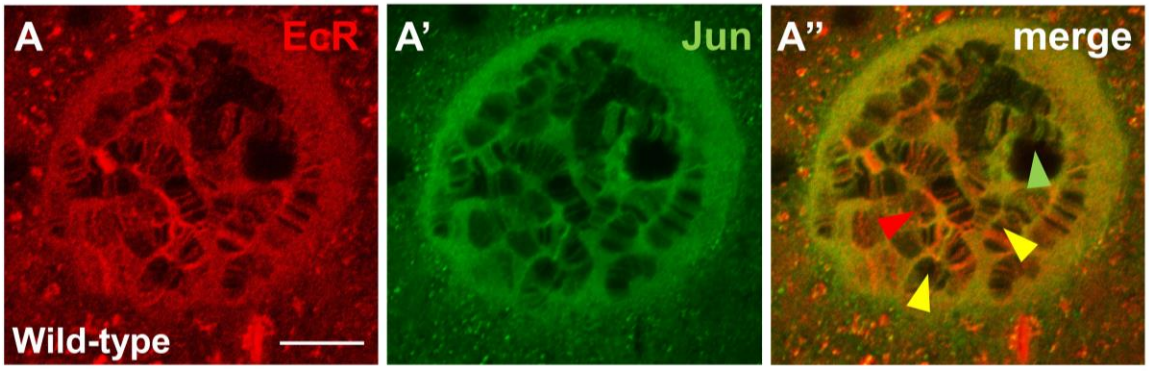


**Figure 3.1.6 EcR and Jun co-immunostain within a salivary gland nucleus.**

Co-immunostain between EcR and Jun on a third instar larval salivary gland nucleus. Shown is a single section (*i.e.* non-stacked) confocal image. (A-A'') EcR (red, A) and Jun (green, A') staining patterns appeared to show a subset of nuclear bands that had a prominent amount of overlap (yellow) between the two signals (indicated by yellow arrowheads). Red and green arrowheads point to bands showing predominately EcR or Jun staining only, respectively.

## 3.2. Identification of other DC participants that are regulated by the EcR-Jun complex

One key to understanding morphogenesis of the AS during DC is identifying the genes that play a role in the process. As previously mentioned, ecdysone, which is produced at high levels in the AS, is required for DC (Chavez et al., 2000; Giesen et al., 2003; Kozlova and Thummel, 2003). Canonical ecdysone signaling involves the formation of an ecdysone-activated EcR-Usp transcription factor that drives the expression of genes containing EcREs (Cherbas et al., 1991; Riddiford et al., 2001; Thummel, 1995). However, the *zip* locus instead contains a novel EcR binding region, which includes consensus AP-1 binding sites but no EcREs (Gauhar et al., 2009). A bioinformatic screen done by the

lab to find genes that contained similar binding sites, *i.e.* at least five AP-1 consensus sites but no EcREs, identified 49 similar regions throughout the genome. Interestingly, at least 13 of these regions are in or near genes encoding known or likely DC participants. They are: *cabut* (*cbt*), *Chd64*, *ecr*, *G protein-coupled receptor kinase 2* (*gprk2*), *insulin-like receptor* (*inr*), *jaguar* (*jar*), *jupiter*, *mesoderm-expressed 2* (*mes2*), *Rho GTPase activating protein at 71E* (*rhogap71e*), *steppke* (*step*), *u-shaped* (*ush*), *ultraspiracle* (*usp*) and *Z band alternatively spliced PDZ-motif protein 52* (*zasp52*) (see Appendix E for the list of the candidate genes and their brief functions). In this section, each candidate gene will be assessed to see if its expression is regulated by the EcR-Jun complex during DC, similar to the work that was done for *zip*.

### 3.2.1. The expression patterns of *cbt*, *ecr*, *jar*, *jupiter*, *mes2*, *rhogap71e*, *ush* and *zasp52* during late embryogenesis are similar to *zip*

FISH against each candidate gene was first performed on wild-type embryos in order to observe their expression patterns during GBR and DC. Available cDNAs for each candidate were used as templates to make the antisense RNA probes (see sections 2.2 and 2.3 for more information). Expression patterns that were similar to *zip* were sought after, as this may indicate that the genes are regulated by similar mechanisms. As discussed, *zip* expression is strongly upregulated in the AS at the onset of GBR (Figure 3.2.1 A). During mid to late GBR, elevated expression in the DME cells can begin to be observed (Figure 3.2.1B). As DC proceeds, however, expression levels wane in the AS but persist in the DME cells (Figure 3.2.1 C).

In confirmation of previous work, *jar*, *jupiter* and *zasp52* shared similar expression patterns to *zip* during late embryogenesis (Ducuing et al., 2015; Kim, 2017). *Drosophila* Jar is the homologue of myosin VI (Ducuing et al., 2015; Kellerman et al., 1992), Jupiter is a microtubule binding protein (Ducuing et al., 2015; Karpova et al., 2006), and Zasp52 is a member of the Alp/Enigma family involved in actin cable formation (Ducuing and Vincent, 2016; Ducuing et al., 2015; Jani and Schock, 2007). Akin to the *zip* expression pattern, *jar*, *jupiter* and *zasp52* transcripts were highly present in the AS during GBR (Figure 3.2.1 D,E,G,H,J,K). However, only *jar* and *zasp52* transcript levels diminished in the AS during DC (Figure 3.2.1 I,L). *jupiter* transcripts persisted throughout DC,and appeared to be located within AS cell nuclei (Figure 3.2.1 F). It is unknown whether persistence of the transcripts at this stage is due to continual expression, nuclear

sequestration, or increased transcript stability. In the DME cells, *jar, jupiter* and *zasp52* transcript levels all accumulated in the DME cells from mid-GBR to DC (Figure 3.2.1 E,F,H,I,K,L).

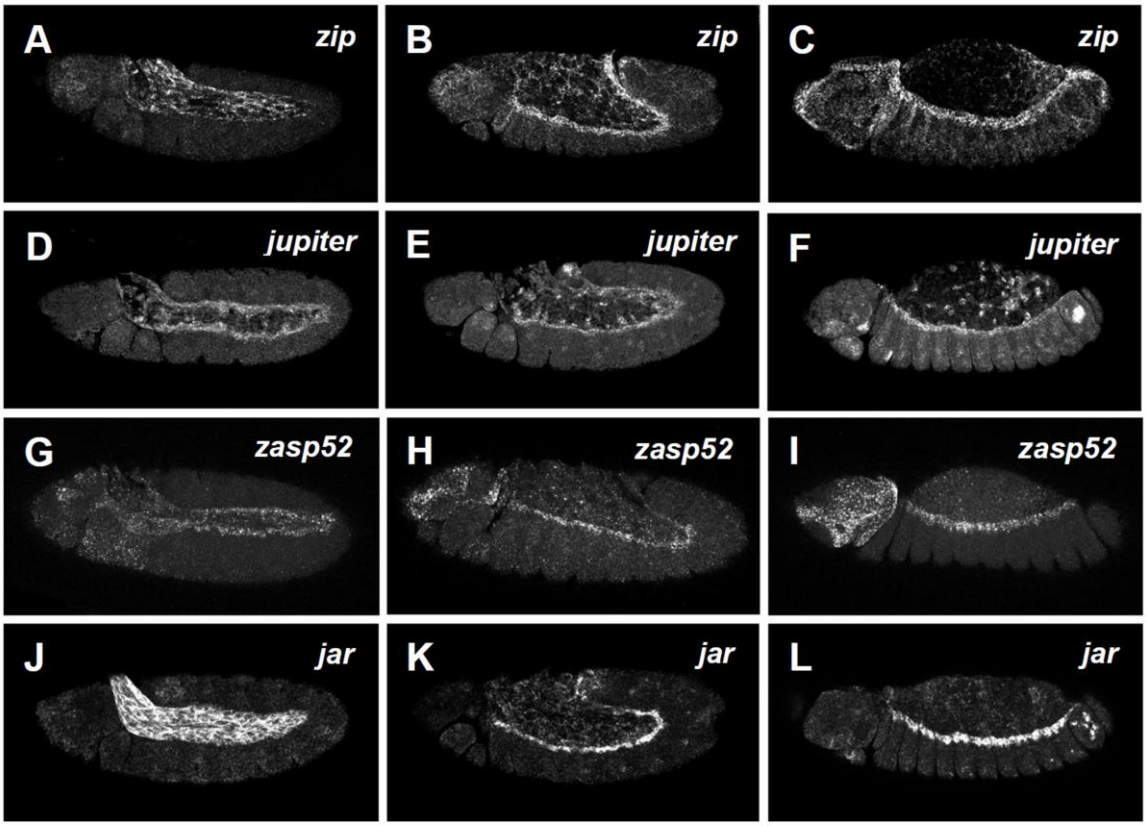


**Figure 3.2.1 *jupiter*, *zasp52* and *jar* expression patterns during GBR and DC.**

FISH against *jupiter*, *zasp52* and *jar* on GBR- and DC-staged wild-type embryos. (A-C) *zip* expression during GBR (A,B) and DC (C). (D-F) Like *zip*, *jupiter* transcripts were found at high levels in the AS during GBR (D,E) and in the DME cells from mid-GBR to DC (E,F). However, *jupiter* transcripts persisted in the AS throughout DC, and appeared to be sequestered within nuclei (F). (G-L) Both *zasp52* (G-I) and *jar* (J-L) expression patterns were comparable to zip.

Expression of *cbt*, which encodes for a transcription factor that is expressed in yolk sac nuclei (Muñoz-Descalzo et al., 2005), was predominately observed in the AS during GBR, though the transcripts appeared to be sequestered within nuclei like *jupiter* (Figure 3.2.2 D-E). In contrast to *zip* during DC, however, *cbt* transcripts in the AS persisted and there were no accumulations in the DME cells (Figure 3.2.2 F). *ecr* transcripts were abundant in the AS during GBR but not during DC, similar to *zip* but accumulations in the DME cells were also not apparent (Figure 3.2.2 G-I). *mes2*, which encodes for a transcription factor with a MADF domain that directs binding to multiple trinucleotide repeat sites (Bhaskar and Courey, 2002; Zimmermann et al., 2006), had an expression pattern comparable to that of *zip*, with the exception of additional transcript accumulations seen in the ventral epidermis in a segmental pattern (Figure 3.2.2 J-L). Minimal in the AS during GBR, *rhogap71e* transcripts were most apparent during DC in the dorsal vessel, *i.e.* the cardiac cells underneath the dorsal epidermis (Figure 3.2.2 M-O). *ush*, which encodes a multitype zinc-finger protein that acts as a GATA transcription factor (Fossett et al., 2000), is present at high levels in both the AS and DME cells from GBR to DC, with prominent AS accumulations at the canthi of the dorsal hole during DC (Figure 3.2.2 P-R).

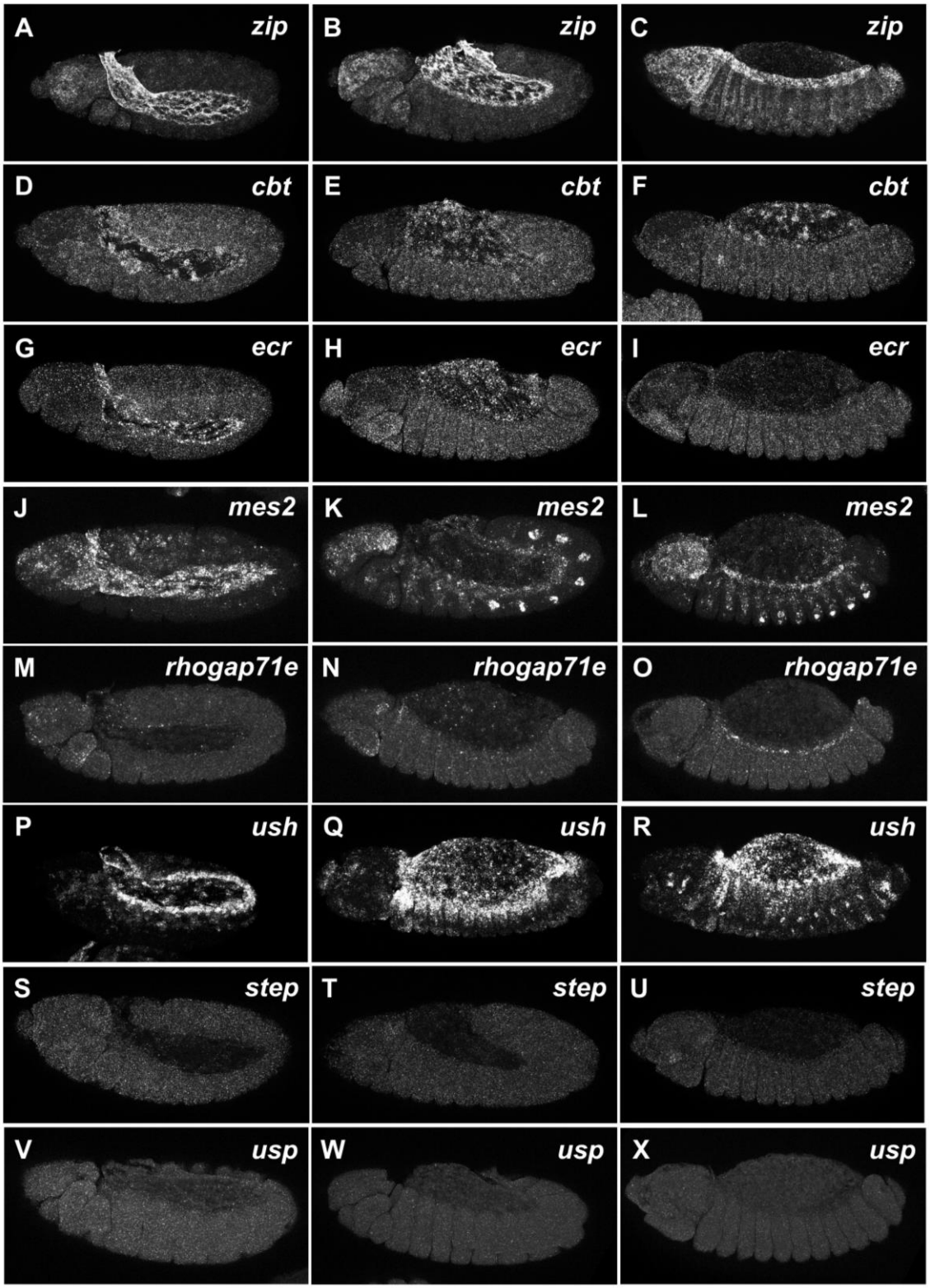
A zip
B zip
C zip
D cbt
E cbt
F cbt
G ecr
H ecr
I ecr
J mes2
K mes2
L mes2
M rhogap71e
N rhogap71e
O rhogap71e
P ush
Q ush
R ush
S step
T step
U step
V usp
W usp
X usp

**Figure 3.2.2 Expression patterns of other candidate genes during GBR and DC.**

FISH against other candidate genes on GBR- and DC-staged wild-type embryos. (A-C) *zip* expression during GBR (A,B) and DC (C). (D-F) *cbt* expression was observed in the AS during GBR, though the transcripts were sequestered in nuclei (D,E). Also, *cbt* transcripts persisted in the AS during DC, and there were no accumulations in the DME cells (F). (G-I) *ecr* transcripts were abundant in the AS during GBR but not during DC (G-I), similar to *zip*. But localizations in the DME cells were not apparent (I). (J-L) *mes2* had an expression pattern akin to *zip* (J-L), with the exception of additional transcripts present in the ventral epidermis in a segmental pattern (K,L). (M-O) *rhogap71e* transcript levels were minimal in the AS during GBR (M,N), but observable in the dorsal vessel during DC (O). (P-R) *ush* expression was high in both the AS and DME cells from GBR to DC (P-R), with prominent AS accumulations at the canthi of the dorsal hole during DC (R). (S-X) No FISH signal was observed for both *step* and *usp*.

No FISH signal was observed for *step*, which encodes for an Arf-GEF (West et al., 2017), and *usp* (Figure 3.2.2 S-X). This may be due to suboptimal binding of the antisense probe to the transcripts *in vivo*. Unfortunately, antisense probes for *Chd64, gprk2* and *inr* were unable to be generated, as restriction digest tests of the cDNAs that were used as templates did not produce the predicted banding patterns (see Appendix B for more information). In the future, different cDNAs can be ordered to make the probes.

Taken together, FISH against the candidate genes on wild-type embryos revealed that *cbt*, *ecr*, *jar*, *jupiter*, *mes2*, *rhogap71e*, *ush* and *zasp52* were expressed in the AS and/or dorsal epidermis during late embryonic development. As their expression patterns shared similarities to that of *zip*, which may indicate a shared regulatory mechanism for gene expression, these candidates were studied further in regards to whether they are also regulated by the EcR-Jun complex. The inclusion of *ecr* as a possible candidate gene may indicate the presence of a positive feedback loop. Due to technical reasons, the expression patterns of *Chd64*, *gprk2*, *inr*, *step* and *usp* could not be evaluated. Thus, further work on these candidates was not pursued in this study.

## 3.2.2. Ecdysone signaling promotes the expression of *ecr, jupiter* and *ush*, but suppresses *rhogap71e, jar and zasp52* expression

Owing that eight of the candidate genes each showed a similar expression pattern to *zip*, and that all them have an EcR binding region with AP-1 consensus sites but no EcREs, it is quite possible that these genes are also regulated by the EcR-Jun complex. In this section, it was first determined if these genes are regulated by ecdysone-activated

EcR. To accomplish this, the transcript levels for each candidate gene was assessed during GBR and DC in embryos mutant for either *spo* or *dib* via FISH analyses (see Table 1 at the end of section 3.2 for a summary of all the results). A detailed description on how the FISH signals were quantified can be found in section 2.9.

Effects on *cbt* and *mes2* transcript levels were not readily apparent in either $spo^{1}$ or $dib^{2}$ homozygous mutants when compared to their heterozygous siblings, which served as a wild-type control for these experiments (Figure 3.2.3 and Figure 3.2.4). *ecr* transcript levels, on the other hand, were significantly reduced in the AS during mid to late GBR in both $spo^{1}$ and $dib^{2}$ homozygous mutants (Figure 3.2.5 A,B,E,F,I,J). Effects in the DME cells or during DC could not be evaluated (Figure 3.2.5 C,D,G,H), as wild-type *ecr* expression in these cells and at this stage is not detectible (Figure 3.2.2 I). For both $spo^{1}$ and $dib^{2}$ homozygous mutants, *jupiter* transcript levels in the DME cells during GBR and DC were revealed to be significantly decreased (Figure 3.2.6 A-I,K). Likewise, significant decreases in transcript levels were also observed in the AS (Figure 3.2.6 A-F,J,L), with the exception of DC-staged $dib^{2}$ homozygotes, where signal variability was too high within the data set to reveal any significant differences (Figure 3.2.6 G,H,L). Lastly, *ush* transcript levels in the DME cells of $spo^{1}$ and $dib^{2}$ homozygous mutants were significantly reduced during GBR and DC (Figure 3.2.7 A-I,K). Significant reductions in transcript levels were observed in the AS as well (Figure 3.2.7 A-D,G,H,J,L), with the exception of GBR-staged $dib^{2}$ homozygotes (Figure 3.2.7 E,F,L). Again, the amount of signal variability was too high within the data set to show any significant differences. Though some data sets were determined to be statistically insignificant, the general trends indicate that ecdysone signaling can promote the expression of *ecr*, *jupiter* and *ush*, but not *cbt* nor *mes2*, during GBR and DC.

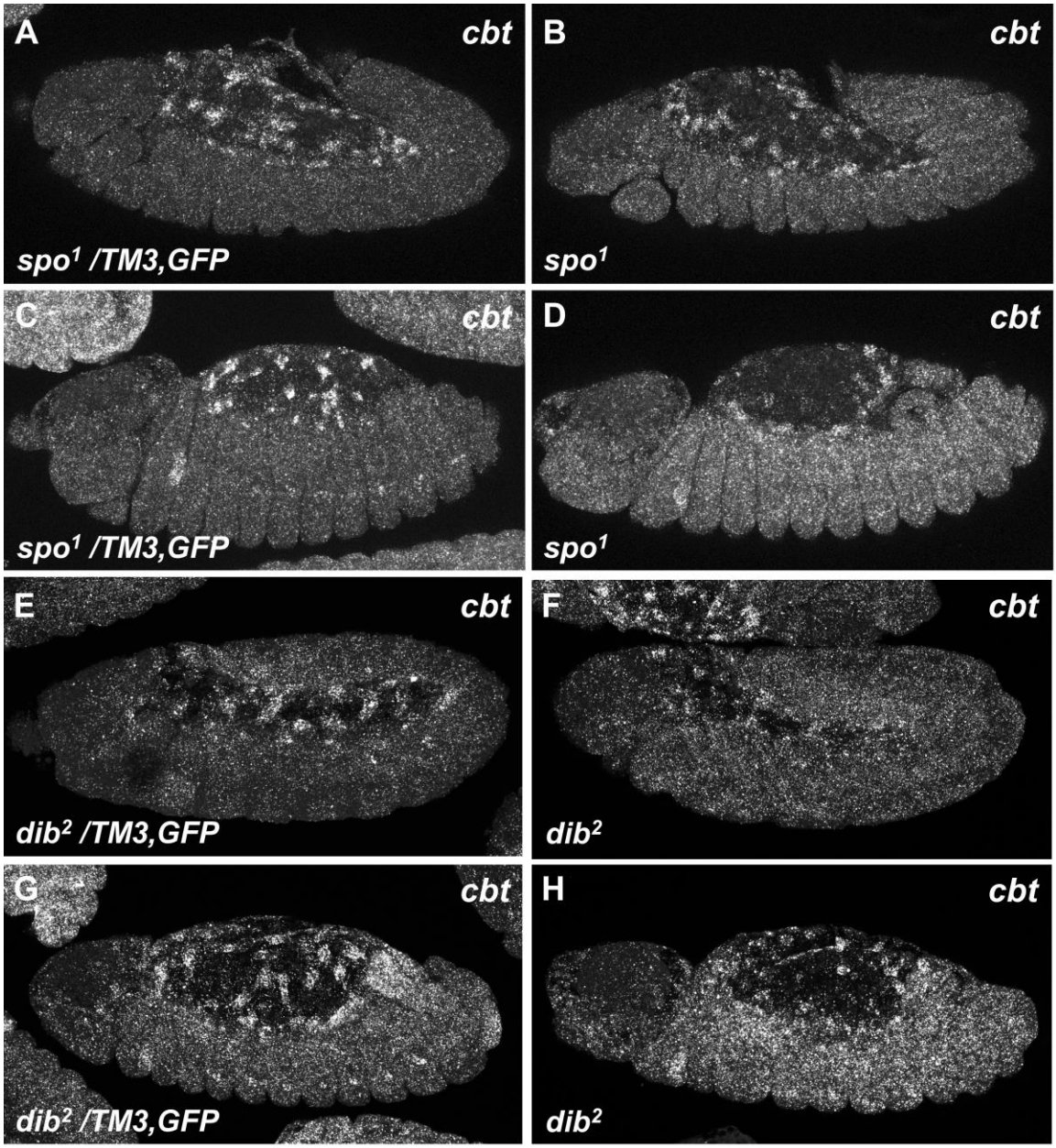


**Figure 3.2.3 Effects of ecdysone signaling on *cbt* expression.**

FISH against *cbt* on GBR- and DC-staged embryos. (A-D) Embryos heterozygous mutant for *spo*$^{1}$, which served as a wild-type control, showed typical *cbt* transcript distributions during GBR (A) and DC (C). In comparison, homozygous mutant embryos displayed no obvious changes in *cbt* transcript levels or distributions during GBR (B) and DC (D). (E-H) Similar results were observed between *dib*$^{2}$ and *spo*$^{1}$.

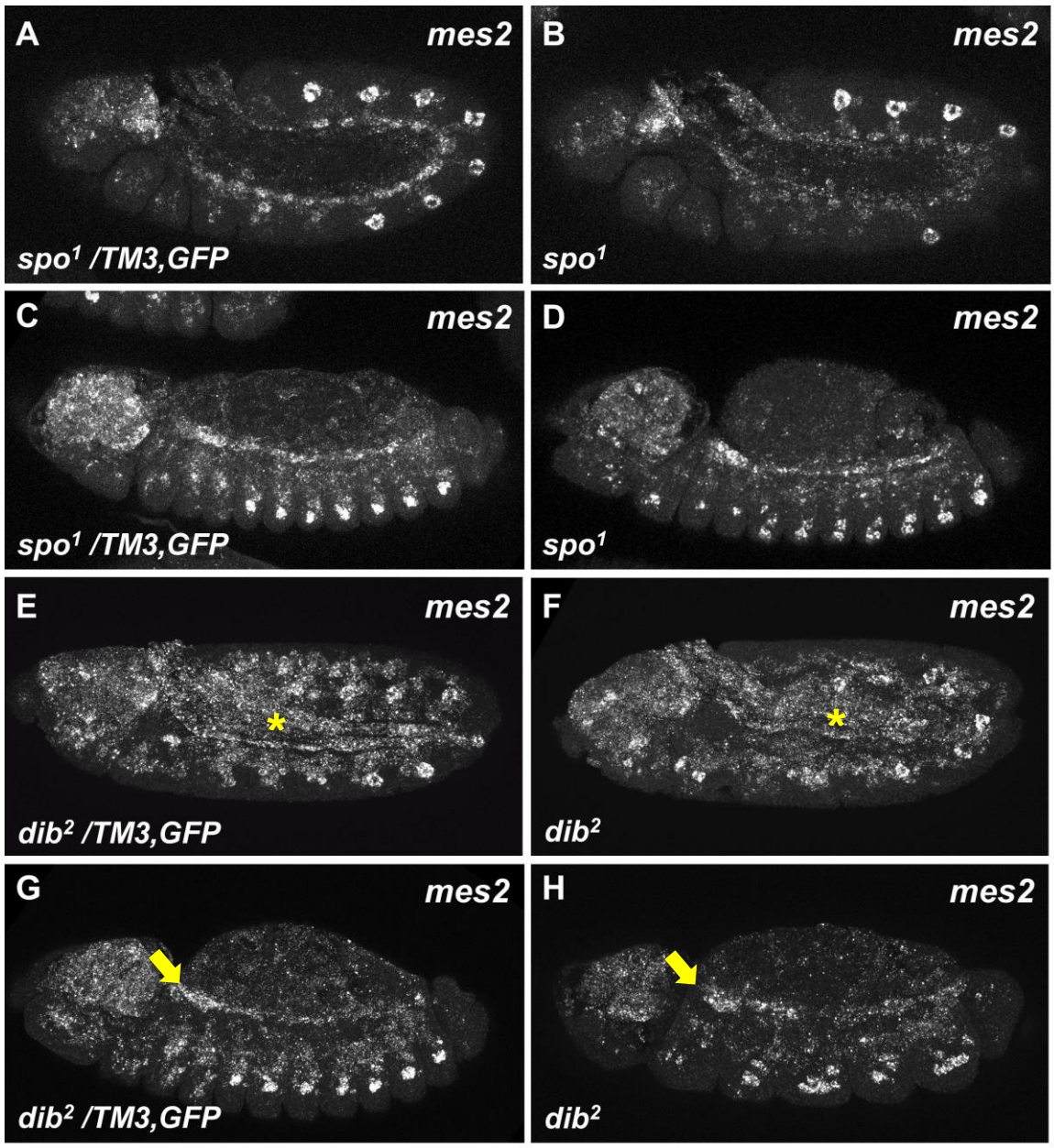


**Figure 3.2.4 Effects of ecdysone signaling on *mes2* expression.**

FISH against *mes2* on GBR- and DC-staged embryos. (A-D) Embryos heterozygous mutant for *spo*$^{1}$, which served as a wild-type control, showed typical *mes2* transcript distributions during GBR (A) and DC (C). In comparison, homozygous mutant embryos displayed no obvious changes in *mes2* transcript levels or distributions during GBR (B) and DC (D). (E-H) Similar results were observed between *dib*$^{2}$ and *spo*$^{1}$. Yellow asterisk indicates the AS. Yellow arrow indicates the boundary between the AS and DME.

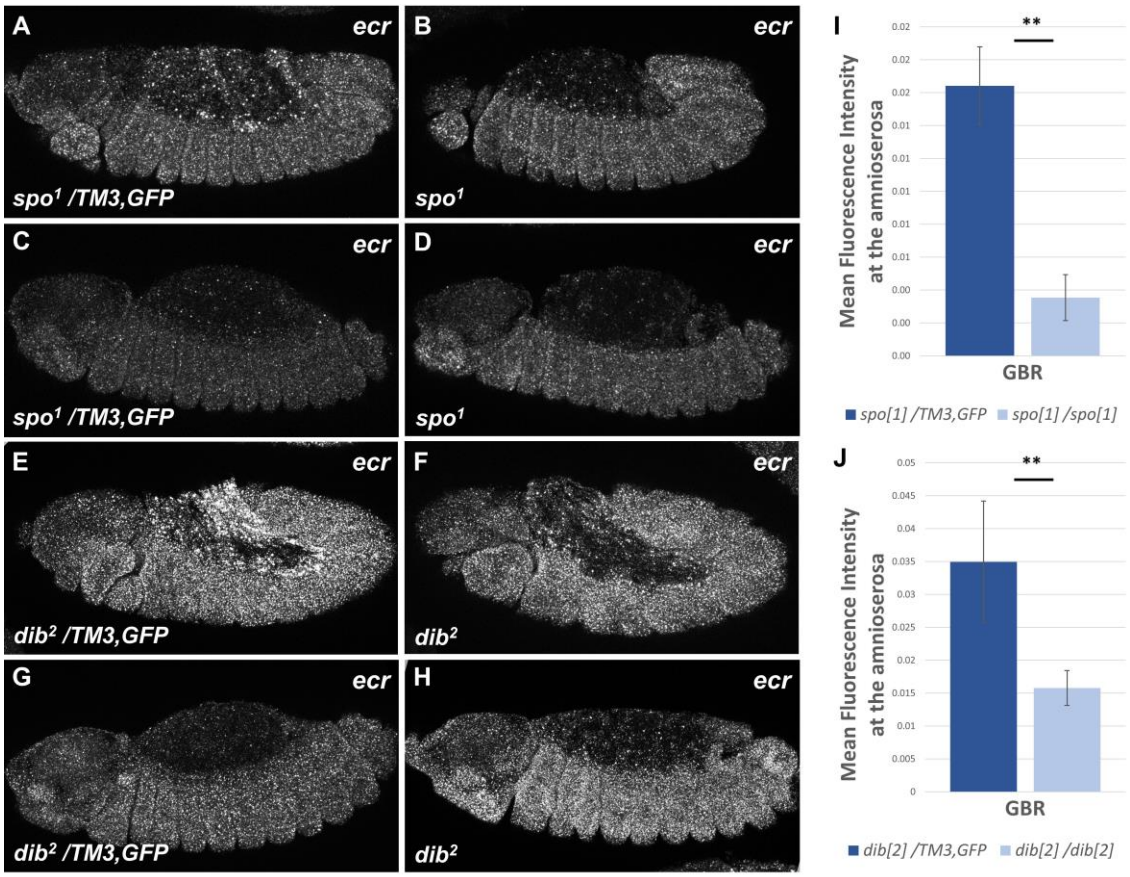


**Figure 3.2.5 Effects of ecdysone signaling on *ecr* expression.**

FISH against *ecr* on GBR- and DC-staged embryos. (A-D) Embryos heterozygous mutant for *spo*$^{1}$, which served as a wild-type control, showed typical *ecr* transcript distributions during GBR (A) and DC (C). Homozygous mutant embryos, however, displayed significantly reduced *ecr* transcript levels in the AS during mid to late GBR (B). Effects in the DME cells or during DC could not be assessed, as control *ecr* expression in these cells and at this stage is not readily observable (C,D). (E-H) Similar results were observed between *dib*$^{2}$ and *spo*$^{1}$. (I,J) Quantification of the FISH signals. Sample sizes are: *spo*$^{1}$ heterozygotes (3 embryos), *spo*$^{1}$ homozygotes (4), *dib*$^{2}$ heterozygous (9), *dib*$^{2}$ homozygotes (13). ** $p<0.01$.

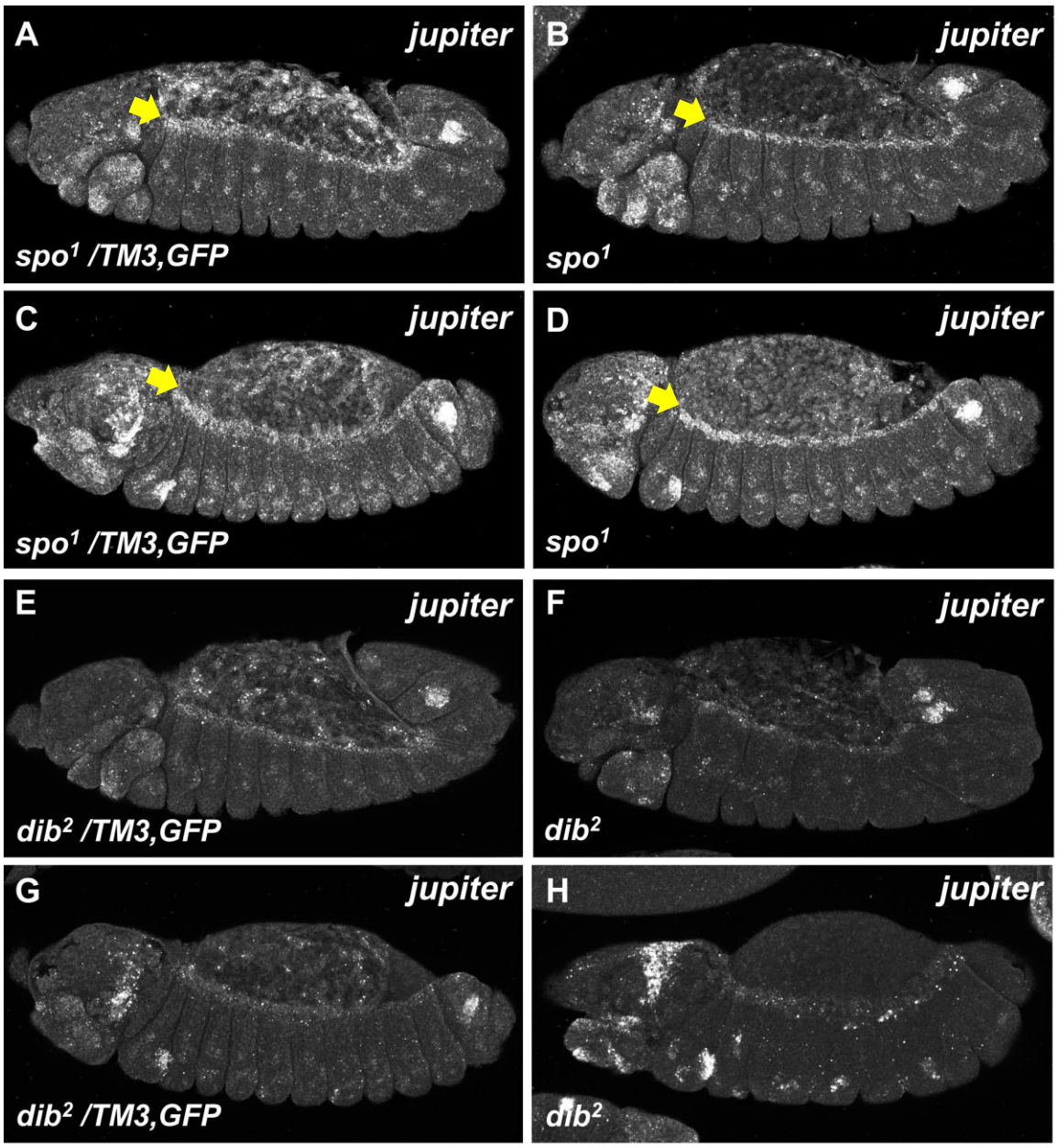


continues on next page…

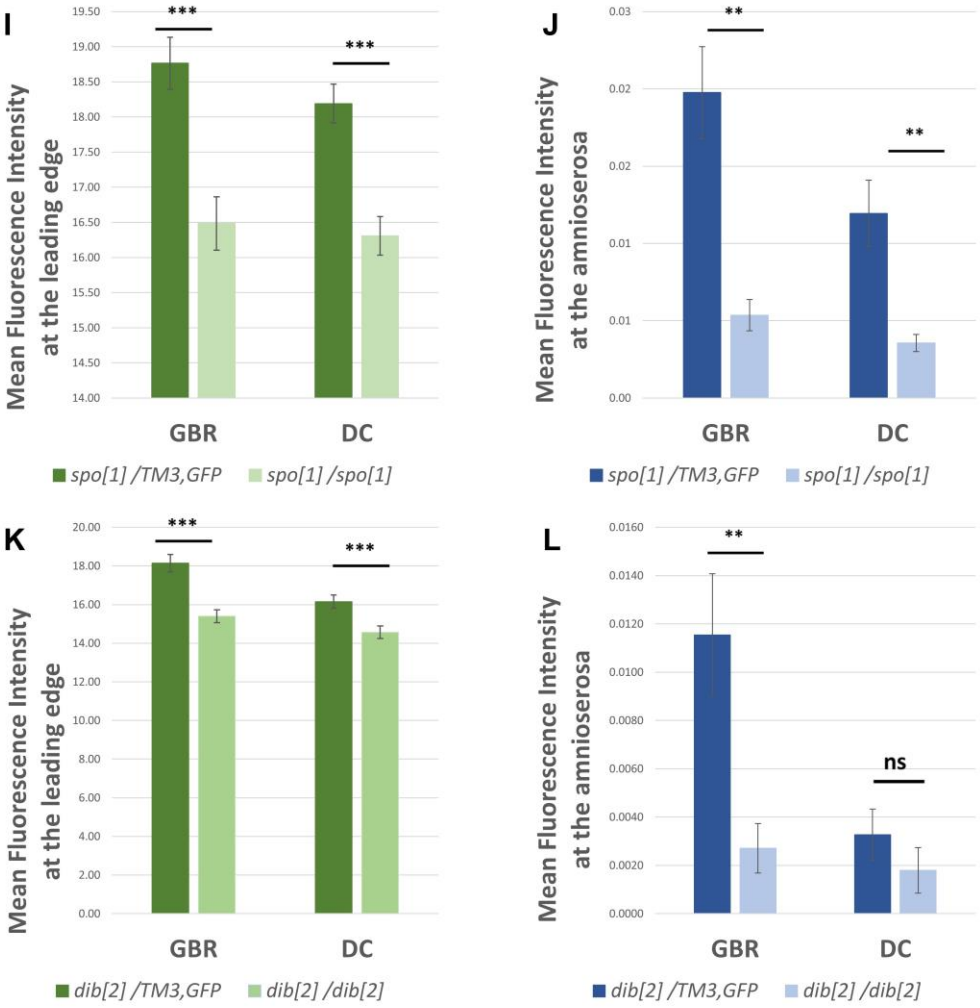


**Figure 3.2.6 Effects of ecdysone signaling on *jupiter* expression.**

FISH against *jupiter* on GBR- and DC-staged embryos. (A-D) Embryos heterozygous mutant for *spo*$^{1}$, which served as a wild-type control, showed typical *jupiter* transcript distributions during GBR (A) and DC (C). Homozygous mutant embryos, however, displayed significantly reduced *jupiter* transcript levels in the AS and DME cells (see yellow arrows) during GBR (B) and DC (D). (E-H) Similar results were observed between *dib*$^{2}$ and *spo*$^{1}$, except that *dib*$^{2}$ homozygotes did not show a significant difference in transcript levels in the AS during DC. (I,J) Quantification of the FISH signals. Sample sizes for DME cell measurements are: *spo*$^{1}$ heterozygotes (GBR = 42 segments in 6 embryos, DC = 35/5), *spo*$^{1}$ homozygotes (GBR + DC = 42/6), *dib*$^{2}$ heterozygotes (GBR + DC = 35/5), *dib*$^{2}$ homozygotes (GBR = 49/7, DC = 28/4). Sample sizes for AS measurements are: *spo*$^{1}$ heterozygotes (GBR = 6 embryos, DC = 5), *spo*$^{1}$ homozygotes (GBR + DC = 6), *dib*$^{2}$ heterozygotes (GBR + DC = 5), *dib*$^{2}$ homozygotes (GBR = 7, DC = 4). **p<0.01, *** p<0.001.

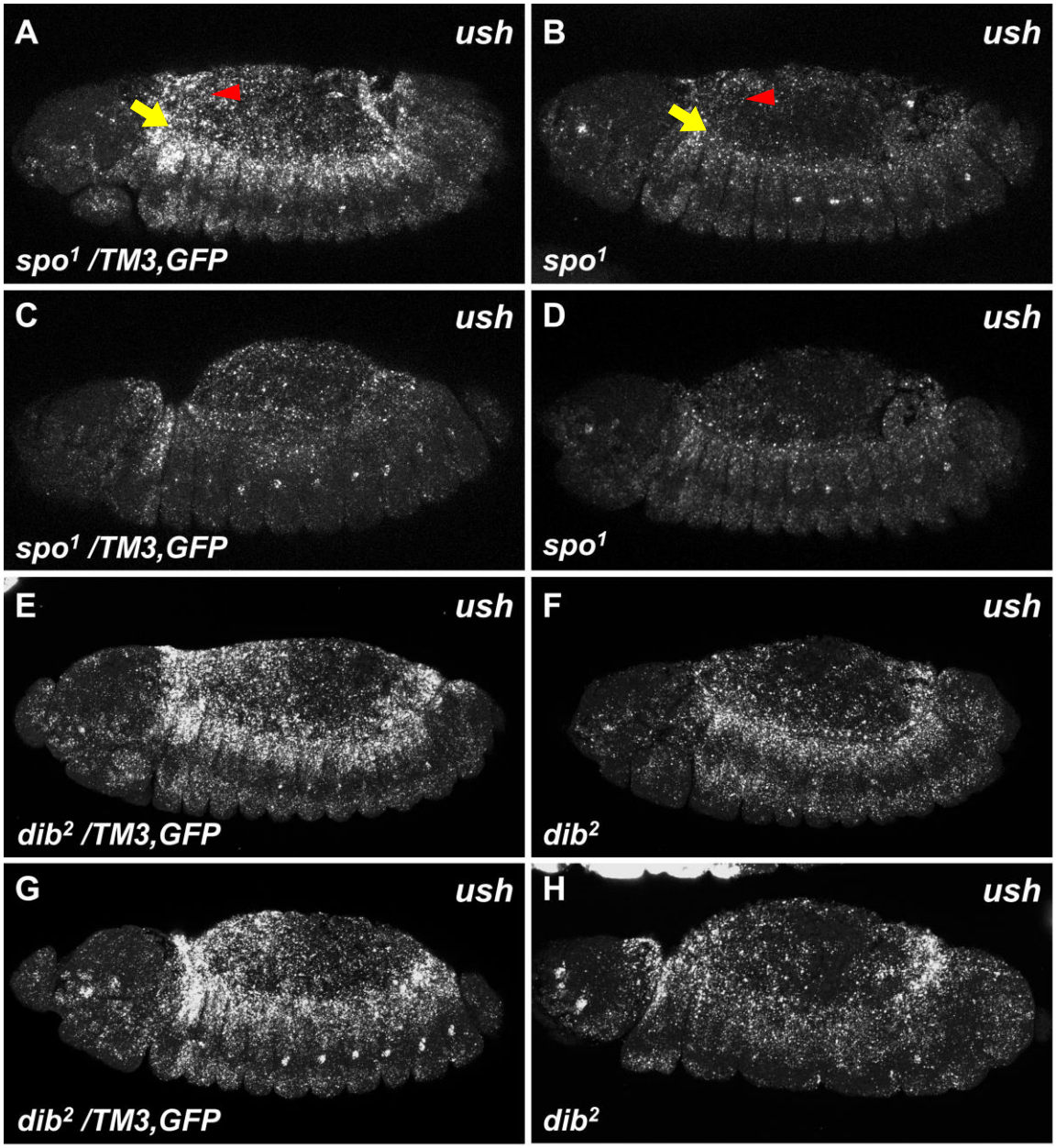


continues on next page…

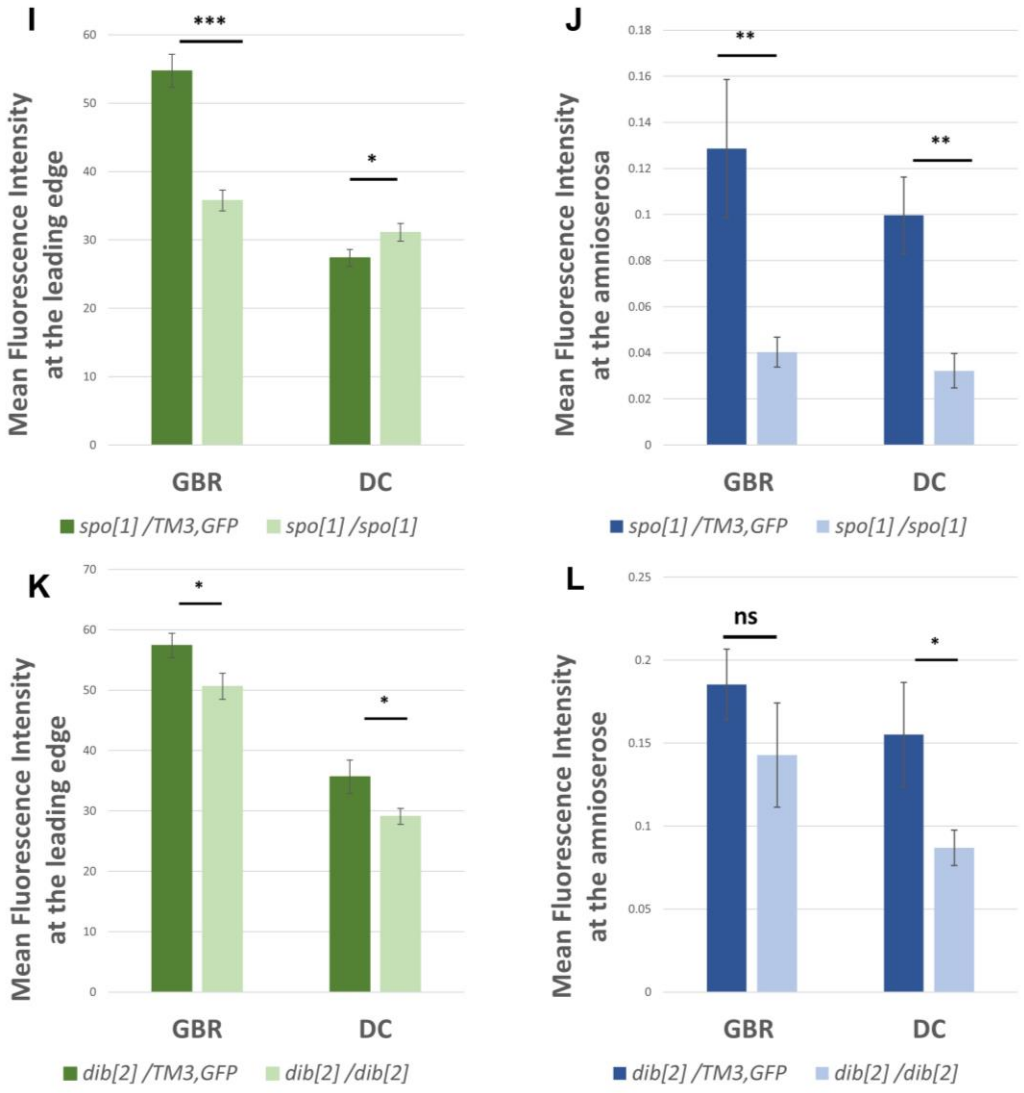


**Figure 3.2.7 Effects of ecdysone signaling on *ush* expression.**

FISH against *ush* on GBR- and DC-staged embryos. (A-D) Embryos heterozygous mutant for *spo*$^{1}$, which served as a wild-type control, showed typical *ush* transcript distributions during GBR (A) and DC (C). Homozygous mutant embryos, however, displayed significantly reduced *ush* transcript levels in the AS (see red arrowhead) and DME cells (yellow arrow indicates the boundary between the AS and DME) during GBR (B) and DC (D). (E-H) Similar results were observed between *dib*$^{2}$ and *spo*$^{1}$, except that *dib*$^{2}$ homozygotes did not show a significant difference in transcript levels in the AS during GBR. (I,J) Quantification of the FISH signals. Sample sizes for DME cell measurements are: *spo*$^{1}$ heterozygotes (GBR = 35 segments in 5 embryos, DC = 56/8), *spo*$^{1}$ homozygotes (GBR + DC = 49/7), *dib*$^{2}$ heterozygotes (GBR = 56/8, DC = 49/7), *dib*$^{2}$ homozygotes (GBR = 42/6, DC = 56/8). Sample sizes for AS measurements are: *spo*$^{1}$ heterozygotes (GBR = 5 embryos, DC = 8), *spo*$^{1}$ homozygotes (GBR + DC = 7), *dib*$^{2}$ heterozygotes (GBR = 8, DC = 7), *dib*$^{2}$ homozygotes (GBR = 6, DC = 8). * $p<0.05$, ** $p<0.01$, *** $p<0.001$.

As some of the data derived from embryos mutant for either *spo* or *dib*, which lack 20E production, were not determined to be statistically significant, gain-of-function analysis was also performed in order to confirm the results. This was accomplished by soaking wild-type embryos in 20E, then performing FISH against the candidate genes in question. In 20E-treated wild-type embryos, both *ecr* and *ush* transcript levels were noticeably elevated in the AS and epidermis when compared to ethanol-treated wild-type embryos, which were used as a negative control (Figure 3.2.8). Unfortunately, effects on *jupiter* transcript levels have yet to be evaluated. In addition to 20E-treatment, *UAS-ecr* was overexpressed in segmental stripes using the *prd-Gal4* driver. However, *zip* and *ush* expression were not elevated in prd[+] stripes (Figure 3.2.9). These results indicate that ecdysone-activated EcR, and not just higher overall levels of EcR, is responsible for gene expression.

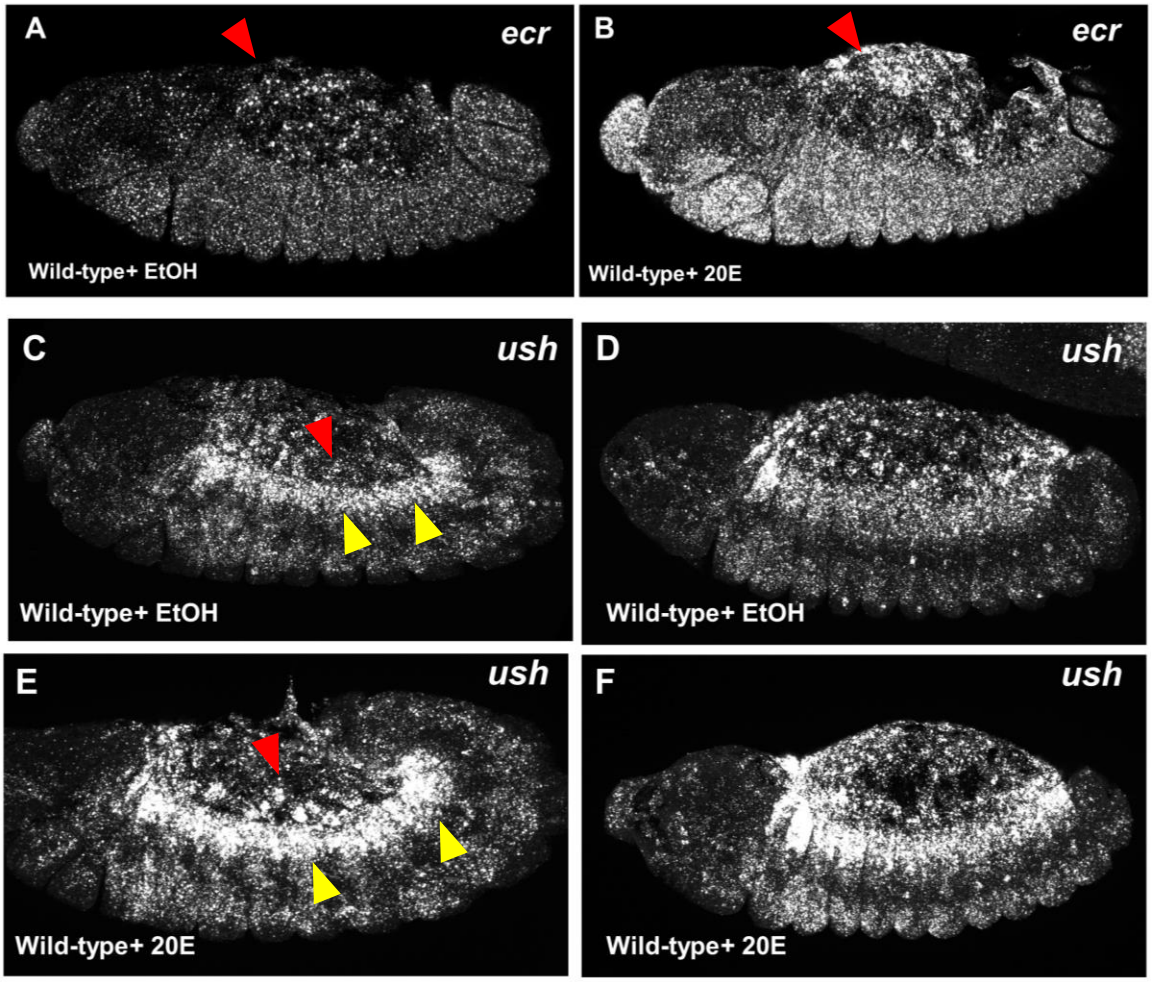


**Figure 3.2.8 Effects of 20E-treatment on *ecr* and *ush* expression.**

FISH against *ecr* and *ush* on GBR- and DC-staged embryos. (A,B) Wild-type embryos treated with exogenous 20E showed elevated *ecr* expression in the AS (see red arrowhead) and epidermis during late GBR (B) in comparison to ethanol-treated embryos (A), which served as a negative control. (C-F) 20E-treated wild-type embryos also displayed elevations in *ush* transcript levels in the AS (red arrowhead) and dorsal epidermis (yellow arrowhead) during late GBR (E) and DC (F) when compared to ethanol-treated wild-type embryos (C,D).

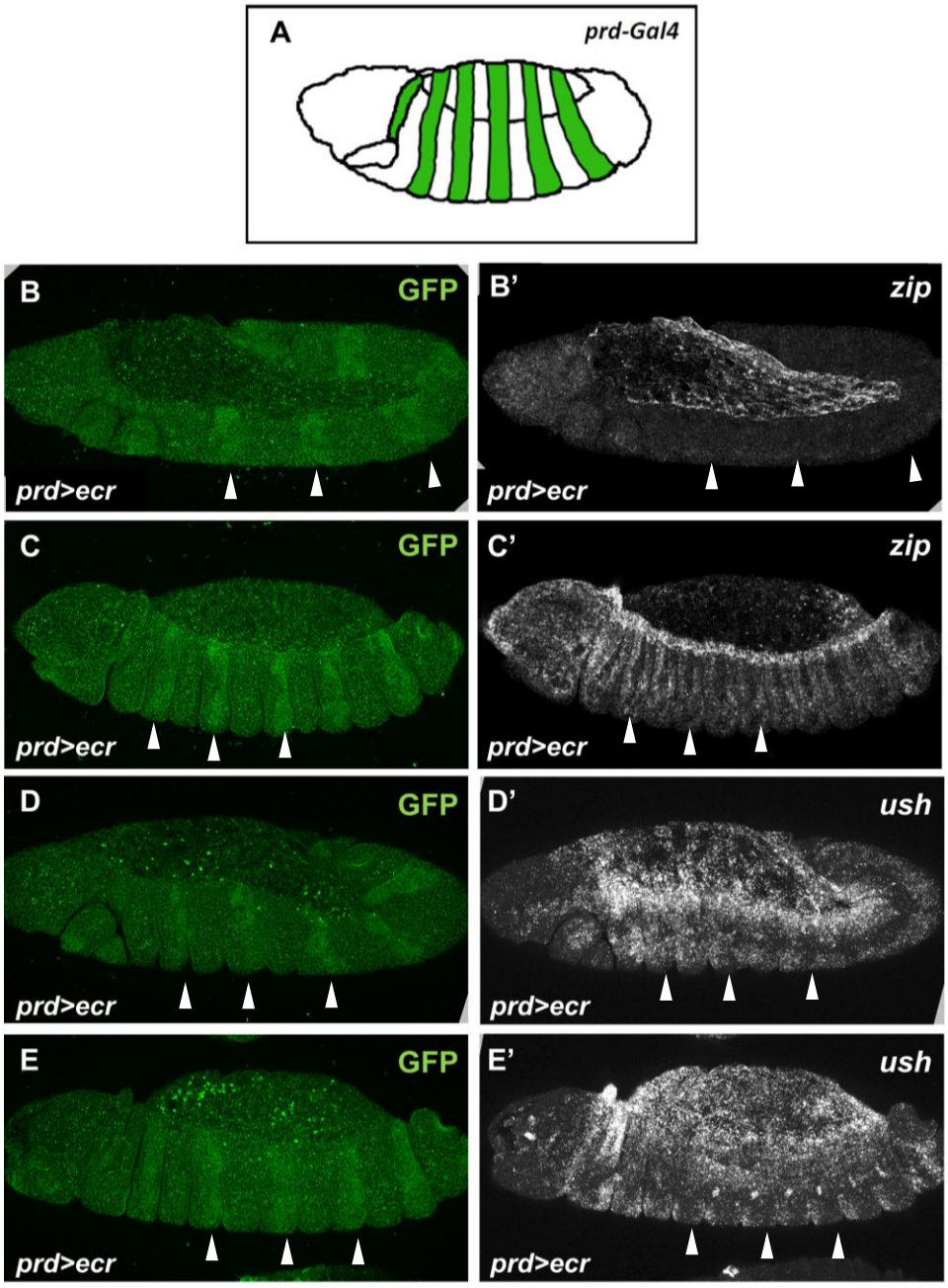


**Figure 3.2.9 Effects of EcR overexpression on *zip* and *ush* expression.**

FISH against *zip* and *ush* on GBR- and DC-staged embryos overexpressing *UAS-ecr* and *UAS-GFP* via the segmental *prd-Gal4* driver (A). (B-C') GFP immunostains demarcate prd[+] stripes (B,C) (see white arrowheads), and indirectly shows where EcR is being overexpressed. Overexpression of EcR does not elevate *zip* expression during GBR (B') or DC (C'). (D-E') Similar negative results were observed for *ush*. (see white arrowheads)

Unexpectedly, the transcript levels for some of the candidate genes appeared to be elevated during GBR and DC when 20E biosynthesis was impaired. *rhogap71e* was only expressed in the dorsal vessel of wild-type embryos during DC (Figure 3.2.10 O). However, ectopic expression was observed in the dorsal epidermis of both *spo*$^{1}$ and *dib*$^{2}$ homozygous mutants during GBR and DC (Figure 3.2.10). In addition, the expressions of *jar* and *zasp52* were generally shown to be significantly elevated in the AS, though some of the data were determined to be statistically insignificant (Figure 3.2.11 and Figure 3.2.12). For both candidates, the transcript levels remained unchanged in the DME cells (quantifications not shown). In all, these results suggest that ecdysone can down-regulate the expression of some genes during late embryogenesis through an as of yet identified mechanism.

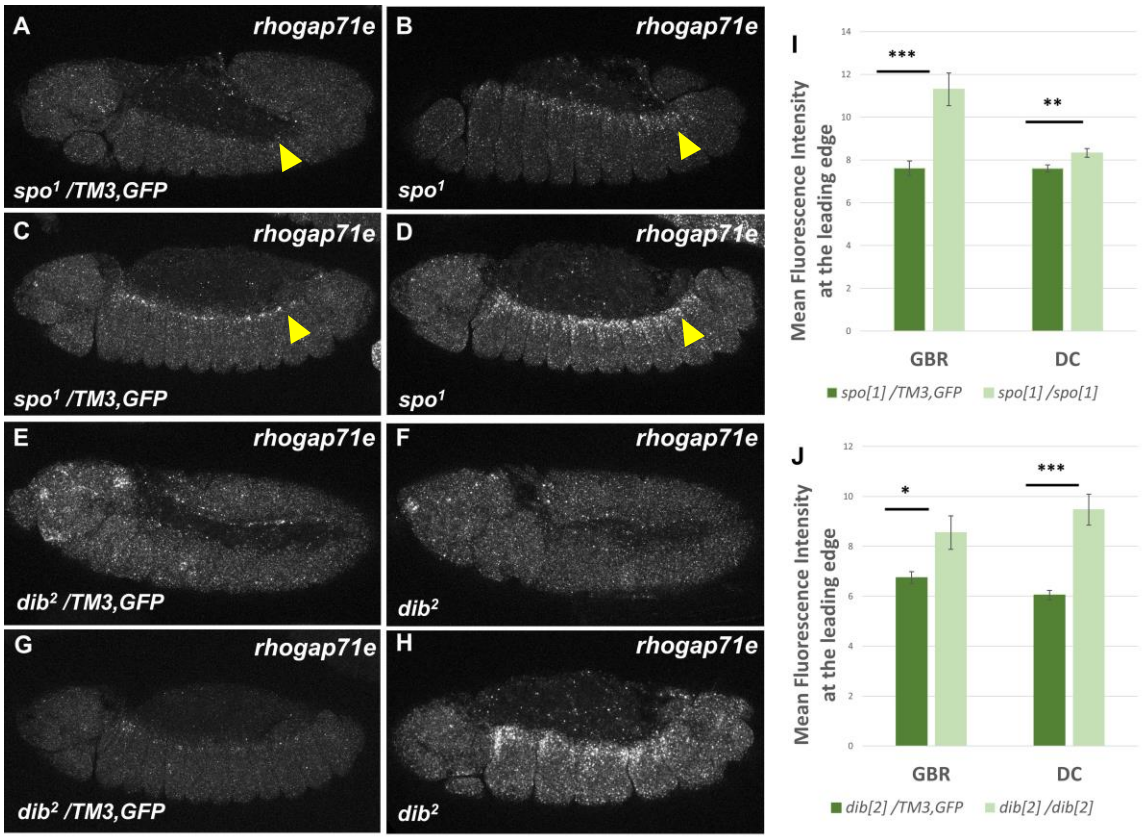


**Figure 3.2.10 Effects of ecdysone signaling on *rhogap71e* expression.**

FISH against *rhogap71e* on GBR- and DC-staged embryos. (A-D) Embryos heterozygous mutant for *spo*$^{1}$, which served as a wild-type control, showed typical *rhogap71e* transcript distributions during GBR (A) and DC (C). Homozygous mutant embryos, however, displayed ectopic elevations of *rhogap71e* transcripts in the dorsal epidermis (see yellow arrowhead) during GBR (B) and DC (D). (E-H) Similar results were observed between *dib*$^{2}$ and *spo*$^{1}$. (I,J) Quantification of the FISH signals. Sample sizes are: *spo*$^{1}$ heterozygotes (GBR = 18 segments in 3 embryos, DC = 32/4), *spo*$^{1}$ homozygotes (GBR = 18/3, DC = 32/4), *dib*$^{2}$ heterozygotes (GBR = 16/3, DC = 24/3), *dib*$^{2}$ homozygotes (GBR = 16/3, DC = 24/3). * p<0.05, p<0.01, *** p<0.001.

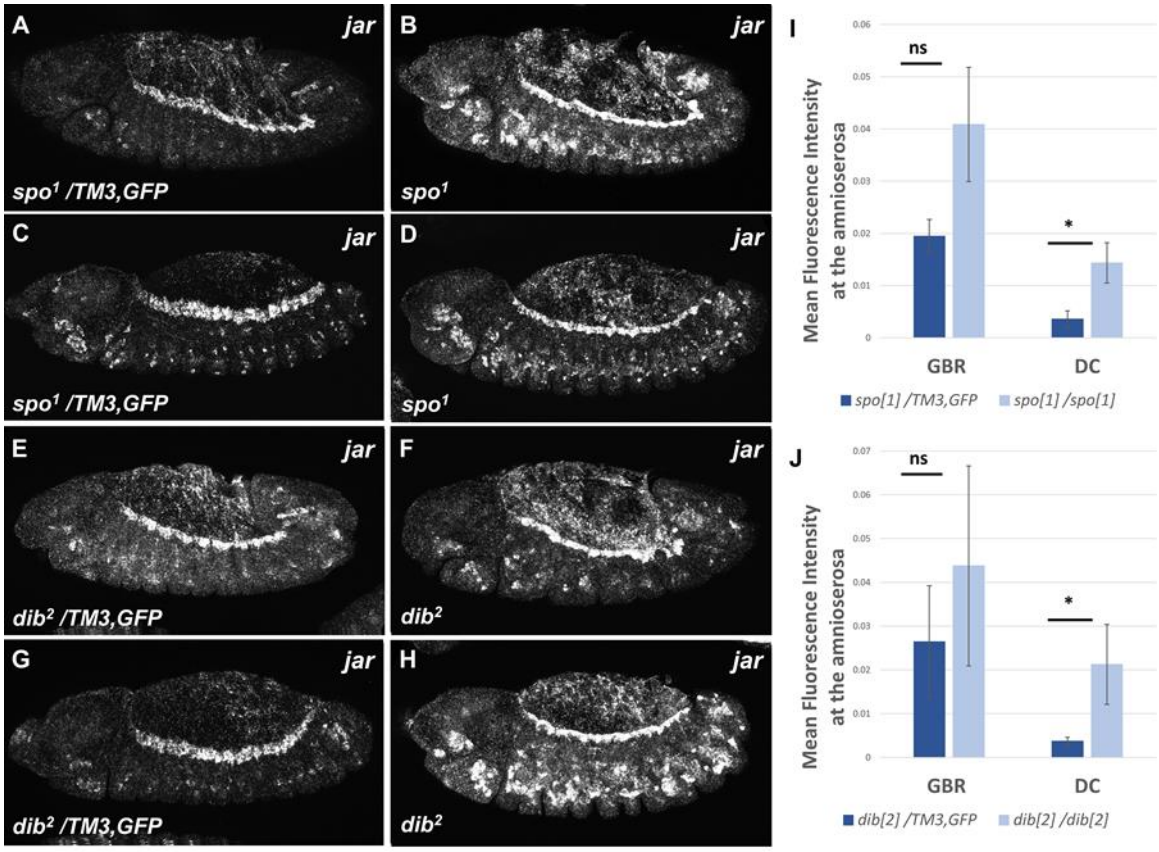


**Figure 3.2.11 Effects of ecdysone signaling on *jar* expression.**

FISH against *jar* on GBR- and DC-staged embryos. (A-D) Embryos heterozygous mutant for *spo*$^{1}$, which served as a wild-type control, showed typical *jar* transcript distributions during GBR (A) and DC (C). Homozygous mutant embryos, however, displayed significantly elevated *jar* transcript levels in the AS during DC (D) but not GBR (B). No significant effects were observed in the DME cells (A-D; quantifications not shown). (E-H) Similar results were observed between *dib*$^{2}$ and *spo*$^{1}$. (I,J) Quantification of the FISH signals. Sample sizes are: *spo*$^{1}$ heterozygotes (GBR = 7 embryos, DC = 8), *spo*$^{1}$ homozygotes (GBR = 6, DC = 11), *dib*$^{2}$ heterozygotes (GBR = 6, DC = 10), *dib*$^{2}$ homozygotes (GBR = 4, DC = 11). * $p<0.05$.

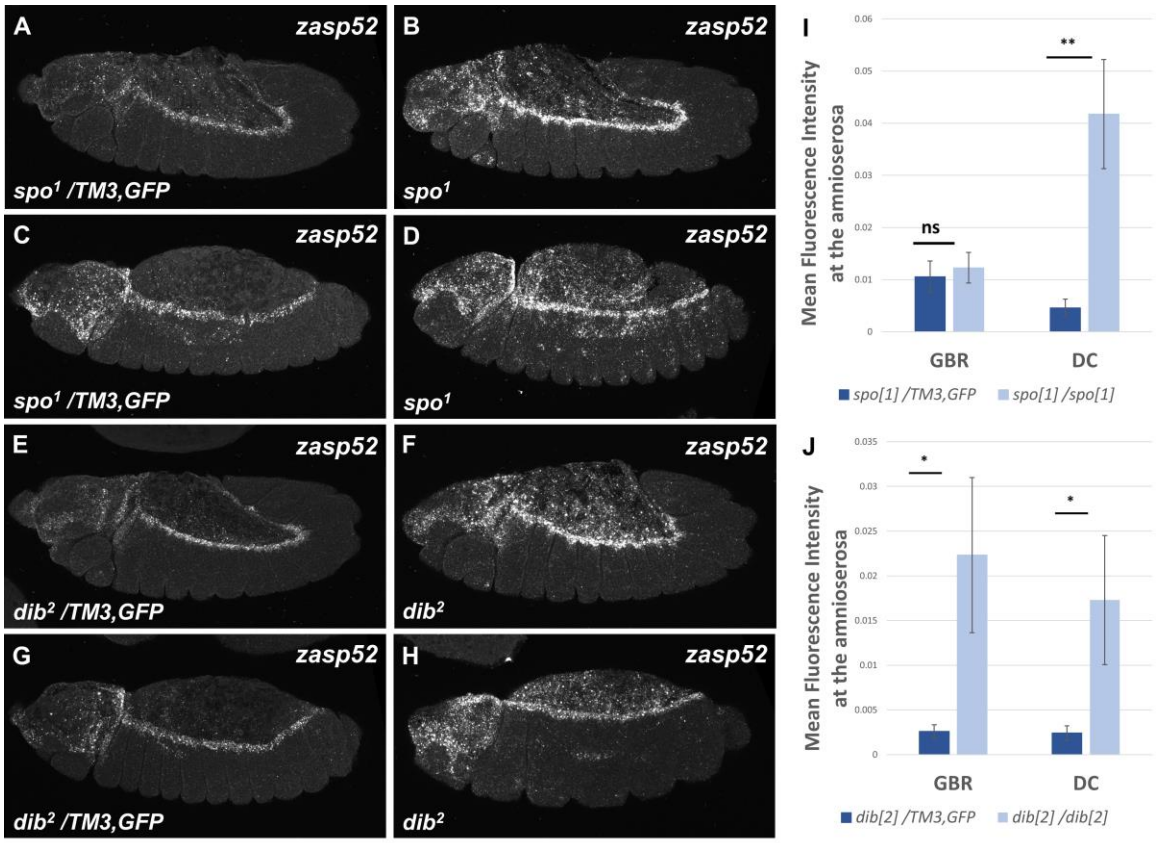


**Figure 3.2.12 Effects of ecdysone signaling on *zasp52* expression.**

FISH against *zasp52* on GBR- and DC-staged embryos. (A-D) Embryos heterozygous mutant for *spo*$^{1}$, which served as a wild-type control, showed typical *zasp52* transcript distributions during GBR (A) and DC (C). Homozygous mutant embryos, however, displayed significantly elevated *zasp52* transcript levels in the AS during DC (D) but not GBR (B). No significant effects were observed in the DME cells (A-D; quantifications not shown). (E-H) Similar results were observed between *dib*$^{2}$ and *spo*$^{1}$, except that *dib*$^{2}$ homozygotes showed a significant difference in transcript levels in the AS during GBR. (I,J) Quantification of the FISH signals. Sample sizes are: *spo*$^{1}$ heterozygotes (GBR = 5 embryos, DC = 8), *spo*$^{1}$ homozygotes (GBR = 6, DC = 10), *dib*$^{2}$ heterozygotes (GBR + DC = 6), *dib*$^{2}$ homozygotes (GBR + DC = 6). * $p<0.05$, ** $p<0.01$.

Considering all of the data above, the expression of *ecr, ush, jupiter* are positively regulated by ecdysone-activated EcR during late embryonic development. As these results show similarities to those pertaining to *zip*, these candidates were characterized further in regards to whether their expressions can also be regulated by Jun. Interestingly, the expressions of *jar*, *rhogap71e* and *zasp52* were shown to be suppressed by ecdysone signaling. *rhogap71e* was chosen for further work as it may function as a GAP for Rho1, which will be discussed in section 3.3.

### 3.2.3. Jun promotes the expression of *ecr*, *jupiter* and *ush*

In the previous section, three of the candidate genes were shown to be positively regulated by ecdysone-activated EcR: *ecr*, *jupiter* and *ush*. Here, it was next assessed whether these candidates can also be regulated by Jun. In order to address this question, FISH against the candidates was performed on *jun* loss-of-function embryos carrying either the *jun* deficiency, *Df(2R)BSC303*, or one of the *jun* mutations, $jun^{lA109}$ and $jun^{76\text{-}19}$ (see Table 1 at the end of section 3.2 for a summary of all the results). A detailed description on how the FISH signals were quantified can be found in section 2.9.

First, *ecr* transcript levels were significantly reduced in the AS during GBR in both *Df(2R)BSC303* and $jun^{76\text{-}19}$ homozygotes when compared to their respective heterozygous siblings, which were used as wild-type controls for these experiments (Figure 3.2.13 A-D,G,H). *ecr* transcript levels also appeared to be reduced in a noticeable subset of $jun^{lA109}$ homozygotes, but high signal variability within the dataset made measurements statistically insignificant (Figure 3.2.13 E,F,I). During GBR and DC, *jupiter* transcript levels were significantly decreased in the DME cells for all three *jun* loss-of-function lines (Figure 3.2.14 A-M,O,Q). Though all the lines also appeared to show an observable decrease in transcript levels in the AS, only $jun^{76\text{-}19}$ homozygotes showed a statistically significant decrease (Figure 3.2.14 A-L,N,P,R). For the other lines, the signal variability was again too high for these datasets to reveal any statistically significant differences. Finally, for all three *jun* loss-of-function lines, *ush* transcript levels were significantly reduced in the DME cells during GBR but not DC (Figure 3.2.15 A-M,O,Q). Significant reductions in transcript levels were also observed in the AS during GBR and DC, but only for $jun^{76\text{-}19}$ homozygotes (Figure 3.2.15 A-L,N,P,R). This may be due to the observation that *Df(2R)BSC303* and $jun^{lA109}$ heterozygotes appeared to have signal intensities equivalent to their homozygous siblings (compare the scale bars for Figure 3.2.15 N,R to P), indicating that *ush* transcript levels may be more sensitive to haploinsufficiency in these lines. Thus, wild-type embryos should have been used for the control. Though some data sets were determined to be statistically insignificant, the general trends indicate that Jun positively regulates the expression of *ecr*, *jupiter* and *ush* during GBR and DC.

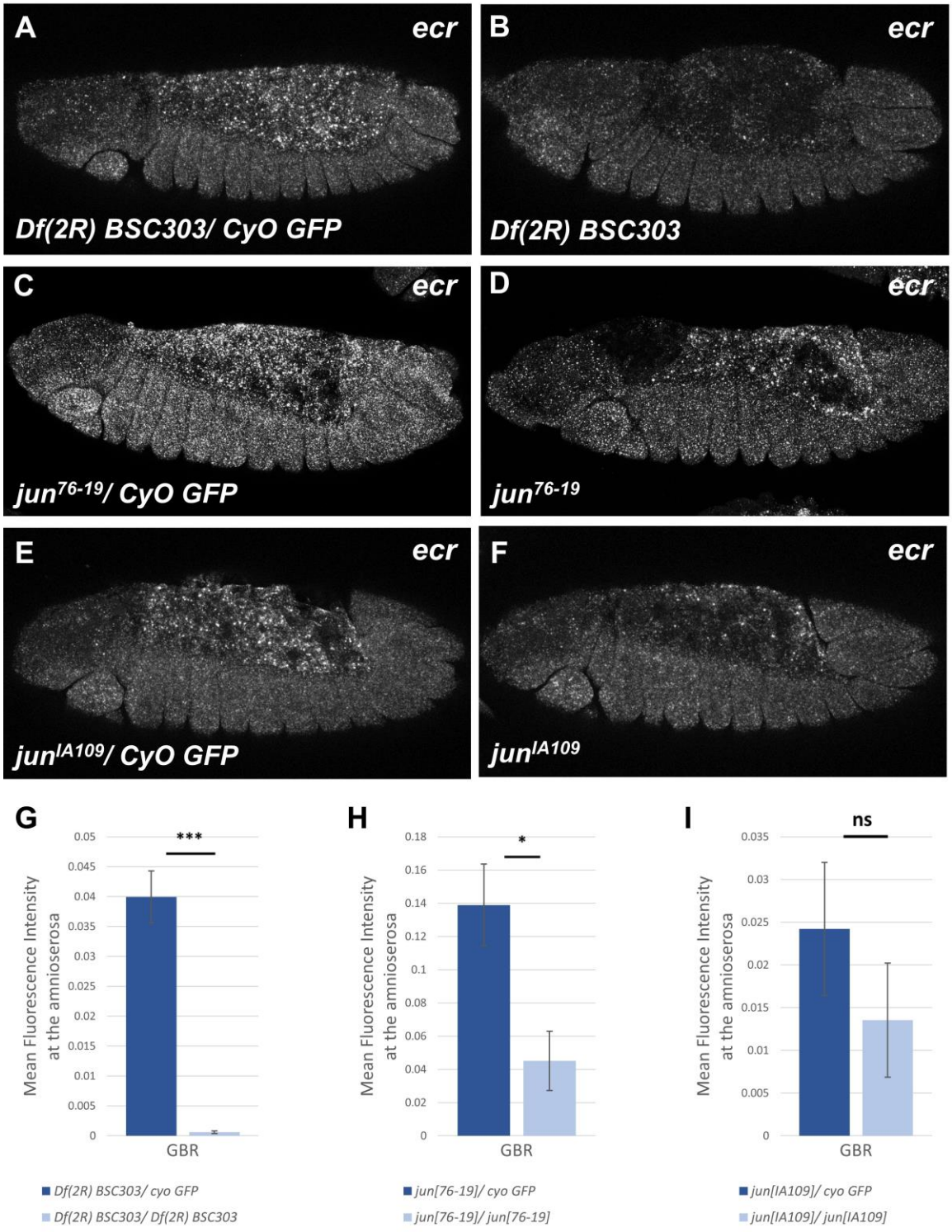


**Figure 3.2.13 *ecr* expression in *jun* decifient and mutant embryos.**

FISH against *ecr* on GBR-staged embryos. (A-B) Embryos heterozygous for the *Df(2R)BSC303* deficiency, which served as a wild-type control, showed typical *ecr* transcript distributions during GBR (A). *Df(2R)BSC303* homozygotes, however, displayed significantly reduced transcript levels

in the AS during GBR (B). (C,D) Similar results were observed for *jun*$^{76\text{-}19}$. (E,F) *jun*$^{lA109}$ homozygotes did not show a significant difference in *ecr* transcript levels in the AS during GBR (F) when compared to their heterozygous siblings (E). (G-I) Quantification of the FISH signals. Sample sizes are: *Df(2R)BSC303* heterozygotes (GBR = 4 embryos), *Df(2R)BSC303* homozygotes (GBR = 4), *jun*$^{76\text{-}19}$ heterozygotes (GBR = 9), *jun*$^{76\text{-}19}$ homozygotes (GBR = 6), *jun*$^{lA109}$ heterozygotes (GBR = 7), *jun*$^{lA109}$ homozygotes (GBR = 8). * $p<0.05$, *** $p<0.001$.

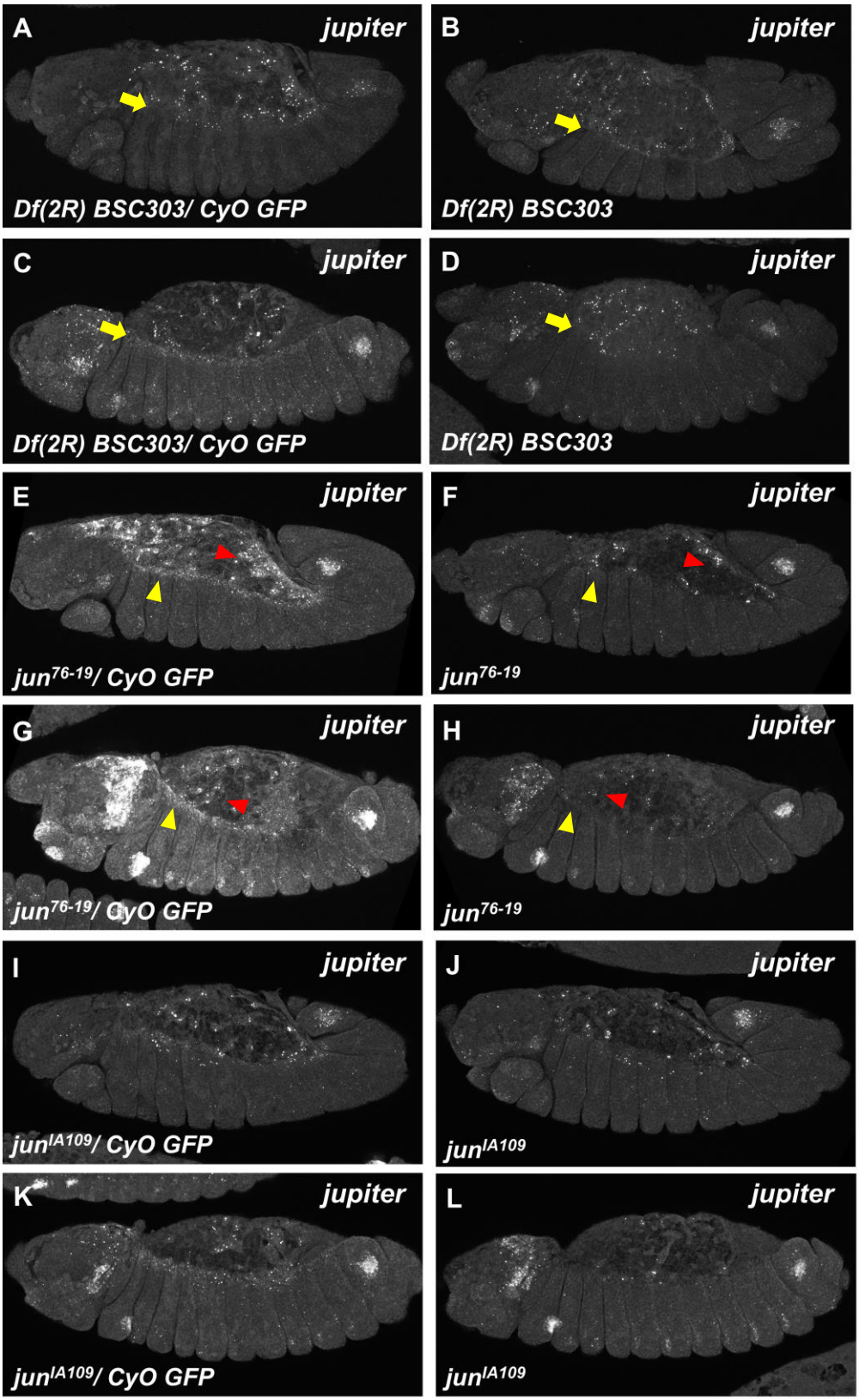


continues on next page…

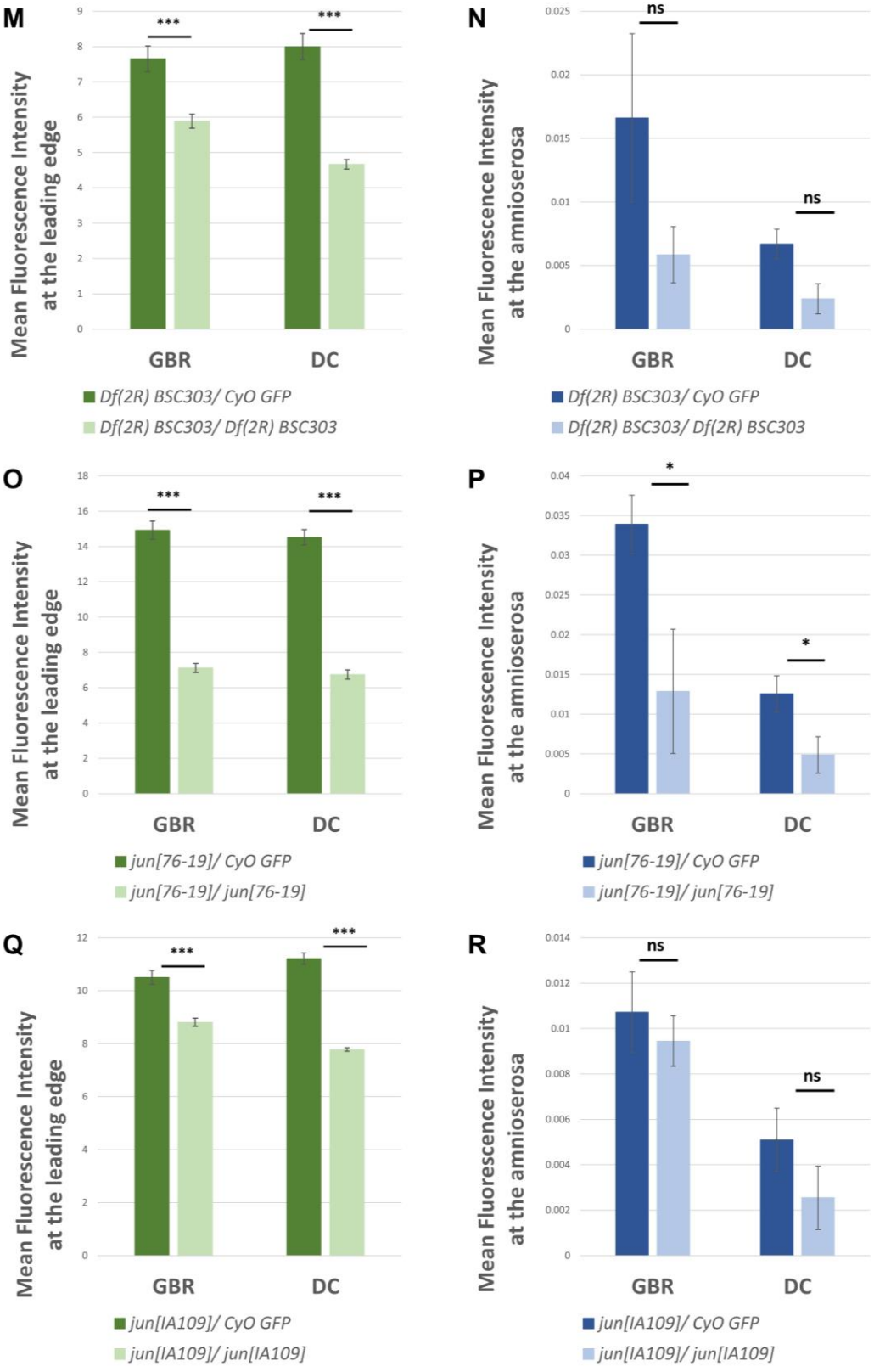
M
Mean Fluorescence Intensity at the leading edge
***
***
GBR
DC
Df(2R) BSC303/ CyO GFP
Df(2R) BSC303/ Df(2R) BSC303
N
Mean Fluorescence Intensity at the amnioserosa
ns
ns
GBR
DC
Df(2R) BSC303/ CyO GFP
Df(2R) BSC303/ Df(2R) BSC303
O
Mean Fluorescence Intensity at the leading edge
***
***
GBR
DC
jun[76-19]/ CyO GFP
jun[76-19]/ jun[76-19]
P
Mean Fluorescence Intensity at the amnioserosa
*
*
GBR
DC
jun[76-19]/ CyO GFP
jun[76-19]/ jun[76-19]
Q
Mean Fluorescence Intensity at the leading edge
***
***
GBR
DC
jun[IA109]/ CyO GFP
jun[IA109]/ jun[IA109]
R
Mean Fluorescence Intensity at the amnioserosa
ns
ns
GBR
DC
jun[IA109]/ CyO GFP
jun[IA109]/ jun[IA109]

**Figure 3.2.14 *jupiter* expression in *jun* decifient and mutant embryos.**

FISH against *jupiter* on GBR- and DC-staged embryos. The boundary between the AS and DME is indicated by yellow arrow. (A-D) Embryos heterozygous for the *Df(2R)BSC303* deficiency, which served as a wild-type control, showed typical *jupiter* transcript distributions during GBR (A) and DC (C). *Df(2R)BSC303* homozygotes, however, displayed significantly reduced transcript levels in the DME cells during GBR (B) and DC (D), but no significant changes in the AS (B,D) (E-H) During GBR and DC, $jun^{76\text{-}19}$ homozygotes showed significant decreases in *jupiter* transcript levels in the DME cells (yellow arrowhead) and AS (red arrowhead) (F,H) when compared to their heterozygous siblings (E,G). (I-L) Similar results were observed between $jun^{lA109}$ and *Df(2R)BSC303*. (M-R) Quantification of the FISH signals. Sample sizes for DME cell measurements are: *Df(2R)BSC303* heterozygotes (GBR = 49 segments in 7 embryos, DC = 35/5), *Df(2R)BSC303* homozygotes (GBR = 49/7, DC = 28/4), $jun^{76\text{-}19}$ heterozygotes (GBR = 35/5, DC = 28/4), $jun^{76\text{-}19}$ homozygotes (GBR = 35/5, DC = 28/4), $jun^{lA109}$ heterozygotes (GBR = 42/6, DC = 49/7), $jun^{lA109}$ homozygotes (GBR + DC = 35/5). Sample sizes for AS measurements are: *Df(2R)BSC303* heterozygotes (GBR = 7 embryos, DC = 5), *Df(2R)BSC303* homozygotes (GBR = 7, DC = 4), $jun^{76\text{-}19}$ heterozygotes (GBR = 5, DC = 4), $jun^{76\text{-}19}$ homozygotes (GBR = 5, DC = 4), $jun^{lA109}$ heterozygotes (GBR = 6, DC = 7), $jun^{lA109}$ homozygotes (GBR + DC = 5). * $p<0.05$, *** $p<0.001$.

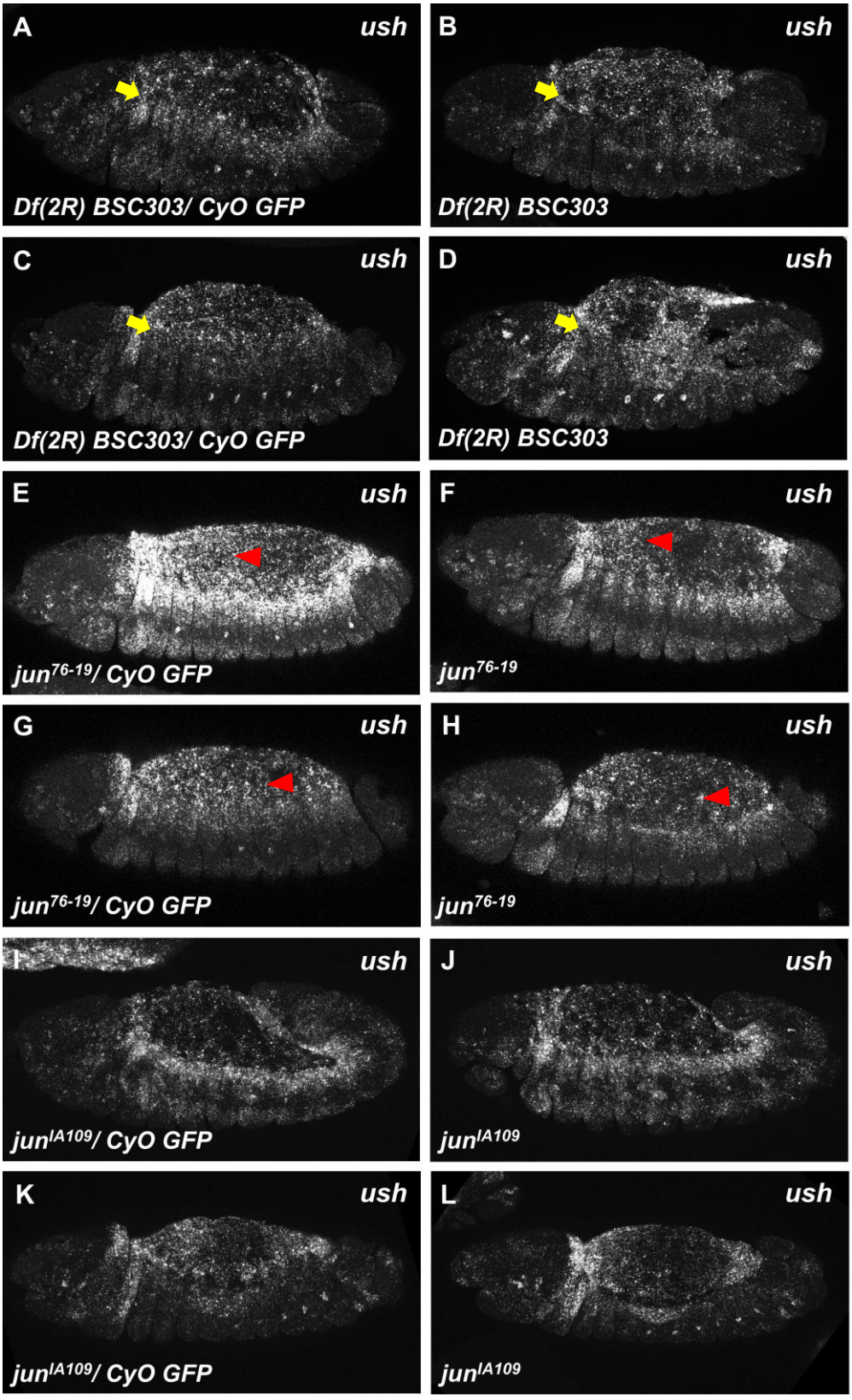


continues on next page…

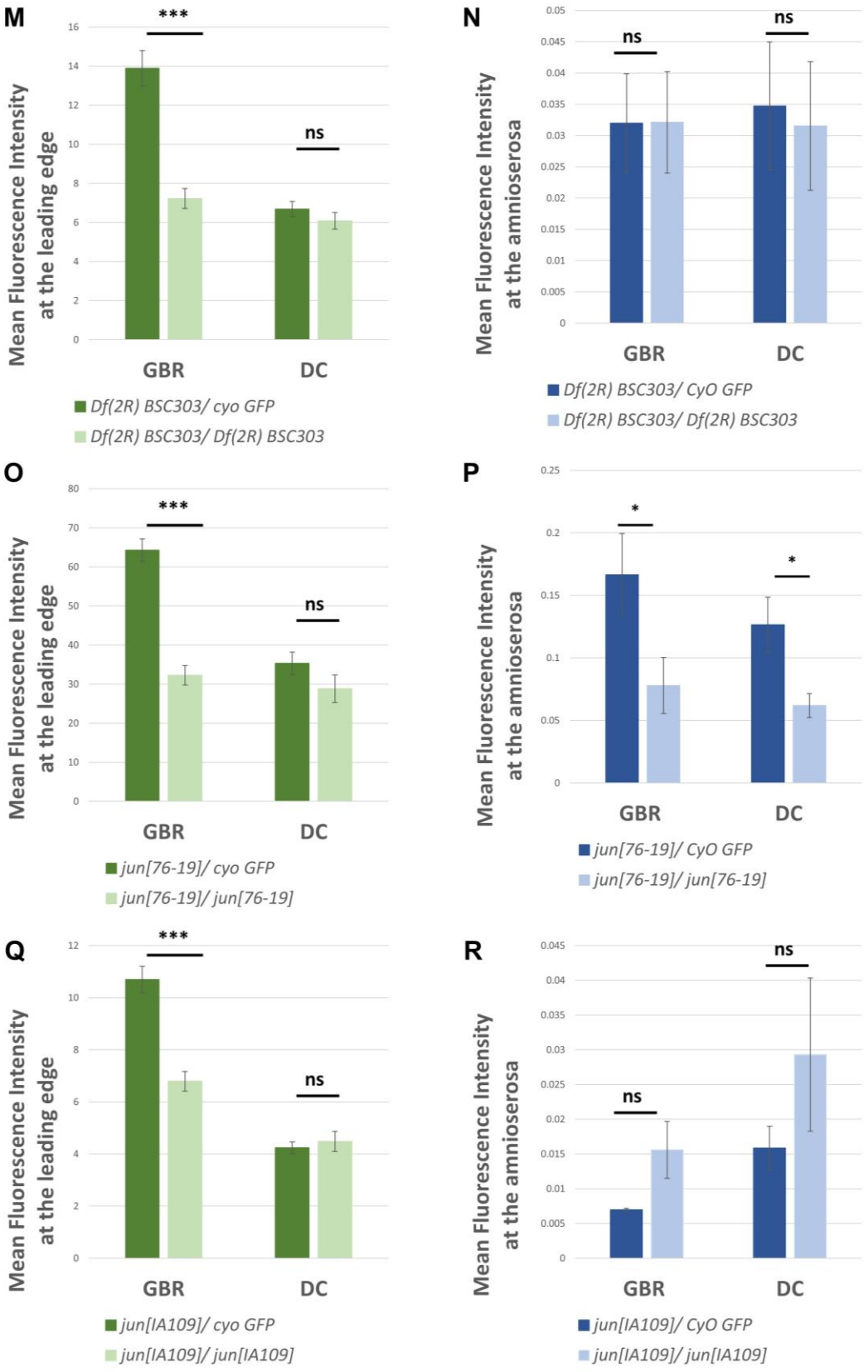
M
***
ns
Mean Fluorescence Intensity at the leading edge
GBR
DC
Df(2R) BSC303/ cyo GFP
Df(2R) BSC303/ Df(2R) BSC303
N
ns
ns
Mean Fluorescence Intensity at the amnioserosa
GBR
DC
Df(2R) BSC303/ CyO GFP
Df(2R) BSC303/ Df(2R) BSC303
O
***
ns
Mean Fluorescence Intensity at the leading edge
GBR
DC
jun[76-19]/ cyo GFP
jun[76-19]/ jun[76-19]
P
*
*
Mean Fluorescence Intensity at the amnioserosa
GBR
DC
jun[76-19]/ CyO GFP
jun[76-19]/ jun[76-19]
Q
***
ns
Mean Fluorescence Intensity at the leading edge
GBR
DC
jun[IA109]/ cyo GFP
jun[IA109]/ jun[IA109]
R
ns
ns
Mean Fluorescence Intensity at the amnioserosa
GBR
DC
jun[IA109]/ CyO GFP
jun[IA109]/ jun[IA109]

**Figure 3.2.15 *ush* expression in *jun* decifient and mutant embryos.**

FISH against *ush* on GBR- and DC-staged embryos. The boundary between the AS and DME is indicated by yellow arrow. (A-D) Embryos heterozygous for the *Df(2R)BSC303* deficiency, which served as a wild-type control, showed typical *ush* transcript distributions during GBR (A) and DC (C). *Df(2R)BSC303* homozygotes, however, displayed significantly reduced transcript levels in the DME cells during GBR (B) but not DC (D). No significant changes in the AS were observed (B,D). (E-H) Similar results were observed between $jun^{iA109}$ and *Df(2R)BSC303*, except that $jun^{76\text{-}19}$ homozygotes showed significant decreases in *ush* transcript levels in the AS during GBR (F) and DC (H) (see red arrowheads) when compared to their heterozygous siblings (E,G). (M-R) Quantification of the FISH signals. Sample sizes for DME cell measurements are: *Df(2R)BSC303* heterozygotes (GBR = 49 segments in 7 embryos, DC = 42/6), *Df(2R)BSC303* homozygotes (GBR = 42/6, DC = 49/7), $jun^{76\text{-}19}$ heterozygotes (GBR = 35/5, DC = 42/6), $jun^{76\text{-}19}$ homozygotes (GBR = 56/8, DC = 35/5), $jun^{lA109}$ heterozygotes (GBR = 35/5, DC = 42/6), $jun^{lA109}$ homozygotes (GBR = 35/5, DC = 42/6). Sample sizes for AS measurements are: *Df(2R)BSC303* heterozygotes (GBR = 7 embryos, DC = 5), *Df(2R)BSC303* homozygotes (GBR = 4, DC = 7), $jun^{76\text{-}19}$ heterozygotes (GBR = 7, DC = 6), $jun^{76\text{-}19}$ homozygotes (GBR = 5, DC = 6), $jun^{lA109}$ heterozygotes (GBR + DC = 5), $jun^{lA109}$ homozygotes (GBR + DC = 6). * $p<0.05$, *** $p<0.001$.

In wild-type embryos, *rhogap71e* was only expressed in the dorsal vessel during DC. Interestingly, ectopic expression was observed in the dorsal epidermis when 20E synthesis was disrupted. To determine whether this mode of regulation requires Jun, *rhogap71e* expression was evaluated in the three *jun* loss-of-function lines. From the analyses, *rhogap71e* transcript levels were only significantly elevated in the dorsal vessel, not the dorsal epidermis, of $jun^{lA109}$ homozygous mutant embryos (Figure 3.2.16). These experiments were only done once, and should be repeated in the near future. But these preliminary results may indicate that Jun-mediated signaling is required for supressing *rhogap71e* expression in the dorsal vessel, whereas ecdysone signaling is required for supressing *rhogap71e* expression in the dorsal epidermis.

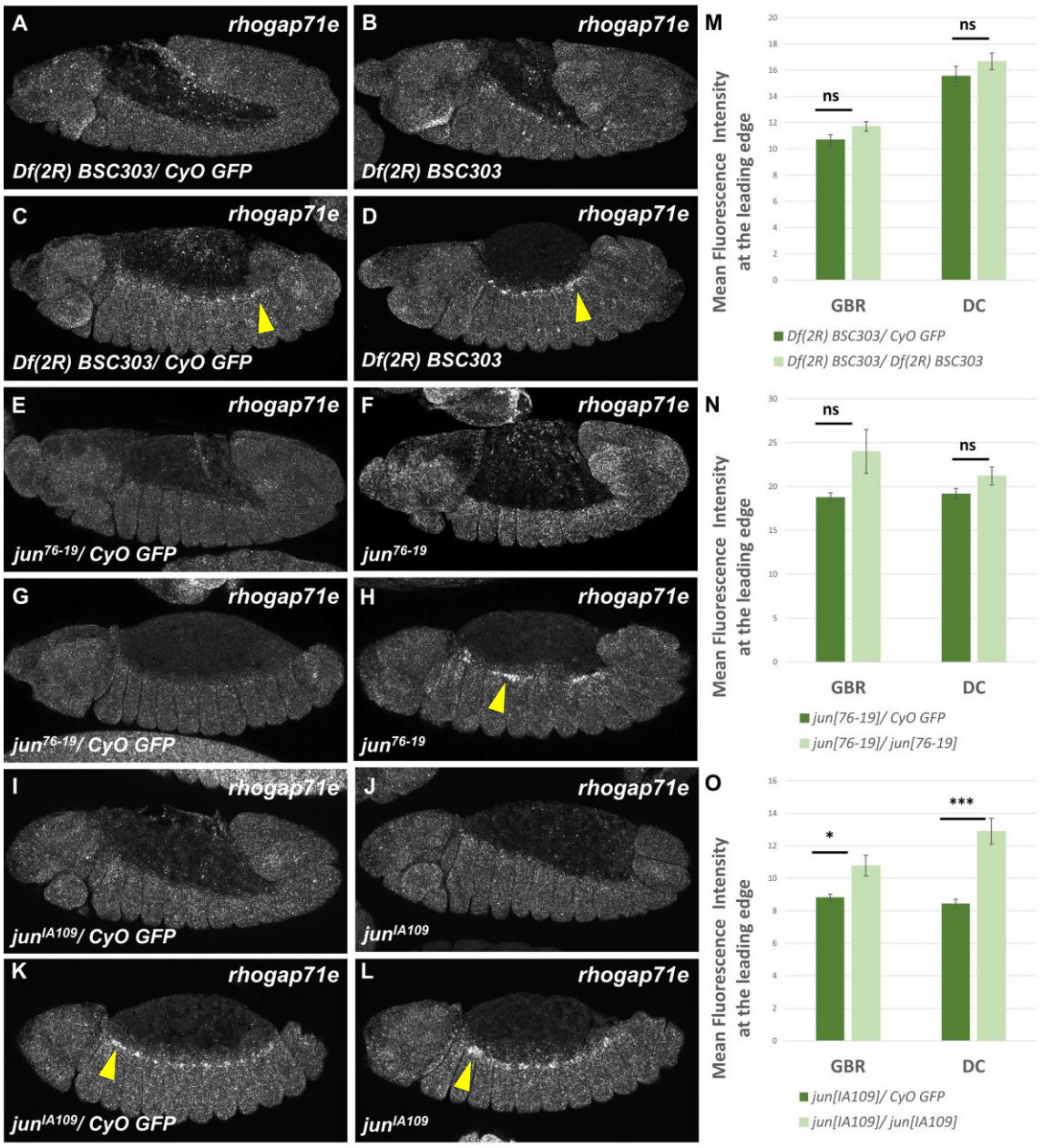


**Figure 3.2.16 *rhogap71e* expression in *jun* decifient and mutant embryos.**

FISH against *rhogap71e* on GBR- and DC-staged embryos. (A-D) Embryos heterozygous for the *Df(2R)BSC303* deficiency, which served as a wild-type control, showed typical *rhogap71e* transcript distributions during GBR (A) and DC (C) which is expression in the dorsal epidermis (indicated by yellow arrowhead). *Df(2R)BSC303* homozygotes showed no significant changes in transcript levels (B,D). (E-H) Similar results were observed between $jun^{76\text{-}19}$ and *Df(2R)BSC303*. (I-L) $jun^{IA109}$ homozygotes showed significant elevations in *rhogap71e* transcript levels in the dorsal vessel during GBR (J) and DC (L) when compared to their heterozygous siblings (I,K) (see yellow arrowhead). (M-O) Quantification of the FISH signals. Sample sizes: *Df(2R)BSC303* heterozygotes (GBR + DC = 35 segments in 5 embryos), *Df(2R)BSC303* homozygotes (GBR = 35/5, DC = 48/6), $jun^{76\text{-}19}$ heterozygotes (GBR = 8/1, DC = 16/2), $jun^{76\text{-}19}$ homozygotes (GBR = 16/2, DC = 24/3),

*jun*$^{lA109}$ heterozygotes (GBR + DC = 21/3), *jun*$^{lA109}$ homozygotes (GBR + DC = 21/3). * p<0.05, *** p<0.001.

### 3.2.4. EcR and Jun cooperate to regulate the expression of *ecr* and *ush*

Previous sections have shown that *ecr*, *jupiter* and *ush* are regulated by ecdysone-activated EcR and Jun. In this section, to confirm if ECR and Jun are cooperating to regulate the expression of these genes, epistatic analysis was performed. FISH against these genes were assessed in *jun* loss-of-function embryos exposed to exogenous 20E (see Table 1 at the end of section 3.2 for a summary of all the results). If ecdysone-activated EcR and Jun function independently of each other, then exogenous 20E should still be able to elevate their expression levels in embryos lacking *jun* to comparable levels observed in 20E-soaked wild-type embryos. A detailed description on how the FISH signals were quantified can be found in section 2.9.

Upon 20E-treatment of *jun*$^{lA109}$ heterozygotes, *ecr* expression was considerably elevated in the AS during GBR in comparison to ethanol-treated *jun*$^{lA109}$ heterozygotes (Figure 3.2.17 A,C,E). No such elevations were seen in 20E-treated *jun*$^{lA109}$ homozygotes (Figure 3.2.17 B,E). In fact, 20E-treated homozygotes showed comparable levels of *ecr* transcripts as ethanol-treated homozygotes (Figure 3.2.17 B,D,E), indicating that there was indeed no increase in expression. Similar results were observed for *ush* during DC (Figure 3.2.18). The experiment for *jupiter* could not be evaluated, as there was no difference in transcript levels detected between 20E-treated and ethanol-treated *jun*$^{76\text{-}19}$ heterozygotes (Figure 3.2.19). This indicates that the 20E-treatment did not work, as we expect to see increased *jupiter* transcript levels when the control embryos are soaked in exogenous 20E. This experiment will be repeated in the near future. Taken together, epistatic analyses strongly indicates that ecdysone-activated EcR cooperates with Jun to promote the expression of *ecr* and *ush* during late embryogenic development. Though the experiment failed, *jupiter* is also likely to be regulated by the EcR-Jun complex. This is because *jupiter* expression is shown to be regulated by both ecdysone signaling and Jun in this study, in addition to the fact the *jupiter* locus carries an EcR binding region that contains AP-1 consensus sites but no EcREs, which is found in *zip*, *ecr* and *ush*.

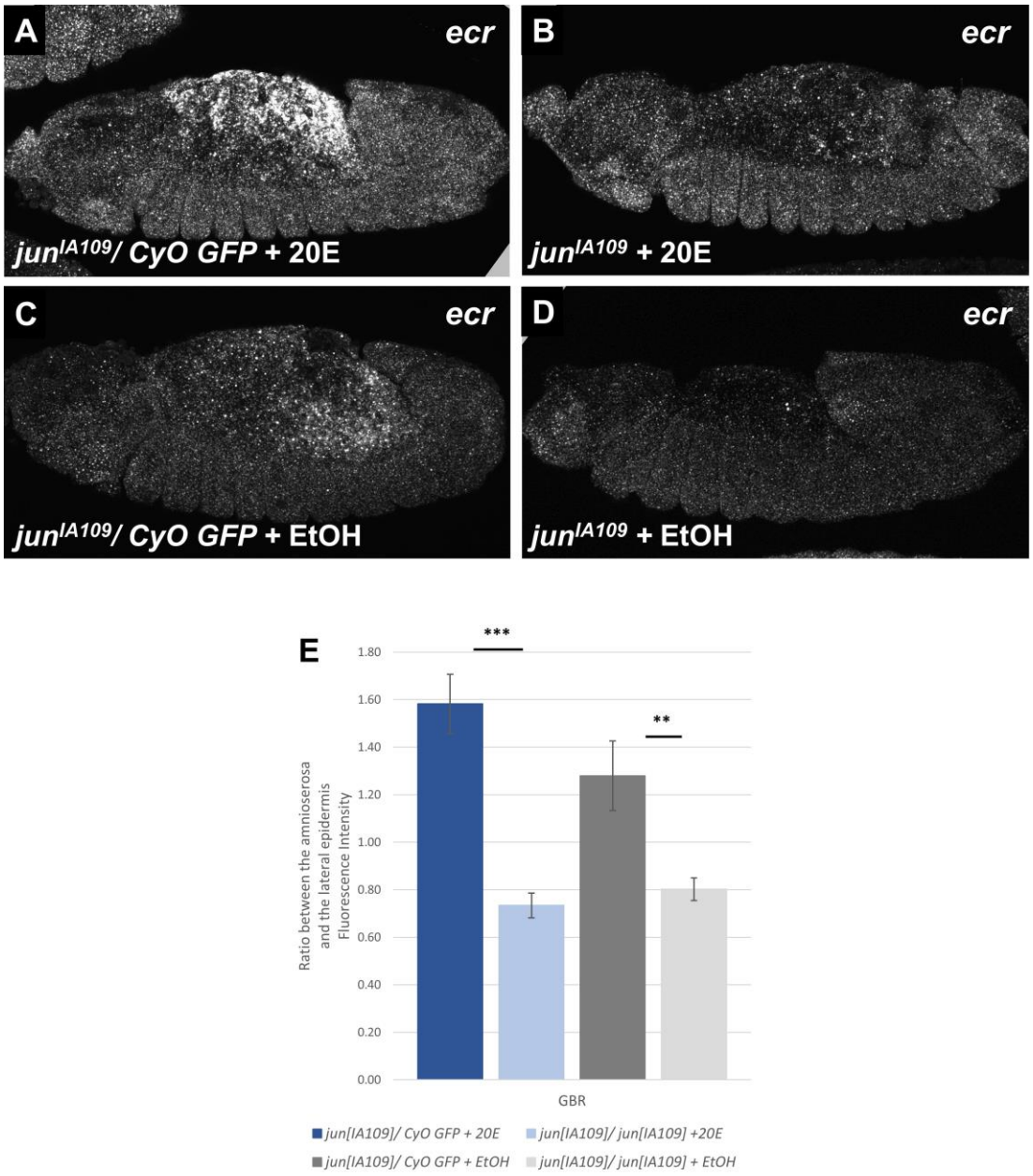


**Figure 3.2.17 Epistatic analysis between ecdysone-activated EcR and Jun in the regulation the expression of *ecr*.**

FISH against *ecr* on GBR-staged embryos. (A-D) 20E-treated *jun*$^{lA109}$ heterozygotes displayed elevated *ecr* transcript levels in the AS (A) when compared to ethanol-treated heterozygotes (C). No elevations were observed in 20E-treated *jun*$^{lA109}$ homozygotes (B), which had comparable transcript levels as ethanol-treated homozygotes (D), indicating no change in expression. (E) Quantification of the FISH signals. Sample sizes: 20E-treated *jun*$^{lA109}$ heterozygotes (64 segments in 12 embryos), 20E-treated *jun*$^{lA109}$ homozygotes (35/7), EtOH-treated *jun*$^{lA109}$ heterozygotes (30/6), EtOH-treated *jun*$^{lA109}$ homozygotes (25/5). **p<0.01, *** p<0.001.

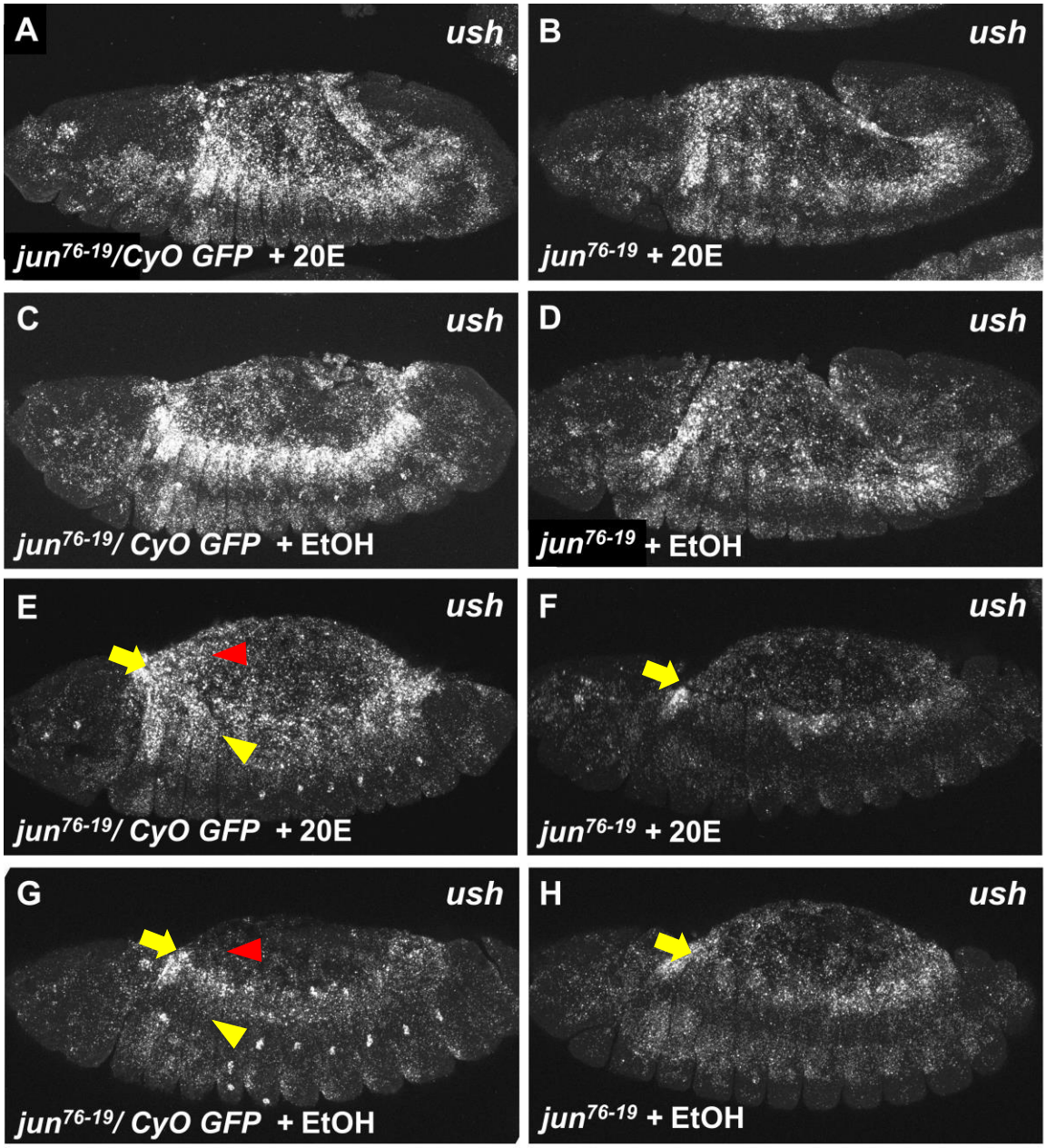


continues on next page…

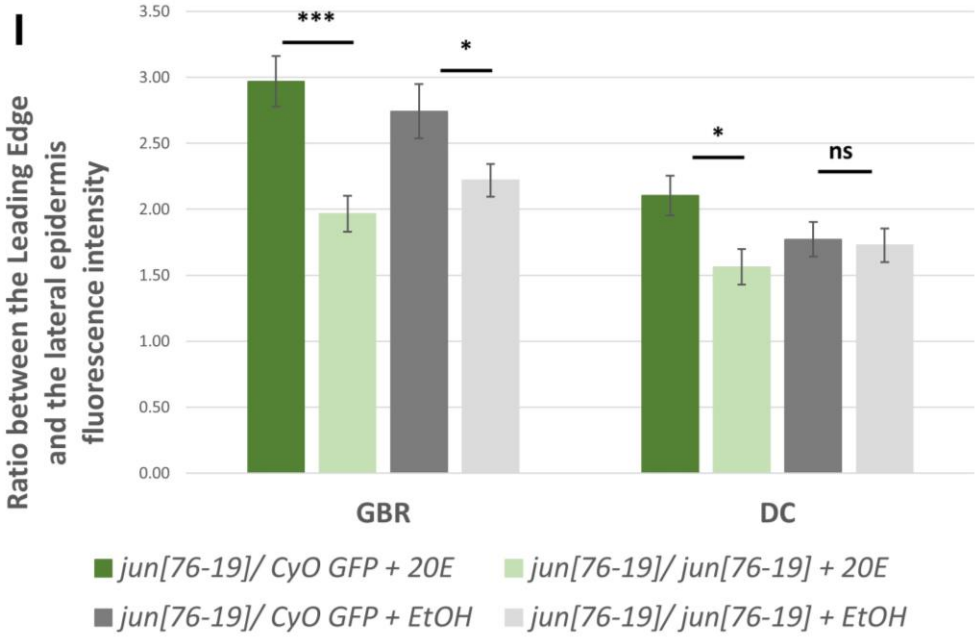
I
Ratio between the Leading Edge and the lateral epidermis fluorescence intensity
3.50
3.00
2.50
2.00
1.50
1.00
0.50
0.00
***
*
*
ns
GBR
DC
jun[76-19]/ CyO GFP + 20E
jun[76-19]/ jun[76-19] + 20E
jun[76-19]/ CyO GFP + EtOH
jun[76-19]/ jun[76-19] + EtOH

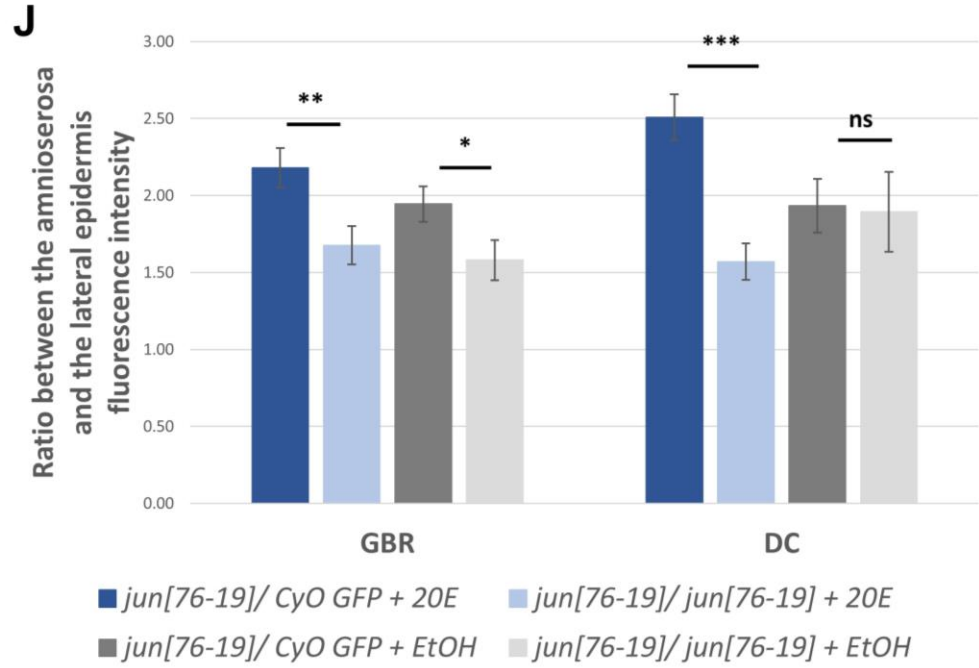
J
Ratio between the amnioserosa and the lateral epidermis fluorescence intensity
3.00
2.50
2.00
1.50
1.00
0.50
0.00
**
*
***
ns
GBR
DC
jun[76-19]/ CyO GFP + 20E
jun[76-19]/ jun[76-19] + 20E
jun[76-19]/ CyO GFP + EtOH
jun[76-19]/ jun[76-19] + EtOH

**Figure 3.2.18 Epistatic analysis between ecdysone-activated EcR and Jun in the regulation the expression of *ush*.**

FISH against *ush* on GBR- and DC-staged embryos. The boundary between the AS and DME cells during DC are indicated by yellow arrow. (A-D) For GBR-staged embryos, the effects on *ush* expression could not be evaluated as there was no difference in transcript levels detected between 20E-treated (A) and ethanol-treated (C) $jun^{76\text{-}19}$ heterozygotes. (E-H) For DC-staged embryos, 20E-treated $jun^{76\text{-}19}$ heterozygotes displayed elevated *ush* transcript levels in the AS (red arrowhead) and DME cells (yellow arrowhead) (E) when compared to ethanol-treated heterozygotes (G). No elevations were observed in 20E-treated $jun^{76\text{-}19}$ homozygotes (F), which had comparable transcript levels as ethanol-treated homozygotes (H), indicating no changes in expression. (I,J) Quantification of the FISH signals. Sample sizes: 20E-treated $jun^{76\text{-}19}$ heterozygotes (GBR = 40 segments in 8 embryos, DC = 25/5), 20E-treated $jun^{76\text{-}19}$ homozygotes (GBR = 35/7, DC = 25/5), EtOH-treated $jun^{76\text{-}19}$ heterozygotes (GBR = 20/4, DC = 15/3), EtOH-treated $jun^{76\text{-}19}$ homozygotes (GBR + DC = 20/4). * $p<0.05$, ** $p<0.01$, *** $p<0.001$.

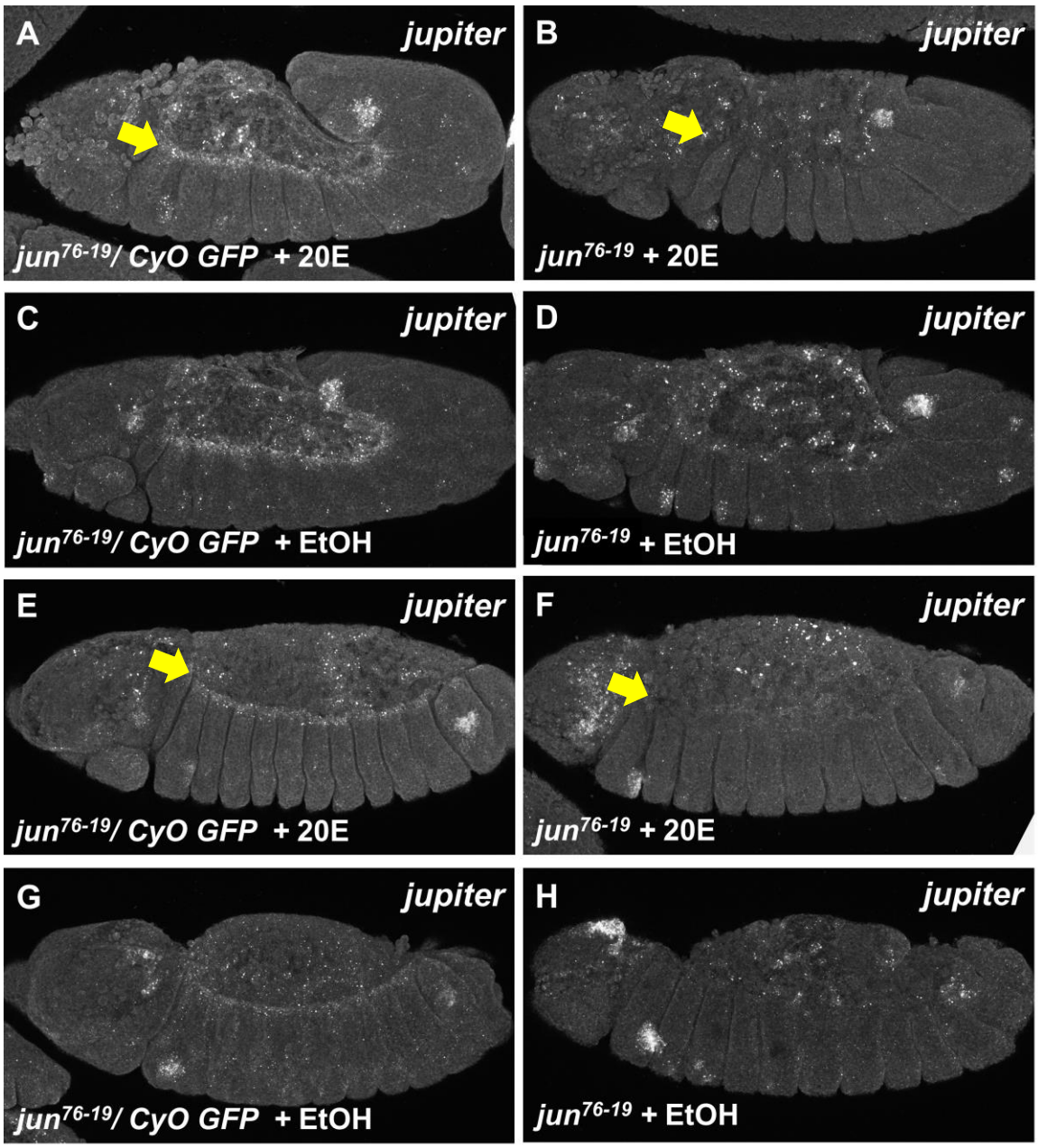


continues on next page…

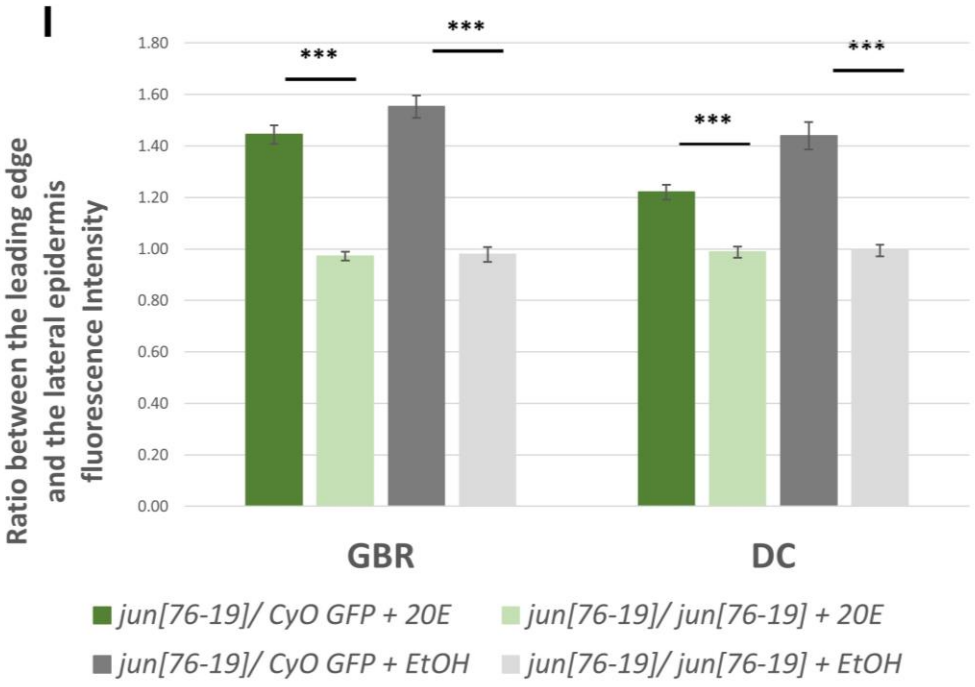
I
Ratio between the leading edge and the lateral epidermis fluorescence Intensity
1.80
1.60
1.40
1.20
1.00
0.80
0.60
0.40
0.20
0.00
***
***
***
***
GBR
DC
jun[76-19]/ CyO GFP + 20E
jun[76-19]/ jun[76-19] + 20E
jun[76-19]/ CyO GFP + EtOH
jun[76-19]/ jun[76-19] + EtOH

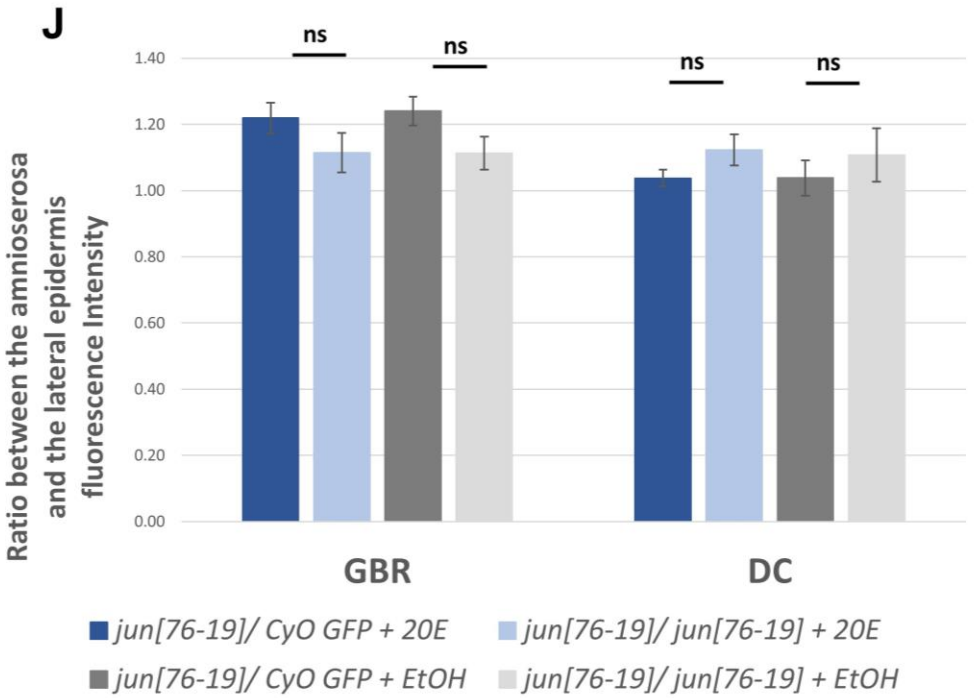
J
Ratio between the amnioserosa and the lateral epidermis fluorescence Intensity
1.40
1.20
1.00
0.80
0.60
0.40
0.20
0.00
ns
ns
ns
ns
GBR
DC
jun[76-19]/ CyO GFP + 20E
jun[76-19]/ jun[76-19] + 20E
jun[76-19]/ CyO GFP + EtOH
jun[76-19]/ jun[76-19] + EtOH

**Figure 3.2.19 Epistatic analysis between ecdysone-activated EcR and Jun in the regulation the expression of *jupiter*.**

FISH against *jupiter* on GBR- and DC-staged embryos. The boundary between the AS and DME is indicated by yellow arrow. (A-H) For GBR- and DC-staged embryos, the effects on *jupiter* expression could not be evaluated as there was no difference in transcript levels detected between 20E-treated (A,E) and ethanol-treated (C,G) $jun^{76\text{-}19}$ heterozygotes. (I,J) Quantification of the FISH signals. Sample sizes: 20E-treated $jun^{76\text{-}19}$ heterozygotes (GBR = 25 segments in 5 embryos, DC = 20/5), 20E-treated $jun^{76\text{-}19}$ homozygotes (GBR + DC = 20/5), EtOH-treated $jun^{76\text{-}19}$ heterozygotes (GBR = 28/7, DC = 20/5), EtOH-treated $jun^{76\text{-}19}$ homozygotes (GBR = 24/6, DC = 20/5). *** $p<0.001$.

**Table 1 Summarized results of FISH against the candidate genes.**

(Blue) decrease in gene expressions. (Pink) increase in gene expressions. (N/A) FISH not performed (GBR) Germband retraction. (DC) Dorsal closure. (AS) Amnioserosa. (LE) Leading edge (or DME)

| | spo[1] | | dib[2] | | Df(2R)BSC303 | | jun[76-19] | | jun[1A109] | | wt +20E | | Df(2R)BSC303 +20E | | jun[76-19] +20E | | jun[1A109] +20E | |
|---|---|---|---|---|---|---|---|---|---|---|---|---|---|---|---|---|---|---|
| | GBR | DC | GBR | DC | GBR | DC | GBR | DC | GBR | DC | GBR | DC | GBR | DC | GBR | DC | GBR | DC |
| cbt | no effect | no effect | no effect | no effect | ↓AS | ↓AS | no effect | no effect | no effect | no effect | N/A | N/A | N/A | N/A | N/A | N/A | N/A | N/A |
| EcR | ↓AS (mid-GBR) | no signal at AS,LE to evaluate | ↓AS (mid-GBR) | no signal at AS,LE to evaluate | ↓AS (mid-GBR) | no signal at AS,LE to evaluate | ↓AS (mid-GBR) | no signal at AS,LE to evaluate | no effect | no signal at AS,LE to evaluate | ↑AS | no signal at AS,LE to evaluate | N/A | N/A | N/A | N/A | ↓AS (mid-GBR) | ↓AS (mid-GBR) |
| jar | no effect | ↑AS | no effect | ↑AS | N/A | N/A | N/A | N/A | N/A | N/A | N/A | N/A | N/A | N/A | N/A | N/A | N/A | N/A |
| jupiter | ↓LE,AS | ↓LE,AS | ↓LE,AS | ↓LE | ↓LE | ↓LE | ↓LE,AS | ↓LE,AS | ↓LE | ↓LE | no effect | no effect | no effect | no effect | no effect | no effect | no effect | no effect |
| mes2 | no effect | no effect | no effect | no effect | no effect | no effect | no effect | no effect | no effect | no effect | N/A | N/A | N/A | N/A | N/A | N/A | N/A | N/A |
| RhoGAP 71E | ↑LE (mid-GBR) | ↑LE | ↑LE (mid-GBR) | ↑LE | no effect | no effect | no effect | no effect | ↑LE | ↑LE | N/A | N/A | N/A | N/A | N/A | N/A | N/A | N/A |
| ush | ↓LE,AS | ↓LE,AS | ↓LE | ↓LE,AS | ↓LE | no effect | ↓LE,AS | ↓AS | ↓LE | no effect | ↑AS,LE | ↑AS,LE | N/A | N/A | ↓LE,AS | ↓LE,AS | N/A | N/A |
| zasp52 | no effect | ↑AS | ↑AS | ↑AS | N/A | N/A | N/A | N/A | N/A | N/A | N/A | N/A | N/A | N/A | N/A | N/A | N/A | N/A |
| zip | ↓AS | ↓LE | ↓AS | ↓LE | ↓AS | ↓LE | ↓AS | ↓LE | ↓AS | ↓LE | ↑AS,LE | ↑AS,LE | ↓AS,LE (late-GBR) | ↓LE | ↓AS,LE (late-GBR) | ↓LE | ↓AS,LE (late-GBR) | ↓LE |

## 3.3. RhoGAP71E may act as a GAP for Rho1 during DC

One of the candidates analyzed in this project is RhoGAP71E, which can function as a GAP for the Rho family small GTPases during ventral furrow formation (Mason et al., 2016). However, it is unknown whether RhoGAP71E can play the same role during DC. As mentioned in the introduction, Rho1 is an upstream regulator of the JNK pathway cascade, and is required for myosin activity in the dorsal epidermis during DC (Harden et al., 1999). Since regulation of Rho1 activity during DC is also not well understood itself, preliminary work was carried out to determine whether RhoGAP71E can serve as a GAP to negatively modulate Rho1 activation during this process.

Prior work in the lab has shown that Rho1 overexpression leads to elevations in *zip* transcript levels during DC (Kim, 2017). Consequently, severe morphological defects are often observed in these embryos due to aberrant actomyosin contraction. To assess if RhoGAP71E can negatively regulate Rho1 activity, RhoGAP71E was co-overexpressed with Rho1 during late embryogenesis. If RhoGAP71E does indeed function as a Rho1 GAP, then co-overexpression of RhoGAP71E is expected to block Rho1 over-expression associated phenotypes. A recombinant stock carrying both the *UAS-rho1* and *UAS-rhogap71e* transgenes was made (see section 2.1 for more information) and crossed to the segmental *prd-Gal4* driver. FISH analysis of these embryos revealed that ectopic *zip* expression in prd[+] stripes was effectively suppressed (Figure 3.3.1 C,D) in comparison to embryos co-expressing *UAS-Rho1* and *UAS-GFP* (Figure 3.3.1 A,B), with the latter serving as a control transgene. This was to exclude the possibility that suppression was due to a titration of GAL4 activity caused by introducing an additional transgene.

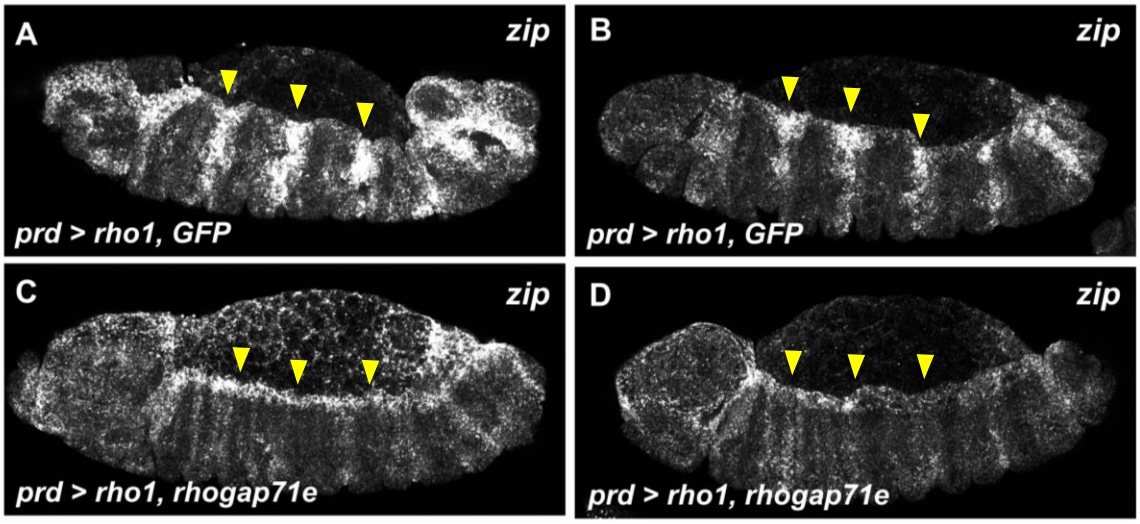


**Figure 3.3.1 RhoGAP71E effects on ectopic *zip* transcript levels associated with Rho1 overexpression.**

FISH against *zip* on late GBR- and mid DC-staged embryos. (A,B) Overexpression of *rho1* and *GFP* (a control transgene) with the *prd-Gal4* driver resulted in ectopic *zip* expression in prd[+] stripes during late GBR (A) and mid DC (B) indicated by yellow arrowheads. Note that healthier-looking mutant embryos were chosen for representative images, and display only slight morphological defects. (C,D) Overexpression of *rhogap71e* with *rho1* suppressed ectopic *zip* expression at both stages (yellow arrowheads). The embryos also displayed a more wild-type morphology.

Suppression was also seen when evaluating embryonic morphology phenotypes through cuticle preparations (Figure 3.3.2 A-D). When crossing *prd-Gal4, UAS-GFP/TM3* females to *UAS-rho1* homozygous males, a high frequency of embryonic morphological defects were observed within the F1 progeny (note that 50% of the progeny were expected to express both *rho1* and *GFP*). This included 35.7% of the total progeny being embryos that displayed some form of a dorsal hole (Figure 3.3.2 E). When crossing *prd-Gal4/TM3* females to *UAS-rho1, UAS-rhogap71e* homozygous males, only 0.6% of the total progeny displayed DC defects (again, 50% of the progeny were expected to express both *rho1* and *rhogap71e*) (Figure 3.3.2 E). Overall, these results provide preliminary evidence that RhoGAP71E can potentially function as a GAP to downregulate Rho1 activity during DC. However, molecular evidence still needs to be provided in the form of Rho activation assays, which can be commercially bought.

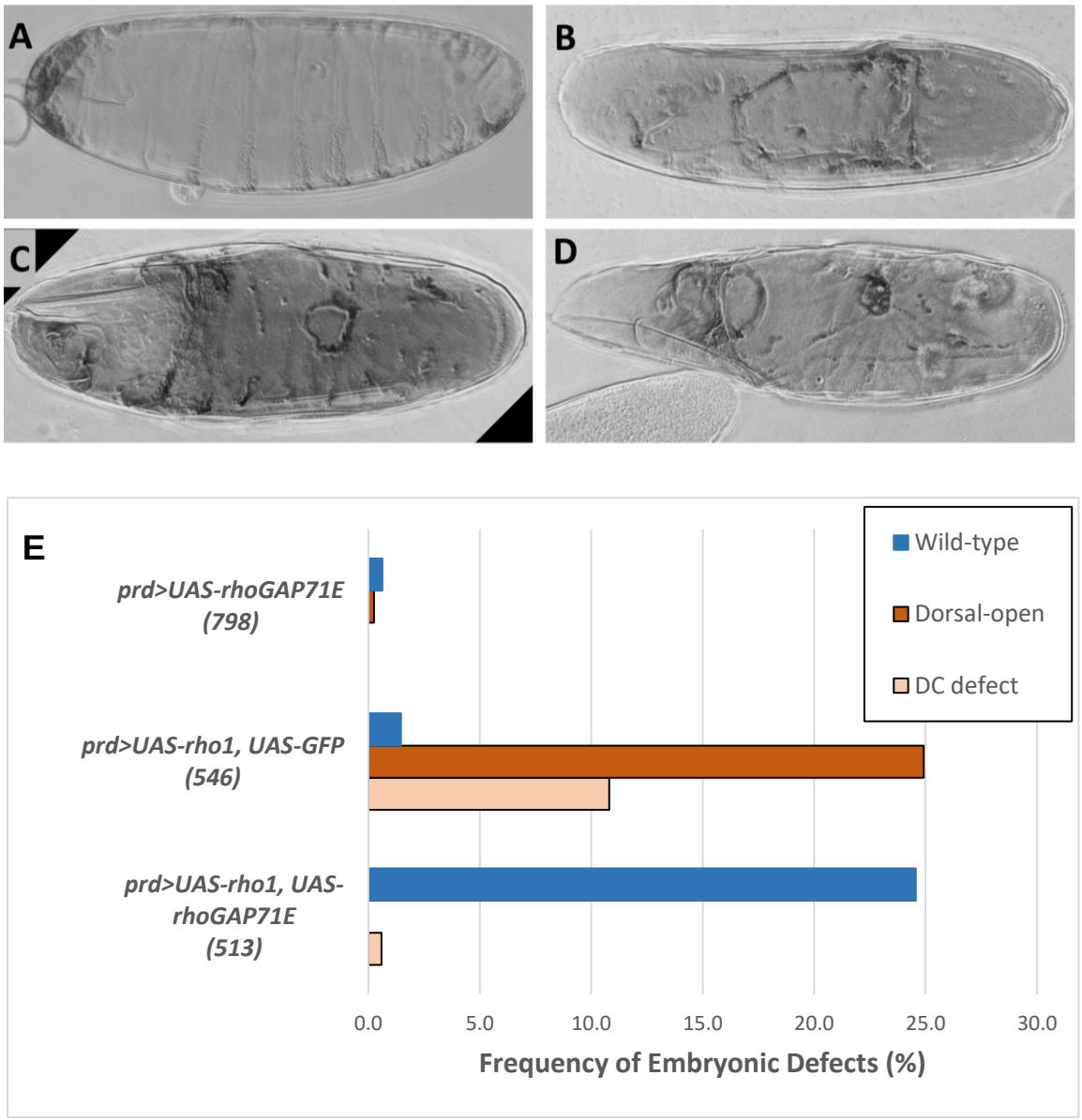


**Figure 3.3.2 RhoGAP71E effects on embryonic phenotypes associated with Rho1 overexpression.**

(A-D) Phase contrast images of representative embryonic morphological defects associated with overexpression of Rho1 via the segmental *prd-Gal4* driver. Predominant phenotypes include: wild-type (A), large dorsal holes ("dorsal-open") (B), small dorsal holes ("DC defect") (C), and head holes (D). (E) Quantification of the frequency of embryonic defects. Crosses are listed to the left of each bar graph, with the F1 sample sizes indicated directly below in brackets. Upon crossing *prd-Gal4, UAS-GFP/TM3* females to *UAS-rho1* homozygous males, 35.7% of the total progeny were dead embryos that displayed some form of a dorsal hole (*n.b.* half the progeny were expected to express *rho1* and *GFP*). When crossing *prd-Gal4/TM3* females to *UAS-rho1, UAS-rhogap71e* homozygous males, only 0.6% of the total progeny displayed DC defects (*n.b.* half the progeny were expected to express *rho1* and *rhogap71e*). Crossing *prd-Gal4/TM3* females to *UAS-rhogap71e* homozygous males resulted in low embryonic lethality.

# Chapter 4. Discussion

Metazoans solved the problem of epithelial closure before the divergence of vertebrates and invertebrates, thus what is learned about DC is likely to be applicable to our understanding of developmental epithelial fusions and wound healing in humans. DC is propelled by actomyosin contractility in both the AS and the DME cells of the dorsal epidermis, though recent evidence indicates that AS morphogenesis is the principle driving force pulling the dorsal hole shut (Ducuing and Vincent, 2016; Pasakarnis et al., 2016). Therefore, understanding the network of signaling pathways that regulate AS contraction is of key importance. Morphogenesis in both the AS and dorsal epidermis requires many of the same genes, and it has been established that much of the gene expression in the dorsal epidermis is promoted by a JNK signaling cascade that activates the AP-1 transcription factor (Riesgo-Escovar and Hafen, 1997b; Zeitlinger et al., 1997). Among the key genes that have been determined to be regulated by the JNK cascade is the myosin heavy chain encoding *zip* locus, which is essential for actomyosin contractility. *zip* is also upregulated in the AS, but this is not due to cell autonomous expression mediated by the JNK cascade, as the pathway is inactive in this tissue (Reed et al., 2001). What is then driving *zip* expression in the AS? One candidate is signaling by the TGF-β superfamily member, Dpp, which is produced in the DME cells and signals to the AS, promoting actomyosin contractility (Fernández et al., 2007; Wada et al., 2007; Zahedi et al., 2008). Another candidate is signaling by the steroid hormone, ecdysone, which is produced at high levels in the AS, and is required for DC (Chavez et al., 2000; Giesen et al., 2003; Kozlova and Thummel, 2003). Prior work in the lab has found that Dpp is an upstream regulator of ecdysone biosynthesis (Chen, 2014). Interestingly, the JNK cascade, AP-1 transcription factor, TGF-β signaling and steroid hormones have all been implicated in vertebrate developmental epithelial closures, and piecing together the DC signaling network involving these components could be very informative in better understanding these events.

Canonical ecdysone signaling involves the formation of a heterodimer between EcR and Usp (Thummel, 1995). In the presence of ecdysone, the ligand binding stabilizes the EcR-Usp complex and initiates binding to EcREs within the genome to promote gene expression (Cherbas et al., 1991; Riddiford et al., 2001). However, expression of two dominant negative versions of EcR, EcR-F465A and EcR-W650A, which block

endogenous EcR by dimerizing with Usp and repressing transcription at EcREs (Cherbas et al., 2003), had no effect on *zip* expression during DC (Chen, 2014). This indicates that ecdysone does not regulate *zip* through EcREs, and is acting in a non-canonical fashion. An interesting possibility is that ecdysone-activated EcR is capable of promoting activity of the AP-1 transcription factor at AP-1 binding sites. Consistent with this, a study to map binding regions for EcR in 20E-treated *Drosophila* Kc167 cells identified a 4-kb region within the *zip* gene that is bound by EcR (Gauhar et al., 2009). This region contains five sequences matching the AP-1 consensus binding site but no consensus EcRE. The main purpose of this study is to investigate further whether non-canonical ecdysone signaling, in cooperation with AP-1, regulates expression in the AS during DC.

## 4.1. EcR and Jun interact and coordinate *zip* regulation in both the AS and the DME cells during DC

The first aim of this study was to find genetic and molecular evidence that EcR and Jun, a component of the AP-1 complex, interact during DC. Comparable interactions have previously been shown in mammals. For example, the estrogen receptor, ERβ, a steroid nuclear receptor similar to EcR, can regulate gene expression in cooperation with AP-1 (Kushner et al., 2000; Teurich and Angel, 1995; Zhao et al., 2010). Moreover, an interaction between JNK and hormone signaling has been reported in mouse eyelid closure (Sanchis et al., 2010). Here, epistatic analysis between ecdysone-activated EcR and Jun revealed that the two proteins cooperate in the regulation of *zip* expression during DC. Wild-type embryos treated with 20E display significant increases in the transcript levels of *zip*, demonstrating that signaling through ecdysone promotes *zip* expression. However, 20E-treated embryos lacking Jun function show no such elevation. This result indicates that ecdysone-activated EcR requires Jun for this process.

EcR-Jun complexes in the nuclei of AS and DME cells during DC have been observed through PLA analysis (Chen, 2014). To characterize the association molecularly, pull-down assays using bacterially expressed GST- and His-tagged proteins were done in order to demonstrate direct binding between the proteins. In these assays, EcR and Jun were determined to specifically bind to each other, at least *in vitro*. Future work in the long-term may involve identifying which domains are required for binding, which will require making tagged truncated and single domain constructs. Interestingly, additional pull-down experiments showed that Kay/Fos (a component of AP-1) can bind to EcR, and Usp (the

binding partner of EcR for ecdysone signaling) can bind to Jun, thus indicating that other proteins may be part of the EcR-Jun complex. In support of this data, both Jun and Fos have been shown to be recruited to the estrogen receptor binding region with AP-1 consensus sites in mammalian cells (Zhao, 2010). Nevertheless, to show that Usp and Kay/Fos are part of the Ecr-Jun complex, *in vivo*, PLA experiments can be performed between Jun and Usp, in addition to EcR and Kay/Fos, on DC-staged embryos.

Considering all of the results from the epistatic analysis and pull-down assays, in addition to the previous PLA experiments, EcR and Jun likely form a complex at the *zip* locus. Further evidence towards EcR and Jun's ability to serve as a transcription factor during DC was provided through ChIP analyses. Using DC-staged embryonic extracts, DNA fragments that were co-immunoprecipitated with either EcR or Jun were amplified using *zip* specific primers. Results showed that EcR and Jun can both associate with the same intronic region corresponding to the EcR-binding region first discovered by Gauhar and colleagues, which contained AP-1 binding sites but no EcREs (Gauhar et al., 2009). No association was observed for a sequence corresponding to the 3' end of the *zip* gene, which was used as a negative control. To provide further evidence that EcR and Jun require each other to form the transcription factor, work in the near future will involve ChIPs performed on *jun* deficient embryonic extracts to see if EcR can still co-immunoprecipitate with the same EcR binding region of *zip*. In regards to long-term future work, it would be interesting to visualize the distribution of EcR and Jun on polytene chromosomes from *Drosophila* salivary glands, which are also regulated by ecdysone signaling (Lehmann et al., 2002). This will involve co-immunostaining chromatin squashes so that the chromosomal positions of overlapping signal between EcR and Jun can be determined. For example, co-localization at cytogenetic position 60E12 (FlyBase) can be assessed in order to see if EcR and Jun bind at the region containing the *zip* locus at the same time. For increased sensitivity, PLA can be performed instead to only show regions bound by EcR-Jun complexes

The work in this section all indicate that an EcR-Jun complex exists in both AS and DME cells during DC to regulate *zip* expression. These results support the hypothesis that EcR is acting non-canonically (*i.e.* independent of binding to EcREs) by forming a complex with Jun at novel sites to mediate gene expression, similar to what is observed in mammalian cells (Bjornstrom, 2005, Zhao, 2010). Described in the next section, a screen was performed that identified other genes containing similar regulatory regions as found

in *zip*. The experiments described above can be applied to some of those candidates to determine if this mode of gene regulation is common to several genes critical for AS morphogenesis.

## 4.2. EcR-AP-1 binding sites are putative DC enhancers

As mentioned, the *zip* locus contains a novel EcR binding region which includes consensus AP-1 binding sites but no EcREs (Gauhar et al., 2009). A bioinformatic screen done by the lab to find genes that contained similar binding sites, *i.e.* at least five AP-1 consensus sites but no EcREs, identified 49 similar regions throughout the genome. Interestingly, at least 13 of these regions are in or near genes encoding known or likely DC participants. They are: *cbt*, *Chd64*, *ecr*, *Gprk2*, *InR*, *jar*, *jupiter*, *mes2*, *rhogap71e*, *step*, *ush*, *usp* and *zasp52*.

Among the 13 candidates, only *ecr, jupiter* and *ush* were found to be positively regulated by both ecdysone-activated EcR and Jun, similar to what is observed for *zip*. *ecr* encodes a ecdysone receptor which forms heterodimer with Usp and acts as a DNA binding transcription factor for gene expressions required for developmental transitions (Riddiford et al., 2001; Thummel, 1995). Its expression is limited during the germband retraction stage. The timing of its expression in the AS correlates with *zip* expression in the AS. There are high levels of *zip* transcripts in the AS during germband retraction and are gradually reduced when DC starts to progress. Similarly, this study has shown that *ecr* expression was reduced in *spo* and *dib* mutant embryos (embryos that lacks 20E) which suggests that EcR mediates a positive feed back regulation. *ecr* was also shown to be regulated by both EcR and AP-1 since incubation of exogenous 20E could not rescue the expression of *ecr* in *jun* mutant embryos.

*jupiter* which encodes microtubule associating protein is expressed in the DME cells and amnioserosa during germband retraction and DC. Modulated gene expression in the epidermis and AS was observed in both 20E lacking and *jun* mutant embryos. However, effect on expression in the DME cells in *jun* mutant embryos was most prominent possibly due to high expression levels in this tissue (Ducuing et al., 2015). Microtubule, although not fully understood, is also suggested to be contributing to the leading edge elongation during DC (Jankovics and Brunner, 2006). Thus it is possible that *jup* expression in the epidermis is more susceptible than in the AS.

It has been proposed that a diffusible signal from the AS to the epidermis is involved in the regulation of germband retraction by members of the U-shaped group of genes, Hindsight (Frank and Rushlow, 1996; Lamka and Lipshitz, 1999). One of our previous results also indicated that the U-shaped group is involved in the regulation of *zip* expression (Zahedi et al., 2008). In the present study, *ush* which is required for the AS maintenance, germband retraction and DC was shown to be regulated by both AP-1 and 20E; it is likely that this gene is one of the genes that is essential for the cross talk between the AS and the epidermis (Frank and Rushlow, 1996; Lada et al., 2012; Reed et al., 2001; Strecker et al., 1995; Stronach and Perrimon, 2001)

As mentioned, *ecr, jupiter* and *ush*, each has its role either in the epidermis or AS during germband retraction and DC (Jankovics and Brunner, 2006; Kozlova and Thummel, 2003; Lada et al., 2012). Thus, it is likely that these genes are modulated in more refined fashion via EcR-AP-1 enhancers not just by JNK or ecdysone signaling on its own.

Why did only 3 out of 13 candidates fit the model? One reason of concern is the way the FISH signals between experimental and control embryos were quantified, which was by measuring immunofluoresence intensity as mean gray values using Photoshop. Embryos from the same experiment sometimes stained inconsistently, where some embryos stained far greater or lesser than others, even if they were treated in the same tube under identical conditions. A way to potentially remedy this issue is to perform qPCR, which should be far more sensitive in detecting differences in transcript levels. However, expression of our genes of interest are cell and stage specific. Thus, signal from tissues that are not of interest may dilute any potential differences between the experiment and the control. Another possible remedy is to perform co-FISH against the gene of interest and a housekeeping gene (*i.e.* a gene not affected by our experiment), measure the signal intensities for both, then normalize the data by dividing the measurement of the gene of interest by the control. This way, if an embryo stained better or worse than others, both signals should be affected similarly and hopefully the ratio will temper out.

One thing to consider is that 3 candidate genes could not be assessed due to the inability to make antisense probes. Another consideration is that 3 genes were affected by ecdysone, but negatively through an unknown mechanism. Similarly, estrogen has been shown to activate some genes through AP-1 but repress others (Bjornstrom and Sjoberg, 2005). In this study, we only focused on candidate genes that were believed to

play a role in DC. Potentially more positive hits could be found work was expanded to the other genes picked up in the screen. Also, if the stringency of the bioinformatics screen was relaxed, more candidates may be uncovered.

The work previously done and this study demonstrate how ecdysone signaling is involved in non-canonical way in the epithelial morphogenesis during germband retraction and DC. Firstly, JNK cascade activates AP-1 transcription factor to induce *dpp* in the dorsal epidermis which then travels to the AS to activate the 20E biosynthetic pathway. The 20E bound EcR interacts with AP-1 to bind to AP-1 consensus site to regulate gene expression (Figure 4.2.1).

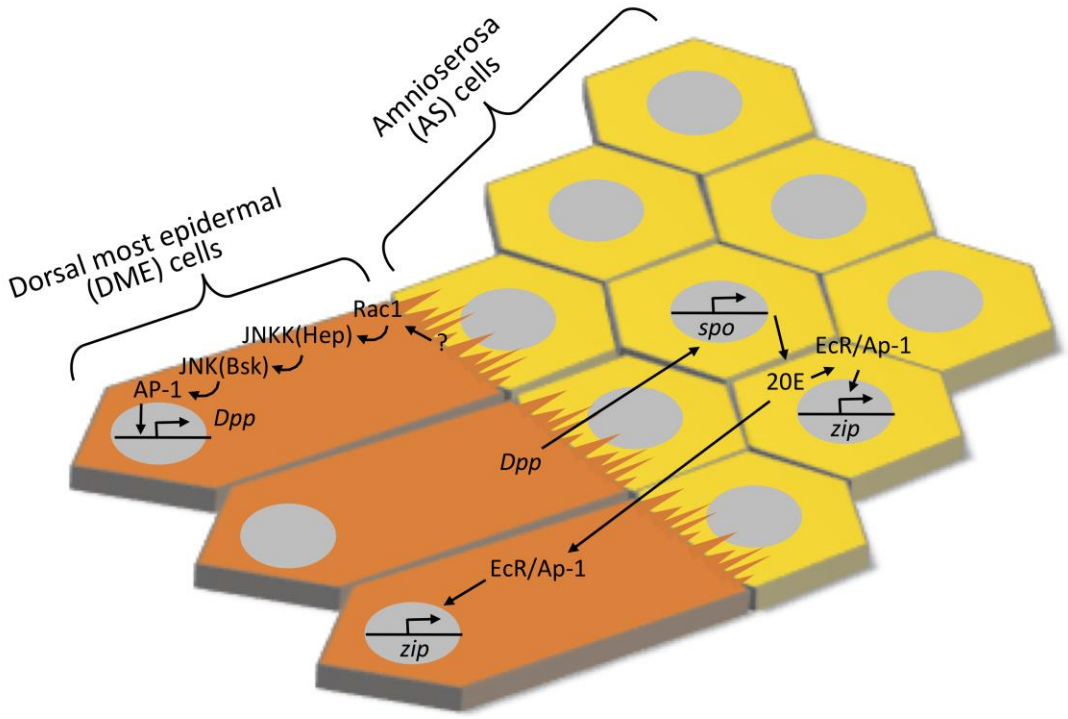


**Figure 4.2.1 Schematic of bi-directional regulation of gene expression during DC by 20E through a putative EcR-Ap-1 enhancer.**

## 4.3. Preliminary evidence that RhoGAP71E is turning off Rho1

Finally, performing *rhogap71e* FISH on embryos lacking 20E raises a possibility that the gene is involved upstream of JNK signaling that regulates *zip.* Both in *Drosophila* and mammals, Rho1 has been shown to regulate myosin accumulation that is required in actomyosin contractility through activation of Rho-associated kinases (ROKs)-Myosin II in cooperation with Ras (Harden, 2002; Harden et al., 1999; Jacinto et al., 2002; Khoo et al., 2013; Stronach and Perrimon, 2001)

Previous grad students investigated the role of the diffusible ligand Fog, a well-known activator of the Rho1 actomyosin contractility pathway during gastrulation (Barrett et al., 1997; Costa et al., 1994; Dawes-Hoang et al., 2005). It was demonstrated that overexpression of Fog caused elevated levels of *zip* in the DME cells during DC, which led to assessments of known downstream components of the Fog pathway such as GTPase Rho1 and RhoGEF2. Mutation of RhoGEF2 led to a decrease in *zip* levels suggesting RhoGEF2 has a role in activating Rho1 that is upstream of the JNK pathway during DC. (Kim, 2017) (Figure 1.3.2). Here I am suggesting that RhoGAP71E is involved in the opposite direction to turn off Rho1.

In this preliminary experiment, I wanted to determine if RhoGAP71E can actually turn off Rho1 and cause reduced *zip* expression. Overexpressing Rho1 alone in paired stripes using *prd-GAL4* led to overexpression of *zip* in paired stripes with defects in embryo morphology. Overexpressing Rho1 and Rhogap71E together in paired stripes not only reduced *zip* expression to the levels of wild-type embryos. The embryo morphology was also rescued which was strongly supported by evaluating embryonic morphology phenotypes via cuticle preparations. In this test, 35.7% of *rho1* overexpressing embryos displayed DC defects (out of approximately 50% of progeny with overexpressed *rho1*) whereas only 0.6% of *rho1* and *rhogap71e* co-expressing embryos displayed such defects.

These results implicate that RhoGAP71E has a role in downregulating *zip.* Since *zip* has to be expressed in the LE during DC for actomyosin contractility, it is likely that 20E is repressing *rhogap71e.*

Future study will involve assessing GTPase activity of Rho1 and its regulation by RhoGAP71E. It will be interesting to test how RhoGAP71E affects other components of the Rho1 pathway and how it fits into the complex signalling regulation DC

## 4.4. Coordinated morphogenesis requires well established networks of signals

DC, a developmental wound-healing event in which a hole in the dorsal side of the embryo is covered by the surrounding epidermal tissues requires both tissues to constrict in a coordinated matter. The AS also undergo autonomous constriction (Agnès et al., 1999; Fernández et al., 2007; Glise et al., 1995; Harden, 2002; Reed et al., 2001; Stronach and Perrimon, 2001; Wada et al., 2007). Communication between these tissues is essential and elucidating this signaling network will provide better insight into coordinated epithelial morphogenesis between different tissues and in other organisms.

Our lab has been trying to elucidate signaling networks involved in the coordinated morphogenesis between the epidermis and the AS by focusing on the expression of *zip* as a target gene. It has been shown that Dpp, a member of TGF-β family, is initiating 20E production in the AS cells and 20E activates its receptor EcR to function in a novel fashion which is to activate *zip* expression by interacting with the AP-1 transcription factor.

Here, I have shown that EcR and Jun, a component of the AP-1 transcription factor are interacting and require each other for *zip* expression in both the LE and the AS. It was shown through epistatic analysis and ChIP analysis that these two proteins are likely binding to the same region in *zip* locus.

Several DC related genes that contained AP-1 consensus sites within or near the gene locus are also bound by EcR, and are likely to be regulated by the EcR/AP-1 complex. These results suggest a role of EcR-AP-1 enhancers in control of gene expression in a spatio-temporal manner during DC. Cooperation of 20E signaling pathway and the JNK pathway through EcR-AP-1 enhancers allows more coordinated and refined regulation of gene expression during DC than JNK on its own. In mammals, steroid hormone receptors such as estrogen receptor and AP-1 bind to each other and form chromatin looping and it will be of interest if the DC enhancer functions in a similar fashion (Le Dily and Beato, 2018).

The knowledge obtained here can also be applied to other developmental processes such as embryonic wound healing, mouse eyelid closure, and neural tube closure in mammals (Geh et al., 2011; Grose and Martin, 1999; Kuan et al., 1999; Martin and Parkhurst, 2004; Sanchis et al., 2010; Xia and Karin, 2004). Some of the signaling pathways involved in DC are conserved in morphogenetic events in other organisms. For example, in the mammalian wound healing process, there is paracrine TGF-β induced contraction of the wound bed (Fernández et al., 2007), which also signals from keratinocytes to fibroblasts to trigger their differentiation into contractile fibroblasts. Also fibroblasts signal back to keratinocytes for proliferation and differentiation (Werner et al., 2007).

Another example of parallels can be seen in mouse embryonic eyelid closure which involves epithelial migration at the tip of the developing eyelid (Geh et al., 2011; Zhang et al., 2003). Similar to DC defects, mice with impaired MAPK signaling show a impaired eyelid closure and are born with eyes open at birth (EOB) phenotype (Geh et al., 2011). In the eyelid closure, MEKK1, a member of the MAPKKK family activates a MAPK cascade, (Zhang et al., 2003). A MEKK1 mutation prevents cell shape change and F-actin formation in the eyelid epithelium, which which is due to abolished c-Jun N-terminal phosphorylation (Xia and Karin, 2004). TGF-β is also involved in this process where it activates MEKK1-JNK pathway. The knockout of TGF-β also impairs eyelid closure just like impaired Dpp signalling leads to DC defects. Most importantly, the eyelid closure also requires a steroid hormone (Sanchis et al., 2010). The glucocorticoid receptor, which is a steroid hormone receptor, modulates epithelial morphogenesis through i binding of GR to AP-1 and interaction with JNK (Sanchis et al., 2010) This is a nice parallrel with our findings of similar intercationsn steroid hormone receptor and AP-1 transcription factor.

Recent studies has also shown that TGF-β promotes expression of a gene called *fascin1* which regulates cytoskeletal structures for cell migration and invasion in some tumor cells (Fu et al., 2009; Yang et al., 2018) through JNK and ERK pathway (Yang et al., 2018). These parallels between different organisms suggests epithelial morphogenesis and signaling pathways are well conserved. This also makes *Drosophila* DC a good model that might also provide insights into the therapeutic strategies for some human diseases such as cancers.

# Chapter 5. Conclusion

In this thesis, I have worked on interactions between the steroid hormone ecdysone pathway and AP-1 transcription factor to regulate genes during DC. This study proposes the ecdysone pathway is acting in a novel fashion in regulating *Drosophila* DC which does not require its DNA recognition site EcRE.

Our data suggest EcR-AP-1 complex not only regulates the expression of *zip* but also other DC related genes such as *ecr, ush* and *jupiter.* The expression of these genes is affected by impairment of 20E or AP-1 pathway or by both. The effects on these DC related gene expressions were observed in both the AS and the surrounding epidermis. Taken together, these results suggest EcR-AP-1 binds enhancers that regulate gene expression in both the AS and the epidermis during DC.

# References


**Abreu-Blanco, M. T., Verboon, J. M. and Parkhurst, S. M.** (2014). Coordination of Rho family GTPase activities to orchestrate cytoskeleton responses during cell wound repair. *Curr. Biol.* **24**, 144–155.

**Affolter, M., Marty, T., Vigano, M. A. and Jaźwińska, A.** (2001). Nuclear interpretation of Dpp signaling in Drosophila. *EMBO J.* **20**, 3298–3305.

**Agnès, F., Suzanne, M. and Noselli, S.** (1999). The Drosophila JNK pathway controls the morphogenesis of imaginal discs during metamorphosis. *Development* **126**, 5453–5462.

**Arquier, N., Perrin, L., Manfruelli, P. and Sémériva, M.** (2001). The Drosophila tumor suppressor gene lethal(2)giant larvae is required for the emission of the Decapentaplegic signal. *Development* **128**, 2209–2220.

**Barrett, K., Leptin, M. and Settleman, J.** (1997). The Rho GTPase and a putative RhoGEF mediate a signaling pathway for the cell shape changes in Drosophila gastrulation. *Cell* **91**, 905–915.

**Belacortu, Y., Weiss, R., Kadener, S. and Paricio, N.** (2011). Gene Expression Patterns Expression of Drosophila Cabut during early embryogenesis , dorsal closure and nervous system development. *Gene Expr. Patterns* **11**, 190–201.

**Bender, M., Imam, F. B., Talbot, W. S., Ganetzky, B. and Hogness, D. S.** (1997). Drosophila ecdysone receptor mutations reveal functional differences among receptor isoforms. *Cell* **91**, 777–788.

**Bhaskar, V. and Courey, A. J.** (2002). The MADF-BESS domain factor Dip3 potentiates synergistic activation by Dorsal and Twist. *Gene* **299**, 173–184.

**Bischof, J., Bjorklund, M., Furger, E., Schertel, C., Taipale, J. and Basler, K.** (2013). A versatile platform for creating a comprehensive UAS-ORFeome library in Drosophila. *Development* **140**, 2434–2442.

**Bishop, A. L. and Hall, A.** (2000). Rho GTPases and their effector proteins. *Biochem. J.* **348**, 241–255.

**Biteau, B., Karpac, J., Hwangbo, D. S. and Jasper, H.** (2011). Regulation of Drosophila lifespan by JNK signaling. *Exp. Gerontol.* **46**, 349–354.

**Blanchard, G. B., Murugesu, S., Adams, R. J., Martinez-Arias, A. and Gorfinkiel, N.** (2010). Cytoskeletal dynamics and supracellular organisation of cell shape fluctuations during dorsal closure. *Development* **137**, 2743–2752.

**Bosch, M., Serras, F., Martin-Blanco, E. and Baguñà, J.** (2005). JNK signaling

pathway required for wound healing in regenerating Drosophila wing imaginal discs. *Dev. Biol.* **280**, 73–86.

**Brennan, C. A., Ashburner, M. and Moses, K.** (1998). Ecdysone pathway is required for furrow progression in the developing Drosophila eye. *Development* **125**, 2653–2664.

**Bresnick, A. R.** (1999). Molecular mechanisms of nonmuscle myosin-II regulation. *Curr. Opin. Cell Biol.* **11**, 26–33.

**Brogiolo, W., Stocker, H., Ikeya, T., Rintelen, F., Fernandez, R. and Hafen, E.** (2001). An evolutionarily conserved function of the drosophila insulin receptor and insulin-like peptides in growth control. *Curr. Biol.* **11**, 213–221.

**Brummel, T. J., Twombly, V., Marqués, G., Wrana, J. L., Newfeld, S. J., Attisano, L., Massagué, J., O'Connor, M. B. and Gelbart, W. M.** (1994). Characterization and relationship of dpp receptors encoded by the saxophone and thick veins genes in Drosophila. *Cell* **78**, 251–261.

**Campbell, G. and Tomlinson, A.** (1999). Transducing the Dpp morphogen gradient in the wing of Drosophila: Regulation of Dpp targets by brinker. *Cell* **96**, 553–562.

**Cargnello, M. and Roux, P. P.** (2011). Activation and Function of the MAPKs and Their Substrates, the MAPK-Activated Protein Kinases. *Microbiol. Mol. Biol. Rev.* **75**, 50–83.

**Chavez, V. M., Marques, G., Delbecque, J. P., Kobayashi, K., Hollingsworth, M., Burr, J., Natzle, J. E. and O'Connor, M. B.** (2000). The Drosophila disembodied gene controls late embryonic morphogenesis and codes for a cytochrome P450 enzyme that regulates embryonic ecdysone levels. *Development* **127**, 4115–4126.

**Chavoshi, T. M., Moussian, B. and Uv, A.** (2010). Tissue-autonomous EcR functions are required for concurrent organ morphogenesis in the Drosophila embryo. *Mech. Dev.* **127**, 308–319.

**Chen, X.** (2014). Bidirectional communication between tissues regulating morphogenesis in a Drosophila model of wound healing by. *Thesis. Sci. Mol. Biol. Biochem.*

**Chen, W., White, M. A. and Cobb, M. H.** (2002). Stimulus-specific requirements for MAP3 kinases in activating the JNK pathway. *J. Biol. Chem.* **277**, 49105–49110.

**Cherbas, L., Lee, K. and Cherbas, P.** (1991). Identification of ecdysone response elements by analysis of the Drosophila Eip28/29 gene. *Genes Dev.* **5**, 120–131.

**Cherbas, L., Hu, X., Zhimulev, I., Belyaeva, E. and Cherbas, P.** (2003). EcR isoforms in Drosophila: Testing tissue-specific requirements by targeted blockade and rescue. *Development* **130**, 271–284.

**Costa, M., Wilson, E. T. and Wieschaus, E.** (1994). A putative cell signal encoded by the folded gastrulation gene coordinates cell shape changes during Drosophila gastrulation. *Cell* **76**, 1075–1089.

**Dawes-Hoang, R. E., Parmar, K. M., Christiansen, A. E., Phelps, C. B., Brand, A. H. and Wieschaus, E. F.** (2005). Folded gastrulation, cell shape change and the control of myosin localization. *Development* **132**, 4165–4178.

**Dobens, L., Rudolph, K. and Berger, E. M.** (1991). Ecdysterone regulatory elements function as both transcriptional activators and repressors. *Mol. Cell. Biol.* **11**, 1846–1853.

**Dobens, L. L., Martin-Blanco, E., Martinez-Arias, A., Kafatos, F. C. and Raftery, L. A.** (2001). Drosophila puckered regulates Fos/Jun levels during follicle cell morphogenesis. *Development* **128**, 1845–1856.

**Dorfman, R. and Shilo, B. Z.** (2001). Biphasic activation of the BMP pathway patterns the Drosophila embryonic dorsal region. *Development* **128**, 965–972.

**Ducuing, A. and Vincent, S.** (2016). The actin cable is dispensable in directing dorsal closure dynamics but neutralizes mechanical stress to prevent scarring in the Drosophila embryo. *Nat. Cell Biol.* **18**, 1149–1160.

**Ducuing, A., Keeley, C., Mollereau, B. and Vincent, S.** (2015). A DPP-mediated feed-forward loop canalizes morphogenesis during Drosophila dorsal closure. *J. Cell Biol.* **208**, 239–248.

**Edwards, K. A., Chang, X. J. and Kiehart, D. P.** (1995). Essential light chain of Drosophila nonmuscle myosin II. *J. Muscle Res. Cell Motil.* **16**, 491–498.

**Fernandez, R., Tabarini, D., Azpiazu, N., Frasch, M. and Schlessinger, J.** (1995). The Drosophila insulin receptor homolog: a gene essential for embryonic development encodes two receptor isoforms with different signaling potential. *EMBO J.* **14**, 3373–3384.

**Fernández, B. G., Arias, A. M. and Jacinto, A.** (2007). Dpp signalling orchestrates dorsal closure by regulating cell shape changes both in the amnioserosa and in the epidermis. *Mech. Dev.* **124**, 884–897.

**Fossett, N., Zhang, Q., Gajewski, K., Choi, C. Y., Kim, Y. and Schulz, R. A.** (2000). The multitype zinc-finger protein U-shaped functions in heart cell specification in the Drosophila embryo. *Proc. Natl. Acad. Sci.* **97**,.

**Frank, L. H. and Rushlow, C.** (1996). A group of genes required for maintenance of the amnioserosa tissue in Drosophila. *Development* **122**, 1343–1352.

**Franke, J. D., Montague, R. A. and Kiehart, D. P.** (2005). Nonmuscle myosin II generates forces that transmit tension and drive contraction in multiple tissues

during dorsal closure. *Curr. Biol.* **15**, 2208–2221.

**Fu, H., Hu, Z., Wen, J., Wang, K. and Liu, Y.** (2009). TGF-β promotes invasion and metastasis of gastric cancer cells by increasing fascin1 expression via ERK and JNK signal pathways. *Acta Biochim. Biophys. Sin. (Shanghai).* **41**, 648–656.

**Fuse, N., Yu, F. and Hirose, S.** (2013). Gprk2 adjusts Fog signaling to organize cell movements in Drosophila gastrulation. *Dev.* **140**, 4246–4255.

**Gallo, K. A. and Johnson, G. L.** (2002). Mixed-lineage kinase control of JNK and p38 MAPK pathways. *Nat. Rev. Mol. Cell Biol.* **3**, 663–672.

**Gauhar, Z., Sun, L. V, Hua, S., Mason, C. E., Fuchs, F., Li, T. R., Boutros, M. and White, K. P.** (2009). Genomic mapping of binding regions for the Ecdysone receptor protein complex. *Genome Res.* **19**, 1006–1013.

**Geh, E., Meng, Q., Mongan, M., Wang, J., Takatori, A., Zheng, Y., Puga, A., Lang, R. A. and Xia, Y.** (2011). Mitogen-activated protein kinase kinase kinase 1 (MAP3K1) integrates developmental signals for eyelid closure. *Proc. Natl. Acad. Sci. U. S. A.* **108**, 17349–17354.

**Giesen, K., Lammel, U., Langehans, D., Krukkert, K., Bunse, I. and Klämbt, C.** (2003). Regulation of glial cell number and differentiation by ecdysone and Fos signaling. *Mech. Dev.* **120**, 401–413.

**Glise, B., Bourbon, H. and Noselli, S.** (1995). hemipterous encodes a novel drosophila MAP kinase kinase, required for epithelial cell sheet movement. *Cell* **83**, 451–461.

**Greenberg, L. and Hatini, V.** (2011). Systematic expression and loss-of-function analysis defines spatially restricted requirements for Drosophila RhoGEFs and RhoGAPs in leg morphogenesis. *Mech. Dev.* **128**, 5–17.

**Grose, R. and Martin, P.** (1999). Parallels between wound repair and morphogenesis in the embryo. *Semin. Cell Dev. Biol.* **10**, 395–404.

**Harden, N.** (2002). Signaling pathways directing the movement and fusion of epithelial sheets : lessons from dorsal closure in Drosophila. *Differentiation* **70**, 181–203.

**Harden, N., Lee, J., Loh, H. Y., Ong, Y. M., Tan, I., Leung, T., Manser, E. and Lim, L.** (1996). A Drosophila homolog of the Rac- and Cdc42-activated serine/threonine kinase PAK is a potential focal adhesion and focal complex protein that colocalizes with dynamic actin structures. *Mol. Cell. Biol.* **16**, 1896–1908.

**Harden, N., Ricos, M., Ong, Y. M., Chia, W. and Lim, L.** (1999). Participation of small GTPases in dorsal closure of the Drosophila embryo: Distinct roles for Rho subfamily proteins in epithelial morphogenesis. *J. Cell Sci.* **112**, 273–284.

**Harrington, W. F. and Rodgers, M. E.** (1984). MYOSIN William. *Annu. Rev. Biochem.*

**53**, 35–73.

**Hashimoto, C., Kim, D. R., Weiss, L. A., Miller, J. W. and Morisato, D.** (2003). Spatial regulation of developmental signaling by a serpin. *Dev. Cell* **5**, 945–950.

**Hayes, P. and Solon, J.** (2017). Mechanisms of Development Drosophila dorsal closure : An orchestra of forces to zip shut the embryo. *Mech. Dev.* **144**, 2–10.

**Heissler, S. M. and Sellers, J. R.** (2014). Myosin light chains: Teaching old dogs new tricks. *Bioarchitecture* **4**, 169–188.

**Holst, J. P., Soldin, O. P., Guo, T. and Soldin, S. J.** (2013). Steroid hormones: relevance and measurement in the clinical laboratory Jennifer. *NIH Public Access* **24**, 105–118.

**Hoodless, P. A., Haerry, T., Abdollah, S., Stapleton, M., O'Connor, M. B., Attisano, L. and Wrana, J. L.** (1996). MADR1, a MAD-related protein that functions in BMP2 signaling pathways. *Cell* **85**, 489–500.

**Hotamisligil, G. S.** (2006). Inflammation and metabolic disorders. *Nature* **444**, 860–867.

**Hou, X. S., Goldstein, E. S. and Perrimon, N.** (1997). Drosophila jun relays the jun amino-terminal kinase signal transduction pathway to the decapentaplegic signal transduction pathway in regulating epithelial cell sheet movement. *Genes Dev.* **11**, 1728–1737.

**Igaki, T.** (2009). Correcting developmental errors by apoptosis: Lessons from Drosophila JNK signaling. *Apoptosis* **14**, 1021–1028.

**Inoue, H., Imamura, T., Ishidou, Y., Takase, M., Udagawa, Y., Oka, Y., Tsuneizumi, K., Tabata, T., Miyazono, K. and Kawabata, M.** (1998). Interplay of signal mediators of decapentaplegic (Dpp): Molecular characterization of Mothers against dpp, Medea, and Daughters against dpp. *Mol. Biol. Cell* **9**, 2145–2156.

**Ip, Y. T. and Davis, R. J.** (1998). Signal transduction by the c-Jun N-terminal kinase (JNK) - From inflammation to development. *Curr. Opin. Cell Biol.* **10**, 205–219.

**Jacinto, A. and Martin, P.** (2001). Morphogenesis: Unravelling the cell biology of hole closure. *Curr. Biol.* **11**, 705–707.

**Jacinto, A., Wood, W., Balayo, T., Turmaine, M., Martinez-Arias, A. and Martin, P.** (2000). Dynamic actin-based epithelial adhesion and cell matching during Drosophila dorsal closure. *Curr. Biol.* **10**, 1420–1426.

**Jacinto, A., Woolner, S. and Martin, P.** (2002). Dynamic analysis of dorsal closure in Drosophila: From genetics to cell biology. *Dev. Cell* **3**, 9–19.

**Jackson, P. D. and Hoffmann, F. M.** (1994). Embryonic expression patterns of the

drosophila decapentaplegic gene: Separate regulatory elements control blastoderm expression and lateral ectodermal expression. *Dev. Dyn.* **199**, 28–44.

**Jani, K. and Schock, F.** (2007). Zasp Is Required for the Assembly of Functional Integrin Adhesion Sites. *J. Cell Biol.* **179**, 1583–1597.

**Jankovics, F. and Brunner, D.** (2006). Transiently Reorganized Microtubules Are Essential for Zippering during Dorsal Closure in Drosophila melanogaster. *Dev. Cell* **11**, 375–385.

**Jennings, B. H.** (2011). Drosophila-a versatile model in biology & medicine. *Mater. Today* **14**, 190–195.

**Johnson, G. L. and Nakamura, K.** (2007). The c-jun kinase/stress-activated pathway: Regulation, function and role in human disease. *Biochim. Biophys. Acta - Mol. Cell Res.* **1773**, 1341–1348.

**Jordan, P. and Karess, R.** (1997). Myosin Light Chain-Activating Phosphorylation Sites Are Required for Oogenesis in Drosophila. *J. Cell Biol.* **139**, 1805–1819.

**Karess, R. E., Chang, X. jia, Edwards, K. A., Kulkarni, S., Aguilera, I. and Kiehart, D. P.** (1991). The regulatory light chain of nonmuscle myosin is encoded by spaghetti-squash, a gene required for cytokinesis in Drosophila. *Cell* **65**, 1177–1189.

**Karpova, N., Bobinnec, Y., Fouix, S., Huitorel, P. and Debec, A.** (2006). Jupiter , a New Drosophila Protein Associated With Microtubules. *Cell Motil. Cytoskeleton* **312**, 301–312.

**Kellerman, K. A., Miller, K. G., Kellerman, K. A. and Miller, K. G.** (1992). An Unconventional Myosin Heavy Chain Gene from Drosophila melanogaster Stable URL : https://www.jstor.org/stable/1615376 REFERENCES Linked references are available on JSTOR for this article : An Unconventional Myosin Heavy Chain Gene from Drosophila melan. *J. Cell Biol.* **119**, 823–834.

**Kennison, J. A.** (2008). Dissection of larval salivary glands and polytene chromosomes preparation. *Cold Spring Harb. Protoc.* **3**, 1–6.

**Khoo, P., Allan, K., Willoughby, L., Brumby, A. M. and Richardson, H. E.** (2013). In Drosophila, RhoGEF2 cooperates with activated Ras in tumorigenesis through a pathway involving Rho1-Rok-Myosin-II and JNK signalling. *DMM Dis. Model. Mech.* **6**, 661–678.

**Kiehart, D. P. and Feghali, R.** (1986). Cytoplasmic Myosin from Drosophila melanogaster. *J. Cell Biol.* **103**, 1517–1525.

**Kiehart, D. P., Galbraith, C. G., Edwards, K. A., Rickoll, W. L. and Montague, R. A.** (2000). Multiple Forces Contribute to Cell Sheet Morphogenesis for Dorsal Closure

in Drosophila. **149**, 1–20.

**Kiehart, D. P., Crawford, J. M., Aristotelous, A., Venakides, S. and Edwards, G. S.** (2017). Cell Sheet Morphogenesis: Dorsal Closure in Drosophila melanogaster as a Model System. *Annu. Rev. Cell Dev. Biol.* **33**, 169–202.

**Kim, H.** (2017). Characterization of signaling pathways enabling coordinated morphogenesis of tissues during Drosophila dorsal closure by. *Thesis. Sci. Mol. Biol. Biochem.*

**Koelle, M. R., Talbot, W. S., Segraves, W. A., Bender, M. T., Cherbas, P. and Hogness, D. S.** (1991). The drosophila EcR gene encodes an ecdysone receptor, a new member of the steroid receptor superfamily. *Cell* **67**, 59–77.

**Kozlova, T. and Thummel, C. S.** (2003). Essential roles for ecdysone signaling during Drosophila mid-embryonic development. *Science (80-. ).* **301**, 1911–1914.

**Kuan, C. Y., Yang, D. D., Samanta Roy, D. R., Davis, R. J., Rakic, P. and Flavell, R. A.** (1999). The Jnk1 and Jnk2 protein kinases are required for regional specific apoptosis during early brain development. *Neuron* **22**, 667–676.

**Kushner, P. J., Agard, D. A., Greene, G. L., Scanlan, T. S., Shiau, A. K., Uht, R. M. and Webb, P.** (2000). <Kushner Et Al 2000 Ap1 Er Review.Pdf>. *J. Steroid Biochem. Mol. Biol.* **74**, 311–317.

**Lacy, M. E. and Hutson, M. S.** (2016). Amnioserosa development and function in Drosophila embryogenesis: Critical mechanical roles for an extraembryonic tissue. *Dev. Dyn.* **245**, 558–568.

**Lada, K., Gorfinkiel, N. and Arias, A. M.** (2012). Interactions between the amnioserosa and the epidermis revealed by the function of the u-shaped gene. *Biol. Open* **1**, 353–361.

**Lamka, M. L. and Lipshitz, H. D.** (1999). Role of the Amnioserosa in Germ Band Retraction of the Drosophila melanogaster Embryo. *Dev. Biol.* **112**, 102–112.

**Le Dily, F. and Beato, M.** (2018). Signaling by steroid hormones in the 3D nuclear space. *Int. J. Mol. Sci.* **19**, 1–16.

**Lécuyer, E., Nećakov, A. S., Céceres, L. and Krause, H. M.** (2008). High resolution flourescent in situ hybridization of Drosophila embryos and tissues. *Cold Spring Harb. Protoc.* **3**, 1–11.

**Lehmann, M., Jiang, C., Ip, Y. T. and Thummel, C. S.** (2002). AP-1, but not NF-κB, is required for efficient steroid-triggered cell death in Drosophila. *Cell Death Differ.* **9**, 581–590.

**Letsou, A., Arora, K., Wrana, J. L., Simin, K., Twombly, V., Jamal, J., Staehling-**

**Hampton, K., Hoffmann, F. M., Gelbart, W. M., Massagué, J., et al.** (1995). Drosophila Dpp signaling is mediated by the punt gene product: A dual ligand-binding type II receptor of the TGFβ receptor family. *Cell* **80**, 899–908.

**Leung, I. W. L. and Lassam, N.** (2001). The kinase activation loop is the key to mixed lineage kinase-3 activation via both autophosphorylation and hematopoetic progenitor kinase 1 phosphorylation. *J. Biol. Chem.* **276**, 1961–1967.

**Li, Y., Zhang, Z., Robinson, G. E. and Palli, S. R.** (2007). Identification and characterization of a juvenile hormone response element and its binding proteins. *J. Biol. Chem.* **282**, 37605–37617.

**Liu, S. L., Fewkes, N., Ricketson, D., Penkert, R. R. and Prehoda, K. E.** (2008). Filament-dependent and -independent localization modes of Drosophila non-muscle myosin II. *J. Biol. Chem.* **283**, 380–387.

**Loubiere, V., Delest, A., Schuettengruber, B., Martinez, A.-M. and Cavalli, G.** (2017). Chromatin Immunoprecipitation Experiments from Whole Drosophila Embryos or Larval Imaginal Discs. *BIO-PROTOCOL* **7**, 1–17.

**Martin-blanco, E.** (1997). Regulation of cell differentiation by the Drosophila Jun kinase cascade. *Curr. Opin. Genet. Dev.* **7**, 666–671.

**Martín-Blanco, E., Gampel, A., Ring, J., Virdee, K., Kirov, N., Tolkovsky, A. M. and Martinez-Arias, A.** (1998). puckered encodes a phosphatase that mediates a feedback loop regulating JNK activity during dorsal closure in Drosophila. *Genes Dev.* **12**, 557–670.

**Martín-Blanco, E., Pastor-Pareja, J. C. and García-Bellido, A.** (2000). JNK and decapentaplegic signaling control adhesiveness and cytoskeleton dynamics during thorax closure in Drosophila. *Proc. Natl. Acad. Sci. U. S. A.* **97**, 7888–7893.

**Martin, P. and Parkhurst, S. M.** (2004). Parallels between tissue repair and embryo morphogenesis. *Development* **131**, 3021–3034.

**Mason, F. M., Xie, S., Vasquez, C. G., Tworoger, M. and Martin, A. C.** (2016). RhoA GTPase inhibition organizes contraction during epithelial morphogenesis. *J. Cell Biol.* **214**, 603–617.

**Mihaly, J., Kockel, L., Gaengel, K., Weber, U., Bohmann, D. and Mlodzik, M.** (2001). The role of the Drosophila TAK homologue dTAK during development. *Mech. Dev.* **102**, 67–79.

**Miller, W. L.** (2017). Disorders in the initial steps of steroid hormone synthesis. *J. Steroid Biochem. Mol. Biol.* **165**, 18–37.

**Millo, H., Leaper, K., Lazou, V. and Bownes, M.** (2004). Myosin VI plays a role in cell-cell adhesion during epithelial morphogenesis. *Mech. Dev.* **121**, 1335–1351.

**Minami, M., Kinoshita, N., Kamoshida, Y., Tanimoto, H. and Tabata, T.** (1999). brinker is a target of Dpp in Drosophila that negatively regulates Dpp- dependent genes. *Nature* **398**, 242–246.

**Mizuno, T., Tsutsui, K. and Nishida, Y.** (2002). Drosophila myosin phosphatase and its role in dorsal closure. *Development* **129**, 1215–1223.

**Mueller, B. K.** (1999). GROWTH CONE GUIDANCE: First Steps Towards a Deeper Understanding. *Annu. Rev. Neurosci.* **22**, 351–388.

**Muliyil, S. and Narasimha, M.** (2014). Mitochondrial ROS Regulates Cytoskeletal and Mitochondrial Remodeling to Tune Cell and Tissue Dynamics in a Model for Wound Healing. *Dev. Cell* **28**, 239–252.

**Muliyil, S., Krishnakumar, P. and Narasimha, M.** (2011). Spatial, temporal and molecular hierarchies in the link between death, delamination and dorsal closure. *Development* **138**, 3043–3054.

**Muller, H.-A. J.** (2008). Immunolabelling of embryos. *Methods Mol. Biol.* **420**, 207–218.

**Muñoz-Descalzo, S., Terol, J. and Paricio, N.** (2005). Cabut, a C2H2 zinc finger transcription factor, is required during Drosophila dorsal closure downstream of JNK signaling. *Dev. Biol.* **287**, 168–179.

**Niwa, R. and Niwa, Y. S.** (2014). Enzymes for ecdysteroid biosynthesis : their biological functions in insects and beyond. *Biosci. Biotechnol. Biochem.* **78**, 1283–1292.

**Niwa, R., Namiki, T., Ito, K., Shimada-Niwa, Y., Kiuchi, M., Kawaoka, S., Kayukawa, T., Banno, Y., Fujimoto, Y., Shigenobu, S., et al.** (2010). Non-molting glossy/shroud encodes a short-chain dehydrogenase/reductase that functions in the “Black Box” of the ecdysteroid biosynthesis pathway. *Development* **137**, 1991–1999.

**Ono, H., Rewitz, K. F., Shinoda, T., Itoyama, K., Petryk, A., Rybczynski, R., Jarcho, M., Warren, J. T., Marqués, G., Shimell, M. J., et al.** (2006). Spook and Spookier code for stage-specific components of the ecdysone biosynthetic pathway in Diptera. *Dev. Biol.* **298**, 555–570.

**Parks, A. L., Cook, K. R., Belvin, M., Dompe, N. A., Fawcett, R., Huppert, K., Tan, L. R., Winter, C. G., Bogart, K. P., Deal, J. E., et al.** (2004). Systematic generation of high-resolution deletion coverage of the Drosophila melanogaster genome. *Nat. Genet.* **36**, 288–292.

**Pasakarnis, L., Frei, E., Caussinus, E., Affolter, M. and Brunner, D.** (2016). Amnioserosa cell constriction but not epidermal actin cable tension autonomously drives dorsal closure. *Nat. Cell Biol.* **18**, 1161–1172.

**Qi, M. and Elion, E. A.** (2005). MAP kinase pathways. *J. Cell Sci.* **118**, 3569–3572.

**Raftery, L. A. and Sutherland, D. J.** (1999). TGF-β family signal transduction in Drosophila development: From Mad to Smads. *Dev. Biol.* **210**, 251–268.

**Ranz, J. M., Maurin, D., Chan, Y. S., Von Grotthuss, M., Hillier, L. D. W., Roote, J., Ashburner, M. and Bergman, C. M.** (2007). Principles of genome evolution in the Drosophila melanogaster species group. *PLoS Biol.* **5**, 1366–1381.

**Reed, B. H., Wilk, R. and Lipshitz, H. D.** (2001). Downregulation of Jun kinase signaling in the amnioserosa is essential for dorsal closure of the Drosophila embryo. *Curr. Biol.* **11**, 1098–1108.

**Ricketson, D., Johnston, C. A. and Prehoda, K. E.** (2010). Multiple tail domain interactions stabilize nonmuscle myosin II bipolar filaments. *Proc. Natl. Acad. Sci. U. S. A.* **107**, 20964–20969.

**Riddiford, L. M., Cherbas, P. and Truman, J. W.** (2001). Ecdysone Receptors and Their Biological Actions. *Vitamis Horm.* **60**, 1–73.

**Riesgo-Escovar, J. R. and Hafen, E.** (1997a). Drosophila jun kinase regulates expression of decapentaplegic via the ets-domain protein Aop and the ap-1 transcription factor Djun during dorsal closure. *Genes Dev.* **11**, 1717–1727.

**Riesgo-Escovar, J. R. and Hafen, E.** (1997b). Common and distinct roles of DFos and DJun during Drosophila development. *Science (80-. ).* **278**, 669–672.

**Riesgo-Escovar, J. R., Jenni, M., Fritz, A. and Hafen, E.** (1996). The Drosophila jun-N-terminal kinase is required for cell morphogenesis but not for DJun-dependent cell fate specification in the eye. *Genes Dev.* **10**, 2759–2768.

**Rodriguez-Diaz, A., Toyama, Y., Abravanel, D. L., Wiemann, J. M., Wells, A. R., Tulu, U. S., Edwards, G. S. and Kiehart, D. P.** (2008). Actomyosin purse strings: Renewable resources that make morphogenesis robust and resilient. *HFSP J.* **2**, 220–237.

**Roote, J. and Prokop, A.** (2013). How to design a genetic mating scheme: a basic training package for Drosophila genetics. *G3 (Bethesda).* **3**, 353–358.

**Rothwell, W. . and Sullivan, W.** (2007a). Drosophila embryo collection. *CSH Protoc.* doi:10.1101/pdb.prot4825.

**Rothwell, W. . and Sullivan, W.** (2007b). Drosophila embryo dechorionation. *CSH Protoc.* doi:10.1101/pdb.prot4826.

**Rothwell, W. . and Sullivan, W.** (2007c). Fixation of Drosophila embryos. *CSH Protoc.* doi:10.1101/pdb.prot4827.

**Ruberte, E., Marty, T., Nellen, D., Affolter, M. and Basler, K.** (1995). An absolute requirement for both the type II and type I receptors, punt and thick veins, for Dpp

signaling in vivo. *Cell* **80**, 889–897.

**Rubin, G. M., Hong, L., Brokstein, P., Evans-holm, M., Frise, E., Stapleton, M. and Harvey, D. A.** (2000). DNA Resource. *Science (80-. ).* **287**, 2222–2224.

**Sanchis, A., Bayo, P., Sevilla, L. M. and Pérez, P.** (2010). Glucocorticoid receptor antagonizes EGFR function to regulate eyelid development. *Int. J. Dev. Biol.* **54**, 1471–1478.

**Sathyanarayana, P., Barthwal, M. K., Lane, M. E., Acevedo, S. F., Skoulakis, E. M. C., Bergmann, A. and Rana, A.** (2003). Drosophila mixed lineage kinase/slipper, a missing biochemical link in Drosophila JNK signaling. *Biochim. Biophys. Acta - Mol. Cell Res.* **1640**, 77–84.

**Sekelsky, J. J., Newfeld, S. J., Raftery, L. A., Chartoff, E. H. and Gelbart, W. M.** (1995). Genetic characterization and cloning of mothers against dpp, a gene required for decapentaplegic function in Drosophila melanogaster. *Genetics* **139**, 1347–1358.

**Simske, J. S. and Hardin, J.** (2001). Getting into shape: Epidermal morphogenesis in Caenorhabditis elegans embryos. *BioEssays* **23**, 12–23.

**Sluss, H. K. and Davis, R. J.** (1997). Embryonic morphogenesis signaling pathway mediated by JNK targets the transcriptions factor JUN and the TGF-β homologue decapentaplegic. *J. Cell. Biochem.* **67**, 1–12.

**Sluss, H. K., Han, Z., Barrett, T., Davis, R. J. and Ip, Y. T.** (1996). A JNK signal transduction pathway that mediates morphogenesis and an immune response in Drosophila. *Genes Dev.* **10**, 2745–2758.

**Söderberg, O., Gullberg, M., Jarvius, M., Ridderstråle, K., Leuchowius, K. J., Jarvius, J., Wester, K., Hydbring, P., Bahram, F., Larsson, L. G., et al.** (2006). Direct observation of individual endogenous protein complexes in situ by proximity ligation. *Nat. Methods* **3**, 995–1000.

**Sokolow, A., Toyama, Y., Kiehart, D. P. and Edwards, G. S.** (2012). Cell ingression and apical shape oscillations during dorsal closure in Drosophila. *Biophys. J.* **102**, 969–979.

**Solon, J., Kaya-Çopur, A., Colombelli, J. and Brunner, D.** (2009). Pulsed Forces Timed by a Ratchet-like Mechanism Drive Directed Tissue Movement during Dorsal Closure. *Cell* **137**, 1331–1342.

**Stapleton, M., Carlson, J., Brokstein, P., Yu, C., Champe, M., George, R., Guarin, H., Kronmiller, B., Pacleb, J., Park, S., et al.** (2002). A Drosophila full-length cDNA resource. *Genome Biol.* **2**, 1–8.

**Stern, D. L. and Sucena, E.** (2011). Preparation of cuticles from unhatched first-instar

drosophila larvae. *Cold Spring Harb. Protoc.* **6**, 1110–1114.

**Strecker, T. R., Li, P., McGhee, S. A., Ham, D., Smith, S. K., Schreck, J. A., Youn, S. J. and Kon, P. S. H.** (1995). The effects of the glucocorticoid, dexamethasone, on the development of the Drosophila embryo. *Roux's Arch. Dev. Biol.* **204**, 359–368.

**Stronach, B. E. and Perrimon, N.** (2001). Investigation of leading edge formation at the interface of amnioserosa and dorsal ectoderm in the Drosophila embryo. *Development* **128**, 2905–2913.

**Stronach, B. and Perrimon, N.** (2002). Activation of the JNK pathway during dorsal closure in Drosophila requires the mixed lineage kinase, slipper. *Genes Dev.* **16**, 377–387.

**Talbot, W. S., Swyryd, E. A. and Hogness, D. S.** (1993). Drosophila tissues with different metamorphic responses to ecdysone express different ecdysone receptor isoforms. *Cell* **73**, 1323–1337.

**Teurich, S. and Angel, P.** (1995). The glucocorticoid receptor synergizes with jun homodimers to activate AP-1-regulated promoters lacking GR binding sites. *Chem. Senses* **20**, 251–255.

**Thummel, C. S.** (1995). From embryogenesis to metamorphosis: The regulation and function of drosophila nuclear receptor superfamily members. *Cell* **83**, 871–877.

**Toyama, Y., Peralta, X. G., Wells, A. R., Kiehart, D. P. and Edwards, G. S.** (2008). Apoptotic force and tissue dynamics during Drosophila embryogenesis. *Science (80-. ).* **321**, 1683–1686.

**Tsai, C. C., Kao, H. Y., Yao, T. P., McKeown, M. and Evans, R. M.** (1999). SMRTER, a Drosophila nuclear receptor coregulator, reveals that EcR-mediated repression is critical for development. *Mol. Cell* **4**, 175–186.

**Vasquez, C. G., Heissler, S. M., Billington, N., Sellers, J. R. and Martin, A. C.** (2016). Drosophila non-muscle myosin II motor activity determines the rate of tissue folding. *Elife* **5**, 1–20.

**Wada, A., Kato, K., Uwo, M. F., Yonemura, S. and Hayashi, S.** (2007). Specialized extraembryonic cells connect embryonic and extraembryonic epidermis in response to Dpp during dorsal closure in Drosophila. *Dev. Biol.* **301**, 340–349.

**Wells, A. R., Zou, R. S., Tulu, U. S., Sokolow, A. C., Crawford, J. M., Edwards, G. S. and Kiehart, D. P.** (2014). Complete canthi removal reveals that forces from the amnioserosa alone are sufficient to drive dorsal closure in Drosophila. *Mol. Biol. Cell* **25**, 3552–3568.

**Werner, S., Krieg, T. and Smola, H.** (2007). Keratinocyte-fibroblast interactions in wound healing. *J. Invest. Dermatol.* **127**, 998–1008.

**West, J. J., Zulueta-Coarasa, T., Maier, J. A., Lee, D. M., Bruce, A. E. E., Fernandez-Gonzalez, R. and Harris, T. J. C.** (2017). An Actomyosin-Arf-GEF Negative Feedback Loop for Tissue Elongation under Stress. *Curr. Biol.* **27**, 2260-2270.e5.

**Xia, Y. and Karin, M.** (2004). The control of cell motility and epithelial morphogenesis by Jun kinases. *Trends Cell Biol.* **14**, 94–101.

**Yang, J., Zhang, N., Gao, R., Zhu, Y., Zhang, Z., Xu, X., Wang, J., Li, Z., Liu, X., Li, Z., et al.** (2018). TGF-β1 induced fascin1 expression facilitates the migration and invasion of kidney carcinoma cells through ERK and JNK signaling pathways. *Biochem. Biophys. Res. Commun.* **501**, 913–919.

**Yao, T. P., Segraves, W. A., Oro, A. E., McKeown, M. and Evans, R. M.** (1992). Drosophila ultraspiracle modulates ecdysone receptor function via heterodimer formation. *Cell* **71**, 63–72.

**Young, P. E., Richman, A. M., Ketchum, A. S. and Kiehart, D. P.** (1993). Morphogenesis in Drosophila requires nonmuscle myosin heavy chain function. *Genes Dev.* **7**, 29–41.

**Zahedi, B., Shen, W., Xu, X., Chen, X., Mahey, M. and Harden, N.** (2008). Leading edge-secreted Dpp cooperates with ACK-dependent signaling from the amnioserosa to regulate myosin levels during dorsal closure. *Dev. Dyn.* **237**, 2936–2946.

**Zeitlinger, J. and Bohmann, D.** (1999). Thorax closure in Drosophila: Involvement of Fos and the JNK pathway. *Development* **126**, 3947–3956.

**Zeitlinger, J., Kockel, L., Peverali, F. A., Jackson, D. B., Mlodzik, M. and Bohmann, D.** (1997). Defective dorsal closure and loss of epidermal decapentaplegic expression in Drosophila fos mutants. *EMBO J.* **16**, 7393–7401.

**Zhang, L., Wang, W., Hayashi, Y., Jester, J. V., Birk, D. E., Gao, M., Liu, C. Y., Kao, W. W. Y., Karin, M. and Xia, Y.** (2003). A role for MEK kinase 1 in TGF-β/activin-induced epithelium movement and embryonic eyelid closure. *EMBO J.* **22**, 4443–4454.

**Zhao, C., Gao, H., Liu, Y., Papoutsi, Z., Jaffrey, S., Gustafsson, J. Å. and Dahlman-Wright, K.** (2010). Genome-wide mapping of estrogen receptor-β-binding regions reveals extensive cross-talk with transcription factor activator protein-1. *Cancer Res.* **70**, 5174–5183.

**Zimmermann, G., Furlong, E. E., Suyama, K. and Scott, M. P.** (2006). Mes2 , a MADF-Containing Transcription Factor Essential for Drosophila Development. *Dev. Dyn.* **235**, 3387–3395.

**Zubeldia-Brenner, L., Roselli, C. E., Recabarren, S. E., Gonzalez Deniselle, M. C. and Lara, H. E.** (2016). Developmental and Functional Effects of Steroid Hormones on the Neuroendocrine Axis and Spinal Cord. *J. Neuroendocrinol.* **28**,.

# Appendix A Rho1, RhoGAP71E recombination stock

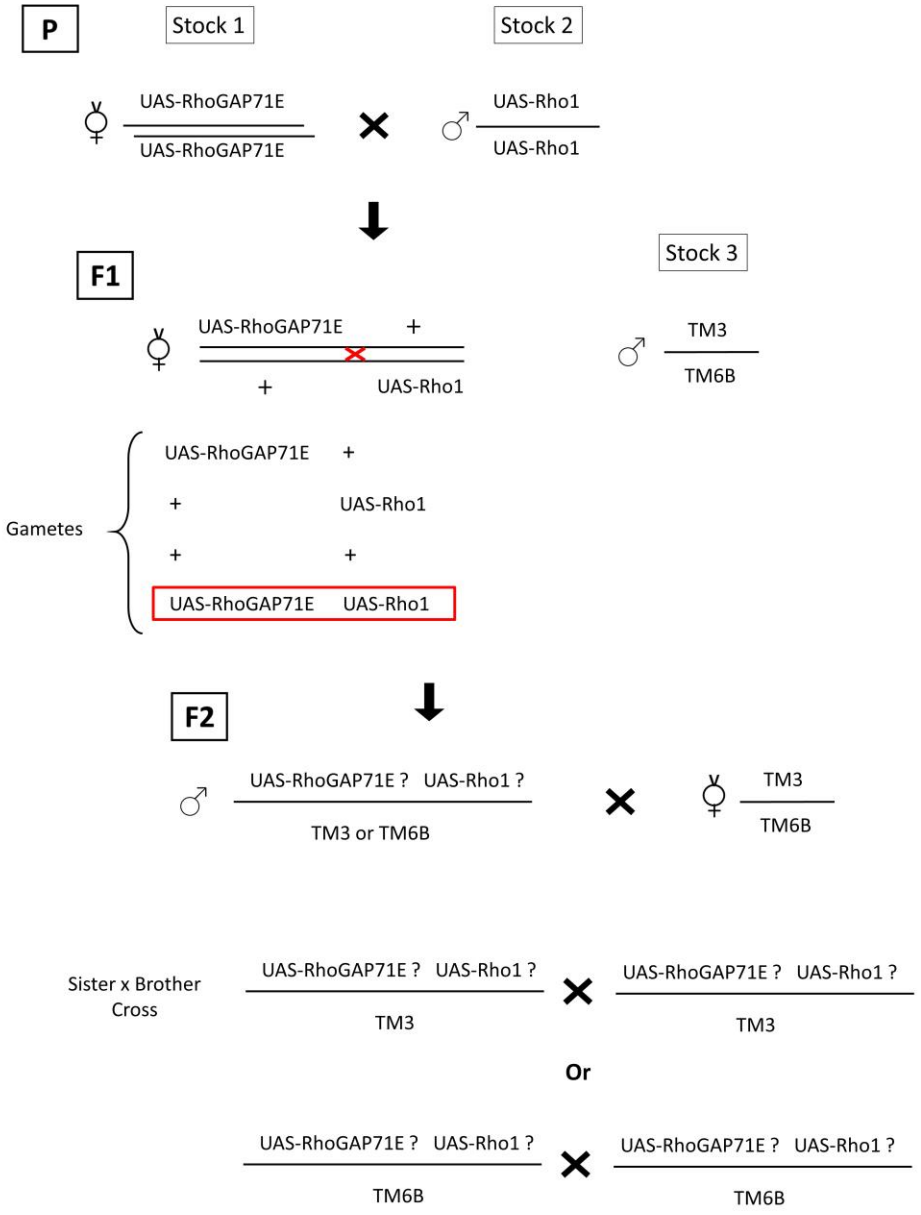


**S.Figure 1 A scheme for constructing Rho1, RhoGAP71E recombination stock**

Only Chromosome 3 is shown here.

# Appendix B Subcloning

**Table 2 List of cDNAs with corresponding antibiotics and restriction enzymes**

| Name | CG | Clone | Vector / Antibiotics | DIGESTION | ANTISENSE |
|---|---|---|---|---|---|
| cabut (cbt) | CG4427 | RE07124 | pFLC-1 Amp | EX (11+1548+3411) | NotI + T3 |
| Chd64 (Chd64) | CG14996 | GH28730 | pOT2 Chl | EX (248+1173+**1665**) | EcoRI + Sp6 |
| Ecdysone receptor (EcR) | CG1765 | RE06878 | pFLC-1 Amp | EX (81+1273+1801+3953) | NotI + T3 |
| G protein-coupled receptor kinase 2 (Gprk2) | CG17998 | LD21923 | pOT2 Chl | EX (**1665**+3075) | EcoRI + Sp6 |
| Insulin-like receptor (InR) | CG18402 | LD06045 | pBS_SK(-) Amp | EX (**2958**+3355 ) | EcoRI + T7 |
| jaguar (jar) | CG5695 | FI18104 | pFLC-1 Amp | BN (**3005**+4571) | NotI + T3 |
| jupiter (jup) | CG31363 | GH10365 | pOT2 Chl | EX (889+**1665**) | EcoRI + Sp6 |
| mesoderm-expressed 2 (mes2) | CG11100 | SD09884 | pOT2 Chl | EX (**1665**+2287) | EcoRI + Sp6 |
| Rho GTPase activating protein at 71E (RhoGAP71E) | CG32149 | LD04071 | pBS_SK(-) Amp | EX (**2958**+3069) | EcoRI + T7 |
| steppke (step) | CG11628 | RE34385 | pFLC-1 Amp | EX (221+4519) | NotI + T3 |
| u-shaped (ush) | CG2762 | LD12631 | pBS_SK(-) Amp | EX (1096+1449+1940+**2958** ) | SmaI/XbaI + T7 |
| ultraspiracle (usp) | CG4380 | LD09973 | pBS_SK(-) Amp | EX (662+1844+**2958** ) | EcoRI + T7 |
| Zasp52 | CG30084 | RH03424 | pFLC-1 Amp | BN (**3005**+3188) | NotI + T3 |
| zipper (zip) | CG15792 | LD21871 | pOT2 Chl | EX (**1665**+2397) | EcoRI + Sp6 |

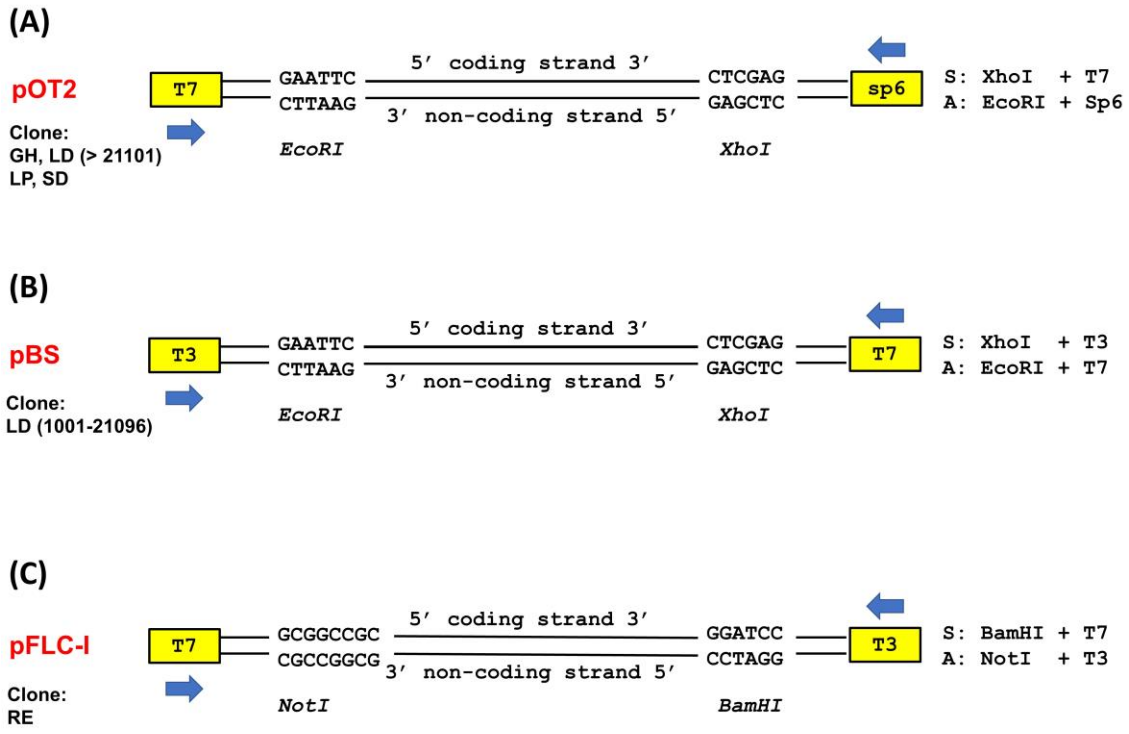


**S.Figure 2 Schematics of cloning sites and promoters in pOT2, pBS and pFLC-1 vectors for probe synthesis.**

(A) cDNAs start with GH, LD (number higher than 21101),LP, SD clone are inserted into pOT2 vectors. (B) cDNAs start with LD (number between 1001-21096) are inserted into pBS, (C) cDNAs start with RE are inserted into pFLC-1. S: sense probe, A: Anti-sense probe

# Appendix C Subcloning for pull-down assay

Coding regions from the clones were inserted in frame into pGEX-4T-1 (GE Healthcare, 28-9545-49) and pET-28a(+) (MilliporeSigma, 69864-3) to create N-terminal, GST- and His-tagged constructs, respectively.

*ultraspiracle (Usp)*/LD09973

F: ATGAATTCATGGACAACTGCGACCAGG (27bp|48.1%|61 ℃)
R: ATGCGGCCGCCTACTCCAGTTTCATCG (27bp|59.3%|66℃)
Internal Primer: TAGCGGTCCAGGTTCGGTAGG (21bp|61.9%|60.7℃)
Forward primer contains EcoRI restriction site
Reverse primer contains NotI restriction site

ATGGACAACTGCGACCAGGACGCCAGCTTTCGGCTGAGCCACATCAAGGAGGAGGTCAAGCCGGA
CATCTCGCAGCTGAACGACAGCAACAACAGCAGCTTTTCGCCCAAGGCCGAGAGTCCCGTGCCCT
TCATGCAGGCCATGTCCATGGTCCACGTGCTGCCCGGCTCCAACTCCGCCAGCTCCAACAACAAC
AGCGCTGGAGATGCCCAAATGGCGCAGGCGCCCAATTCGGCTGGAGGCTCTGCCGCCGCTGCAGT
CCAGCAGCAGTATCCGCCTAACCATCCGCTGAGCGGCAGCAAGCACCTCTGCTCTATTTGCGGGG
ATCGGGCCAGTGGCAAGCACTACGGCGTGTACAGCTGTGAGGGCTGCAAGGGCTTCTTTAAACGC
ACAGTGCGCAAGGATCTCACATACGCTTGCAGGGAGAACCGCAACTGCATCATAGACAAGCGGCA
GAGGAACCGCTGCCAGTACTGCCGCTACCAGAAGTGCCTAACCTGCGGCATGAAGCGCGAAGCGG
TCCAGGAGGAGCGTCAACGCGGCGCCCGCAATGCGGCGGGTAGGCTCAGCGCCAGCGGAGGCGGC
AGTAGCGGTCCAGGTTCGGTAGGCGGATCCAGCTCTCAAGGCGGAGGAGGAGGAGGCGGCGTTTC
TGGCGGAATGGGCAGCGGCAACGGTTCTGATGACTTCATGACCAATAGCGTGTCCAGGGATTTCT
CGATCGAGCGCATCATAGAGGCCGAGCAGCGAGCGGAGACCCAATGCGGCGATCGTGCACTGACG
TTCCTGCGCGTTGGTCCCTATTCCACAGTCCAGCCGGACTACAAGGGTGCCGTGTCGGCCCTGTG
CCAAGTGGTCAACAAACAGCTCTTCCAGATGGTCGAATACGCGCGCATGATGCCGCACTTTGCCC
AGGTGCCGCTGGACGACCAGGTGATTCTGCTGAAAGCCGCTTGGATCGAGCTGCTCATTGCGAAC
GTGGCCTGGTGCAGCATCGTTTCGCTGGATGACGGCGGTGCCGGCGGCGGGGGCGGTGGACTAGG
CCACGATGGCTCCTTTGAGCGACGATCACCGGGCCTTCAGCCCCAGCAGCTGTTCCTCAACCAGA
GCTTCTCGTACCATCGCAACAGTGCGATCAAAGCCGGTGTGTCAGCCATCTTCGACCGCATATTG
TCGGAGCTGAGTGTAAAGATGAAGCGGCTGAATCTCGACCGACGCGAGCTGTCCTGCTTGAAGGC
CATCATACTGTACAACCCGGACATACGCGGGATCAAGAGCCGGGCGGAGATCGAGATGTGCCGCG
AGAAGGTGTACGCTTGCCTGGACGAGCACTGCCGCCTGGAACATCCGGGCGACGATGGACGCTTT
GCGCAACTGCTGCTGCGTCTGCCCGCTTTGCGATCGATCAGCCTGAAGTGCCAGGATCACCTGTT
CCTCTTCCGCATTACCAGCGACCGGCCGCTGGAGGAGCTCTTTCTCGAGCAGCTGGAGGCGCCGC
CGCCACCCGGCCTGGCGATGAAACTGGAGTAG

*Kayak (kay)* / LP01201

F: ATGAATTCATGAAAGTCAAAGTGGAGCG (28bp|39.3%|57.9℃)
R: ATCTCGAGTTATAAGCTGACCAGC (24bp|45.8%|56.3℃)
Internal Primer: ATACGCAGATGAACGAGGAGC (21bp|52.4%|57℃)

Forward primer contains EcoRI restriction site
Reverse primer contains XhoI restriction site

ATGAAAGTCAAAGTGGAGCGCACAACGAAAAAGCCCGCCATCAGAAAGCCCGAGGATCCAGATCC
GGCGGAAGAGGACAGGGTCAAGATGGTGCAGGATGACCCAGAGGACCAGGAGAACCAGGCGGTGG
ATGAGGAGGAGCTGGACTTTCTGCCCGCCGATCTAAGCGCTGCGATATCGACGGCGACAACGAAA
ATAGCAACACCGACGCGCAATCTTATCCTCGGCAACTTTGAGACCGGCCAGAGTGTTCTCACACT
GACGACGCCCACGTTGACGCCGACCACCACGCGCAACATCGAGGACACACTGGGCCACTTGCTCT
CGGACACGCAGACCGATCGTGTGGCTGGTTGCGCGGGATTTGCAGTGCCAAAGGTGCTACCCAAT
GCCATTGATGTCCTGGGCATGGGTATTCCCACCGGTGTTTCGTCGCTCCCACTTCAGCAGACATT
CGATTTGAGCCTGGGGCAGGGCAGCGAGTCCGAGGACTCCAACGCTTCGTACAACGATACGCAGA
TGAACGAGGAGCAGGACACGACCGATACTTCAAGTGCCCATACGGACAGCACCTCGTACCAAGCT
GGCCACATCATGGCGGGCAGCGTGAACGGCGGCGGTGTCAACAACTTCTCCAATGTCCTGGCCGC
CGTGAGCTCTAGCCGCGGATCGGCGTCGGTGGGCAGCAGCAACGCGAATACCTCAAATACGCCGG
CTCGTCGTGGCGGTGGCAGACGCCCCAACCGGTCGACGAACATGACCCCGGAGGAGGAGCAGAAG
CGGGCCGTGCGCCGGGAGCGGAACAAACAGGCGGCGGCCCGTTGCCGCAAGAGGCGCGTGGACCA
GACCAACGAGCTCACCGAGGAGGTGGAGCAGCTGGAGAAGCGGGGCGAGAGCATGCGCAAGGAGA
TCGAGGTGCTGACGAATAGCAAGAATCAGCTGGAGTACCTTCTGGCCACCCACCGGGCCACCTGC
CAAAAGATTCGCTCCGACATGCTGAGCGTGGTCACCTGCAACGGTCTGATTGCCCCGGCCGGACT
CCTGAGTGCAGGGAGCAGCGGCAGCGGCGCGAGCAGCCATCACAACCACAACAGCAACGACAGCA
GCAACGGCACGATTACGGGCATGGACGCCACGCTGAACTCCACCGGGAGGAGCAATTCACCCTTG
GATCTCAAGCCGGCGGCGAACATCGATAGCCTGCTGATGCACATCAAGGACGAGCCACTCGATGG
CGCCATCGACTCAGGATCCAGCCTGGACCAGGACGGTCCGCCGCCCAGCAAGCGCATCACCTTGC
CGCCCATGTCCACGATGCCGCACGTTCACTTGTCCACGATATTAACGCCCACCGGCGCCTCGTCG
GGATCTCTGCAGACGCCGATCACGAGCACGGCGCCCGGCGGATTCGGCAGCGCCTTCCCGGTGAC
CTCCAACGGCAGCAGCATCAACAACATCAACAGCATCGGCAACAACATGAACTCTCCCACGCTGA
ATGCGCATAACAAGGTGCCTAAGGAGCGGCCCAATACGCTGGCTTTCCAGCGTCCTCTGGGCCAG
ATGCACCTCACCATGGCCAACAACAAGGCGGGTGGGCCCACGCAGATCCAGGGCGTGCCCATCCA
GACGCCCTCGACCGGCACCTTCAACTTCGACTCCCTGATGGACGGCGGCACTGGGCTAACGCCCG
TCTCCGGACCCCTCGTACCGAACAGCTCCTCCACGAACAAGCACCCGCTGGAGCTGCCCACGCCC
ACCGCCGAGCCGTCCAAGCTGGTCAGCTTATAA

# Appendix D Primers for ChIP

The following primers were used to perform PCR to confirm ChIP result. Primers either contain or flank AP-1 consensus sequence.

**Genomic *zipper* (Flybase ID: FBgn0265434)**

F1: ATGTTTCGTGACCGTATAAGGC (23bp|43.5%|64.0°C)
R1: GCTTAGAAGTGGCAATGACTCG (20bp|45.0%|61.0°C)

Product Length: 167bp

F2: ACATTGGTGTAAGATTATCCGACGC (25bp|44.0%|67.8°C)
R2: GAAGAAATTGTTCCATCAATCGAGC (25bp|40.0%|67.6°C)

Product Length: 132bp

F3:GTTG**TGAATCA**TAATCCCAAACTGGTTTCC (30bp|40%|58.9°C)
R3:**TGAGTCA**TCTCCCGGCGCGACGTTA (25bp|60%|62.6°C)
Product Length: 165bp

**Primers for negative control**
NEG-ZIP-F1: CAAGAACTGATTCGAAGAGAGG (22bp|45.5%|62.3°C)
NEG-ZIP-R1: CGTAGTTCATTTAGTTGGACCG (22bp|45.5%|62.6°C)

Product Length: 110bp

NEG-ZIP-F2: GCTACATGAACATTATCTTTCCTTGGG (27bp|40.7%|67.2°C)
NEG-ZIP-R2: TGTAAACATATAGTCGCCAGTTACC (25bp|40.0%|62.2°C)

Product Length: 185bp

consensus AP-1 sequences
EcR binding site
flanking genomic regions

TGATTCAAGCGCGGACCTTCACCGTTCCTCGAAAAATTCAAAATTAACTGAAAGTATCCGCACATCCG
CGCATTAACCCAACGGTTTATTGAAGTTTGGTTTTACCAAGAACTGATtcgaagagaggacagcacgc
gagaccccgcaaaacaccaaaaacaaaaaggcggtaaggtattttgatgttgtcgtgcggtccaacta
aatgaactACGTATATGTCAAAAGTAAAATCGACATATACGATACTTAGCTTGCACTAATTTGACCAA
TATTATAAATTGAAAAGTGAGTTGGAAACATCCTTTGCTACATCTGAATATGCAAGTGAGTGAAATCG
GCAAAATAATTTAATCTCATTTCTATTCCGGAAGTATTCGATTCCAATCGACACCGCTTGGCTTGAAG
CCGCGAATATTTCGATCTTAAGTGCAGTCATGAACCAGAGGAAGCTGATGCGATACTTTGCTAAAAAC
TTAGATATTCTGTTATAGAGGAATACAATGGCCGACCTGAAAAAATGTTACAGGTGTGTGCTTTAAAC
AAAATCTAGATGCGATCCATATGTAGAATTTTAATCAGTGTTGACATATCGATGTATGTGTTTTCAGA
AAGCGCTGCCGCGGCCGTCGTGTGAACTACGACATATCGATGCATCGATATGTCCGAATGGAATCGGA
AGGCATCGATTACCATCGAACTCGAAAAGTACTCGGTCGGCAAAACGGCAAGCGGCGAAAAACAGTGA
AAAAAAAAGGGGGAAAGCGAAAAGACGTGCTCAGGAACTGCGGTCGAAGTCTTTGTGAGTGTGTGTGG
GTGCAGCTGTCGCCAAACAAATGAAAAGCGCCTGGCTTGCATTAAAATCGGTAAAAAAAAAATCGGAA
ATGTGCACAGGCATCCAGCGAATGCAGCGACCTATTCGCCGGCGTCGGGACGCCGCCAGCTGAAACTG
CACGGTCGAATTTGGCTGCATTTGCACAAACGCTGTGCTGACGCGGGGAAATGGGAGCATAAAAACCG
AAACTTGTGTGCGAAATATGCGAATATGCGAAACCTTGGCTCCCAGTGCGATCTATGTGTGTGTGTGT
GTGAGCCGTGCTGTGTGTCGGTGTTGCAGAACGAACCAAGTGGGAAGCAAAGCGAGAGAAGACGAAGA

GGAAGAAAAAGAGCCGCTTGTACCTGCTCCGAAAACTGAAACATCCGAAATCGGAGGTGAAAAGGTGC
TCTGATAGTGTTTAGCTGCAGTTTTAGGAGATGCAAACTGGTTAATTGCTACGTAACGCTATTTTTCC
GCTAAATTACTTCACCACCCCTTCTTCTACGTTCAGCGGTGACTTTGGCTTAAGAAAATGAAAATGTG
TGGCCATATTTTTTCCTCTCCGTCTTTCTTTCGCCTTCGCGCTCTCCCTTTTGAAACTCTCGCCGCGC
GCTGTTCTCGCCGCCTCCGTTTTGTGCCGCACTTCCGAGATAAAGAACGCAAACGCGAGATAAATGCG
AAATATTGTATCTGAGGAGCGAGGCAACATACTCATTGTTCTCATCGATTTGTTTTGTCCGACAGAAA
AGTGCATTGCATCCGAAAAGCGAATATCCAGTATCCAATATCCATTATCCGAAAGCAGCTAATTACCG
ACAGACAAGGAATTATTTAGAGATCGCCGCCAAAATGTCGGAGGAAGTAGATCGCAACGATCCGGAGC
TCAAGTACCTCTCGGTGGAGCGCAACCAGTTCAACGATCCGGCCACGCAGGCCGAGTGGACACAGAAG
CGTCTGGTGTGGGTGCCACACGAGAACCAGGTGAGTCTACTTAAATGTAATGCCTACCCGTAGAGCAT
GTTCCTACTCTGGACGCAACCTCTGCTACGGGATTTCTACCCCGGAAGCCACGCCCGTTTCAGTGAAC
TACCTGAATAGACCCTATAGATAGCCTAAATGCAACAGGAACTGCTACAACTGAGATAAAAATACAGT
CGATACATCATAACGCTGTTTATTTCGTGAAGTCGGTAGTCATTAGCCCATTATGGTTTTTTTTTTTT
TTTTTGTAAAATTACCAAATGTACTTAATTTTCGTTTAATTTTCATATTCTTTTGCGTAAAAAATTGC
TACATGTAACTATCTAATATCTAAGTATTACTTCGCAGTGAATGGTTATTATAGAACATAGTGTGTTC
GACACATCGTGATAATATTTTAGCCCTAGCTGTACGTGCTCTAATCAATTTTCACAGTGTTTGTCCCC
GGCTTTGCGCTTCTTATCAGCCAACACCTTTTGAGCCATCCGACTCACTCATCGATTGGTCATGAATC
ACGCTTCACCGATCCGTTTATTTTTAATTTTGAACAGGCCCAACTTCTTTGAATTTTCATTACATTCG
CACCGCGGTGATAAACTTGGGTAAACATCCGTTGGCGTCGATGCTGAATCACTCTTTTCTCCTGCGCT
GATGCTGAATTAATCTCACCGTAGTAGTGTGACACATTTAACTTCTTACTTGGTCAAATCCGCGACCA
TTTGGTACCAATTTGCATGCAGACGCTCTTCGACTCAGTGACTCACCTCCGAGGGAGAGTGGAAGCAG
GAATGGCCCCAGTTCGCAGTTCCCACTAAGAGCGGGCCAAAACAAGTTTTCAATGTGGCTAGGTATTT
GTGGTGTGGACTTGCTTGTGTGGGGCTTTCTGGCCTCAACCACACAGCCAGGCCAGCAAAGAAACGAG
CCGAGATTGCGCCAAAGAATCGCTTCCCTCGGAGTTCGGGCGCCCGCTCTTGGCCTATAAATTCAAAT
TCAAAACTTTGGTCGACTGCTAGCGATCAAGCCTTATGATAACAAGCCGATTGTTTTGCTAATTTCGG
TGTGGCTTGTTATTCTCTTCTTCAGTTTAAAGCGATTTCATTCAGGTGTCATTCAACTGCATTCCAAC
GACTTAATTTCAAGACCATAAAAAACGTAAACAGATAAAATTATCAACCGCTCCTTTCTCCCCTGGCT
GCCCGTAATTGCTGTATTTGCCAGAGATAATTCCGTACATAGAATGGTAGCACTTTTGGGTGACTTCG
TATAATAAAAGCAACATCGAAAACAAAAGCCAACAACTTCACATTTTTGTGTAATTACGCGATCACTT
TAACAGACATTTACTTTACAATGGAATCTCACAAAAAGACAACGGCAGAGATAAAACCCAGAAATAAA
ACGAAAATAACGAAACGCTCGATTGTCATGAGTGGTCCGTCAGATTGTCTAAAGGCTAAAATTTCTTT
GCGACTGACGAACGGCACATGAGACGGGTGGAAATAGTTAAGAAATTTGCATATAGCGCAACTGTTGC
TCCGCTGGAATGTCCACAGATACAGCTACGTCTTAACGGGAACGGACCCGTCCAAAAGGGTATTCGCC
AATTGTGTCAACACTCGTTTCGTTTCCAGCAACTGTTCCAGCTTTTCGAAATGTAAGCGAATTCGCTG
AATAATGGCGGCGTCAGTCCACGTACGTGATATCCAAATTCAGTAATTTACTGGTGGATACACAAGGA
GACCTTTTGTTCGTGGCTACATTTCGTTTCATGTTGTTTGCTGAACAGCGATGATTCATCGAATCAAT
TGCACAGAGAGCAAGTTTATTGGTGGGGATTAGATATATTGTACATTGAAGGTTTCGGGTTATAGGTT
AATGTATATTTGCGATCTTGAAACTATTTAAATGCTTTTAATAGTTCATAGCTTACTTTTCCATTGTC
CAACGATGAAATTGAAAAGTTAATACTTTGGAATTCGTGAACACGGTGGAAATGTGTTTACACCTCTT
TTCTTTTTTCCCTCTTCTTCAGCGCTAATGCTCTTCTTATCCGCTGTCTTTGTTCAGGCATTCCTGAA
CGCCTCACTCCCGAGACCAATCTGAAAACTTTTTATATTGTTAGCCAAATTGAAGTCGGCTTAACCTT
CGTCATGTCCAGAGAATCGATTCGATTGTAACGAACGGCGATCATTAGGGGGTCTCTGCTCACCCACA
CATGCTGCGTTTCATACTTCCACGCTTGTATGTGTGCTGCTCGTATTTATAACCAAAGAAACCACTTT
GGACTTTGTTTGCGACCACTCCCACTCCGCTTCCGCGCCCCCGCCCTTTGGCGTGCCGCGATTGGTTC
TGGCGGAGATGCCCGTGCCGCGCGAGTGTGTGTTTTCTTTTCGGTTACGGCAATGACAAACGTAGCCA
GCTTTCGACTCTCGTCCGTCCGGTTTACGGTCAACGAACCTGCGCCTCGTATCACGTATGTGTAATAT
ACGCTTCTTACCCTCTCCATCTCCACTTCCATCCTCAACAATGCATATACGTTGATCGATTAAGCGAA
GGAATAAAATAAAAGAGTAACAAATTTTAATGGGCCCATCGAACGTTCGCATTTGGATCGTGATGGAA
AAAGGGGGACCGGAGACATCTATTCATTATTCTGTTCATATTTACATTTTCGGAATAGTGTAAACAAA
AGAAGTTGGCGAAAAACATACGCTCCCAGAGAGTAAATAATGGCCACAGATATATCTCAAAATCACCA
ATATTCTTATGTGTGCTGTTCGGCCGATACCTTGGCATGTTCAAGGTTGCGGTTGGGCACCCAAAAAT
AGTCAAACCCAAATCGGGGGCTCCCCTCTGGAATGCACTCCTTCCCAACATTCTTACTTTGATTCCCG
CCTGTCTGATCATCACCAACATCTAGGTGTTGTTGATATATTTTCTTTGGTTTCGCTTCACCGATTGC
CTGGAATGCCCGAGATGCCGTTGAGCGAGAATCCGAGACTGATGACCTCATATGCCCCAGCCTCTCGC

GGCTGCCTCGCTGGGTAACTTCGGACAACTTCCCTGGACCGATAACTCCAATTCCTCTCTTGTGGGGC
ATTCCAATATCGTGATTCACGCACCAACTGTCGCAGCGGCTATAGCATTTTCCGATTCGGCGAACTTT
TAGCTTCTTCTGCCACTGTCGCAAGCCTTGTGTATTTGTTTGTCCAAAGTGTCAAACGTTTTATGCAC
AAATGTTTTGCAGGCTGACAGCGGCTGCCCACAAAAAAGGCAGACGCCTGGGAAATGAATTTAGATAC
AGCGAAAGTACTCAAAATTTAGGCCTATATACATGCAGACGACTTTACCTTATGACTAATCTGTAAAC
TTTTCGCAGCGCGAAAATAATTTGCCGTAGGACCCAGCTGAGTATTCTAAAGAAGTCGTTACATGCTC
TAAATGGTTTCATATACGCCATATATGCCCGAGAATAACGACTTTCTTATGGCTGTTTATCAACAGTA
CCGGAAAAGCGCAAAGATAACACAGGCAAGGCAAGAACCACCACGTCTCTGGTTTTTCCGAAACTGAT
CGCTGGGGCGTGTGCGTATTTAACTTAATGGACCCGAACCGGGCTGGGATGTATTGCAGATGCTTCTG
CCCTGCATCGGCAGGCCGTTGTTGGTCTTAATGCATTTCTGTTTTGCAGCGGCGGCACGCCACTCCAC
CCTTTAATGACTGAGTTACGGGTTGCCCCTGATTTGATTAATGCCAATGCGTCGCGTGAACATGCTTC
CCTTTGTTGTTGTTTCACTTGACTTCTAATTGAGGATGTTATTCTGTTGGTGTTCGATTAAATTTCAT
GCAGACGTTTCGGAGAAGACTCGGAAGTAAACCCCATTTGGTACCCTAAATTAGTTATGGGTACTGCG
CTGCGAACGGTTCAACATCAAAACTGTGATGCTTCCCCAAAATCCGCGCCTTGAACTTGCTAAGTACC
CGGGTCGGAGAGAAGGAACCAGACAAGCGGACAGACAGTTGCATCTGCCTCCCGTTGTTCTGGGTTGG
TTCTTGCTTCGTCTTCTATGCATTCTTCTCTATGCATTTCAATTGGCAGCGAGAGAGCGGAGGCTGAG
TGGTTTTTCTTCTGGCGCTTGACTCATGCGGCGTCATTGCACTTGTTGTGTTTATCGCCTTCCCGCTG
AGATGAAGAACAGAAGCGTACCCGTCCTGTTTTCGCGTAACACACTCATACCACACTGCAGAGAAACA
GAGATGGCAACCGTGAATAACTCTTTCTATTTTCTTTTACAGGGCTTCGTGGCCGCCAGTATTAAACG
GGAGCATGGCGACGAGGTCGAAGTGGAGTTGGCCGAAACCGGCAAGCGGGTGATGATCCTACGTGACG
ACATACAGAAGATGAATCCGCCTAAGTTCGACAAAGTCGAGGACATGGCCGAGCTTACGTGTCTAAAC
GAAGCCTCCGTTTTGCACAACATCAAGGACAGATACTACTCTGGCCTAATCTATGTGAGTACCTCGTA
CATATTCCCTATCTTATATGTTTGTGTTGGCTGCCCCAAGTTTCCGCCGCGCCAGCTGCCGGTAATGT
GACGATGATGATGAAACTAAGTAAACAGCCCCCCCCCCTTTCACACATTTGATTTCGCTTAACTGGAA
ATTTTGAAAGGCCAAACTTTATAAAGGCGTCTTGCCTCATCGCATATCTATTTATTTAAAAGCATCGC
AAATATTTAAGACTCCAAAGCTCAATCACTCAATTCATTGCTGCATTCGTCACAGGCCAAATGATTTA
TAACCATTAACTCACTCTTTCGTCCTCTGTTCACCCGATCACCCGCAAAGCATATCCGCTGTTAATTG
GCATGCCAAAAGCGCTTTGGTCTGAGTAGAAAGCCAGCAAAAAGTTCATTTTCGATTCGATGAGAAAC
GAATTTCAAGTGGCGCGTTTAAATTCGACTCCATAAATCCCAGCTGCTTTGCTTTGCGACTGTTCCTC
TTATAAATATAACTTATTGCAGTATTTACAATGGCGGGCTGCAATTGATAAAGATTTATCTTTTGACA
TACCTTATCATACAAGTTAAATTTAAAGTGAGGGCTAGTTATGTTTTCTAAAGTTGGTAAATGTTTAT
TAGACTTTTTGGATTTGTAGATTAATAAAAACATCTAAAACAATTTTTGAATTAATTGAAAATAAATA
ACATCCTTAAGTAGCTCGTTAAATATATAAATCAAGTTTTTTCTTGACTTCAGTAGACTCGCTTTTCC
TGAATTCTATGATGACAAATGCAGCTCATTTATGATTTTCCTATGCTAACGATCGTTATACAAACCTA
CTTTTCGTCACTGAGCAATGTCTAGCAACAACATGTTTCAAGGAAATGTTGCCAAACTTGGCCTCAGT
TCTGGATGCTTGTCTATGCCACGCCTCTTAGCCTTGATTCTCTGTTGATTCCCTGAGGCAGGTTCATT
GCGACTTATTTTTTCATTGTTATAACAAATTATGTGCCGCTTTTAAAATACTTTATGTACTGCGCCTG
CTACTTATCGCAGTCTTTCTCCCTCTCGCCTGCACGTTTTAATTTAGTGCACAAATGGTTGTTGCTGC
CAGTTTTTGATGTGGGCGCGAACTACTTTAAATTTGTTTATATCATTGTTGGCAAGCCATGCTTCAGC
GCACTTGCCATTGTCGTTGTTGTTGCTAAATTCGAGCGCCGCTTTACTGTTTACACAACCATGCCACG
CACACATCTTGCGTCCCTTTGTCGCTCTTACCACGGCCTGTCCCACTTAATTCTCTTGCCAATTGTTG
CTAACTTGTTGCATGAACAATGGGGGATTGAGACGGCGAGGGAGCGGCAGCGGGGGCTGCACTTAACG
GCATAATTATTATAATTTGTTGACATTTAATTCGATTTTTAAATTTCATTTAAATTAATTCGCCTGGC
AGCTGCCGGCTGACGGTAGCTTGTAATCTAATTAATATGCGTCGGCAAGAAGAATGTGTCTTGCACGG
CCACGCACACTCATGGCGCTTTGCTCAAATATGCTAATCAAATTGTCAACACTTTAGCAACACCTTAG
AAAATCGAAAATTCGGAAGCAAAAGCGACAAGTATAGACCATATTATTCTTTTTTGTAATTGAAGTGA
TAATTATAAATATTTTTTACTGTCAATAAGTCTATTGAAAAATGTCTAGTCTTGTAATTTTATCAAAC
ATCTCCTTCTGATGCGCTTGTTTACATATGAAATCGGGTTTGAAATATTTTACAAAACATTTGCTTCT
GCCCCTGTTGTTGTTGTAATTAATTGATTTACGTCAACCGTGTGACTGGGTGCAATTGCTCAAAAGCA
GTCTTAATATTACCTAATATATTTCGTGTGCTTTTTGCGCGGCTGCGTTGGCATCTAAAAGAATCGCA
CTTGACAACGCAGCAGCGTGAAGGAGATGATGACGTTGGCATCTTGGCTGTTGCTGTTGTCTCAATTC
CCAGTCGGTCCTGACTATCTGTAAGAGGCACTAATTAAACTGACCAGCAGAATTAGACAGGATGACTT
AATAATGTAGGGTTGCAGTGACAACCAGAGCCAAGTGGCTTCCTTGGCCAGATTTAAATAAGGAATGT
AAATGAACCACGACATGTGGTAAATAAAATATGATTCCCGCATCAGCTAAGCAATTTGTTCGCAGATA

TTGGCAAAACTAACACCTCCGTCTGTCGAGCACATAATTAACAAAAAAGGCTCTGTTCCAATGCCCGC
CCGTGCATTCTTAACTTTTTTATGTTTCTCTCCAGGCTCACGTTCTTTGTATTCTTTGTTTAAAATTC
TTTCACGTTTCCTTTCCAAAACTCCAAGATGTAATTATATCTCGCTGTAATTTAAATGCCTTGCGGCC
GTTTGCTAAACTTGCAAAATATTATGTTTCGTGACCGTATAAGGCTTTATATCAGGTCCGGTTAAGTG
ATTAATGACATTCAAGGGGACTGTAGAAATATGCACCAGGACAATGAGTCAAGCCAACATAACCGATG
TGATTCAAAGACGAGGGGAGCAAACATCGTCACGAGTCATTGCCACTTCTAAGCGGTTGCCAAAACAG
CAGACACTGAGAAAACAATTTCTTATACCATTTTTGGATGCCTCACACACGCACACACACACATACAA
GGAAGGTGGCTGATTGGCAAGACGTGATTTTGACTGTTAATTGCGGGCCTAAAAGTGATTCGTTTTCC
TGCCGCCCTCATCACACTCACCTGTGCAAAAAGTTGAGGGCATTTTCTCTACTACAATAATTGCCAGC
GGTACTTTCCATTTCGATTTGTGTGGGCTGGCCCACACTTCTCCGCCCCCTTTGATACACTCTTGCGC
GCTGCCGTGAAGCTCGAGGCACTCGCATCTAATGTTTGGGTAGATATGTATTTAAATGGTACAACAAA
TAGCAAAGCCGCATACTTAGTGCCCACGCCGCAGTCTCGGTCCCAATCACAGTCGCAGTTATGTAGGC
TGCCGCTCGATAGATACCACCAACGGATTCGGATACAGATGGAGCGGCAGATACAGATACATGCGTTC
GCTGCTTATGGTGCTGGCCAACTTTAAAGCACATGTCACGTTGACTTGGACACACATGCGAGAGTGTT
AGCATTTGGGCAACAATAACTAGGGCACAAAAAGCAGTTGCCGGTGTCCAAAGCTGCCGTTAGTCCAA
GCATCACTTTGATTACCTGCAGCCCAGTGGATAGCATTTATAGCTGGAAAATTATCAACTTTAAGAAT
GGGAATACATTGGTGTAAGATTATCCGACGCGATTTATTAATATTACCTCATGTTTTGAATCATACTC
CTAAAAGCCCTTCATTCAAGCATTAAGTATACCTAACAATAAATCCCTCGATTGATGGAACAATTTCT
TCATTTCAGACATATTCCGGTCTTTTCTGTGTTGTGGTCAACCCGTACAAGAAACTTCCGATCTACAC
CGAAAAGATAATGGAACGGTACAAGGGCATAAAACGACACGAAGTGCCTCCGCATGTATTTGCAATCA
CGGATAGTGCCTATAGAAACATGTTGGGTGGTAAGTATCTCGATCCTGCACTTACGTTCCCTTTTCGC
TCCACAGCTGCACATACATATGGGAGATGGAATGCCAGAATTATCAACAGCCTTTCCTTTTTTCTCTG
GAGCGCGATTTCTGGTCGCTATCAAAATTCCATTCTCCAAATAAGCAAGCGAAATTTTTTTCAGAGCT
GATTAGATAAGGCGTGGAAAAGTATATAAGGGAGGGGCATTTCCAGGAATAACGTTGAAGCGGGGTCC
ATACATGACACACTTTGCAGATATAACTCCAAAGAGGTGCATTAGCATTCGAATTCATACAAATGTTG
TGAATCATAATCCCAAACTGGTTTCCTTTTTCGGTATGAATTTTCAAATGAGATTTTTTCAGGTTTCC
TTTTCACTTCTGTGCTTTTTAGTTCGGGCTTCACTGAGTTTCGATGGTTTGCATGTCCGTTCCAAGCG
TAACGTCGCGCCGGGAGATGACTCACGGCGCTGGCTCCAGCGCAGCAGAGACTCCAGCTCGAGGCCAG
GCGTATCTTACTGCGGCCATATCTATAGGTTCCTACATGTGTGTGTTGTGTTTCCTCTGCTTGAGATT
GGTTAACTAATATTGCGTATACGTGTCATTACCATATTTGGATCTAAAACTGAGCCCGGCTTCGCTTG
GACAGCAGGCAACTTTGTTTGCCCCATCATCAGCTATATTTTTGTTGTCGTAAAAATGTTTAAACATA
TCGACACCTCACTCTGGCTCACCATATATCACGCTTATTAATTTTCGGCATATGCACATTTTCTTGGT
CGTATATTCGCGGTATAAATTTTTTTCGAGAAGTTCGCTCTCAAAGCCAAGCCATTGGGGAGTGGCAT
TTAATTTGATTTATTTCACTGGCCTTTAATAAACTAAGCCCAGCCCCATCGCCTCCGACTCCATTGCC
CTGGAACATTGGGGAGTTGGACAAACGTCACAAACATTTATCTTTCTGTGATTCTCCAGCTGCTCCCC
CAACTCGGAGCAATCGCAAATCTTCCAACTTCCAATCTTCCAAAGTTCCAATTTTCATGGAATTCGTG
ATAAAATGAACACGCCCTGCCTACATGCACATATATAGCAGTTAAAACCGTCGCGAAATTTCCGATAC
TGGGCAGATGTTTTACCTGTACGTATTTTTTCAGTTGTTTAAAGAAGTTTATTTTGGGAGTGAAGTCT
GCTGTGTGATACAAAATAAAAAGTTTTTACAGCTCTTCAACAAGTGCAAAAAGTGAATGAATGAAACT
TATGATCGATTGTAGCTTCGAGCCATAAAATGCATTGGCTATCAATGACACATATTTCGCATACCCCT
TATTCGCAGCGTAATAATTTGAGAAACTCTTAATTCGCCTTCTGAGCATTAAATTTATTAATGACAAA
AAAAACTGTGAAAAAATTTCCATAAAATGAAGTGTGGAGATACAAAAATTAGGCCCATGTATGGTCGA
ATATAGAATGTAGCTTGTATGTACGTATAGATATGTGACTGGGTCTATCCATAAAAATAAATAAGTAC
GGGGTCGTGATATGGAAGCTGTTTGGTTGTTTGGAGCTCCATGTCTCAGAGTAGATACATATATCTTA
CTCGCGTCTCTCTGCCTGAATTTGTGGTTAGCTTAATGCTGGATCGTATGACGAGGCTGTCAGTTGCG
GTGGGGGGTGTGGTGATCCCGGGGTGCAGTGCGAATCTAGTTCGCTGTATTCTACATGGGATCATTGG
CGCCATACCAAGCAACAGCAATTTACTGCTTGTGTGTGTCTGTTGTCTTTTGTATCTTTCAGATATGC
ACGCTGAAATCAACTGTTTTATTTTTAATTTCAAAATAACAGTTGAGCATTGAAGCCTAAGCGAAAAT
CGGTTGATAGTTATTTGCATGCTATGATTTCATTTGATGTATGTCCCATTTATCACCCATCAACTATT
CTGGGTTTTACTTTCTGGGCTCGTTTTTTGCCCGTTTAAATTTGGGTCAACAGAAAATTCAAGCTGAG
GTGCGCATTTAACATTTTAATTACATTTTTGGCTGGTCAGCCGCATTGTTCCGCATATGAAGCAAGTG
ACAGCTTACCTTCTTACACTTTCACTTTCATTTTTTTTTTTTTTTGCAGATCGCGAAGACCAATCGAT
TTTGTGTACTGGCGAATCGGGTGCTGGCAAAACGGAGAACACCAAGAAGGTCATCCAATTTCTAGCCT
ATGTGGCAGCTTCGAAACCCAAGGGCTCGGGTGCGGTAAGTACAGAAGAGCAAAATCAGAAATGAGAC

CCTAGATCGGAAGCAAATGCAAAGTTGTATGCCCCATTGGGTGGTGATATCTGCCGGAGAAATACAGC
CCCATATGGGGTTTTTCACTAGAAGTGCTTATTAAACTCACATTAATTGCACGCAAGCCAGACACTTG
TTATTATTTGGTATTGTAATTAATGAGACCAACAACGTTAGCGGGAATTTCACGACGCTAACATAAGC
ACATATGTATATGTTTGTTGTCGGCAGATTGGCTTTAAACCCCCTTCTAATCTAGAACTTATTCGTGG
GAGTATGCAGTATATCTGTTTTAAATTAGCAATATCAGTCAAGTTTTAAATTTATTAGGCTTAACAGA
GCAATCAGATCCGCTGACATTGCTATTTATACATATATAGGTTGTAAAAGCTATTCCTCAATAACGAC
CTCAAGAACTAGAATAAACTTCAGTTGAATTCAGAGATTCAGAGTGCTAAACTGATGCTCCCCATATG
GTGGATGGATGGCCGAGGGTAACGCTTAAATATGTGGATGGCTGATGACATGGCAGCTGGCTTATGTG
CTTTGTGATCCCGGGAGCCGGAGCACACTTCATTAATCAAGAGCCATAGTTGCTGACAAATTTTGTCG
TTTACAGCAATAAAATAAACACCATAAAAAAGTTGGGAGAATTGAAATTGAAAGGCAATTGATAAAAA
AAAAAAAAAAAATTAAATCGCGAAAATTGCGACATTCGATAAATTTCTGGGGCAGCAATTGCTGCTCT
GTACAGTTTGCTACTGTTGGGGTTGCCATATCCATAACTGTGGGGACAAGCCGTTTTTAGTGCATTTC
GGACTTGCTCAATCCTTTCGAGATCAAACAAGCTGTTCTTGAGCTCCAAACACACTTTTTACTATGTT
TTATTTGTTTACTGCCTTATATGACCCTGGTGCTGAAGCTGCAGACGAAGTTGAGATTATTTTTCTGC
TGTGAACGTGATAAGCTGCAAATATACTTAAAAAGCTTCTTAAGACATTAAACAAATCTACAAGCCTT
TTATTTGAACCATTCAGAGATCTTGCATAAGCATATCGCTTTATACCTTGCTGTTCATACCTTATTTT
AAGAAAAAATTGTCTATGTGGTATTATCTCTGATTCTAAGTTCCATAAATATACGCTGACGATAAAAA
ACCATATAACATTGTCTGCAGTGAATCATAGCAAGTTACTGTAGAACTGAATTGAACCAAAGGTAATT
TTCGTTAGTTTGATTAGAAAATGTGTGTTTTAGTGGTACTTATCAGGTCAAGATAAGAGGAGCGATAA
GAAAACCCGAAAACAAACATGGATATAACTTTGCATTTGTTTAAAAATGATATCGTTTTTTTTTTTCA
TGACTTCAGTTCTTATCAAATATTTTTGCTTGATGCTGAGGATGAGGCAAAATTTAAATTGATTTTTG
ATCTGATATAATTATTATTTATTATTGATCTTATTTATTTTCATGTCCTACACATAAACACTCCACTA
TGCTACACAACACACCTATAAATATACGCACACTCACCCTGTACATTGGACTTTGGTTGTTGTCTTCA
CTCTAAACTCTGATCAATATGTTTATAAAATTTGTAAATATAATTTGTATAAAATGCTGCCAAATGTC
ACAATCAATCCAAATATCCAACAACCAAATCAAACCTCAACACCTCCAACCAATTGACACCAACTCCG
ACAGGTGCCGCATCCCGCCGTGCTCATTGTAAGTATTCGAGGATTGAGAATCCTGAAACGTTTTCCCT
CTTTGTGTTTCAAAATTAACTCGAATTATTTAACCCCGTTCATTGTTTAATTAAACTTACTTTTCACC
CACTGTCTATTTCTGATCCCAACAACACCCTTGATTTCCAAACGTTATTTTCTTAATCCTTTAAATGT
GGCCGAAATATTACTATTAACCCTCTCCGAATGAACTCTCCCAACTCTTCGTTTGGTTCCCTTGTTGC
TGTCCCATCCAAGTCAACACTCATCTACTCAATCTCATCTCTCTGCTCTGCTTTGATCTGCTCCCTCA
TTGTACAACATATGCCAACGAAATTCTAGAGTAGTCATCAAGAGACATTTGCGGTAAAGTATGCTTGA
CGTCCAAAAATTCTTTTAAATATAATTTTGTAGTAAATTGTCGTGCCGTAGGCTTCGATTCATTTGTA
CCTGTGTATTTCGAAATCTAAGCATGGTTTTAAGGCTGGATAGATCAATGCGCGTAATAAACGATGAG
AGTCATCAAGAAATCCTGGAATATCCACCCCGTACCCCATAATCCCATTCCCACCTAATTGCAGAACT
TCTCGGTCAACACAAACAAGTACATAAAGGTCAAGATTATGGCCCAAAATCAGAATCAGACGATCGAG
GTAGTCAATGGATTGAAGATGGTGGAAGTTAATTCCAACTGTCAAGAGGTAAACCGGGTGATGCCATT
GCGCCGGCATTGATCGTGAGAAGCTGTAGGATATCGTCCAGTGTTTATTGTCCTTCGTTATGCTTGGC
TTTGTCTCCTTTCTGCATGATTTATTAAGCTAACCATATCTAGTTTTGTAGATACTTTATGTTGCTTG
TGATGTTACTGTTCTTGTGTTAAGACTGCTTTCGTAAATATATGTGTCTAACCCCTAACCTTACATAA
CGTGAAACGTATTAACCTAACATAAATATAATCTTGTCTATCCTCTAAACAGGGCGAGCTGGAGCAAC
AGCTGCTGCAGGCAAATCCCATTCTGGAGGCCTTTGGCAACGCCAAGACGGTCAAAAACGATAACTCT
TCACGTTTTGTAAGTTGTTTGCTTCTTTGTTTTACAACACAGAATGCCAATTTCCGTTTGCCTCATTG
TAGGGTAAATTCATACGGATCAATTTCGATGCCTCGGGATTTATCTCGGGAGCCAACATCGAAACATA
TCTGCTGGAGAAGTCGCGTGCCATTCGTCAAGCAAAGGACGAACGAACATTCCATATATTCTACCAGT
TGCTGGCTGGGGCCACGCCGGAGCAGCGCGAGAAGTTCATACTGGATGACGTTAAATCGTATGCATTC
CTTTCCAATGGCAGCCTGCCTGTACCTGGCGTGGACGATTACGCCGAGTTTCAGGCAACGGTTAAGTC
CATGAACATCATGGGCATGACATCAGAGGATTTCAACTCGATATTTCGCATCGTGAGCGCCGTCCTAC
TGTTCGGTAGCATGAAATTCCGTCAGGAGCGCAACAACGATCAGGCAACTCTACCAGACAACACGGTG
GCCCAGAAGATTGCGCATCTACTCGGACTTAGTGTGACAGACATGACCAGGGCTTTCCTGACGCCACG
CATTAAAGTGGGTCGTGACTTTGTTACGAAGGCCCAAACAAAGGAGCAGGTGGAGTTCGCCGTGGAGG
CCATTGCTAAGGCGTGTTACGAGCGAATGTTCAAGTGGCTTGTGAACCGGATTAACCGTTCTTTAGAC
CGCACCAAGCGCCAAGGAGCCTCCTTTATTGGCATTCTCGATATGGCGGGTTTTGAAATATTTGAACT
CAACTCCTTTGAGCAGCTGTGTATAAACTACACTAACGAGAAACTGCAGCAGCTCTTTAACCACACCA
TGTTTATCCTGGAGCAGGAAGAGTACCAGCGCGAGGGTATTGAGTGGAAGTTCATCGACTTTGGGTTG

GACCTGCAGCCTACCATCGACCTGATCGATAAGCCCGGCGGCATCATGGCACTGCTGGATGAGGAGTG
CTGGTTCCCTAAAGCCACTGACAAGACGTTTGTAGATAAACTCGTATCGGCCCACTCTATGCACCCCA
AGTTTATGAAGACAGACTTTCGAGGAGTCGCAGACTTTGCAATAGTGCATTACGCCGGGCGTGTTGAC
TACTCGGCGGCCAAGTGGCTGATGAAGAACATGGACCCATTGAACGAGAACATCGTGTCGCTCCTCCA
GGGCTCCCAGGATCCGTTCGTGGTGAACATCTGGAAGGATGCTGAAATCGTTGGCATGGCACAGCAGG
CCCTGACTGATACCCAGTTCGGGGCCCGCACCCGCAAGGGCATGTTCCGCACCGTGTCCCATCTGTAC
AAGGAGCAGCTGGCTAAGTTGATGGACACTCTGCGCAACACGAACCCGAACTTTGTGCGCTGTATCAT
ACCGAACCACGAGAAGCGCGCCGGCAAGATCGATGCTCCCTTGGTGCTTGACCAGTTGCGCTGCAACG
GTGTGCTCGAGGGTATTCGTATCTGCCGCCAGGGCTTCCCAAATCGCATTCCCTTCCAGGAGTTCCGC
CAACGATACGAACTCCTTACACCCAACGTGATTCCCAAAGGATTCATGGACGGAAAGAAGGCCTGCGA
GAAGATGATTCAGGCGCTGGAGCTTGACTCGAACTTGTACCGAGTGGGCCAGTCGAAGATCTTCTTCC
GCGCTGGTGTCCTCGCTCACCTGGAGGAGGAGCGTGATTTCAAGATATCCGATCTTATCGTTAACTTC
CAGGCCTTCTGTCGTGGCTTCCTTGCGCGTCGCAACTACCAAAAGCGCTTGCAGCAACTAAACGCTAT
TCGAATCATCCAGCGGAATTGTGCCGCCTACCTTAAGCTTCGGAACTGGCAGTGGTGGCGCCTCTATA
CTAAGGTCAAGCCCCTGTTGGAAGTTACAAAGCAGGAAGAGAAGCTTGTCCAGAAGGAGGATGAGCTG
AAGCAGGTACGCGAGAAGCTTGACACTCTGGCCAAGAATACGCAGGAGTACGAGCGCAAGTACCAGCA
GGCTTTGGTGGAGAAGACCACTCTAGCAGAGCAGCTTCAAGCCGAAATCGAACTTTGCGCCGAGGCCG
AGGAGTCGCGCTCTAGACTAATGGCACGCAAACAAGAACTGGAGGATATGATGCAAGAGCTTGAGACG
CGCATCGAAGAAGAAGAGGAACGAGTCCTCGCGCTTGGAGGCGAAAAAAAGAAACTTGAGCTTAATAT
TCAAGATCTGGAAGAGCAACTCGAAGAAGAAGAGGCCGCACGCCAAAAACTACAATTGGAGAAAGTGC
AGCTCGACGCTAAAATTAAAAAGTACGAAGAAGATCTTGCGTTAACTGACGACCAGAACCAAAAGCTT
CTGAAGGAAAAGAAGCTATTGGAAGAGCGTGCTAACGATCTGTCCCAGACACTTGCTGAGGAGGAGGA
AAAGGCTAAACACCTGGCCAAGCTGAAAGCCAAGCACGAAGCCACAATCTCGGAGCTCGAGGAACGTT
TGCACAAGGATCAGCAGCAGCGACAGGAGTCTGATCGATCTAAGCGGAAGATCGAGACTGAAGTTGCT
GATCTTAAAGAACAGCTGAACGAACGGCGCGTACAAGTAGATGAAATGCAGGCTCAACTGGCCAAACG
CGAGGAAGAACTTACCCAGACTCTGTTGCGCATTGACGAGGAATCGGCCACGAAGGCCACCGCACAAA
AGGCTCAACGCGAGCTGGAGTCGCAGCTGGCCGAGATTCAAGAGGACCTAGAGGCCGAAAAGGCGGCC
CGTGCCAAGGCGGAGAAGGTTAGACGCGACCTTAGCGAGGAACTAGAGGCTCTCAAGAATGAGTTGCT
GGACTCGCTGGACACCACAGCCGGTAAGACTAAGCATCTATATTTTAAAAATGTTTTCAAGAAATCCG
TATCATTACCACTATTAAATTAAAAAAATTTTTTTTGACAAACAGCTCAGCAAGAATTGCGTTCTAAA
CGCGAGCAGGAGTTGGCTACCCTAAAAAAGTCTCTCGAAGAGGAGACTGTTAACCACGAAGGTGTTTT
GGCCGACATGCGACACAAACATTCGCAGGAGCTCAACAGCATCAACGATCAGCTTGAAAACCTACGAA
AAGCCAAAACAGTCCTTGAAAAAGCCAAGGGCACCTTGGAGGCGGAAAACGCCGACTTGGCCACTGAA
CTGCGCAGCGTCAACAGCTCCCGGCAAGAAAACGACCGACGGCGCAAGCAGGCAGAGTCGCAGATTGC
TGAATTGCAGGTAAATAATCACGAAAAATGTGTGATATATATAAATATGATATTTCTATAAAAAAAAA
ATAACGTATATGTATGCCTATGTTTTGGACAGGTAAAACTGGCTGAGATTGAACGCGCCCGCTCGGAA
CTTCAGGAGAAGTGCACAAAACTGCAACAGGAAGCTGAGAACATAACAAACCAGCTGGAGGAAGCCGA
ACTAAAAGCCTCGGCCGCCGTAAAGTCTGCAAGCAACATGGAATCACAGCTTACTGAAGCCCAGCAGC
TGTTGGAAGAGGAAACGCGCCAAAAGTTGGGTCTCAGCTCCAAGCTGCGTCAGATCGAGTCAGAGAAG
GAGGCTCTACAAGAGCAGCTTGAGGAGGATGATGAAGCCAAACGTAATTACGAACGAAAACTGGCCGA
AGTCACCACCCAAATGCAAGAAATTAAAAAGAAGGCCGAGGAAGATGCAGATCTGGCCAAAGAACTGG
AAGAGGGGAAGAAGCGGCTCAATAAGGATATCGAGGCATTAGAACGGCAGGTTAAGGAACTTATTGCC
CAAAACGACCGCCTCGACAAAAGCAAAAAAAAGATACAGTCGGAGCTTGAAGATGCCACCATTGAGTT
GGAAGCGCAACGTACGAAGGTGAGTTTTTGTCTGAATTAAATAAACTAGTTCTAATAAAAAAATTGCA
TGTCCTTGGTCAGGTGCTCGAATTGGAGAAAAAACAAAAAAACTTCGACAAAATTCTTGCCGAGGAGA
AAGCCATATCAGAACAGATCGCCCAAGAGCGTGATACTGCAGAACGAGAGGCCCGCGAAAAGGAGACC
AAGGTGCTGTCGGTTTCCCGCGAGCTAGACGAAGCCTTTGACAAAATTGAAGATCTTGAGAACAAGCG
AAAGACCCTCCAAAATGAACTCGATGACTTGGCCAACACACAGGGTACAGCCGATAAAAACGTCCACG
AACTGGAGAAAGCGAAGCGGGCGCTAGAGTCTCAGCTGGCTGAACTGAAAGCACAAAACGAGGAACTT
GAGGACGACCTACAGCTGACCGAAGACGCGAAATTGCGCCTAGAGGTGAACATGCAGGCCCTTCGTTC
CCAGTTTGAACGCGACCTGCTAGCTAAGGAAGAGGGTGCCGAGGAGAAAAGACGCGGACTTGTCAAGC
AACTGCGGGATCTTGAGACCGAACTAGACGAGGAACGTAAACAGCGCACGGCTGCTGTGGCGTCAAAA
AAGAAACTGGAGGGCGACCTGAAAGAGATCGAAACCACCATGGAGATGCATAACAAGGTGAAGGAAGA
TGCGTTGAAGCATGCGAAGAAGCTGCAAGCACAAGTCAAGGACGCGCTGCGCGACGCCGAGGAGGCAA

AGGCCGCCAAGGAAGAGCTACAGGCGTTGAGCAAGGAGGCGGAGCGCAAGGTCAAGGCCCTGGAGGCA
GAAGTATTACAGCTGACTGAAGATCTGGCCAGCTCAGAGAGGGCGCGACGTGCTGCCGAAACGGAGCG
TGACGAATTGGCCGAAGAAATTGCCAACAATGCCAACAAGGGATCCTTAATGATCGACGAGAAGCGCC
GATTGGAAGCCCGCATTGCCACTCTTGAGGAGGAGTTGGAGGAGGAACAGTCCAACTCTGAGGTGCTG
CTGGATCGCAGCCGCAAGGCGCAGCTGCAGATTGAGCAGCTGACCACTGAGTTGGCAAACGAAAAATC
GAACTCTCAGAAGAACGAAAACGGGCGCGCTCTGCTCGAACGCCAAAACAAGGAGCTGAAGGCTAAGC
TTGCCGAAATAGAGACAGCACAGCGCACTAAAGTAAAGGCGACAATCGCCACGCTAGAGGCCAAGATC
GCCAACCTAGAAGAGCAGCTGGAGAATGAGGGCAAGGAGAGGCTGTTGCAGCAAAAGGCCAATCGGAA
GATGGACAAGAAGATTAAGGAGCTTACAATGAACATCGAGGATGAACGGAGACACGTCGACCAGCACA
AGGAGCAAATGGATAAGGTAAATAATAAAATGGCTCATTAATACGAATTCCTACTGAAAAGTATTTGC
TTTTATAGCTGAATAGCCGCATTAAACTGCTCAAGCGCAACTTGGACGAGACCGAAGAGGAATTGCAG
AAGGAGAAGACGCAGAAGCGCAAATACCAGCGTGAGTGCGAGGACATGATTGAATCGCAGGAAGCCAT
GAATCGTGAGATAAACTCACTTAAAACGAAACTACGGTGAGTCTTGGACTGTGTCAACATATTTCTTC
TATGATCATGACGGGGGTTCCTTAGTTCTCTCTTGGAGATGCAATTTGATTATTGTTTGAAATTTATC
TTTGGTTTAAGCTCCATACAAGTAGCCGAGACTGAAAAGGCCAAGGCATATTCGCCAAAAAAGGATGC
CGCACTCATTATGAATTGTGAGGGTCTGCATTAGGTTTCGTTTCGCTTCGATTCGCTTCGTTTCCTTC
TCGTAGGCTGTAAGTGCTGATGTTCGCCCTGATCCTTAGAACCAGTGAATGTCAACCGAACCCAGCAA
CCAAAAAATTGTGTTTTCTTTGCATGTTAGGAACAGAACTCACGTAAAGACCAAACTGCAAATTTATG
CAATTCTCCAAACTTCCTCAAAAAAAGTTCTTAGTCGTGAACCCTCCAACGTACCCCTGTTTGGACTT
GTGTATATGTTGCCCCTGCACTGCACGCTCACAGAAAGACGGAAAATACGTCCTGAACAGAAATACTA
ATTATATGTCGTGGTCTATTCCTTCCTAGACGCACCGGCGGCATTGGTCTCAGCTCCAGTCGGCTCAC
GGGTACACCTTCATCAAAGCGTGCAGGAGGAGGCGGTGGCGGCGACGACTCATCGGTCCAGGATGAAT
CATTAGATGGAGAGGATTCTGCCAATTGACGCGTTAATTATTAGATGAAGAAAAAGTTGAATCGCAGG
AAGAAGGTGATGATGAAGAGCAAAATAAACGATTATATTTAATGTTTCTTTTATATAATTTCTCTGTT
ATTTTTTATATAAACTATTATACATACTTAAATTAAAACGTAAACGAAAAAACCAACATTTTTATAAC
GACAAAACTTAAACAAAAAAAAAAAAACAATGTTGTAAACACACACACTCAAGAATTTTCGCATCCCTC
GAATGACGGCGTATTTAAGTGGTCAACGAAATCAAGTAAAATAATACAACACACACATCAACCAATAA
ACGTATTAACTCTCAGATCCAGAAACCCGCAAACACCAATAAAGAGAGACTAAATCCACAGAAAATTG
ATTTCTAAATTTTTTCTACCTTAATATAAAACCGATAGAATTACTCGATGCAATGTAATTTACGCATT
TAACAACTAAAACGGTTTTCAAACAGAACAAAGATCATAACAGAAAATCAAATGTTGAACACGCAACT
AATATACGAATTTCGTTTTTGTTTAGAAACTTAACAATAAAATATTTGCTACatgaacattatctttc
cttgggcaaataagtgttgcaatgtggccaacttaatttattatagggaaaacatataaatattAACA
GTTATAGGTAATGAACAGTTTATTAAACGATTCTACATATATTTACATACATCAGATGACTAAAGACT
AAAGGTAACTGGCGACTATATGTTTACAAACTATTCTATAATTAATGCAGACAAATTCGAAAATCTCA
TTTAAGTTTGAATTTTCCCCATACCCGCCCTTAACTAAACAACTAGTGGCACTT

# Appendix E

**Table 3 List of candidate genes and functions**

| Gene name | Functions during DC | DC participant | Reference |
|---|---|---|---|
| *cabut (cbt)* | Transcription factor with $C_2H_2$ zinc finger motifs. It functions down stream of the JNK cascade and regulates *dpp* expression. Cbt is expressed in the lateral epidermis, the yolk cell and the amnioserosa. | Yes | (Belacortu et al., 2011; Muñoz-Descalzo et al., 2005) |
| *chd64* | Involved in juvenile hormone pathway and 20E pathway by binding to EcR/Usp complex | Yes | (Li et al., 2007) |
| *ecdysone receptor (ecr)* | A nuclear hormone (20E) receptor. Forms heterodimer with Usp and acts as a DNA binding transcription factor to initiate downstream gene expressions necessary for developmental transitions. | Yes | (Riddiford et al., 2001; Thummel, 1995) |
| *g protein-coupled receptor kinase 2 (Gprk2)* | A member of a family of serine/threonine kinases which modulates G-protein coupled receptor activity. In embryonic development, it is involved in cell morphogenesis such as gastrulation in embryonic development. | Potential | (Fuse et al., 2013) |
| *Insulin-like receptor (InR)* | Receptor tyrosine kinase. It is required for normal development including formation of the embryonic epidermis and nervous systems. | Yes | (Brogiolo et al., 2001; Fernandez et al., 1995) |
| *jaguar (jar)* | Myosin VI homologue. Required for cell-cell adhesion and rigidity of the cell during DC. | Yes | (Kellerman et al., 1992; Millo et al., 2004) |
| *jupiter (jup)* | Encodes microtubule associating protein. It is involved in polymerization of microtubule. | Yes | (Karpova et al., 2006) |
| *mesoderm-expressed 2 (mes2)* | It is expressed in the eaerly mesoderm during embryonic development, encodes a member of MADF family transcription factor. | Yes | (Zimmermann et al., 2006) |
| *Rho GTPase activating protein at 71E (RhoGAP71E)* | A GAP for the Rho family small GTPases | Unknown | (Mason et al., 2016) |
| *steppke (step)* | Encodes a member of the cytohesin family of Arf-guanine nucleotide exchange factors (GEFs). It relaxes tissue tension in response to the assembly of actomyosin cables at cell-cell junctions. | Yes | (West et al., 2017) |

| | | | |
|---|---|---|---|
| *u-shaped (ush)* | Encodes a member of the friend of GATA (FOG) multitype zinc finger protein. It is required for maintenance of amnioserosa during embryonic development. Known target gene of Dpp signaling. | Yes | (Frank and Rushlow, 1996; Lada et al., 2012) |
| *Ultraspiracle (usp)* | Nuclear receptor which forms heterodimer with EcR. | Yes | (Riddiford et al., 2001; Thummel, 1995) |
| *Z band alternatively spliced PDZ-motif protein 52 (zasp52)* | A member of the Alp/Enigma family involved in actin cable formation. The protein maintains actin anchorage at the z line of muscle cells with α-actinin, and regulate integrin mediated adhesion sites. | Yes | (Jani and Schock, 2007) |
| *zipper* | Encoding non-muscle myosin II heavy chain. See section | Yes | (Young et al., 1993) |